# Enhanced Polymeric Nanoparticles for Gene Delivery

by

Jordan Jamieson Green

B.S. Biomedical Engineering and Chemical Engineering
Carnegie Mellon University, 2003

SUBMITTED TO THE DIVISION OF BIOLOGICAL ENGINEERING IN PARTIAL FULFILLMENT OF THE REQUIREMENTS FOR THE DEGREE OF

DOCTOR OF PHILOSOPHY IN BIOLOGICAL ENGINEERING
AT THE
MASSACHUSETTS INSTITUTE OF TECHNOLOGY

SEPTEMBER 2007



Signature of Author: _____
Division of Biological Engineering
July 20, 2007

Certified by: _____
Robert S. Langer
Institute Professor
Thesis Supervisor

Accepted by: _____
Alan J. Grodzinsky
Professor of Electrical, Mechanical, and Biological Engineering
Chair, Biological Engineering Graduate Program Committee

This doctoral thesis has been examined by a committee of the Biological Engineering Division as follows:

Thesis Committee Chair:

Douglas A. Lauffenburger
Director and Professor of Biological Engineering
Professor of Chemical Engineering and Biology

Thesis Supervisor, Committee Member:

Robert S. Langer
Institute Professor

Committee Member:

John M. Essigmann
Professor of Biological Engineering and Chemistry

**Enhanced Polymeric Nanoparticles for Gene Delivery**

by Jordan Jamieson Green

Submitted to the Division of Biological Engineering on July 20, 2007
in Partial Fulfillment of the Requirements for the
Degree of Doctor of Philosophy in Biological Engineering

# Abstract

The potential of gene therapy to treat disease and improve human health is tremendous. The failure of viral gene therapy clinical trials due to toxicity, immunogenicity, and carcinogenicity has been tragic and strongly motivates a non-viral approach. However, non-viral gene delivery is currently ineffective.

Here, we show that polymeric nanoparticles composed of poly(β-amino esters) (PBAEs) and DNA can be formulated to be stable in the presence of serum proteins and have high gene delivery without toxicity to human primary cells. The biophysical properties of PBAE/DNA nanoparticles have good correlation to transfection efficacy when tested in the appropriate media conditions.

We also show that electrostatic interactions can drive peptide coating of nanoparticles and enable ligand-specific gene delivery. A biphasic efficacy relationship exists for peptide weight ratio, overall charge ratio, and ligand length, with intermediate values of coating being optimal. A balance is required when seeking to design nanoparticles that have reduced non-specific uptake, but increased ligand-specific uptake.

We develop a high-throughput assay to quantify polymer/DNA binding as a gene delivery bottleneck and find that a biphasic relationship exists between polymer/DNA binding constant, $K_a$, and delivery efficacy.

We also show that end-modified PBAEs can be as effective as adenovirus for gene delivery. In comparison to the previous "gold standard" for polymeric transfection, 25 kDa polyethylenimine, the PBAE nanoparticles presented here have 100x higher efficacy while simultaneously having 100x lower toxicity. Small structural changes were found to have dramatic effects on multiple steps of gene delivery including the DNA binding affinity, nanoparticle size, intracellular DNA uptake, and final protein expression. We show that small modifications to the termini of a polymer can significantly increase its *in vivo* activity and demonstrate potential utility of these polymers in the fields of cancer therapy, genetic vaccines, and stem cell engineering. As the enhanced polymeric gene delivery nanoparticles described here have many attractive properties over a virus including high safety, low immunogenicity, high nucleic acid cargo capacity, ease in manufacture, a coating method for targeted delivery, and flexibility for future design improvements, we believe that these polymeric nanoparticles may be promising alternatives for therapeutic gene delivery applications.

Thesis supervisor: Robert S. Langer, Sc.D.
Title: Institute Professor

# Acknowledgements

First and foremost, I am grateful to my advisor, Bob Langer. His inspiration, vision, and encouragement have been a great source of strength and his mentoring of both my research and personal development has been invaluable. I am also very appreciative of my thesis committee members, Doug Lauffenburger and John Essigmann, for their continued advice and guidance. I also have a special sense of gratitude to Dan Anderson for his kindness in mentoring me since I joined the Langer Lab.

Furthermore, I am very appreciative of the Biological Engineering program at MIT. The program and its vision have both challenged me and empowered me with new tools and a new outlook that I will carry with me long after this thesis work. I feel extremely fortunate to have been part of both BE and the Langer Lab, a place where there is fantastic opportunity to learn, discover, and create.

I am appreciative of all the members of Langer Lab that I have worked with, bounced ideas off, and laughed with over the years. I would like to especially thank the undergraduate and graduate students whom I mentored and worked with closely, Julie Shi, Eugene Chiu, Liz Leshchiner, and Lauren Tashima, for their tireless work and assistance. I would also like to thank my collaborators and friends in the lab, particularly Greg Zugates, Dave Nguyen, and Naushad Hossain for their excellent work and our great discussions.

Last, but not least, I would like to thank my family. I thank my parents, Henry and Elizabeth Green for their unending love and support, for nurturing me to believe in myself and my abilities, and for taking me so many times to the Miami Museum of Science when I was growing up. Finally I would like to thank Steph, my beautiful wife, for all of her love and encouragement.

I would also like to deeply thank the Whitaker Foundation and the National Science Foundation (NSF) for graduate fellowship support of this work. This work was also supported in part by NIH Grant EB 00244. Any opinions, findings, conclusions or recommendations expressed in this work are those of the author and do not necessarily reflect the views of the Whitaker Foundation, NSF, or NIH.

To Kai,

May the curiosity and wonder in the world you feel as a child
only grow stronger as you grow older

*"Everything is simpler than you think and at the same time
more complex than you imagine"*

- Goethe

*"The impossible just takes a little more time"*

- Sidney Green, my grandfather

# Table of Contents

**Abstract** ..... 3

**Acknowledgements** ..... 4

**List of Figures** ..... 10

**List of Tables** ..... 13

**List of Abbreviations** ..... 14

**Chapter 1: Introduction** ..... 16

**Chapter 2: Background** ..... 18

*2.1 THE PROMISE OF GENE THERAPY* ..... *18*
2.1.1 A Short History ..... 18
2.1.2 Clinical Trials ..... 19
2.1.3 Evolution's Way: Viral Gene Therapy ..... 22

*2.2 GENE DELIVERY MECHANISM AND BOTTLENECKS* ..... *26*
2.2.1 Overview ..... 26
2.2.2 Polymer/DNA Binding and Particle Self-Assembly ..... 28
2.2.3 Particle Uptake ..... 29
2.2.4 Endosomal Escape ..... 30
2.2.5 Intracellular Transport ..... 31
2.2.6 DNA Unpacking ..... 32
2.2.7 Nuclear Entry ..... 33
2.2.8 Biomaterial Degradability ..... 34
2.2.9 From In Vitro to In Vivo: Serum Interactions and Targeting Challenges ..... 35

*2.3 NON-VIRAL GENE DELIVERY: DESIGNING SMART NANO-BIOMATERIALS* ..... *37*
2.3.1 Overview ..... 37
2.3.2 Inorganic Materials ..... 38
2.3.3 Cationic Lipids ..... 39
2.3.4 Polysaccharides ..... 41
2.3.5 Polymers ..... 43

**Chapter 3: Poly(β-amino esters): Procedures for Synthesis and Gene Delivery** ..... 66

*3.1 INTRODUCTION* ..... *66*

*3.2 MATERIALS* ..... *67*
3.2.1 Polymer Synthesis ..... 67
3.2.2 Cell Culture ..... 68
3.2.3 Standard Gene Delivery Transfection ..... 69
3.2.4 High-throughput Gene Delivery Transfection ..... 69

*3.3 METHODS* ..... *71*
3.3.1 Polymer Synthesis ..... 71
3.3.2 Standard Transfection ..... 72
3.3.3 High-throughput Screening ..... 76

*3.4 NOTES* ..... *80*
3.4.1 Cell Line ..... 80

3.4.2 Plasmid DNA ..... 81
3.4.3 Polymer/DNA Self-Assembly ..... 81
3.4.4 Low Transfection ..... 82
3.4.5 High Cytotoxicity ..... 82
3.4.6 High-Throughput Screening Advantages/Limitations ..... 82
*3.5 REFERENCES* ..... *83*

**Chapter 4: Design of Biodegradable Polymeric Vectors** ..... **85**
*4.1 INTRODUCTION* ..... *85*
*4.2 EXPERIMENTAL PROCEDURES* ..... *87*
4.2.1 Cell Culture ..... 87
4.2.2 Polymer Synthesis ..... 87
4.2.3 Polymeric Vectors ..... 88
4.2.4 Biophysical Characterization ..... 89
4.2.5 Luciferase Transfections ..... 89
4.2.6 GFP Transfections ..... 91
4.2.7 Flow Cytometry ..... 91
4.2.8 Cell Viability Measurements ..... 92
4.2.9 Statistics ..... 92
*4.3 RESULTS AND DISCUSSION* ..... *92*
4.3.1 Polymer Synthesis and Gene Delivery Vector Formulation ..... 92
4.3.2 Biophysical Characterization ..... 94
4.3.3 Luciferase Transfections ..... 100
4.3.4 GFP Transfections ..... 102
4.3.5 Cell Viability ..... 110
*4.4 CONCLUSIONS* ..... *112*
*4.5 REFERENCES* ..... *112*

**Chapter 5: Nanoparticle Coatings for Ligand-Specific Delivery** ..... **116**
*5.1 INTRODUCTION* ..... *116*
*5.2 EXPERIMENTAL PROCEDURES* ..... *118*
5.2.1 Cell Culture ..... 118
5.2.2 Polymer Synthesis ..... 119
5.2.3 Peptide-Coated Polymeric Nanoparticles ..... 119
5.2.4 Transmission Electron Microscopy (TEM) ..... 120
5.2.5 Agarose Gel Electrophoresis Retardation Assay ..... 120
5.2.6 Biophysical Characterization ..... 121
5.2.7 GFP Transfections ..... 121
5.2.8 Flow Cytometry ..... 122
5.2.9 Cell Viability Measurements ..... 123
*5.3 RESULTS AND DISCUSSION* ..... *124*
5.3.1 Nanoparticle Formation and Peptide Coating ..... 124
5.3.2 Biophysical Characterization ..... 126
5.3.3 GFP Transfections ..... 131
5.3.4 Cell Viability ..... 132
5.3.5 Glutamic Acid-based Coats Enable Ligand-Specific Gene Delivery of Poly(β-amino ester)/DNA nanoparticles to Human Primary Cells ..... 133
5.3.6 Polymer Weight Ratio, Overall Charge Ratio, and Peptide Length are Important Parameters for Ligand-Specific Gene Delivery ..... 135
5.3.7 Statistics ..... 139

*5.4 CONCLUSIONS* ..... *139*

*5.5 REFERENCES* ..... *141*

**Chapter 6: Investigation of Polymer/DNA Binding as a Gene Delivery Bottleneck** ..... **144**

*6.1 INTRODUCTION* ..... *144*

*6.2 EXPERIMENTAL PROCEDURES* ..... *146*
6.2.1 Polymer Synthesis ..... 146
6.2.2 DNA Binding Assay ..... 149
6.2.3 Cell Culture and Transfection ..... 154

*6.3 RESULTS AND DISCUSSION* ..... *156*
6.3.1 Determination of YO-PRO-1 Binding Constant and Site Size ..... 156
6.3.2 Determination of Polymer/DNA Binding Constants ..... 158
6.3.3 Polymer/DNA Binding Constant Correlates to Transfection Efficacy ..... 164
6.3.4 Small Modifications of C32 Base Polymer Enables Polymer/DNA Binding Constant Tuning and Increased Transfection Efficacy ..... 168

*6.4 CONCLUSIONS* ..... *176*

*6.5 REFERENCES* ..... *177*

**Chapter 7: Poly(β-amino ester) Nanoparticles With Efficacy Comparable to Adenovirus** ..... **180**

*7.1 INTRODUCTION* ..... *180*

*7.2 EXPERIMENTAL PROCEDURES* ..... *182*
7.2.1 Materials ..... 182
7.2.2 Polymer Synthesis ..... 183
7.2.3 Luciferase Transfection ..... 185
7.2.4 DNA Binding Assay ..... 186
7.2.5 Particle Sizing ..... 187
7.2.6 DNA Uptake Assay ..... 187
7.2.7 GFP Transfection ..... 188
7.2.8 Mice ..... 190
7.2.9 Intraperitoneal Administration ..... 190
7.2.10 Optical Imaging ..... 191
7.2.11 Statistics ..... 191

*7.3 RESULTS AND DISCUSSION* ..... *192*

*7.4 CONCLUSIONS* ..... *199*

*7.5 REFERENCES* ..... *199*

**Chapter 8: Applications to Genetic Vaccines** ..... **202**

*8.1 INTRODUCTION* ..... *202*

*8.2 METHODS* ..... *204*

*8.3 RESULTS AND DISCUSSION* ..... *206*

*8.4 REFERENCES* ..... *213*

**Chapter 9: Future Directions** ..... **214**

*9.1 SUMMARY* ..... *214*

*9.2 FUTURE DIRECTIONS* ..... *217*
9.2.1 Applications to Stem Cells and Tissue Engineering ..... 217
9.2.2 Towards Further Rational Design ..... 222

*9.3 REFERENCES.....224*

**Chapter 10: Conclusions.....227**

# List of Figures


FIGURE 2.1. INDICATIONS ADDRESSED BY GENE THERAPY CLINICAL TRIALS ..... 21
FIGURE 2.2. CANDIDATE DISEASES FOR GENE THERAPY ..... 21
FIGURE 2.3. VECTORS USED IN GENE THERAPY CLINICAL TRIALS ..... 22
FIGURE 2.4. ADENOVIRUS STRUCTURE ..... 23
FIGURE 2.5. RETROVIRUS STRUCTURE ..... 24
FIGURE 2.6. COMPARISON OF VIRAL VECTOR PROPERTIES ..... 25
FIGURE 2.7. MECHANISM OF NON-VIRAL GENE DELIVERY ..... 27
FIGURE 2.8. STRUCTURES OF CATIONIC AND NEUTRAL LIPIDS ..... 41
FIGURE 2.9. SUGAR-BASED GENE DELIVERY BIOMATERIALS ..... 43
FIGURE 2.10. DENDRIMER STRUCTURE ..... 48
FIGURE 2.11 SYNTHESIS OF PBAES BY CONJUGATE ADDITION ..... 49
FIGURE 2.12. DIACRYLATE MONOMERS USED TO SYNTHESIZE PBAES ..... 51
FIGURE 2.13. AMINE MONOMERS USED TO SYNTHESIZE PBAES ..... 52
FIGURE 2.14. SUBSET OF DIACRYLATE AND AMINE ALCOHOL MONOMERS ESPECIALLY PROMISING FOR GENE DELIVERY ..... 54
FIGURE 3.1. POLYMERIZATION OF 1,4-BUTANEDIOL DIACRYLATE AND 5-AMINOPENTANOL TO FORM GENE DELIVERY POLYMER C32 ..... 71
FIGURE 3.2. REPRESENTATIVE HUVEC TRANSFECTION EFFICACY OF C32 AND METHOD FOR FACS GATING ..... 76
FIGURE 3.3. HIGH-THROUGHPUT SCREENING METHOD ..... 80
FIGURE 4.1A. DIACRYLATE ESTERS AND AMINE MONOMERS ..... 93
FIGURE 4.1B. SYNTHESIS OF POLY(B-AMINO ESTERS) ..... 93
FIGURE 4.2. C32/DNA (50 W/W) PARTICLE SIZE AND STABILITY IS DEPENDENT ON MEDIA TYPE AND SERUM CONCENTRATION AND CAN CHANGE DYNAMICALLY IN TIME ..... 95
FIGURE 4.3. PARTICLE SIZE AND STABILITY IS DEPENDENT ON POLYMER TYPE ..... 97
FIGURE 4.4. PARTICLE SIZE AND STABILITY IN 12% SERUM IS DEPENDENT ON POLYMER TYPE AND THE N/P (AND W/W) RATIOS OF POLYMER TO DNA ..... 98
FIGURE 4.5. C32/DNA (50 W/W) PARTICLES ARE STABLE OVER A LONG TIME PERIOD WHILE IN VARIOUS MEDIA CONDITIONS ..... 99
FIGURE 4.6A. HIGH-THROUGHPUT SCREENING OF VECTORS ..... 101
FIGURE 4.6B AND C. OPTIMAL TRANSFECTION (RLU) IS DEPENDENT ON DNA LOADING, POLYMER WEIGHT RATIO (N/P RATIO), TYPE OF POLYMER, AND PRESENCE OF SERUM ..... 103
FIGURE 4.6D. HIGH-THROUGHPUT SCREENING OF VECTORS ..... 104
FIGURE 4.7. (A) FACS DENSITY PLOT AND GATING FOR NEGATIVE CONTROL (0% POSITIVE) AND COMPARISON TO (B) C32/DNA VECTOR TRANSFECTION (44.7% POSITIVE). (C) THE SAME FACS DATA SHOWN IN A ONE-DIMENSIONAL HISTOGRAM PLOT ..... 106
FIGURE 4.8. HUVEC FACS TRANSFECTION RESULTS IN 12% SERUM MEDIA ..... 108
FIGURE 4.9. COMPARISON OF VECTORS FOR HUVEC TRANSFECTION IN 12% SERUM-CONTAINING MEDIA ..... 109
FIGURE 4.10. POLY(β-AMINO ESTER) C32 IS NON-CYTOTOXIC TO HUVECS IN CONTRAST TO THE PREMIERE COMMERCIALLY AVAILABLE POLYMERIC VECTOR JETPEI ..... 111
FIGURE 5.1. SYNTHESIS SCHEMES. (A) POLY(β-AMINO ESTER) C32 STRUCTURE AND SYNTHESIS; (B) ELECTROSTATIC SELF-ASSEMBLY OF LIGAND COATED NANOPARTICLE. ..... 124
FIGURE 5.2. 40 W/W C32 PARTICLES COATED WITH 19 W/W E12RGD IN SERUM MEDIA. ..... 126
FIGURE 5.3. GEL SHOWING FULL DNA ENCAPSULATION OF PARTICLES ..... 127
FIGURE 5.4. LIGAND COATED NANOPARTICLES ARE SLIGHTLY LARGER IN SIZE THAN UNCOATED NANOPARTICLES. . 129

FIGURE 5.5. LIGAND COATED 40 W/W C32/DNA NANOPARTICLES HAVE EQUIVALENT NEGATIVE CHARGE TO UNCOATED NANOPARTICLES WHILE IN 12% SERUM-CONTAINING MEDIA WHEREAS 50 W/W C32/DNA NANOPARTICLES ARE SLIGHTLY MORE NEUTRALLY CHARGED. ..... 130
FIGURE 5.6. FACS RESULTS SHOWING THE GATING OF TRANSFECTED HUVECS ..... 132
FIGURE 5.7. (A) EFFICACY AND SPECIFICITY OF E12-RGD/E12-RDG LIGAND COATED GENE DELIVERY NANOPARTICLES IS DEPENDENT ON W/W PEPTIDE AND N/P RATIO. NANOPARTICLES ARE FORMED AT 50 W/W C32 AND ARE DELIVERED TO HUVECS IN 12% SERUM CONTAINING MEDIA. ERROR BARS ARE STANDARD DEVIATIONS AND (*) AND (**) INDICATE STATISTICAL SIGNIFICANCE OF $P<0.05$ AND $P<0.01$ RESPECTIVELY... 134
FIGURE 5.8. EFFICACY AND SPECIFICITY OF E12-RGD/E12-RDG LIGAND COATED GENE DELIVERY NANOPARTICLES IS DEPENDENT ON W/W C32 AND N/P RATIO ..... 136
FIGURE 5.9. COMPETITIVE INHIBITION EXPERIMENT WITH E12-RGD (LIGAND) AND E12-RDG (CONTROL) COATED GENE DELIVERY NANOPARTICLES AND FREE RGDS PEPTIDE FRAGMENT ..... 137
FIGURE 5.10. EFFICACY AND SPECIFICITY OF E12-RGD (LIGAND) AND E12-RDG (CONTROL) COATED GENE DELIVERY NANOPARTICLES IS DEPENDENT ON PEPTIDE LENGTH AND N/P RATIO ..... 138
FIGURE 6.1A. AMINE AND ACRYLATE MONOMERS USED FOR POLY(β-AMINO ESTER) SYNTHESIS ..... 148
FIGURE 6.1B. SYNTHESIS OF POLY(β-AMINO ESTERS) ..... 149
FIGURE 6.2A. SYNTHESIS OF END-MODIFIED POLY(β-AMINO ESTERS) BY REACTION OF ACRYLATE-TERMINATED C32 POLYMER WITH PRIMARY DIAMINE MOLECULES IN DMSO ..... 149
FIGURE 6.2B. STRUCTURES OF AMINE-CAPPING MOLECULES ..... 149
FIGURE 6.3. MCGHEE AND VON HIPPEL BINDING ISOTHERM FOR A LIGAND BINDING TO AN INFINITE LATTICE ..... 152
FIGURE 6.4. MODIFIED MCGHEE AND VON HIPPEL BINDING ISOTHERM FOR TWO LIGANDS COMPETING TO BIND TO AN INFINITE LATTICE ..... 153
FIGURE 6.5. PLOT SHOWING THE BINDING OF YO-PRO-1 TO DNA ..... 156
FIGURE 6.6. PLOT SHOWING FIT TO MCGHEE AND VON HIPPEL BINDING ISOTHERM FOR YO-PRO-1/DNA ..... 157
FIGURE 6.7. C32 AND YO-PRO-1 COMPETING TO BIND DNA. ..... 158
FIGURE 6.8. DEMONSTRATION OF FITTING POLYMER/DNA BINDING TO THE MCGHEE AND VON HIPPEL BINDING ISOTHERM ..... 159
FIGURE 6.9. DEMONSTRATION OF FITTING POLYMER/DNA BINDING TO THE MCGHEE AND VON HIPPEL BINDING ISOTHERM. ..... 160
FIGURE 6.10. COMPARISON OF POLY(β-AMINO ESTERS) BINDING TO DNA (V.S. CONCENTRATION OF POLYMER) ..... 161
FIGURE 6.11. COMPARISON OF POLY(β-AMINO ESTERS) BINDING TO DNA (VS. CONCENTRATION OF MONOMER UNITS COMPRISING POLYMER) ..... 162
FIGURE 6.12. BINDING ASSOCIATION CONSTANTS FOR TOP-PERFORMING POLYMERS IN THE POLY(β-AMINO ESTER) LIBRARY ..... 165
FIGURE 6.13. TRANSFECTION EFFICACY OF POLY(β-AMINO ESTERS) IN HUVECS ..... 166
FIGURE 6.14. END-MODIFIED C32 POLYMER ISOTHERMS. ..... 170
FIGURE 6.15. SMALL STRUCTURAL CHANGES TO DIAMINE MONOMERS USED TO END-CAP C32-AC BASE POLYMER TUNE THE OVERALL POLYMER/DNA BINDING CONSTANT FOR THE WHOLE POLYMER ..... 173
FIGURE 6.16. HUVEC TRANSFECTION IN SERUM CONTAINING MEDIA ..... 173
FIGURE 6.17. COMPARISON OF $K_A$ VS. TRANSFECTION EFFICACY ..... 175
FIGURE 7.1. (A) SYNTHESIS OF END-MODIFIED POLY(β-AMINO ESTER)S BY REACTION OF ACRYLATE-TERMINATED C32 POLYMER WITH PRIMARY DIAMINE MOLECULES IN DMSO; (B) STRUCTURES OF AMINE-CAPPING MOLECULES. ..... 183
FIGURE 7.2. COMPARISON OF OPTIMIZED FORMULATIONS OF UNMODIFIED C32 TO MODIFIED C32-103 AND C32-117 FOR ABILITY TO BIND DNA, FORM NANOPARTICLES, AND FACILITATE DNA UPTAKE INTO COS-7 CELLS ..... 193
FIGURE 7.3. GENE EXPRESSION OF LEADING NON-VIRAL POLYMERIC VECTORS AS COMPARED TO ADENOVIRUS VECTORS ..... 195
FIGURE 7.4. (A) OPTICAL IMAGES OF OVARIAN TUMORS AND UTERI FROM MISIIR/TAG MICE 6 HR FOLLOWING *I.P.* INJECTION WITH POLYMER/DNA (PCAG/LUC) COMPLEXES. (B) QUANTIFICATION OF LUCIFERASE EXPRESSION

IN OVARIAN TUMORS 6 HR FOLLOWING *I.P.* INJECTION WITH C32 (N = 6) OR C32-117 (N = 9) DELIVERED PCAG/LUC DNA (100 μG) ..... 198
FIGURE 8.1. OVERVIEW OF DNA VACCINE MECHANISM ..... 203
FIGURE 8.2. SYNTHESIS OF END-MODIFIED C32 POLY(β-AMINO ESTERS). ..... 206
FIGURE 8.3. END-CAPPING MONOMERS USED TO CREATE C32-BASED POLY(β-AMINO ESTERS) FOR USE AS GENETIC VACCINES ..... 206
FIGURE 8.4. TRANSFECTION OF DENDRITIC CELL LINE DC 2.4 IN SERUM CONTAINING MEDIA ..... 207
FIGURE 8.5. FLUORESCENT MICROGRAPHS OF DC 2.4 EGFP TRANSFECTION USING PBAE NANOPARTICLES. ..... 208
FIGURE 8.6. TRANSFECTION OF DENDRITIC CELL LINE DC 2.4 IN SERUM CONTAINING MEDIA ..... 209
FIGURE 8.7. VIABILITY OF DENDRITIC CELL LINE DC 2.4 IN SERUM CONTAINING MEDIA ..... 210
FIGURE 8.8. ANTIBODY PRODUCTION IN MICE FOLLOWING INJECTION OF PBAE NANOPARTICLES ..... 211
FIGURE 8.9. IN VIVO ANTIBODY PRODUCTION AT 6 WEEKS ..... 212
FIGURE 9.1. COMBINED GENE AND STEM CELL THERAPY ..... 218
FIGURE 9.3. TRANSFECTION OF HES COLONY BY LIPOFECTAMINE 2000 ..... 221
FIGURE 9.4. PBAE GENE DELIVERY TO UNDIFFERENTIATED HES COLONIES. ..... 222

# List of Tables

TABLE 3.1 CELL PLATING ..... 72
TABLE 3.2 POLYMER PREPARATION ..... 74
TABLE 3.3 GENE DELIVERY NANOPARTICLE DOSE ..... 75
TABLE 4.1 OPTIMIZED POLYMER WEIGHT RATIOS (W/W), NITROGEN TO PHOSPHATE CHARGE RATIOS ..... 100
TABLE 6.1. TABLE OF POLYMER PROPERTIES. THIS TABLE SHOWS MOLECULAR WEIGHTS (MW), THE MAXIMUM AND OBSERVED LATTICE BINDING SITE SIZE ($N_{MAX}$ AND $N_{OBS}$), AND THE ASSOCIATION CONSTANT, $K_A$. ..... 163
TABLE 6.2 TABLE OF END-MODIFIED C32 POLYMER PROPERTIES. THIS TABLE SHOWS THE MAXIMUM AND OBSERVED LATTICE BINDING SITE SIZE ($N_{MAX}$ AND $N_{OBS}$), AND THE ASSOCIATION CONSTANT, $K_A$. ..... 171

# List of Abbreviations

| | |
|---|---|
| AAV | Adeno-associated virus |
| APC | Antigen presenting cell |
| bp | Base pairs (of DNA) |
| β-gal | β-galactosidase |
| CD | Cyclodextrins |
| C32 | Leading PBAE, Poly(5-amino-1-pentanol-co-1,4-butanediol diacrylate) |
| D | Lattice concentration |
| DC | Dendritic cell |
| DMSO | Dimethyl sulfoxide |
| DNA | Deoxyribonucleic acid |
| DOTMA | N-[1-(2,3-dioleyloxy)propyl]-N,N,N-trimethylammonium chloride |
| E12-RDG | Peptide sequence EEEEEEEEEEEEGGGGGGGRDGS |
| E12-RGD | Peptide sequence EEEEEEEEEEEEGGGGGGGRGDS |
| EGFP | Enhanced green fluorescent protein |
| f | Fraction of lattice free |
| FACS | Fluorescence activated cell sorting |
| FBS | Fetal bovine serum |
| $F_{Bound}$ | Fluorescence per bound ligand |
| $F_{Free}$ | Fluorescence per free unbound ligand |
| $F_{obs}$ | Observed fluorescence |
| GPC | Gel-permeation chromatography |
| hES | Human embryonic stem cell |
| HUVEC | Human umbilical vein endothelial cell |
| $K_a$ | Binding association constant |
| $K_d$ | Binding dissociation constant |
| $L_{Bound}$ | Concentration of bound ligand |
| $L_{Free}$ | Concentration of free ligand |
| $L_{Total}$ | Total concentration of free ligand |
| Luc | Luciferase |
| MOI | Multiplicity of infection |
| MW | Molecular weight |
| n | Lattice-ligand binding site size |
| $n_{max}$ | Maximum possible lattice-ligand binding site size |
| $n_{obs}$ | Observed lattice-ligand binding site size |
| NaAc | Sodium acetate |
| NLS | Nuclear localization sequence |
| N/P | Polymer nitrogen to DNA phosphate charge ratio |
| PAMAM | Poly(amidoamine) |
| PBAE | Poly(β-amino ester) |
| PBS | Phosphate buffered saline |
| PEG | Poly(ethylenegylcol) |
| PEI | Polyethylenimine |
| PLL | Poly(L-lysine) |

| | |
|---|---|
| PNA | Peptide nucleic acid |
| RFP | Red fluorescent protein |
| RGD | Peptide sequence arginine-glycine-aspartic acid |
| RLU | Relative light units |
| SCID | Severe combined immunodeficiency disorder |
| TEM | Transmission electron microscopy |
| v | Fraction of lattice bound by ligand(s) |
| w/w | Weight ratio of polymer (or peptide) to DNA |

# Chapter 1: Introduction

*"There are only three problems in gene therapy - delivery, delivery, and delivery"*

-Inder Verma, Salk Institute and President of the Am. Soc. of Gene Therapy, *TIME*, Jan 11, 1999

Gene therapy is the use of genes, units of heritable traits that are stored in every organism's DNA, as a therapeutic. The potential of gene therapy to benefit human health is tremendous as almost all human diseases have a genetic component, from cancer to heart disease. Furthermore, many untreatable genetic disorders, both common and rare, can be potentially cured via gene therapy.

Unfortunately, a method for gene therapy that is both effective and safe has remained elusive. The principle problem is that it is extremely challenging to design a delivery vehicle capable of efficiently delivering varying payloads of genes to target tissues of the body with high expression and high safety. In many ways though this is not surprising—the human body and its immune system has evolved for millions of years just to prevent such a potentially catastrophic event from occurring.

This thesis describes a promising strategy to the gene delivery problem: the design of biodegradable polymers that are able to deliver DNA like a synthetic virus. However, unlike an actual virus, these polymers form nanoparticles that are non-toxic, minimize the body's immune response, have the flexibility to deliver potentially any sized gene to any target tissue, and are relatively easy and inexpensive to manufacture on either small or large scale.

The background literature is reviewed in Chapter 2, including the most recent gene delivery vehicles, viral vectors and non-viral biomaterials. Chapter 3 describes methods for synthesis, formulation, and transfection of poly(β-amino esters). Chapter 4 describes the design of biodegradable polymeric vectors for gene delivery. The methodology includes initial high-throughput screening to find optimal gene delivery conditions and then a detailed look at polymer structure/function relationships and how biophysical properties affect gene delivery performance. Chapter 5 explores ways to enhance functionality by coating gene delivery nanoparticles for targeted delivery. Multiple coating parameters, but particularly charge ratio, are discussed and found to be critical to form nanoparticles that have both high efficacy and high specificity. Chapter 6 investigates polymer/DNA binding as a gene delivery bottleneck and how polymer structure correlates to binding affinity. Chapter 7 demonstrates that combinatorial modifications to poly(β-amino esters) can lead to the creation of non-viral polymeric nanoparticles that can achieve virus-like efficacy in human primary cells and greatly enhanced efficacy *in vivo*. Chapter 8 discusses applications of these nanoparticles to genetic vaccines and Chapter 9 discusses further directions. Finally, Chapter 10 states the conclusions of this work.

# Chapter 2: Background

## 2.1 THE PROMISE OF GENE THERAPY

Gene therapy represents a powerful new paradigm for treating a myriad of diseases, from cystic fibrosis to cancer, at the genetic level. However, a safe and effective method for gene delivery has not yet been found and the application of gene delivery to treat human disease has so far been limited. New insights into understanding and controlling the mechanism of gene delivery are required to further advance the field.

### *2.1.1 A Short History*

The history of gene therapy in many ways begins with mid-twentieth century discoveries in molecular biology and the subsequent biotechnology revolution in the 1970s. In 1944, Avery, MacLeod, and McCarty's classically showed for the first time that "nucleic acid of the deoxyribose type is the fundamental unit" in transmitting "inheritable and specific alterations in cell structure and function."[1] Other key discoveries soon followed including Watson and Cricks' discovery of DNA's structure[2] in 1953, and subsequent work by others to elucidate the "central dogma" of molecular biology, how DNA functions to encode proteins. In the early 1970s, recombinant DNA was discovered by Paul Berg and Stanley Cohen at Stanford University and

Herbert Boyer at the University of California, San Francisco and thus, it finally became possible to *design* biological products. This started the biopharmaceutical industry (Genentech, Biogen, Amgen, etc.) which was interested in gene transfer to cells in culture to produce commercially relevant proteins such as human insulin and human growth hormone.[3]

In human health, molecular biology and genetics were showing an increasing number of diseases that were determined to have genetic causes. Most treatments were based on using small molecules to treat the symptoms of the diseases, if treatments existed at all. However, if the genetic defect were to be repaired, rather than just treating disease symptoms, the disease itself could be theoretically cured. Thus the idea of gene *therapy*, where the gene itself acts as a therapeutic drug, was proposed. The initial targets for gene therapy were and still are monogenic diseases such as cystic fibrosis, severe combined immunodeficiency disorder (SCID), and hemophilia as well as many types of cancer. However, unlike early successes at transferring genes to bacteria growing in culture to produce protein, delivering genes to animals *in vivo* to produce therapeutic effects was soon found to be much more challenging.

### *2.1.2 Clinical Trials*

The uses of gene therapy in clinical trials to date are shown in Figure 2.1.. Two-thirds of all clinical trials have been for cancer diseases. This is due both to the fact that cancer is a leading cause of death in the United States and Europe without satisfactory available treatments and that for many cancer applications, unlike with most monogenic disorders, gene expression only needs to last a relatively short duration (until the cancer is destroyed) rather than lasting indefinitely. Currently in the United States, an estimated 1,445,000 new cases of cancer and

560,000 deaths will occur in 2007.[4] Some anti-cancer strategies involve using a cytotoxic or apoptosis-causing gene such as diphtheria toxin[5] or p53[6] to cause cancer death. Another complementary strategy is anti-angiogenesis gene therapy targeting endothelial cells, which can starve a growing cancer of oxygen and nutrients.[7, 8] Monogenic diseases make up a substantial portion of gene therapy trials because gene therapy, unlike conventional pharmaceuticals, is ideally suited to treat and cure these diseases. In recent years vascular diseases, the leading cause of death in the United States, are increasingly being considered for gene therapy treatment. 79,400,000 Americans have cardiovascular disease and 871,500 die each year as a result.[9] Gene therapy has the potential to treat many cardiovascular conditions including peripheral arterial disease, restenosis, and myocardial ischemia as gene delivery enables long term expression of target genes useful for treatments such as therapeutic angiogenesis and inhibition of cell proliferation.[10-12] Infectious diseases also have increasingly been looked at for gene therapy applications as DNA-based genetic vaccines would potentially have numerous advantages over conventional viral or protein based vaccines. These include high induction of cellular immunity, potentially high safety, ease in manufacture, cost-savings, and the potential for co-expression of multiple antigens.[13] The above mentioned diseases and other diseases that are potentially treatable by gene therapy are listed in further detail in Figure 2.2..

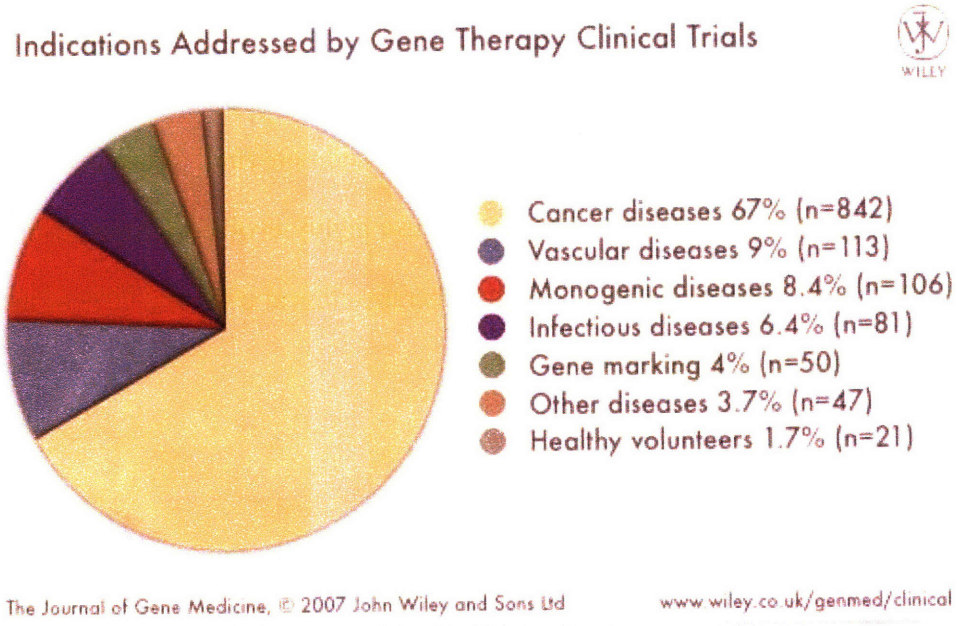


**Figure 2.1.** Indications addressed by gene therapy clinical trials.[14]

| *Disease* | *Defect* | *Incidence* | *Target cells* |
|---|---|---|---|
| **Genetic** | | | |
| Severe combined immunodeficiency (SCID/ADA) | Adenosine deaminase (ADA) in ~25% of SCID patients | Rare | Bone-marrow cells or T lymphocytes |
| Haemophilia A | Factor VII deficiency | 1:10,000 males | Liver, muscle, fibroblasts or bone-marrow cells |
| Haemophilia B | Factor IX deficiency | 1:30,000 males | |
| Familial hypercholesterolaemia | Deficiency of low-density lipoprotein (LDL) receptor | 1:1 million | Liver |
| Cystic fibrosis | Faulty transport of salt in lung epithelium. Loss of *CFTR* gene | 1:3,000 Caucasians | Airways in the lungs |
| Haemoglobinopathies: thalassaemias / sickle-cell anaemia | Structural defects in $\alpha$- or $\beta$-globin gene | 1:600 in certain ethnic groups | Bone-marrow cells, giving rise to red blood cells |
| Gaucher's disease | Defect in the enzyme glucocerebrosidase | 1:450 in Ashkenazi Jews | Bone-marrow cells, macrophages |
| $\alpha_1$-antitrypsin deficiency: inherited emphysema | Lack of $\alpha_1$-antitrypsin | 1:3,500 | Lung or liver cells |
| **Acquired** | | | |
| Cancer | Many causes, including genetic and environmental | 1 million/year in USA | Variety of cancer-cell types; liver, brain, pancreas, breast, kidney |
| Neurological diseases | Parkinson's, Alzheimer's, spinal-cord injury | 1 million Parkinson's and 4 million Alzheimer's patients in USA | Direct injection in the brain, neurons, glial cells, Schwann cells |
| Cardiovascular | Restinosis, arteriosclerosis | 13 million in USA | Arteries, vascular endothelial cells |
| Infectious diseases | AIDS, hepatitis B | Increasing numbers | T cells, liver, macrophages |

**Figure 2.2.** Candidate diseases for gene therapy[15]

### 2.1.3 *Evolution's Way: Viral Gene Therapy*

There are two main approaches to gene delivery: viral and non-viral. Viral delivery is the more conventional approach because it is attractive to use highly-evolved viruses to infect cells. As of April 2007, there have been over 1,250 gene therapy clinical trials and 70% of these trials use a viral vector as shown in Figure 2.2..[14]

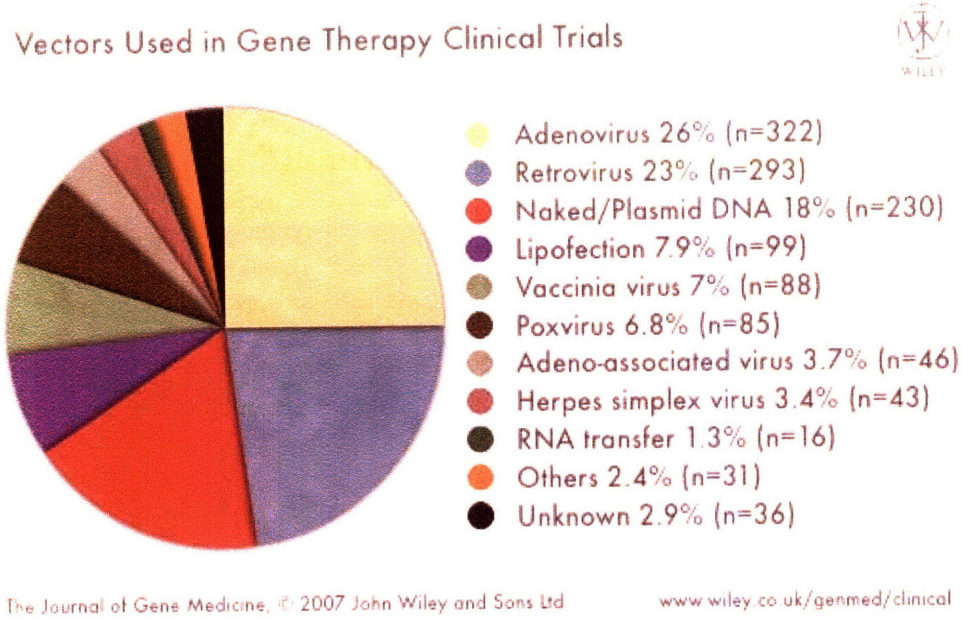


**Figure 2.3.** Vectors used in gene therapy clinical trials.[14]

The main viral approaches used to date are adenovirus and retrovirus. Adenoviruses are double-stranded DNA viruses that are packaged in a non-enveloped icosahedral protein capsid (Figure 2.4.). The advantages of adenovirus are infection of a wide range of human cell types, ability to infect non-dividing cells, and minimal risk of insertional mutagenesis.[16] However, adenovirus

expression is short-lived[15] and adenoviruses can cause a severe, even lethal, inflammatory response.[17] Retroviruses, on the other hand, are single-stranded RNA viruses that are packaged in a protein capsid that is coated with a lipid bilayer envelope that originates from the cell membrane of a host cell (Figure 2.5.). The main advantage of retroviruses is that they can integrate into the host for long-term expression; Their main disadvantage is this integration can cause mutagenesis and potentially cancer.[18] Retroviruses are also further limited by their inability to infect non-dividing cells.[16]

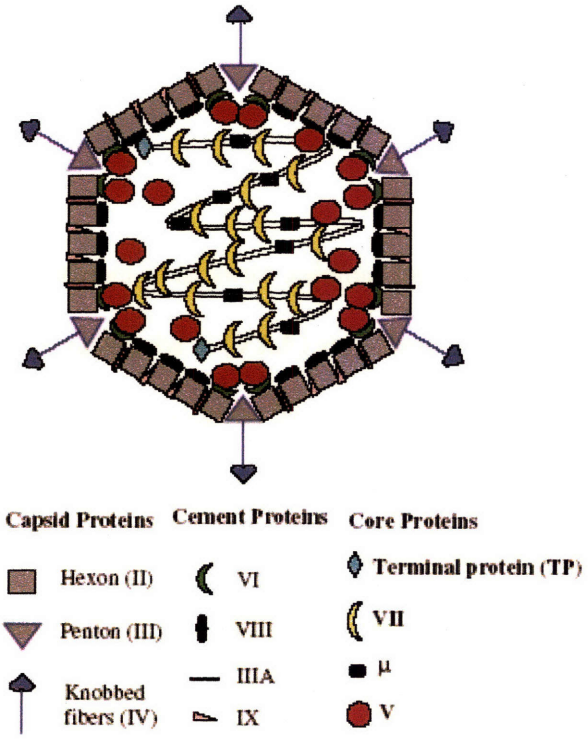


**Figure 2.4.** Adenovirus structure[16]

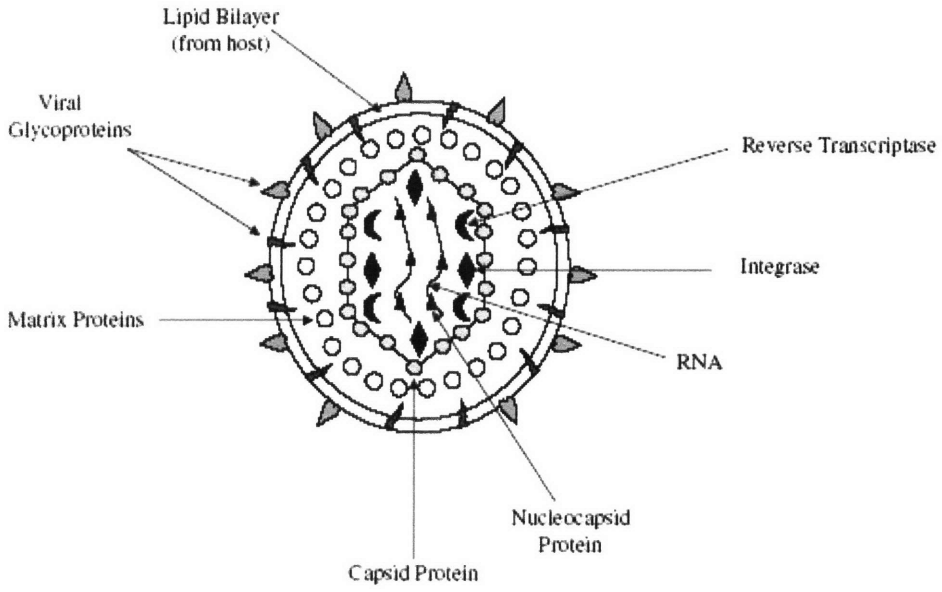


**Figure 2.5.** Retrovirus structure[16]

Recently, adeno-associated virus, lentivirus, and herpes simplex virus have increasingly been utilized as alternative viral vectors.[16, 19] Adeno-associated virus (AAV) is advantageous in that, unlike adenovirus, it has minimal toxicity. However, production of adeno-associated virus is much more labor intensive, the cargo capacity of the virus is relatively small at < 5kb limiting the genes that the virus can carry, and AAV can cause insertional mutagenesis.[20] Lentiviruses, such as HIV, are a subset of complex retroviruses. While they are able to transfect both dividing and non-dividing cells and have long-term expression, they are still limited by their small cargo size and potentially carcinogenic insertional mutagenesis.[20] Finally, herpes simplex virus has a large cargo capacity, but is inflammatory and only causes transient expression in most cells, although it has been particularly effective for gene delivery to neurons.[19] A summary of the advantages and disadvantages of various viral gene therapy approaches is seen in Figure 2.6..

| Vector | Genetic material | Packaging capacity | Tropism | Inflammatory potential | Vector genome forms | Main limitations | Main advantages |
|---|---|---|---|---|---|---|---|
| *Enveloped* | | | | | | | |
| Retrovirus | RNA | 8 kb | Dividing cells only | Low | Integrated | Only transduces dividing cells; integration might induce oncogenesis in some applications | Persistent gene transfer in dividing cells |
| Lentivirus | RNA | 8 kb | Broad | Low | Integrated | Integration might induce oncogenesis in some applications | Persistent gene transfer in most tissues |
| HSV-1 | dsDNA | 40 kb* 150 kb‡ | Strong for neurons | High | Episomal | Inflammatory; transient transgene expression in cells other than neurons | Large packaging capacity; strong tropism for neurons |
| *Non-enveloped* | | | | | | | |
| AAV | ssDNA | <5 kb | Broad, with the possible exception of haematopoietic cells | Low | Episomal (>90%) Integrated (<10%) | Small packaging capacity | Non-inflammatory; non-pathogenic |
| Adenovirus | dsDNA | 8 kb* 30 kb§ | Broad | High | Episomal | Capsid mediates a potent inflammatory response | Extremely efficient transduction of most tissues |

*Replication defective. ‡Amplicon. §Helper dependent. AAV, adeno-associated viral vector; dsDNA, double-stranded DNA; HSV-1, herpes simplex virus-1; ssDNA, single-stranded DNA.

**Figure 2.6.** Comparison of viral vector properties[19]

While there have been some limited successes in using viral gene therapy and many clinical trials are currently ongoing, overall the field has had many disappointments and a premiere technology for gene delivery has still not been developed. As previously mentioned, problems with viral gene therapy include limited cargo capacity, resistance to repeated infection, production and quality control issues, and safety.[20, 21] Ideally, one would want to design a flexible vector that could accommodate DNA cargo of any size and possibly transport multiple therapeutic genes for synergistic effects. Unlimited cargo capacity is not currently possible for viral systems, as they have evolved to carry only a small cargo of fixed size. The manufacture and quality control of producing large amounts of virus is also a challenge. Though cargo capacity and production are problems with a viral approach, a low level of safety is the primary disadvantage of this technique. Specific safety concerns include acute toxicity, cellular immune response, humoral immune response to the gene product, and oncogenicity due to insertional

mutagenesis.[20] Clinical trials have underscored these safety risks as a patient receiving adenovirus-based treatment for partial ornithine transcarbamylase deficiency tragically died due to a severe immune response in 1999.[17] Other viral gene therapy trials have been halted following the recent announcement that a third child being treated for severe combined immunodeficiency disease has developed cancer and that one of the two children who previously developed leukemia from this retroviral approach has died.[22, 23] Finally, there is also a risk that the viral gene therapy could reach germ-line cells as a recent clinical study found viral gene sequences in a patient's semen.[24] For these reasons, new attention has been focused on non-viral approaches for gene therapy as these have the potential to overcome many of the inherent challenges of viral vectors.

## 2.2 GENE DELIVERY MECHANISM AND BOTTLENECKS

### *2.2.1 Overview*

Instead of using a biological virus for gene therapy, an alternative approach is to design a synthetic virus. To rationally design an artificial virus to deliver therapeutic genes, one promising approach is to deconstruct the overall process into specific mechanistic steps of transport and identify bottlenecks. Recent work in the field has identified several key steps including vector binding/condensation of DNA, cellular uptake, endosomal escape, intracellular trafficking, nuclear translocation, and vector unpacking. Though these steps have been identified, they are still not well-understood and it is still largely unknown how a general gene delivery

vector's physical and chemical properties quantitatively influences each stage of delivery. The putative mechanism of non-viral gene delivery is shown below in Figure 2.7.

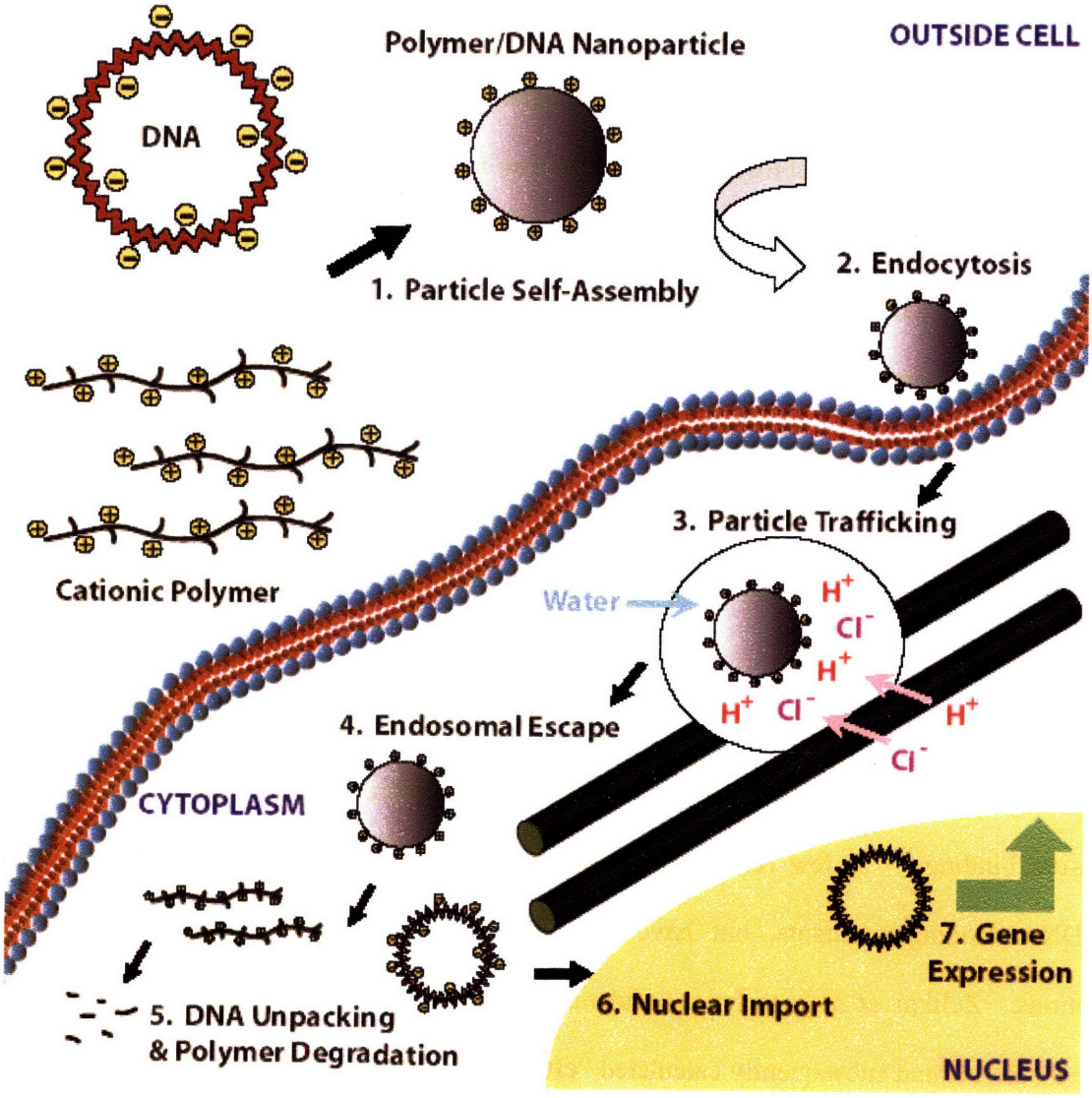


**Figure 2.7.** Mechanism of non-viral gene delivery

### *2.2.2 Polymer/DNA Binding and Particle Self-Assembly*

The first step of non-viral polymeric gene delivery is formation of the gene delivery nanoparticle. Polycations condense DNA in a reversible transition from linear polymer to globule.[25] For efficient transfection, it is crucial that DNA is condensed to protect the DNA, maintain particle stability, and allow for efficient uptake of the complexes.[25, 26] Polymer/DNA binding determines particle stability, which can be key to ensure that the DNA stays protected from nucleases and degradation. Furthermore, stable DNA-encapsulating particles are needed for efficient uptake. DNA uptake efficiency is significantly reduced if the DNA is released by the encapsulating particles prematurely. However, it is also important to consider that the particle should not bind or encapsulate the DNA so tightly, as to prevent the timely release of the DNA into the cytoplasm once the gene delivery particle has entered the cell. Lastly, polymer/DNA interactions are also important in shaping the biophysical properties of the resulting nanoparticle complex.

Gene delivery researchers have for the most part looked at DNA/vector binding qualitatively, rather than quantitatively, by using techniques such as agarose gel electrophoresis to measure binding.[27] A few researchers have recently quantitatively investigated non-viral vector/DNA binding constants, but have done so only after making several simplifying assumptions. Zelikin *et al.*'s technique did not take into account McGhee and von Hippel binding isotherms and subsequently calculated "effective" relative binding constants.[28] Plank *et al.*'s work, though more rigorous in form, required making assumptions about the binding constant of the reference ligand and of the site size of the known and unknown ligands.[29] An improved high-throughput assay that can determine absolute DNA binding constants for

unknown vector ligands and uses minimal assumptions has yet to be formulated. The application of such an assay to a large library of biomaterials to measure quantitatively nucleic acid binding constants would allow discovery of structure/function relationships and aid in increased sophistication of vector design.

### *2.2.3 Particle Uptake*

Once the particles are formed, the next key step is cellular uptake. Uptake can be non-specific or targeted to specific receptors on cell types of interest. For efficient non-specific uptake, it is important for the complexes to have an overall positive charge so that they will be electrostatically attracted to the negatively charged proteoglycan cell surface.[30] It has been shown that the size of the gene delivery particles influences uptake and small particles ~100 nm are taken up the best.[26] However, there are conflicting reports over whether smaller or larger particles exhibit higher overall transfection.[26, 30, 31] This demonstrates the potential ambiguity of analysis of these complexes as biophysical parameters such as particle size are coupled together with other parameters such as polymer molecular weight and charge ratio. This example also highlights the differences between an *in vitro* experiment where larger particles could sediment and increase transfection, and a systemic *in vivo* application, where larger particles would be problematic for physical delivery to distant sites. An exception to this is delivery to the lung, where it has been shown that large aggregating PEI/DNA particles passively target the lung following tail-vein injection.[32, 33] For receptor-specific endocytosis, ligands such as epidermal growth factor (EGF)[34], transferrin[35], folic acid[36], and RGD peptide[37] have been utilized to increase cell specificity and overall uptake *in vitro* and *in vivo*. Though targeting often increases

transfection, some experiments show that uptake that is both specific and efficient only occurs at a narrow window of charge ratios or not at all.[34, 37]

### *2.2.4 Endosomal Escape*

During uptake and internalization, the particles are packaged into vesicles and become part of the endosomal sorting pathway. Without any action by the vector, DNA would typically be degraded by the acidic environment of late endosomes, enzymatically degraded by lysosomes, and/or recycled out of the cell. In the earlier days of non-viral gene delivery, chloroquine was routinely added to cells along with the gene delivery particles to facilitate endosomal escape.[29, 31]

Polyethylenimine (PEI) vectors and other cationic polymers containing titratable amine groups are able to avoid this fate by buffering the endosome through the "proton sponge" mechanism.[38, 39] This hypothesis was recently proven by Sonawane *et al.* who showed that endosomes containing vectors with physiologically titratable amine groups like those formed from PEI, but not vectors lacking these groups like vectors formed from polylysine, buffered $H^+$ ions, increased the counter ion $Cl^-$ concentration within the endosome, swelled the endosome in size, and led to lysis of the endosome.[40] This process is highlighted in Figure 2.7.. These studies highlight the importance of physiologically titratable amine groups in polymeric vector construction. An alternative approach for endosomal escape is the use fusogenic peptides that can destabilize an endosomal membrane through other mechanisms such as pore formation.[41]

### *2.2.5 Intracellular Transport*

Once the vector is free in the cytosol, the next step in gene delivery is intracellular trafficking through the cell to the nucleus. The diffusion of DNA in the cytoplasm has been shown to be rate limiting. For a 2 kilobase pairs (kbp) fragment of DNA, diffusion in the cytoplasm is more than two orders of magnitude lower than diffusion in water and diffusion in the nucleus is essentially non-existent.[42]

Particle tracking can be utilized to investigate intracellular trafficking of individual gene delivery complexes with high sensitivity. Godbey *et al.* first tracked PEI vectors intracellularly in 1999 to demonstrate the mechanistic steps of transfection from endocytosis to gene expression.[43] Though this work showed qualitative localization of PEI and DNA within the cell, dynamic data was not available. The following year it was shown that individual proteins can be tracked intracellularly in live mammalian cells to calculate cellular diffusion constants.[44] Recently, Suh *et al.* conducted multiple particle tracking (MPT) experiments of live cells in real-time to show that a subset of PEI/DNA complexes can undergo motor-protein driven active transport to the nucleus on microtubules.[45] Similar transport has previously been seen with adeno-associated virus during the dynamics of infection.[46] It was shown that though the majority of PEI/DNA nanoparticles exhibited subdiffusive or immobile transport, a subset of the nanoparticles displayed active transport along microtubules with an effective diffusion constant over an order of magnitude higher than the non-actively transported particles.[47] Thus, real-time particle tracking has been shown to be a valuable tool for quantitatively determining rates of transport of individual gene delivery nanoparticles. However, further research must be done to

understand what physical and chemical properties of a gene delivery complex enable this active transport.

### *2.2.6 DNA Unpacking*

For DNA transcription to occur, the DNA must unpack from the gene delivery vector and translocate into the nucleus. The order of nuclear import and vector unpacking is still unclear as it has been demonstrated that PEI/DNA complexes can be found in the nucleus as associated complexes.[43] However, since the polymer/DNA particles are relatively large (>100 nm diameter) compared to a nuclear pore complex channel (25 nm for active transport and 9 nm for diffusion[48]), it is likely that DNA unbinding must occur prior to nuclear translocation.

Furthermore, one inside the nucleus, the transported DNA must eventually be free from polymer and other potentially competing binding biomolecules so that it can be efficiently transcribed into mRNA. It has been shown that polymeric vector/DNA complexation significantly inhibits RNA synthesis and that above an optimal length, overall transfection decreases as polylysine length increases.[49] Similarly, 25 kDa PEI vectors are known to have higher transfection efficacy that those formed with higher molecular weight PEIs.[25] However, it is also known that PEI and poly(β-amino ester)s with molecular weights below 10 kDa exhibit poor transfection as compared to higher molecular weight versions.[50] Thus, it appears that there may be a biphasic relationship between vector/DNA binding and transfection efficacy among a broad range of polymers. If DNA binding constants from a polymeric vector library could be calculated quickly and easily and correlated to structural properties and transfection efficacy, these vectors could be rationally designed to better overcome this bottleneck. Similarly,

improved understanding of structure/function relationships for cellular targeting and uptake, intracellular transport, and nuclear targeting would also significantly improve design of an enhanced non-viral gene delivery vector.

### *2.2.7 Nuclear Entry*

Unlike many drug treatments, in order for gene therapy to be successful therapeutically, it is not enough that the drug (DNA) is delivered to the cell, is internalized by the cell, and escapes the endosomal compartment into the cytoplasm. In addition, the DNA must make its way inside the nucleus, be transcribed into mRNA, and subsequently translated into protein. Whereas many viruses have evolved mechanisms for efficiently transmitting their genetic material into the nucleus for high expression[19], plasmid DNA does not have this advantage as it is primarily constructed to be replicated in bacteria.

Nuclear import, the final known gene delivery transport bottleneck, is a significant rate-limiting step. Through the use of synchronized cells, it has been demonstrated that mitosis can play a key role in gene delivery.[30] Rapidly dividing cells with frequent nuclear membrane breakdown are much more likely to be transfected than non-dividing cells due to easier nuclear uptake of DNA. To improve nuclear transport, nuclear localization sequences (NLS) can be added to the DNA and this technique can potentially increase transfection up to three orders of magnitude.[51] One approach is to incorporate an NLS by using either peptide nucleic acid (PNA) to hybridize to DNA[52] or covalent modification of DNA to include an NLS.[51] An alternative approach is to incorporate a nucleic acid sequence within the DNA that will bind to endogenous DNA-binding proteins that will facilitate nuclear transport.[53] However, the current literature is

unclear on the efficacy of these approaches with some researchers demonstrating increased efficacy and others showing little to no improvement.[54-56] Further research is required to ascertain which type and extent of NLS signal incorporation is the most effective. Following DNA delivery to the nucleus, an additional hurdle to gene therapy is the continued long-term expression of the therapeutic gene. This is a challenge as plasmid DNA may be either degraded[57], reduced in dividing cells through dilution[58], or methylated and transcriptionaly silenced[59], attenuating the expression. These concerns can be addressed in part through plasmid engineering such that functionalities can also be incorporated into the plasmid DNA itself including a choice of episomal expression or site-specific integration and the ability to regulate gene expression on or off.[21]

### *2.2.8 Biomaterial Degradability*

To reduce toxicity and complement system activation, the use of biocompatible and biodegradable materials would be beneficial. For example, the commonly used gene delivery polymer, PEI, is problematic as it has high cytotoxicity in vitro and in vivo by both necrotic and apoptotic mechanisms.[60, 61] The field of drug delivery has shown many approaches to safely deliver various payloads of therapeutics throughout the body using polymers.[62] One polymeric delivery approach that is useful for gene delivery in particular is the use of poly(β-amino esters).[27, 63] These cationic polymers, unlike PEI, are hydrolytically degradable via ester linkages. Beyond reducing cytotoxicity, degradable polymers are also promising for gene delivery as they provide an additional mechanism for DNA release once the gene delivery nanoparticle is internalized.

### 2.2.9 *From In Vitro to In Vivo: Serum Interactions and Targeting Challenges*

While non-viral gene delivery vectors formed with PEI have been found to be relatively effective for *in vitro* transfection under certain conditions, these vectors have much lower efficacy *in vivo*. Specific challenges include preventing serum protein interactions that inhibit transfection, minimizing activation of the complement system, minimizing toxicity, and insuring targeted delivery to only the tissues and cell-types of interest.[29, 64, 65] It is becoming apparent that optimization of a non-viral vector in serum-free *in vitro* conditions may be of limited use in designing a non-viral vector for *in vivo* application. This is due in part to the fact that many important vector properties such as size, zeta potential, particle stability, and polymer degradation are dependent on the local aqueous environment and complexes demonstrated to have certain biophysical characteristics in a buffer may not have the same characteristics in the presence of serum or *in vivo*. An *in vitro* study conducted in the presence of serum would alleviate many of these problems.

Another main problem is that positively charged complexes are known to have the highest transfection *in vitro*, but not *in vivo*. Having a high level of positive charge ensures that the polymer can adequately condense and protect the DNA. In many investigations, a positive charge of the complex is also required *in vitro* for cellular uptake and endocytosis.[30] Finally, having a high concentration of polymer in the particle is also necessary to ensure buffering of the endosome and endosomal escape as previously described. Unfortunately, complexes that have high positive charge also bind to blood constituents such as albumin, immunoglobulins, and fibrinogen, interact with macrophages and neutrophils, and non-specifically bind to many other untargeted tissues and cell types.[64-66] It is also known that these interactions increase clearance and lead to a shorter plasma half-life of the vectors.[66]

It has been shown that direct intratumoral delivery of PEI complexes has resulted in low gene expression.[67] To address the issue of high positive charge, covalent modification of PEI to include poly(ethylenegylcol) (PEG) and/or targeting ligands such as EGF[34], transferrin[68] and RGD[37, 69] peptide have been used to shield positive charge and to improve specific uptake. The results of these experiments have been promising but mixed, with some researchers demonstrating improved targeting and others showing no improvement over passive accumulation due to leaky vasculature.[25, 30, 36, 37, 68] Some of the most promising recent *in vivo* targeting results came from a system that uses blends of PEI, PEI-PEG, and PEI-PEG-ligand to complex DNA. This system showed 1 to 2 orders of magnitude higher gene expression at distant tumors as compared to other tissues following tail vein injection to tumor bearing mice.[36] However, in a related tumor model study, these nanoparticles caused a variable response and only rarely caused regression of tumors following tail vein injection to tumor bearing mice.[68]

One problem with covalent coupling of targeting ligands to a polymer is that it can change the biophysical properties of that polymer and of the corresponding polymer/DNA nanoparticle. For example, several researchers have found that as ligand substitution (either targeting or shielding) increases, overall gene delivery can decrease, presumably due to alteration of the original polymer's functionality for DNA condensation and endosomal buffering.[68, 69] Furthermore, gene delivery nanoparticles are generally positively charged, and it is known that these positively charged nanoparticles are taken up non-specifically.[25] Cell-specific nanoparticulate delivery requires both specific uptake by the target cell and inhibition of delivery to non-specific cell types. Coatings that reduce the positive charge of gene delivery nanoparticles could potentially reduce this non-specific uptake while still enabling receptor-mediated uptake. Gene delivery nanoparticles at overall neutral or negative charge may also be

desirable to prevent unwanted serum interactions.[64] An improved understanding of *in vivo* delivery, including cell targeting and blood serum interactions, and a rational design based on this understanding is required for successful targeted gene delivery.

## 2.3 NON-VIRAL GENE DELIVERY: DESIGNING SMART NANO-BIOMATERIALS

### *2.3.1 Overview*

The alternative approach to viral gene delivery is to develop a non-viral system and make use of physical methods and/or a synthetic chemical vector to deliver the gene of interest. Originally, non-viral gene delivery was simply delivery of naked plasmid DNA. To improve transfection, physical strategies such as hydrodynamic delivery, electroporation, a gene gun, ultrasound, jet injection, magnetofection, and photochemical internalization have been used.[65] Though these techniques can aid in delivery of nucleic acids, there are problems due to inefficient uptake and poor bio-stability.

To improve stability and uptake of DNA, numerous biomaterials have been used to create synthetic gene delivery vectors. The main biomaterials that have been studied include inorganic nanoparticles,[70, 71] cationic lipids,[72-75] polysaccharides,[76, 77] cationic polymers,[27, 38, 78] and dendrimers.[79, 80] These biomaterials either bind to, complex with, and/or encapsulate DNA to form safe, flexible systems that are comparatively easier to manufacture and scale-up than viral systems.[21, 66] These non-viral delivery systems also have large cargo capacities to shuttle DNA containing genes of interest of virtually any size. Research into non-viral gene delivery has been

ongoing since the 1970s, and as understanding of the mechanisms of gene delivery grew, the design of synthetic biomaterials has become more advanced.

### *2.3.2 Inorganic Materials*

Early chemical methods of increasing the efficacy of gene delivery focused on co-precipitation of the DNA. The first demonstration of using inorganic salts to precipitate DNA into nanoparticles was with Graham and van der Eb in 1973.[70] It was determined that calcium phosphate could be used to form gene delivery nanoparticles. First, DNA was mixed in a calcium ion containing solution to associate the anionic DNA with the cationic calcium ions. Then, this solution is added to a phosphate ion containing solution, causing calcium phosphate precipitation. This method and related techniques have since been used successfully over the years for gene delivery to different cell types.[71, 81] Although this approach has been popular for *in vitro* transfections as it is inexpensive and easy to use, the overall efficacy is rather poor compared to other biomaterials now commercially available.

Recently, inorganic materials have also been combined with polymers to form hybrid gene delivery nanoparticles. For example, organically modified silica nanoparticles have been shown to delivery genes *in vivo*.[82] Gold nanoparticles have also been combined with PEI for hybrid gene delivery systems. Electrostatically associated PEI/colloidal gold scaffolds were found to be useful in modulating biophysical properties including size and surface charge of the resulting gene delivery particles and also enabling facile ligand conjuation.[83] In an alternative approach, covalently conjugated gold-PEI nanoparticles were found to increase the efficacy of PEI by three-fold compared to 25 kDa PEI.[84] Combining these gold-PEI nanoparticles with an

N-dodecyl modified version of 2 kDa PEI, further doubled gene delivery efficacy to 6-fold over regular 25 kDa PEI, although this ternary combination also decreased cell viability to 67%.[84] While these hybrid systems are promising, it is important to note that their efficacy is still significantly below that of viruses.

### *2.3.3 Cationic Lipids*

Cationic lipids are the most widely used biomaterials for non-viral gene delivery. They were first used in 1987 by Felger et al. who showed that N-[1-(2,3-dioleyloxy)propyl]-N,N,N-trimethylammonium chloride (DOTMA) was able to form small lipid/DNA complexes that were 6-fold to 80-fold better at transfection than calcium phosphate across several different cell types.[72] DOTMA and other cationic (DMRIE, DODAB, DOTAP, DC-Chol) and neutral (DOPE, DOPC, Chol) lipid biomaterials can be seen in Figure 2.12.. As this figure demonstrates, the main components of a cationic lipid are: a positively charged head group, a linker group, and a hydrophobic group typically composed of either two long hydrocarbon tails or cholesterol. The positively charged head group is important for associating with DNA, the linker group is important for the stability and degradability of the lipid, and the hydrophobic group determines the flexibility of the lipid bilayer.[73]

Cationic lipids condense DNA into a lipid/DNA complex referred to as a lipoplex. Neutral lipids or lipid-like materials such as DOPE or cholesterol are also used in conjunction with cationic lipids to form enhanced gene delivery liposomes.[85] There are many important parameters when formulating liposomes including the structures of the lipids used, the ratio of the lipids to each other, the lipid to DNA ratio, the mixing conditions used (concentration,

temperature, buffer, etc.), and potential extrusion procedures utilized.[74, 85] The resulting biophysical properties of a lipoplex is dependent on its lipid components, the formation conditions used, and also the lipoplex structure, whether it is a micelle, large unilamellar cationic liposome (LUV), small unilamellar cationic liposome (SUV), multilamellar liposome (MLVs), or globular aggregate.[75]

There are many different liposomal formulations used for gene delivery in numerous *in vitro* and *in vivo* studies. These include a Phase II clinical study that showed that direct intratumoral gene delivery using a lipoplex composed of genes HLA-B7 and beta2-microglobulin complexed with a cationic lipid mixture of DMRIE and DOPE can regress melanoma lesions in 18% of the patients, including one complete response.[86] One of the most effective and widely used liposomal reagents is Invitrogen's Lipofectamine™ 2000 which has been shown to be superior to many other commercially available transfection agents for *in vitro* gene delivery.[87] Unfortunately even with the most advanced lipid materials, most lipoplexes are toxic, interact non-specifically with serum proteins and cells, aggregate quickly, activate the complement system, and have low *in vivo* efficacy.[73, 74] More recently PEG groups have been added to liposomes to potentially alleviate some of these problems by reduce binding to serum protein components. However, these modifications have also been shown to reduce transfection efficacy.[75]

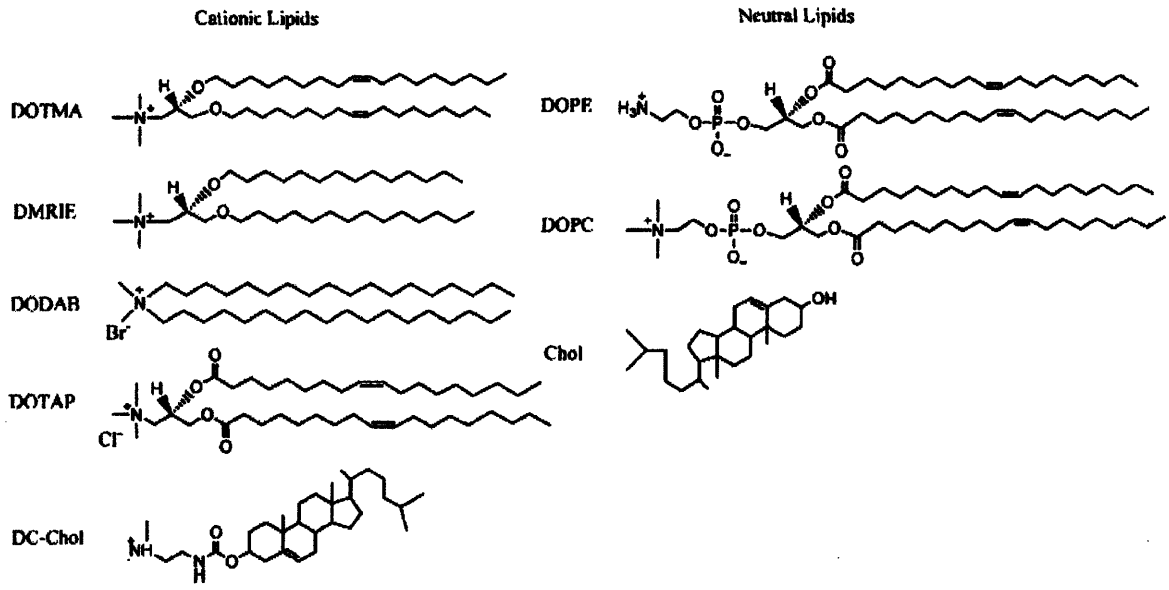


**Figure 2.8.** Structures of cationic and neutral lipids[73]

### *2.3.4 Polysaccharides*

The two main groups of polysaccharides used in non-viral gene delivery are chitosan and cyclodextrins, which are shown in Figure 2.12.. Chitosan is a linear cationic polysaccharide that is made from the deacetylation of chitin, which is a naturally occurring polymer and the major component of crustacean exoskeletons. Low molecular weight chitosan is highly soluble and generally non-toxic.[88] Chitosan can be used to condense DNA into 100-200 nm nanoparticles, although they can have variable stability in the presence of serum proteins.[77] Transfection using lactosylated chitosan was found to be comparable to PEI for *in vitro* delivery to HeLa cells and chitosan/DNA particles have also been shown to work *in vivo* for intratracheal delivery to epithelial cells in the central airways of mice.[77] One application where chitosans may be

particularly useful is for DNA vaccines as immunological protection following vaccination *in vivo* has been demonstrated.[89, 90]

Cyclodextrins (CDs) are cyclic oligomers of glucose that form a hydrophilic cup. They are particularly useful as they can form water soluble inclusion complexes to carry various cargos including nucleic acids and other drugs and are biocompatible with low toxicities.[76] They are named according to their number of glucose units: α-CD (hexamer), β-CD (heptamer), or γ-CD (octamer). For use in gene delivery, CDs are copolymerized with cationic monomers to form positively charged cyclodextrin-based polymers. Several properties can be tuned to change gene delivery efficacy and toxicity including carbohydrate size, distance from charge center, and type of charge center.[91, 92] β-CD-bPEI copolymers have both lower cytotoxicity and lower efficacy than its parent 25 kDa branched PEI polymer (bPEI), but β-CD-lPEI copolymers have comparable efficacy and reduced cytotoxicity compared to its parent linear PEI polymer (lPEI).[93] CD-based polymer/DNA particles are very interesting in that adamantane conjugates containing PEG and/or ligands can easily be added to form inclusion complexes with cyclodextrins on the surface of the particles to modify surface properties including size and stability.[94] CD-based polymers can be modified with adamantane-PEG-galactose conjugates for *in vitro* targeting of HepG2 hepatocytes or modified with adamantane-PEG-transferrin conjugates for tumor targeting *in vivo*.[93]

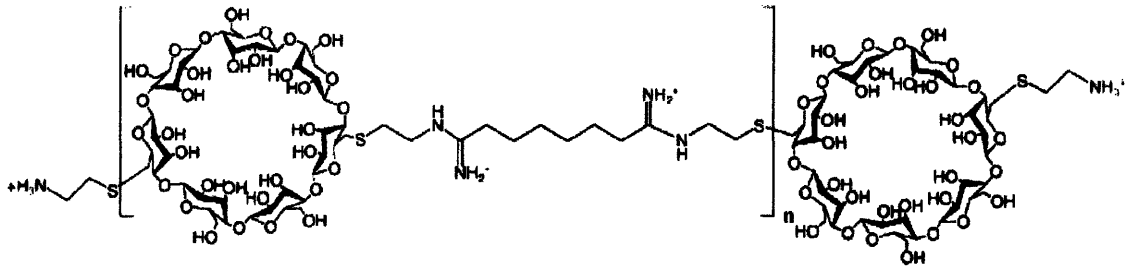

**6D-di(2-aminoethanethio) β-cyclodextrin**

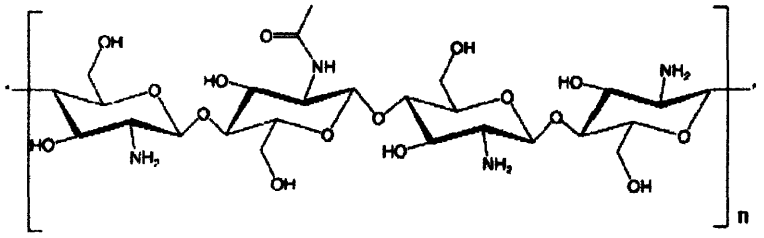

**Chitosan**

**Figure 2.9.** Sugar-based gene delivery biomaterials[88]

### *2.3.5 Polymers*

Commonly used "off-the-shelf" cationic polymers for gene delivery include poly(L-lysine) (PLL) and polyethylenimine (PEI) and are shown in Figure 2.12..[78] These materials electrostatically bind and condense plasmid DNA into nanometer sized complexes. In addition to "off-the-shelf" polymers, numerous research groups world-wide have also created new synthetic polymers, designed especially for gene delivery. While polymeric gene delivery is promising due its large design flexibility, overall efficacy is still significantly lower than that of viral gene delivery.

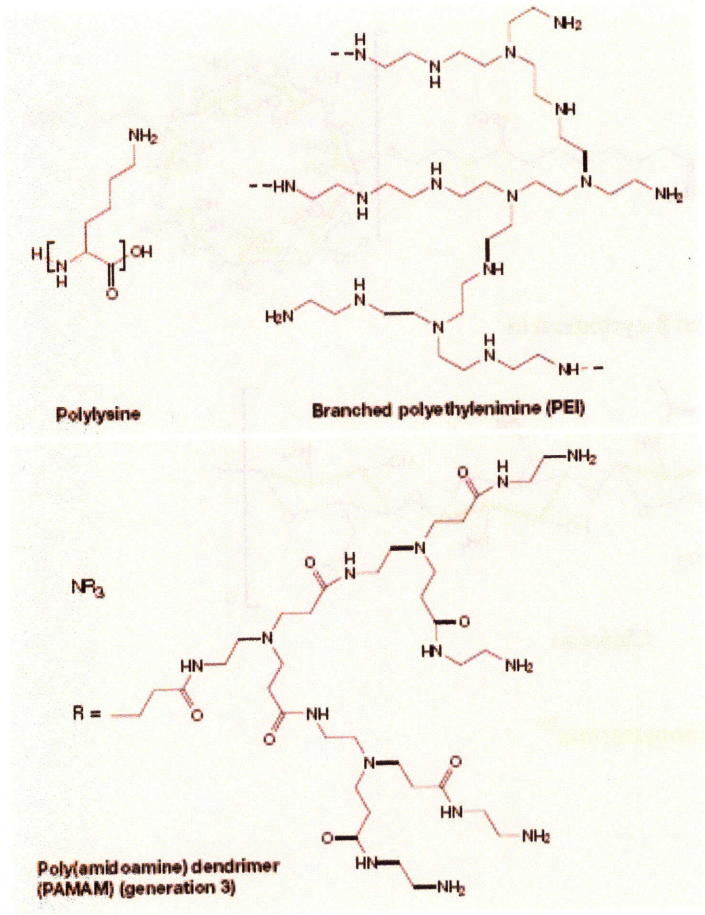


Structures of commonly used gene delivery polymers[78]

### 2.3.5.1 Poly-L-lysine (PLL)

One of the first gene delivery polymers was simply a chain of naturally occurring amino acids, polylysine. It has been demonstrated since the early 1970s that PLL could condense DNA into small doughnut-like structures.[95, 96] Polylysine is also useful as a gene delivery polymer since, as a natural peptide, it is biodegradable. Depending on the mixing conditions and procedure used, PLL and DNA can complex to form particles sized 15-30 nm, 50-150 nm, or even large aggregates.[97] However even though PLL can be used to form small gene delivery

particles, PLL has not been shown to be an effective polymeric vector by itself as it does not have an efficient mechanism for endosomal escape (Step 4 of Figure 2.7.). Consequently, in order to have DNA released to the cytoplasm when using PLL, an additional endosomolytic agent is also required (usually chloroquine). To increase the efficacy of polylysine, PLL has also been conjugated to various targeting ligands including transferrin, sugar, folate, RGD peptide, and antibodies.[78, 97] Although polylysine has been widely studied for gene delivery and improvements to PLL-based systems have been made, overall efficacy still remains low. New synthetic polymers that do not require the addition of endosomolytic agents, such as PEI, have now largely replaced the use of PLL for gene delivery.

#### 2.3.5.2 PEI

A major advance to the field of non-viral gene delivery was the discovery by Boussif et al. of polyethylenimine (PEI) as a gene delivery polymer with successful transfection ability *in vitro* and in *vivo*.[38] PEI was chosen as a vector since it has the highest cationic-charge-density potential of any organic macromolecule. As with polylysine, a high density of positively charged groups on the polymer is important to bind and condense DNA into a small particle. In addition, PEI is more effective than PLL due to a high density of near neutral $pK_a$ groups on the polymer that are important to buffer the acidic environment of the endosome through the "proton sponge" mechanism.[40, 98] Through this mechanism, PEI/DNA particles avoid the lysosomal pathway by osmotic rupture of the endosome and escape to the cytoplasm.

PEI also allows for incorporation of specific targeting ligands such as transferring,[32, 99] epidermal growth factor,[100, 101] and RGD peptides,[37, 69] which have been shown to improve

uptake and transfection efficiency *in vitro* and *in vivo*. Though first shown to be effective for gene delivery in 1995, PEI remains in many ways the "gold standard" for transfection efficacy a decade later. PEI is not ideal however, as its efficacy is still considerably lower than that of a virus, it is not biodegradable, and it causes considerable cytotoxicity via necrosis and apoptosis.[61]

One promising approach to overcome some of these concerns is chemically modifying the PEI polymer. Thomas and Klibanov recently found that N-acylation of branched 25 kDa PEI can double its gene delivery efficacy while reducing its cytotoxicity and dodecylation of 2 kDa PEI can create a non-toxic polymer 5-fold better than branched 25 kDa PEI.[102] Subsequent work showed linear PEIs could be synthesized by the acid-catalyzed hydrolysis of poly(2-ethyl-2-oxazoline) to form PEI87 and PEI217, polymers that are two orders of magnitude more effective than "off-the-shelf" linear PEI (PEI25), although these polymers still show cytotoxicity.[103] PEI87 also delivered DNA *in vivo* as efficiently as deacylated PEI25, which was 10,000-fold higher than "off-the-shelf" linear PEI25, and with 200-fold specificity to the lungs. These are very promising results for gene delivery to the lungs and demonstrate how polymer structure is important to gene delivery function. Although PEI's structure is clearly more effective than other polymers such as polylysine, there are still many unexplored possible gene delivery polymer structures, including biodegradable structures, with the potential to be even more efficacious and simultaneously less toxic.

### 2.3.5.3 Dendrimers

Dendrimers are repeatedly branched cascade polymers that are synthesized from a central core and branch outward like a bush or tree. With each increasing synthesis generation, dendrimers become more branched, larger in size, and have a multiplicative increase in the number of end groups. Dendrimer structure as a function of generation can be seen in Figure 2.10.. Like PEI, several dendrimers including poly(amidoamine) (PAMAM), make effective gene delivery polymers due to their large number of secondary and tertiary amines that can buffer the endosome. Particular advantages of dendrimers are: they are much closer to being monodisperse than other polymers which are typically polydisperse; dendrimer generation number can be tuned for desired application (and thereby tune dendrimer size, number of functional groups, etc.); and dendrimers also have a much higher ligand density than linear polymers which allows higher avidity for multivalent interactions.[79] A disadvantage of dendrimers is that they require a multi-step synthesis that can be more expensive and time-consuming than the synthesis of linear polymers.

Dendrimers do not need to be in their perfect spherical shape to function. In fact, efficacy can be improved by effectively pruning the branches of the dendrimer or by using the branches themselves. Partially degraded or "fractured" PAMAM dendrimers have been shown to have dramatic >50-fold enhancement for gene delivery as compared to complete PAMAM.[104] Alternatively, the core of the dendrimer can be removed, leaving identical branch fragments known as dendrons. An interesting recent approach to build on dendrimer technology is the development of hybrid linear dendrons for targeted gene delivery. Block co-polymers composed of linear poly(amidoamine) (PAMAM) dendrons and functionalized poly(ethylene glycol) (PEG)

self-assemble with DNA to form targeted delivery nanoparticles composed of disparate "shells."[80] In this rationally designed system, the terminal ends of dendrons contain a high density of primary amines to bind DNA, the interior of the dendrons contain secondary and tertiary amines for endosomal buffering, the PEG reduces serum interactions, and the end of the PEG can be functionalized with a ligand specific to the cell type of interest. *In vitro*, these polymers show efficacy 4-8 fold better than PEI in serum conditions while having reduced cytotoxicity.

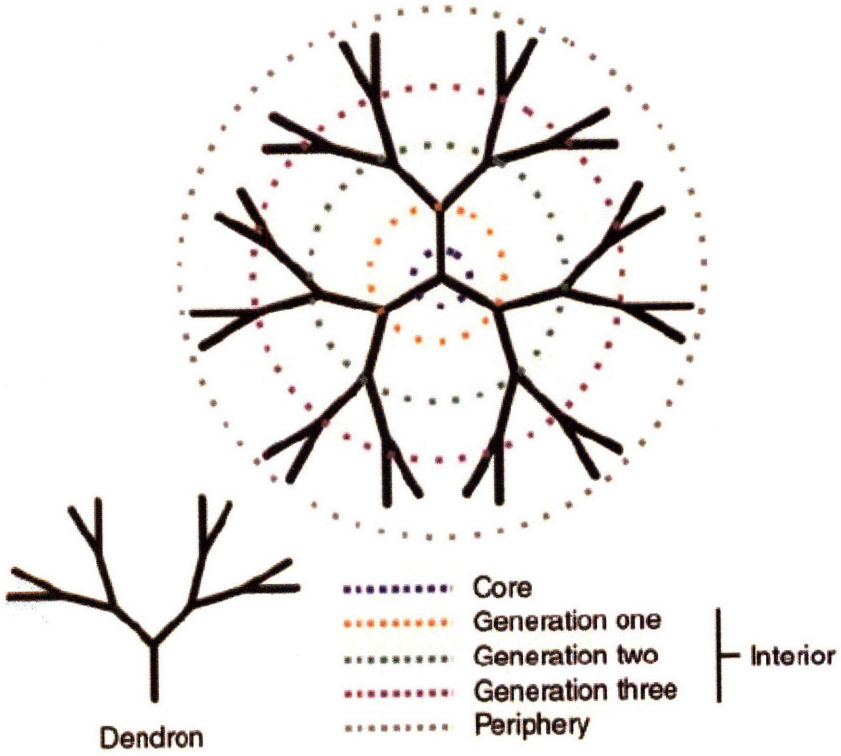


**Figure 2.10.** Dendrimer structure.[79]

### 2.3.5.4 Poly(β-amino) esters

One particularly interesting class of polymers for gene delivery are poly(β-amino esters) which were first developed by Lynn et al. in 2000.[27] Poly(β-amino esters) (PBAEs) are promising as compared to PEI due to their biodegradability via hydrolytically degradable ester groups, their reduced cytotoxicity, their ability for triggered DNA release within the cell, and their potential for structural diversity.[27, 105] They are easily synthesized by the conjugate addition of amine monomers to diacrylates, a one step reaction without the production of any byproducts (Figure 2.12.). These starting materials are also inexpensive and commercially available.

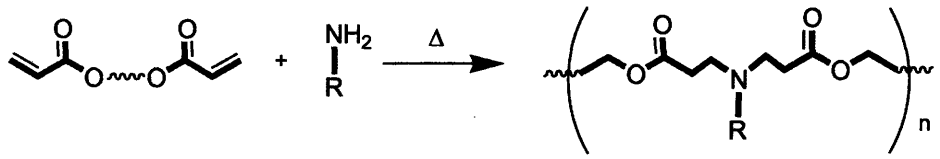


**Figure 2.11 Synthesis of PBAEs by conjugate addition**

Initial studies of this polymer class showed that the polymer molecular weight can be varied from 2,000 to 50,000 Da.[105] In physiological conditions, these polymers have a degradation half-life on the order of hours, but this is slowed considerably at a pH of 5 and/or when the polymers electrostatically condense DNA and form nanoparticles.[27] Importantly, it was demonstrated that a wide range of poly(β-amino esters) were able to self-assemble with DNA to form cationic nanoparticles.[27, 106] Investigative studies on the proton sponge mechanism

and endosomal release also revealed that PBAEs can successfully buffer the endosomal compartment, similarly to PEI.[39, 106] A library of 140 poly(β-amino esters) composed of 7 diacrylate monomers and 20 amine monomers was synthesized in parallel and screened for gene delivery efficacy.[105, 106] In general, the best performing complexes were found to have effective diameters smaller than 250 nm and positive zeta potentials in 10 mM HEPES buffer. While it was determined that the majority of PBAE/DNA particles tested were limited by poor cell uptake, two of the polymers had high uptake and mediated gene delivery 4-8 fold higher than PEI, comparable to the efficacy of Lipofectamine 2000. These two lead poly(β-amino esters) were also able to successfully buffer the endosomal compartment and escape from the lysosomal pathway.[106] However, the cytotoxicity profiles of these two poly(β-amino esters) were quite different, with one being highly cytotoxic and the other being generally non-toxic. These studies demonstrated the utility of using parallel synthesis and screening of a polymer library to identify novel gene delivery polymers with efficacy greater than PEI.

Two poly(β-amino esters) were also further optimized by varying polymer molecular weight, polymer end group, and polymer to DNA weight ratio.[107] Interestingly, it was discovered that polymers terminated with diacrylate monomers were unable to deliver DNA to cells, unlike the near identical polymers that were terminated with amino alcohol monomers instead. Higher molecular weight (~13 kDa), amine-terminated poly(β-amino esters) were found to transfect best for both types of polymers, although the optimal polymer to DNA weight ratio for these two polymers varied considerably between 30 w/w and 150 w/w.[107] Optimal PBAE/DNA nanoparticles had gene delivery efficacy comparable to PEI and Lipofectamine 2000.

In 2003, Daniel Anderson et al. created a large library of 2350 structurally unique poly(β-amino esters) using automation and high-throughput combinatorial chemistry.[63] The diacrylate monomers used are shown in Figure 2.12. and the amine monomers used are shown in Figure 2.13.

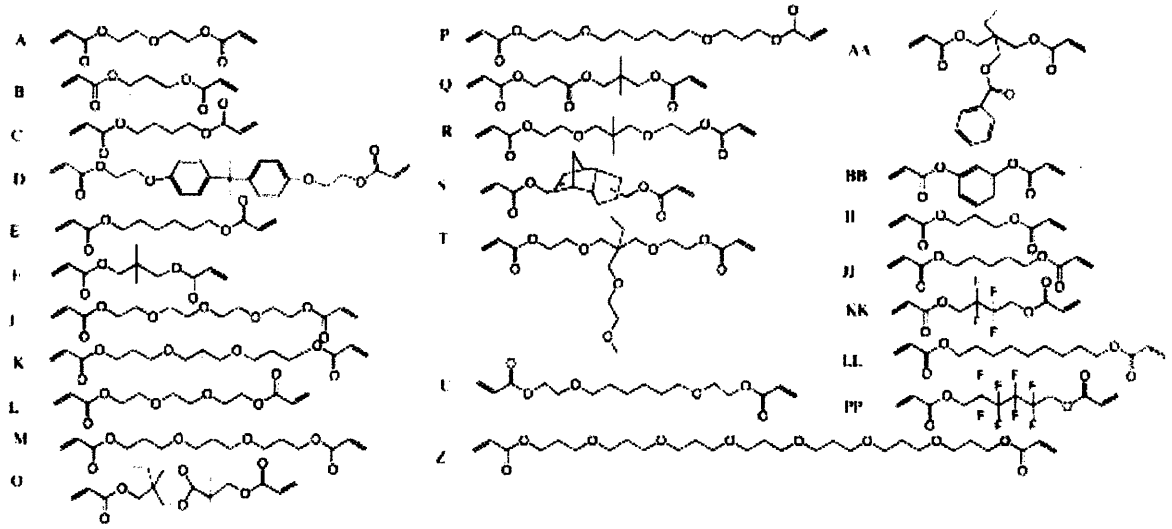

**Figure 2.12.** Diacrylate monomers used to synthesize PBAEs.[63]

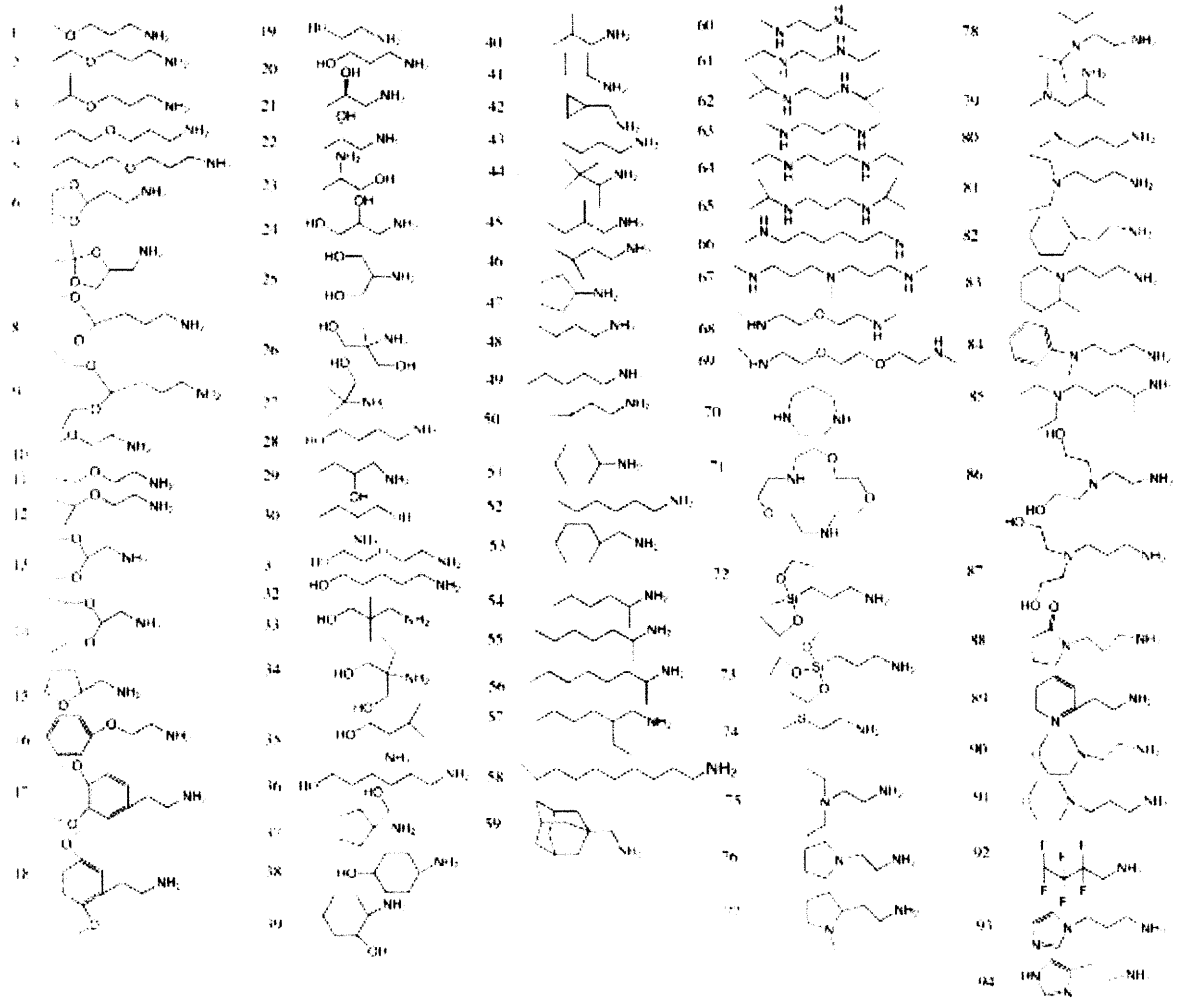

**Figure 2.13.** Amine monomers used to synthesize PBAEs.[63]

This large library of polymers was screened to determine which polymers could efficiently bind DNA and transfect COS-7 cells in serum-free conditions, an easy-to-transfect cell system useful for high-throughput biological assays. From this study, forty-six poly(β-amino esters) were found to transfect as well or better than PEI.[63] The best-performing polymers were next analyzed and refined to a library of 486 second-generation polymers.[50] Analysis of these poly(β-amino esters) revealed that the top performing polymer complexes had sizes smaller than 150 nm,

positive zeta potentials, polymer weight to DNA weight ratios greater than or equal to 40, molecular weights above 10,000, and structural similarities. The top nine polymers were all formed from amino alcohols and hydrophobic diacrylate monomers and the three best performing polymers converged in structure. A subset of diacrylate and amine alcohol monomers from the PBAE library containing the top structures that are especially promising for gene delivery are shown in Figure 2.14.

Though these studies paint a clearer picture of what characteristics an optimal vector should have, many of the properties that were found with the best performing polymers were also found in polymers that had relatively poorer transfection efficacy.[50] In order to better understand what properties an optimal vector should possess, other parameters to potentially consider are polymer/DNA binding[49], nitrogen/phosphate charge ratio (N/P)[83], DNA loading, and particle morphology. As many of these biophysical properties are coupled, a method of uncoupling some of these parameters would also be advantageous. Finally, many important vector properties such as size, zeta potential, particle stability, and polymer degradation are dependent on the local aqueous environment and complexes demonstrated to have particular biophysical characteristics in a buffer may not have the same characteristics in the presence of serum or *in vivo*. Through modification of polymer structure, formulation conditions, surface charge, and targeting ligands, and also through improved understanding of polymeric nanoparticle structure/function relationships, it is believed that poly(β-amino ester) vectors can be improved for efficacious gene delivery to difficult-to-transfect human primary cells and for *in vivo* administration.

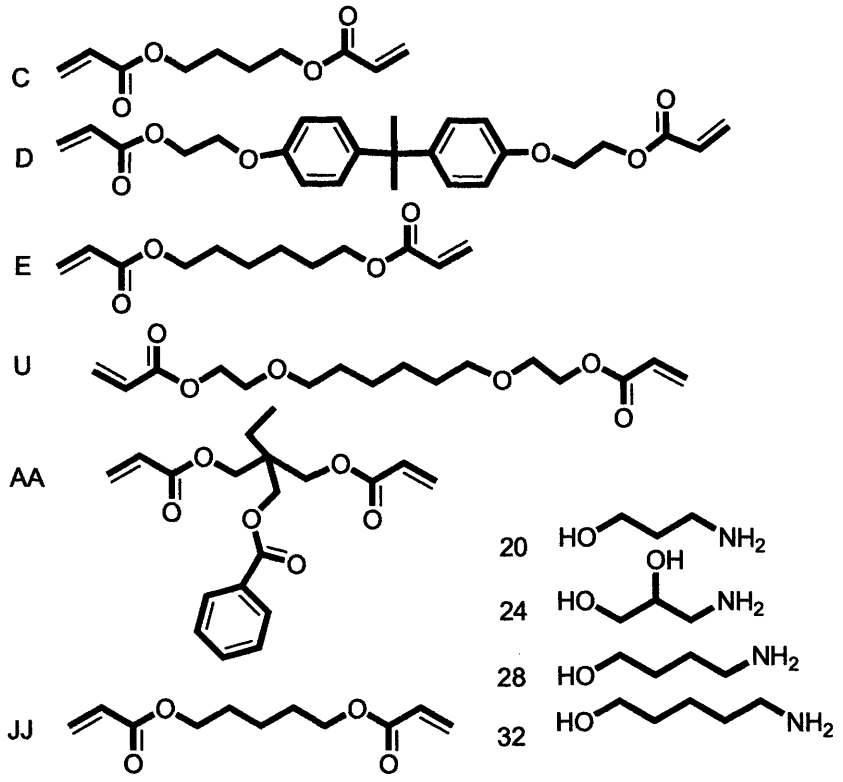


**Figure 2.14.** Subset of diacrylate and amine alcohol monomers especially promising for gene delivery.

## References

1. Avery, O., MacLeod, C. & McCarty, M. Studies on the Chemical Nature of the Substance Inducing Transformation of the Pneumococcal Types. *J Exp Med* **79**, 137-158 (1944).

2. Watson, J.D. & Crick, F.H. Molecular structure of nucleic acids; a structure for deoxyribose nucleic acid. *Nature* **171**, 737-738 (1953).

3. Demain, A.L. Molecular genetics and industrial microbiology--30 years of marriage. *J Ind Microbiol Biotechnol* **27**, 352-356 (2001).

4. www.cancer.org. Estimated new cancer cases and deaths by sex for all sites, US, 2007. (American Cancer Society, 2007).

5. Anderson, D.G. et al. A polymer library approach to suicide gene therapy for cancer. *Proc. Natl. Acad. Sci. U.S.A.* **101**, 16028-16033 (2004).

6. Ndoye, A. et al. Eradication of p53-mutated head and neck squamous cell carcinoma xenografts using nonviral p53 gene therapy and photochemical internalization. *Mol Ther* **13**, 1156-1162 (2006).

7. Segura, I. et al. Inhibition of programmed cell death impairs in vitro vascular-like structure formation and reduces in vivo angiogenesis. *FASEB J* **16**, 833-841 (2002).

8. Muller, K., Nahde, T., Fahr, A., Muller, R. & Brusselbach, S. Highly efficient transduction of endothelial cells by targeted artificial virus-like particles. *Cancer Gene Ther* **8**, 107-117 (2001).

9. www.americanheart.org Cardiovascular Disease Statistics. (American Heart Association, 2007).

10. Nabel, E.G. Gene therapy for cardiovascular diseases. *Journal of Nuclear Cardiology* **6**, 69-75 (1999).

11. Shah, P.B. & Losordo, D.W. Non-viral vectors for gene therapy: clinical trials in cardiovascular disease. *Adv Genet* **54**, 339-361 (2005).

12. Jones, J.M. & Koch, W.J. Gene therapy approaches to cardiovascular disease. *Methods Mol Med* **112**, 15-35 (2005).

13. Bivas-Benita, M., Ottenhoff, T.H., Junginger, H.E. & Borchard, G. Pulmonary DNA vaccination: concepts, possibilities and perspectives. *J Control Release* **107**, 1-29 (2005).

14. www.wiley.co.uk/genetherapy/clinical/ Gene therapy clinical trials worldwide. (J Gene Medicine, 2007).

15. Verma, I.M. & Somia, N. Gene therapy -- promises, problems and prospects. *Nature* **389**, 239-242 (1997).

16. Zhang, X. & Godbey, W.T. Viral vectors for gene delivery in tissue engineering. *Adv Drug Deliv Rev* **58**, 515-534 (2006).

17. Hollon, T. Researchers and regulators reflect on first gene therapy death. *Nature Medicine* **6**, 6-6 (2000).

18. Check, E. Cancer fears cast doubts on future of gene therapy. *Nature* **421**, 678 (2003).

19. Thomas, C.E., Ehrhardt, A. & Kay, M.A. Progress and problems with the use of viral vectors for gene therapy. *Nat Rev Genet* **4**, 346-358 (2003).

20. Kay, M.A., Glorioso, J.C. & Naldini, L. Viral vectors for gene therapy: the art of turning infectious agents into vehicles of therapeutics. *Nature Medicine* **7**, 33-40 (2001).

21. Partridge, K.A. & Oreffo, R.O.C. Gene delivery in bone tissue engineering: Progress and prospects using viral and nonviral strategies. *Tissue Eng* **10**, 295-307 (2004).

22. Check, E. Second cancer case halts gene-therapy trials. *Nature* **421**, 305-305 (2003).

23. Check, E. Gene therapy put on hold as third child develops cancer. *Nature* **433**, 561-561 (2005).

24. Boyce, N. Trial halted after gene shows up in semen. *Nature* **414**, 677-677 (2001).

25. Thomas, M. & Klibanov, A.M. Non-viral gene therapy: polycation-mediated DNA delivery. *Appl Microbiol Biotechnol* **62**, 27-34 (2003).

26. Ogris, M., Steinlein, P., Carotta, S., Brunner, S. & Wagner, E. DNA/polyethylenimine transfection particles: Influence of ligands, polymer size, and PEGylation on internalization and gene expression. *Aaps Pharmsci* **3**, art. no. 21 (2001).

27. Lynn, D.M. & Langer, R. Degradable poly(beta-amino esters): Synthesis, characterization, and self-assembly with plasmid DNA. *J Am Chem Soc* **122**, 10761-10768 (2000).

28. Zelikin, A.N., Trukhanova, E.S., Putnam, D., Izumrudov, V.A. & Litmanovich, A.A. Competitive reactions in solutions of poly-L-histidine, calf thymus DNA, and synthetic polyanions: Determining the binding constants of polyelectrolytes. *J Am Chem Soc* **125**, 13693-13699 (2003).

29. Plank, C., Tang, M.X., Wolfe, A.R. & Szoka, F.C. Branched cationic peptides for gene delivery: Role of type and number of cationic residues in formation and in vitro activity of DNA polyplexes. *Hum Gene Ther* **10**, 319-332 (1999).

30. Zuber, G., Dauty, E., Nothisen, M., Belguise, P. & Behr, J.P. Towards synthetic viruses. *Adv Drug Delivery Rev* **52**, 245-253 (2001).

31. Ogris, M. et al. The size of DNA/transferrin-PEI complexes is an important factor for gene expression in cultured cells. *Gene Ther* **5**, 1425-1433 (1998).

32. Kircheis, R. et al. Polyethylenimine/DNA complexes shielded by transferrin target gene expression to tumors after systemic application. *Gene Ther* **8**, 28-40 (2001).

33. Wightman, L. et al. Different behavior of branched and linear polyethylenimine for gene delivery in vitro and in vivo. *J Gene Med* **3**, 362-372 (2001).

34. Schaffer, D.V. & Lauffenburger, D.A. Optimization of cell surface binding enhances efficiency and specificity of molecular conjugate gene delivery. *J Biol Chem* **273**, 28004-28009 (1998).

35. Zuber, G., Zammut-Italiano, L., Dauty, E. & Behr, J.P. Targeted gene delivery to cancer cells: Directed assembly of nanometric DNA particles coated with folic acid. *Ang. Chem. Int. Edn* **42**, 2666-2669 (2003).

36. Ogris, M. et al. Tumor-targeted gene therapy: strategies for the preparation of ligand-polyethylene glycol-polyethylenimine/DNA complexes. *J. Controlled Release* **91**, 173-181 (2003).

37. Kunath, K., Merdan, T., Hegener, O., Haberlein, H. & Kissel, T. Integrin targeting using RGD-PEI conjugates for in vitro gene transfer. *J Gene Med* **5**, 588-599 (2003).

38. Boussif, O. et al. A versatile vector for gene and oligonucleotide transfer into cells in culture and in vivo: polyethylenimine. *Proc Natl Acad Sci U S A* **92**, 7297-7301 (1995).

39. Akinc, A. & Langer, R. Measuring the pH environment of DNA delivered using nonviral vectors: Implications for lysosomal trafficking. *Biotechnol Bioeng* **78**, 503-508 (2002).

40. Sonawane, N.D., Szoka, F.C. & Verkman, A.S. Chloride accumulation and swelling in endosomes enhances DNA transfer by polyamine-DNA polyplexes. *J Biol Chem* **278**, 44826-44831 (2003).

41. Martin, M.E. & Rice, K.G. Peptide-guided gene delivery. *Aaps J* **9**, E18-29 (2007).

42. Lukacs, G.L. et al. Size-dependent DNA mobility in cytoplasm and nucleus. *J Biol Chem* **275**, 1625-1629 (2000).

43. Godbey, W.T., Wu, K.K. & Mikos, A.G. Tracking the intracellular path of poly(ethylenimine)/DNA complexes for gene delivery. *Proc Natl Acad Sci U S A* **96**, 5177-5181 (1999).

44. Goulian, M. & Simon, S.M. Tracking single proteins within cells. *Biophys J* **79**, 2188-2198 (2000).

45. Suh, J., Wirtz, D. & Hanes, J. Efficient active transport of gene nanocarriers to the cell nucleus. *Proc Natl Acad Sci U S A* **100**, 3878-3882 (2003).

46. Seisenberger, G. et al. Real-time single-molecule imaging of the infection pathway of an adeno-associated virus. *Science* **294**, 1929-1932 (2001).

47. Suh, J., Dawson, M. & Hanes, J. Real-time multiple-particle tracking: applications to drug and gene delivery. *Adv Drug Delivery Rev* **57**, 63-78 (2005).

48. Ohno, M., Fornerod, M. & Mattaj, I.W. Nucleocytoplasmic transport: the last 200 nanometers. *Cell* **92**, 327-336 (1998).

49. Schaffer, D.V., Fidelman, N.A., Dan, N. & Lauffenburger, D.A. Vector unpacking as a potential barrier for receptor-mediated polyplex gene delivery. *Biotechnol Bioeng* **67**, 598-606 (2000).

50. Anderson, D.G., Akinc, A., Hossain, N. & Langer, R. Structure/property studies of polymeric gene delivery using a library of poly(beta-amino esters). *Mol Ther* **11**, 426-434 (2005).

51. Zanta, M.A., Belguise-Valladier, P. & Behr, J.P. Gene delivery: A single nuclear localization signal peptide is sufficient to carry DNA to the cell nucleus. *Proc Natl Acad Sci U S A* **96**, 91-96 (1999).

52. Branden, L.J., Mohamed, A.J. & Smith, C.I.E. A peptide nucleic acid-nuclear localization signal fusion that mediates nuclear transport of DNA. *Nat Biotechnol* **17**, 784-787 (1999).

53. Dean, D.A., Dean, B.S., Muller, S. & Smith, L.C. Sequence requirements for plasmid nuclear import. *Exp Cell Res* **253**, 713-722 (1999).

54. van der Aa, M.A.E.A. et al. An NLS peptide covalently linked to linear DNA does not enhance transfection efficiency of cationic polymer based gene delivery systems. *J Gene Med* **7**, 208-217 (2005).

55. Escriou, V., Carriere, M., Scherman, D. & Wils, P. NLS bioconjugates for targeting therapeutic genes to the nucleus. *Adv Drug Deliv Rev* **55**, 295-306 (2003).

56. Dean, D.A., Strong, D.D. & Zimmer, W.E. Nuclear entry of nonviral vectors. *Gene Ther* **12**, 881-890 (2005).

57. Abdelhady, H.G. et al. Direct real-time molecular scale visualisation of the degradation of condensed DNA complexes exposed to DNase I. *Nucleic Acids Res* **31**, 4001-4005 (2003).

58. Biamonti, G. et al. Fate of exogenous recombinant plasmids introduced into mouse and human cells. *Nucleic Acids Res* **13**, 5545-5561 (1985).

59. Hodges, B.L., Taylor, K.M., Joseph, M.F., Bourgeois, S.A. & Scheule, R.K. Long-term transgene expression from plasmid DNA gene therapy vectors is negatively affected by CpG dinucleotides. *Mol Ther* **10**, 269-278 (2004).

60. Kircheis, R. et al. Polycation-based DNA complexes for tumor-targeted gene delivery in vivo. *J Gene Med* **1**, 111-120 (1999).

61. Moghimi, S.M. et al. A two-stage poly(ethylenimine)-mediated cytotoxicity: implications for gene transfer/therapy. *Mol Ther* **11**, 990-995 (2005).

62. Langer, R. & Peppas, N. Advances in Biomaterials, Drug Delivery, and Bionanotechnology. *AIChE Journal* **49**, 2990-3006 (2003).

63. Anderson, D.G., Lynn, D.M. & Langer, R. Semi-automated synthesis and screening of a large library of degradable cationic polymers for gene delivery. *Ang. Chem. Int. Edn* **42**, 3153-3158 (2003).

64. Trubetskoy, V.S. et al. Recharging cationic DNA complexes with highly charged polyanions for in vitro and in vivo gene delivery. *Gene Ther* **10**, 261-271 (2003).

65. Wagner, E., Kircheis, R. & Walker, G.F. Targeted nucleic acid delivery into tumors: new avenues for cancer therapy. *Biomed Pharmacother* **58**, 152-161 (2004).

66. Merdan, T., Kopecek, J. & Kissel, T. Prospects for cationic polymers in gene and oligonucleotide therapy against cancer. *Adv Drug Delivery Rev* **54**, 715-758 (2002).

67. Wagner, E., Kircheis, R. & Walker, G.F. Targeted nucleic acid deliver into tumors: new avenues for cancer therapy. *Biomedicine & Pharmacotherapy* **58**, 152-161 (2004).

68. Kursa, M. et al. Novel shielded transferrin-polyethylene glycol-polyethylenimine/DNA complexes for systemic tumor-targeted gene transfer. *Bioconjug Chem* **14**, 222-231 (2003).

69. Suh, W., Han, S.O., Yu, L. & Kim, S.W. An angiogenic, endothelial-cell-targeted polymeric gene carrier. *Mol Ther* **6**, 664-672 (2002).

70. Graham, F.L. & van der Eb, A.J. Transformation of rat cells by DNA of human adenovirus 5. *Virology* **54**, 536-539 (1973).

71. Welzel, T., Meyer-Zaika, W. & Epple, M. Continuous preparation of functionalised calcium phosphate nanoparticles with adjustable crystallinity. *Chem Commun (Camb)*, 1204-1205 (2004).

72. Felgner, P.L. et al. Lipofection: a highly efficient, lipid-mediated DNA-transfection procedure. *Proc Natl Acad Sci U S A* **84**, 7413-7417 (1987).

73. Segura, T. & Shea, L.D. Materials for non-viral gene delivery. *Ann Rev Mater Res* **31**, 25-46 (2001).

74. Mahato, R.I. Water insoluble and soluble lipids for gene delivery. *Adv Drug Deliv Rev* **57**, 699-712 (2005).

75. Pedroso de Lima, M.C., Simoes, S., Pires, P., Faneca, H. & Duzgunes, N. Cationic lipid-DNA complexes in gene delivery: from biophysics to biological applications. *Adv Drug Deliv Rev* **47**, 277-294 (2001).

76. Davis, M.E. & Brewster, M.E. Cyclodextrin-based pharmaceutics: past, present and future. *Nat Rev Drug Discov* **3**, 1023-1035 (2004).

77. Borchard, G. & Bivas-Benita, M. in. *Polymeric Gene Delivery* (ed. M.M. Amiji) 301-310 (CRC Press, New York; 2005).

78. Pack, D.W., Hoffman, A.S., Pun, S. & Stayton, P.S. Design and development of polymers for gene delivery. *Nature Reviews Drug Discovery* **4**, 581-593 (2005).

79. Lee, C.C., MacKay, J.A., Frechet, J.M. & Szoka, F.C. Designing dendrimers for biological applications. *Nat Biotechnol* **23**, 1517-1526 (2005).

80. Wood, K.C., Little, S.R., Langer, R. & Hammond, P.T. A family of hierarchically self-assembling linear-dendritic hybrid polymers for highly efficient targeted gene delivery. *Ang. Chem. Int. Edn* **44**, 6704-6708 (2005).

81. Shih, C., Shilo, B.Z., Goldfarb, M.P., Dannenberg, A. & Weinberg, R.A. Passage of phenotypes of chemically transformed cells via transfection of DNA and chromatin. *Proc Natl Acad Sci U S A* **76**, 5714-5718 (1979).

82. Bharali, D.J. et al. Organically modified silica nanoparticles: a nonviral vector for in vivo gene delivery and expression in the brain. *Proc Natl Acad Sci U S A* **102**, 11539-11544 (2005).

83. Sullivan, M.M.O., Green, J.J. & Przybycien, T.M. Development of a novel gene delivery scaffold utilizing colloidal gold-polyethylenimine conjugates for DNA condensation. *Gene Ther* **10**, 1882-1890 (2003).

84. Thomas, M. & Klibanov, A.M. Conjugation to gold nanoparticles enhances polyethylenimine's transfer of plasmid DNA into mammalian cells. *Proc Natl Acad Sci U S A* **100**, 9138-9143 (2003).

85. Smith, J., Niven, R. & Zhang, Y. Toward development of a non-viral gene therapeutic. *Adv Drug Deliv Rev* **26**, 135-150 (1997).

86. Stopeck, A.T. et al. Phase II study of direct intralesional gene transfer of allovectin-7, an HLA-B7/beta2-microglobulin DNA-liposome complex, in patients with metastatic melanoma. *Clin Cancer Res* **7**, 2285-2291 (2001).

87. Dalby, B. et al. Advanced transfection with Lipofectamine 2000 reagent: primary neurons, siRNA, and high-throughput applications. *Methods* **33**, 95-103 (2004).

88. Park, T.G., Jeong, J.H. & Kim, S.W. Current status of polymeric gene delivery systems. *Adv Drug Delivery Rev* **58**, 467-486 (2006).

89. Roy, K., Mao, H.Q., Huang, S.K. & Leong, K.W. Oral gene delivery with chitosan--DNA nanoparticles generates immunologic protection in a murine model of peanut allergy. *Nat Med* **5**, 387-391 (1999).

90. van der Lubben, I.M., Verhoef, J.C., Borchard, G. & Junginger, H.E. Chitosan for mucosal vaccination. *Adv Drug Deliv Rev* **52**, 139-144 (2001).

91. Reineke, T.M. & Davis, M.E. Structural effects of carbohydrate-containing polycations on gene delivery. 1. Carbohydrate size and its distance from charge centers. *Bioconjug Chem* **14**, 247-254 (2003).

92. Reineke, T.M. & Davis, M.E. Structural effects of carbohydrate-containing polycations on gene delivery. 2. Charge center type. *Bioconjug Chem* **14**, 255-261 (2003).

93. Pun, S.H. & Davis, M.E. in. *Polymeric Gene Delivery* (ed. M.M. Amiji) 187-210 (CRC Press, New York; 2005).

94. Pun, S.H. et al. Cyclodextrin-modified polyethylenimine polymers for gene delivery. *Bioconjug Chem* **15**, 831-840 (2004).

95. Olins, D.E. & Olins, A.L. Model nucleohistones: the interaction of F1 and F2al histones with native T7 DNA. *J Mol Biol* **57**, 437-455 (1971).

96. Laemmli, U.K. Characterization of DNA condensates induced by poly(ethylene oxide) and polylysine. *Proc Natl Acad Sci U S A* **72**, 4288-4292 (1975).

97. Zauner, W., Ogris, M. & Wagner, E. Polylysine-based transfection systems utilizing receptor-mediated delivery. *Adv Drug Delivery Rev* **30**, 97–113 (1998).

98. Akinc, A., Thomas, M., Klibanov, A.M. & Langer, R. Exploring polyethylenimine-mediated DNA transfection and the proton sponge hypothesis. *J Gene Med* **7**, 657-663 (2005).

99. Kircheis, R., Wightman, L. & Wagner, E. Design and gene delivery activity of modified polyethylenimines. *Adv Drug Delivery Rev* **53**, 341-358 (2001).

100. Ogris, M. & Wagner, E. Tumor-targeted gene transfer with DNA polyplexes. *Somat Cell Mol Genet* **27**, 85-95 (2002).

101. Shir, A., Ogris, M., Wagner, E. & Levitzki, A. EGF receptor-targeted synthetic double-stranded RNA eliminates glioblastoma, breast cancer, and adenocarcinoma tumors in mice. *PLoS Med* **3**, e6 (2006).

102. Thomas, M. & Klibanov, A.M. Enhancing polyethylenimine's delivery of plasmid DNA into mammalian cells. *Proc Natl Acad Sci U S A* **99**, 14640-14645 (2002).

103. Thomas, M. et al. Full deacylation of polyethylenimine dramatically boosts its gene delivery efficiency and specificity to mouse lung. *Proc Natl Acad Sci U S A* **102**, 5679-5684 (2005).

104. Tang, M.X., Redemann, C.T. & Szoka, F.C., Jr. In vitro gene delivery by degraded polyamidoamine dendrimers. *Bioconjug Chem* **7**, 703-714 (1996).

105. Lynn, D.M., Anderson, D.G., Putnam, D. & Langer, R. Accelerated discovery of synthetic transfection vectors: parallel synthesis and screening of a degradable polymer library. *J Am Chem Soc* **123**, 8155-8156 (2001).

106. Akinc, A., Lynn, D.M., Anderson, D.G. & Langer, R. Parallel synthesis and biophysical characterization of a degradable polymer library for gene delivery. *J Am Chem Soc* **125**, 5316-5323 (2003).

107. Akinc, A., Anderson, D.G., Lynn, D.M. & Langer, R. Synthesis of poly(beta-amino ester)s optimized for highly effective gene delivery. *Bioconjug Chem* **14**, 979-988 (2003).

108. Anderson, D.G. et al. A polymer library approach to suicide gene therapy for cancer. *Proc Natl Acad Sci U S A* **101**, 16028-16033 (2004).

# Chapter 3: Poly(β-amino esters): Procedures for Synthesis and Gene Delivery

## 3.1 INTRODUCTION

Gene delivery is a valuable research tool and also has strong therapeutic potential to treat many human diseases, from monogenic diseases to cancer. However, this potential has not yet been fully realized because a safe and efficient method for gene delivery has not yet been developed. Viral vectors have several safety concerns (e.g., immunogenicity, reversion to the wild type), limited DNA carrying capacity, and production/quality control challenges.[1, 2] Engineered gene delivery biomaterials have increasingly been shown to address these concerns, but have lower efficiency than viruses.[3] Many biomaterials have been used for gene delivery including cationic polymers, liposomes, dendrimers, chitosans, and inorganic nanoparticles.[1, 4] Cationic polymers, in particular, have been shown to be a flexible system to condense DNA into nanoparticles that are effective for gene delivery.[5]

A specific class of cationic polymers, poly(β-amino esters) (PBAEs), are promising as they condense DNA into nanoparticles, are biodegradable via hydrolytic cleavage of their ester groups and have lower cytotoxicity compared to other cationic polymers such as polyethylenimine (PEI).[6-8] These polymers may act through the "proton sponge mechanism" to enable escape from the endosomal compartment to the cytoplasm.[9-11]

PBAEs have also been developed as gene delivery systems for the *in vivo* treatment of prostate cancer,[12] targeted delivery systems using electrostatic coatings of peptide ligands,[13] and transfection agents that rival the efficacy of viral gene delivery systems.[14]

Methods to transfect new cell types or quantify the transfection efficiency of novel biomaterials are fundamental to development of polymeric gene delivery vectors. This chapter discusses high-throughput methods for screening new gene delivery biomaterials while varying important design parameters such as polymer structure, DNA loading basis, and polymer to DNA weight ratio in parallel. These approaches can be used to quickly characterize and optimize new gene delivery formulations.

## 3.2 MATERIALS

### *3.2.1 Polymer Synthesis*

1. For synthesis of one lead polymer, poly(5-amino-1-pentanol-co-1,4-butanediol diacrylate) (referred to as C32), 5-amino-1-pentanol (Aldrich) and 1,4-butanediol diacrylate (Scientific Polymer Products Inc.) are required. Additional amine and diacrylate monomers can be purchased and used following the same protocol to create structurally diverse polymers that are useful for gene delivery. These monomers can be purchased from Aldrich (Milwaukee, WI, USA), Scientific Polymer Products Inc. (Ontario, NY, USA), TCI (Portland, OR, USA), Pfaltz & Bauer (Waterbury, CT, USA), Matrix Scientific (Columbia, SC, USA), and Dajac Monomer–Polymer (Feasterville, PA, USA).

2. Teflon-lined screw cap glass vials, 8 mL; VWR
3. Teflon-coated magnetitic micro stir bars that fit in vials; VWR
4. Magnetic stir plate
5. Incubator/Oven (95°C)

### *3.2.2 Cell Culture*

*COS-7 Cells:*

1. COS-7 cells, African green monkey kidney fibroblast-like cell line; ATCC #CRL-1651
2. Media: 500 mL DMEM containing 10% Fetal Bovine Serum (50 mL FBS) and 1% Penicillin-Streptomycin (5 mL); Invitrogen
3. Trypsin; Invitrogen
4. Phosphate Buffered Saline (PBS); Invitrogen

*Or Human Umbilical Vein Endothelial Cells (HUVECs):*

1. HUVECs, primary human endothelial cells; Lonza #C2519A
2. Media: 500 mL EGM-2 media supplemented with SingleQuot kit; Lonza
3. ReagentPack kit (Trypsin/EDTA, Trypsin Neutralizing Solution, HEPES Buffered Saline); Lonza

*Additional Materials:*

1. Hemocytometer; VWR
2. Incubator (37°C, 5% $CO_2$); Forma Scientific

### *3.2.3 Standard Gene Delivery Transfection*

1. Gene delivery polymer(s). From synthesis in section 3.2.1 and/or bought commercially such as polyethylenimine (PEI), $M_w$ ~ 25 kDa branched from Sigma or PBAEs can be bought directly from Open Biosystems as Leopard™ Transfection Array polymers.
2. Dimethyl sulfoxide (DMSO), >99.7% and sterile; Sigma
3. Tissue culture filter unit, 500 mL, 0.2 micron cellulose acetate, sterile; Nalgene
4. 3 M sodium acetate solution, pH 5.2, 0.2 um filtered; Sigma
5. 1 mg/mL pEGFP DNA in water, stored at -20°C; Elim Biopharmaceuticals
6. Single channel pipettes (Ex: 1-10 μL, 10-100 μL, 100-1000 μL)
7. Eppendorf tubes, 1.5 mL, sterile; VWR
8. Pipette tips (sterilized by autoclaving for 30 minutes at 18 psi and 120°C)
9. 6-channel aspirator wand (autoclaved); V&P Scientific
10. Clear, sterile, tissue culture treated multi-well plates (6-well, 12-well, or 24-well, etc.)
11. Vortex-Genie; VWR
12. Fluorescent microscope and/or flow cytometer to measure green fluorescent protein gene expression.

### *3.2.4 High-throughput Gene Delivery Transfection*

1. Gene delivery polymer(s). These could include materials derived from synthesis as described in section 3.2.1 and/or bought commercially, such as polyethylenimine (PEI),

$M_w$ ~ 25 kDa branched from Sigma, or PBAEs bought directly from Open Biosystems as Leopard™ Transfection Array polymers.

2. Dimethyl sulfoxide (DMSO), >99.7% and sterile; Sigma
3. Tissue culture filter unit, 500 mL, 0.2 micron cellulose acetate, sterile; Nalgene
4. 3 M sodium acetate solution, pH 5.2, 0.2 um filtered; Sigma
5. 1 mg/mL pCMV-Luc DNA in water, stored at -20°C; Elim Biopharmaceuticals
6. Single channel pipettes (Ex: 1-10 μL, 10-100 μL, 100-1000 μL)
7. Eppendorf tubes, 1.5 mL, sterile; VWR
8. 12-channel pipettes (5-50 μL and 50-300 μL); Finnpipette
9. Pipette tips (sterilized by autoclaving for 30 minutes at 18 psi and 120°C)
10. Pipetting reservoirs, sterile; VWR
11. 12-channel aspirator wand (autoclaved); V&P Scientific
12. Clear 96-well half area plate (sterilized by UV treatment in cell culture hood for at least 1 hour); Corning #3695
13. White, opaque, sterile, tissue culture treated 96-well plate; Costar #3917
14. Clear 96-well flat-bottom plates with lids, sterile; BD Falcon #353072
15. Polypropylene 96-well plates (2.4 mL, V-bottom); Sigma #M1561
16. Bright-Glo™ kits; Promega
17. Firefly luciferase protein; Promega
18. 96-well plate luminometer to measure luciferase gene expression

## 3.3 METHODS

### *3.3.1 Polymer Synthesis*

1. Weigh 400 mg of 5-amino-1-pentanol (or other amine monomer) into a 5 mL sample vial with a teflon-lined screw cap.
2. Add acrylate monomer to amine monomer at an amine/diacrylate stoichiometric ratio of 1.2:1. For polymer C32, add 640 mg of 1,4-butanediol diacrylate to the 400 mg of 5-aminopentanol.
3. Add a small teflon-coated magnetitic stir bar to the vial.
4. To polymerize, stir the monomers on a magnetic stir plate in an oven at 95°C for 12 hours.
5. Remove polymer vial and store in the dark at 4°C until ready to use.

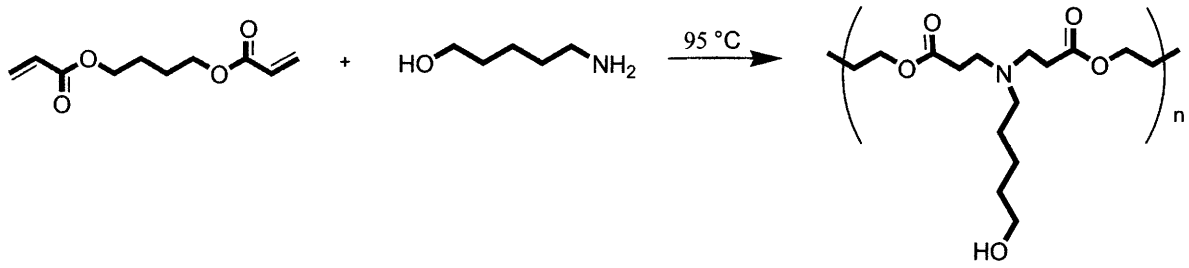


**Figure 3.1.** Polymerization of 1,4-butanediol diacrylate and 5-aminopentanol to form gene delivery polymer C32.

### *3.3.2 Standard Transfection*

Researchers should be familiar with basic sterile cell culture techniques required to grow, passage and plate cells. All work is conducted in a laminar flow biosafety cabinet using sterilized reagents and equipment.

1. **Cell plating.** Twenty-four hours prior to transfection, seed cells to a clear tissue culture muti-well plate at 150 cells/μL according to Table 3.1:

| Wells/plate | Volume/well | Cells/well |
|---|---|---|
| 6 | 2 mL | 300,000 |
| 12 | 1 mL | 150,000 |
| 24 | 500 μL | 75,000 |
| 96 | 100 μL | 15,000 |

**Table 3.1** Cell Plating

2. **Preparation of polymer stock solutions.** Dissolve 50 mg of each synthesized polymer in 500 μL of DMSO in a sterilized eppendorf tubes. Vortex to mix to prepare 100 mg/mL polymer stock solutions. For PEI, dissolve 1 mg in 1 mL of water to prepare a 1 mg/mL PEI stock solution.

3. **Preparation of sodium acetate buffer.** To prepare sodium acetate (NaAc) buffer (pH = 5.2), dilute 4.2 mL of 3 M sodium acetate into 495.8 mL of deionized water. Sterilize by vacuum filtration through a 0.2 μm filter.
4. **Change cell media**. On the day of transfection, warm fresh media in a 37°C water bath. Aspirate out the old media from each cell well and replace with equivalent volume of fresh media. Note: The cells should look healthy as determined by light microscopy. Transfections are typically performed at 70-100% confluence.
5. **DNA preparation.** Thaw the DNA stock solution at room temperature. Dilute an aliquot of the 1 mg/mL DNA stock solution with 25 mM sodium acetate buffer to a final concentration of 0.060 mg/mL. For a 24-well plate, this requires 90 ug of DNA in a final volume of 1.5 mL of 25 mM sodium acetate. Aliquot out 60 μL of diluted DNA to a small volume sterile eppendorf tube for each sample to be made (24 typically).
6. **Aqueous polymer preparation.** Prior to complexation with DNA, each 100 mg/mL polymer/DMSO solution must be diluted in sodium acetate. The dilution is dependent on the final polymer:DNA weight ratios desired. For polymer C32, a weight ratio (w/w) of 30:1 polymer:DNA is typically optimal. However, this may vary with different polymers and different cell systems. Generally, it is advisable to try initially a range of weight ratios and then select the best-performing w/w for future experiments. The aqueous polymer solution should be vigorously mixed prior to use to ensure homogeneity. Table 3.2 shows a protocol for typical formulations in a 24-well plate format assuming polymer preparation for triplicate samples (200 μL aqueous polymer solution). (For different plate formats, all volumes are scaled in proportion to the cell seeding density used in step 1.) PEI is prepared analogously except that a low 1:1 polymer to DNA weight ratio is

generally optimal and the PEI (and the DNA used to complex PEI) is diluted in 150 mM sodium chloride rather than 25 mM sodium acetate.

| Polymer:DNA w/w | Polymer (μg) | Polymer/DMSO (μL) | NaAc (μL) | Polymer Concentration (μg/μL) |
|---|---|---|---|---|
| 1 | 12 | 1.2 | 199 | 0.06 |
| 5 | 60 | 6.0 | 194 | 0.30 |
| 10 | 120 | 12 | 188 | 0.60 |
| 20 | 240 | 24 | 176 | 1.20 |
| 30 | 360 | 36 | 164 | 1.80 |
| 50 | 600 | 60 | 140 | 3.00 |
| 100 | 1200 | 120 | 80 | 6.00 |

**Table 3.2** Polymer Preparation

7. **Polymer-DNA complexation / nanoparticle formation.** For each polymer replicate sample, add 60 μL of polymer to an eppendorf tube containing 60 μL DNA. Mix by vortexing on a medium setting for 10 seconds. Time 10 min on a timer to allow for polymer/DNA self-assembly prior to use.
8. **Add polymer/DNA nanoparticles to the cells.** Prior to addition of the polymer/DNA particles, the media over the seeded cells may be optionally removed and replaced with new media with altered composition for the transfection (serum-free or high serum media

for example), although this is not required. Polymeric gene delivery particles are then added to each well according to Table 3.3:

| Wells/plate | Volume/well | Particle volume/well (μL) | DNA/well (μg) |
|---|---|---|---|
| 6 | 2 mL | 400 | 12 |
| 12 | 1 mL | 200 | 6 |
| 24 | 500 μL | 100 | 3 |
| 96 | 100 μL | 20 | 0.6 |

**Table 3.3** Gene Delivery Nanoparticle Dose

When finished, swirl the plate, return the cells to the incubator, and start a timer.

9. **Remove polymer/DNA particles from the cells.** Typically, particles are incubated on the cells for 1-4 hours. Depending on the concentration and toxicity of materials, in some case overnight incubations are helpful. After incubation, aspirate the polymer/DNA particles from each well using either a 6-channel aspirating wand or a pasteur pipette. Add a volume of fresh, warm media equal to the initial cell seeding volume used in each well (i.e., 500 μL for a 24-well plate). Return the cells to the incubator.
10. **GFP expression measurement.** Alternate strategies may be used to quantify GFP gene expression. Initial study can be performed using a fluorescent microscope to measure the percentage of green, expressing cells vs. total cells counted in the bright field image. Typically however, fluorescence activated cell sorting (FACS) is used to quickly count 10,000 or more live cells per sample and gate the GFP positive cells from the GFP

negative cells. For analysis of GFP positive cells, it is recommended that two-dimensional gating rather than a one-dimensional histogram is used. For two-dimensional gating, the green channel is plotted on the x-axis and the yellow channel is plotted on the y-axis. In this manner, GFP positive cells can be better differentiated from increased background auto-fluorescence as shown in Figure 3.2.

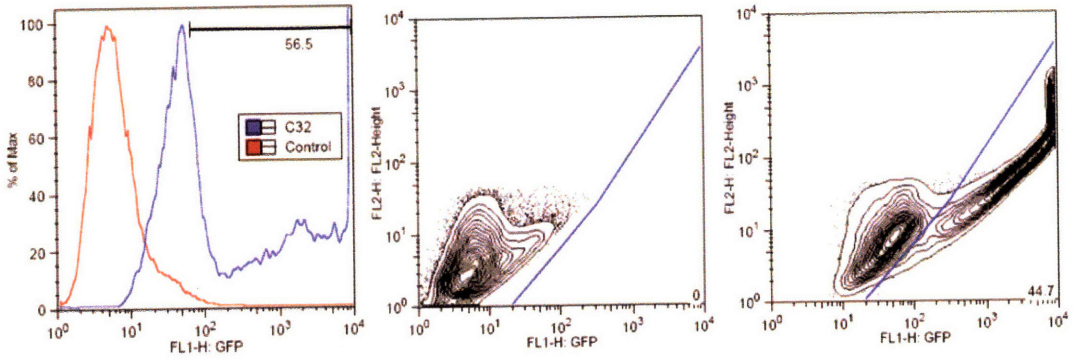


**Figure 3.2.** Representative HUVEC transfection efficacy of C32 and method for FACS gating. The one dimensional histogram of C32/DNA transfected cells (56.5% positive) (left) includes some falsely positive cells that are excluded during the two-dimensional analysis of the same data set as shown by the FACS density plot gating for the negative control (0% positive) (middle) and the C32/DNA transfection (44.7% positive) (right). Ratio of GFP fluorescence (x-axis) to background fluorescence (y-axis) is used to accurately gate positive cells.

### *3.3.3 High-throughput Screening*

The following protocol[15] is for one 96-well plate testing 11 different polymers (columns 1-11 are for each polymer and column 12 is for controls). Each polymer is tested in quadruplicate at two different polymer to DNA w/w ratios (20 w/w is tested in the top half of the plate (rows A-D) and 100 w/w is tested in the bottom half of the plate (rows E-H)).

1. **Cell plating.** Twenty-four hours prior to transfection, seed 15,000 cells/well to a white 96-well tissue culture plate.
2. **Preparation of polymer stock solutions.** Dissolve 50 mg of each synthesized polymer in 500 μL of DMSO in a sterilized eppendorf tubes. Vortex to mix to prepare 100 mg/mL polymer stock solutions. For PEI, dissolve 1 mg in 1 mL of water to prepare a 1 mg/mL PEI stock solution.
3. **Preparation of sodium acetate buffer.** To prepare sodium acetate (NaAc) buffer (pH = 5.2), dilute 4.2 mL of 3 M sodium acetate into 495.8 mL of deionized water. Sterilize by vacuum filtration through a 0.2 μm filter.
4. **Plating sodium acetate buffer.** First, transfer 30 mL of sodium acetate buffer to a pipetting reservoir. Using a multi-channel pipette, add 900 μL/well NaAc to row A of a 2.4 mL deep 96-well plate (Figure 3.3., plate #1). Next, in a clear 96-well plate, add 176 μL/well NaAc to row A (for 20 w/w polymer to DNA particles) and 80 μL/well NaAc to row B (for 100 w/w polymer to DNA particles) (Figure 3.3., plate #2).
5. **DNA preparation and plating.** Thaw the pCMV-Luc DNA stock solution at room temperature. Dilute 600 μL of the 1 mg/mL DNA stock with 9.4 mL of sodium acetate buffer in a 15 mL sterile tube. Transfer the diluted DNA solution to a pipetting reservoir and add 25 μL/well to all wells of a 96-well half area plate (Figure 3.3., plate #3).
6. **Plating media.** Warm 25 mL of media in a 37°C water bath, transfer the media to a pipetting reservoir, and add 200 μL /well to each well of a new clear 96-well plate (Figure 3.3, plate #4).

7. **Aqueous polymer preparation.** For each 100 mg/mL polymer/DMSO solution and the positive control, add 100 μL of concentrated polymer to a single well (#1-12) in row A of the 2.4 mL deep 96-well plate containing 900 μL of sodium acetate buffer (Figure 3.3., plate #1). Vigorously pipette the solution several times to ensure that the polymers are dissolved fully in the buffer.

NOTE: For steps #8-13, all pipetting is done using 12-channel pipettes. Change pipette tips after each use.

8. **Polymer dilutions (Figure 3.3., step 1).** Add 24 μL of polymer solution from row A of the 2.4 mL deep 96-well plate (plate #1) to row A of the polymer dilution plate (plate #2) containing 176 μL of sodium acetate buffer. Similarly add 120 μL of polymer solution from row A of the 2.4 mL deep 96-well plate (plate #1) to row B of the polymer dilution plate (plate #2) containing 80 μL of sodium acetate buffer. Vigorously pipette the solutions multiple times to ensure that they are well-mixed.
9. **Polymer-DNA complexation / nanoparticle formation (Figure 3.3., step 2).** For quadruplicate samples, add 25 μL of polymer from row A of the polymer dilution plate (plate #2) to 25 μL of DNA in rows A, B, C, and D of the DNA plate (plate #3). Add 25 μL of polymer from row B of the polymer dilution plate (plate #2) to 25 μL of DNA in rows E, F, G, and H of the DNA plate (plate #3). For each addition, vigorously pipette the solution several times to promote polymer/DNA self-assembly. To generate reproducible particles, it is important to be consistent with the mixing technique. Start a five minute timer once the plate is finished.

10. **Polymer/DNA particles dilution (Figure 3.3., step 3).** At the end of five minutes, add 30 μL of polymer/DNA particles from row A of the DNA plate (plate #3) to row A of the media plate (plate #4) containing 200 μL of media. Repeat for rows B-H.
11. **Add polymer/DNA particles to the cells (Figure 3.3., step 4).** Use a 12-channel aspiration wand to remove the media from the cells seeded to the white 96-well plate previously (step #1). Add 150 μL of polymer/DNA particles from row A of the media plate (plate #4) to row A of the cell plate. Repeat for rows B-H, being careful to pipette against the side of the wells as opposed to directly over top the cells which can dislodge the cells if not careful.
12. **Remove polymer/DNA particles from the cells.** After a 1-4 hour incubation time, aspirate the polymer/DNA solution from the cells and add 100 μL of warm fresh media to each well. Return the cells to the incubator.
13. **Luciferase protein assay.** This assay is generally performed 2-3 days post-transfection. Thaw the BrightGlo™ Luciferase Assay Kit by warming the buffer in a room temperature water bath. Remove the cells from the incubator and allow them to equilibrate to room temperature as well. Add the buffer to the substrate vial, re-cap, invert to mix, and then dispense into a reservoir. Using a multi-channel pipette, add 100 μL of the solution to each 100 μL well of the cell plate. After the last addition, time two minutes on a timer. Place the plate on an orbital shaker or manually shake to promote mixing during this time. After two minutes, measure the luminescence in a plate reader using an integration time of one second/well. Compare the relative luminescence to a standard curve to obtain the mass of luciferase protein in each well.

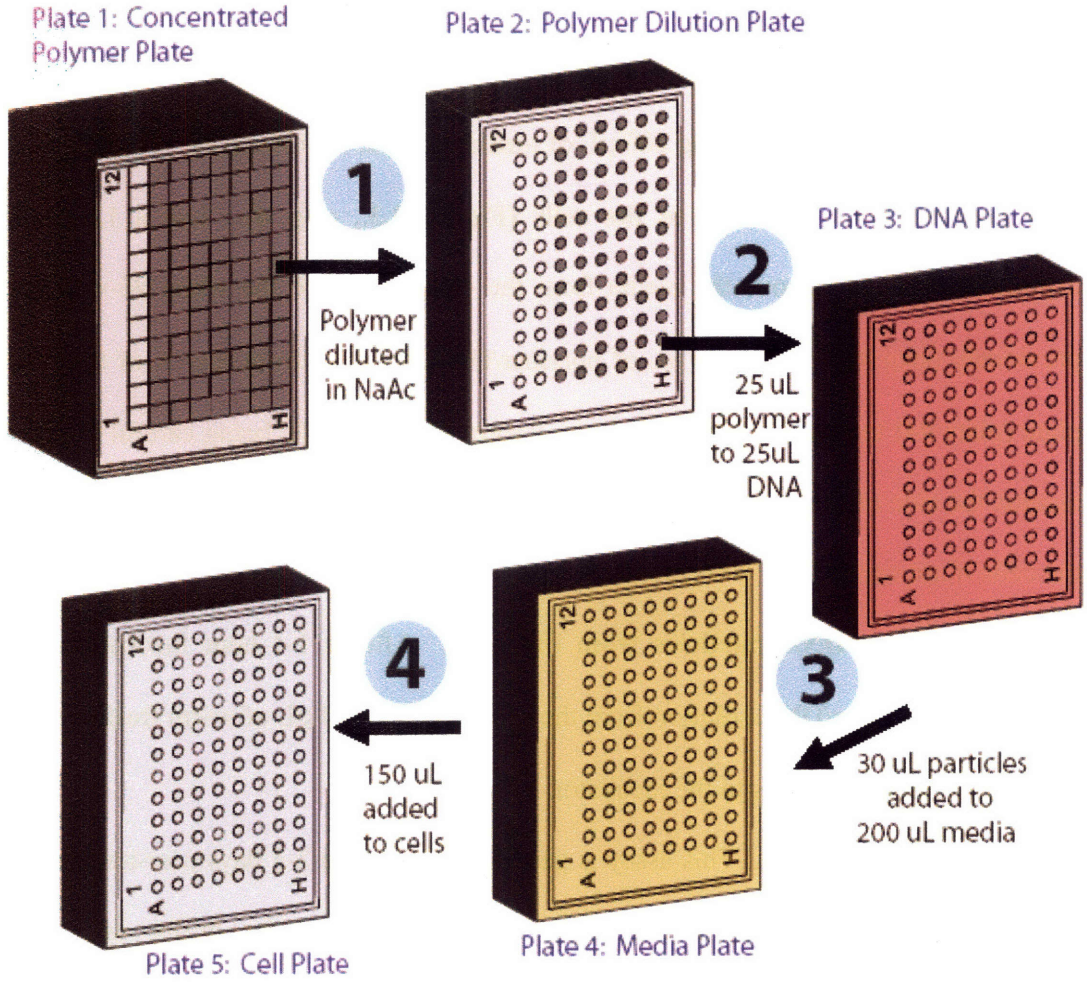


**Figure 3.3.** High-throughput screening method.

## 3.4 NOTES

### *3.4.1 Cell Line*

In general, any adherent cell type may be used following these same protocols. COS-7 and HUVEC cell protocols are shown as examples of an easier-to-transfect mammalian cell

line and more difficult-to-transfect human primary cells, respectively. Typical transfection of COS-7 cells using polymer C32 is ~90-100% whereas for HUVECs it is ~40-50%.

### *3.4.2 Plasmid DNA*

Different sized plasmid DNA may be used to create these polymer/DNA particles. For easy visual inspection of gene expression and quantitative cell population information enhanced green fluorescent protein (EGFP) DNA is often used. For high-throughput screening applications, luciferase (Luc) DNA is often used instead.

### *3.4.3 Polymer/DNA Self-Assembly*

It is important that the cationic polymers are added to the anionic DNA, rather than the reverse. It is also important that the two components are very well mixed. We suggest vortexing at medium speed rather than simply pipetting up and down. The optimal self-assembly incubation time is between 10-15 min. Leaving the assembled polymer/DNA particles for longer than 40 min before use may reduce activity. A slightly shorter self-assembly waiting time is typically used when performing high-throughput methods.

### *3.4.4 Low Transfection*

If for a given application transfection is lower than desired, increase the polymer to DNA weight ratio and/or the DNA loading basis per cell well. For example, in a 24-well plate use a 6 μg DNA / well basis instead of a 3 μg DNA / well basis. Additionally, increasing the time that the polymer/DNA particles incubate the cells or reducing the serum concentration can increase efficacy. Lastly, reducing the cell confluence to 50-70% confluent at the time of transfection can increase efficacy.

### *3.4.5 High Cytotoxicity*

If for a given application cytotoxicity occurs, decrease the polymer to DNA weight ratio and/or the DNA loading basis per cell well.

### *3.4.6 High-Throughput Screening Advantages/Limitations*

Advantages:

- Allows for testing of hundreds of polymers, in quadruplicate, in a single day
- Minimizes amount of reagents used

Limitations:

- Many pipette tip boxes and plate types must be stocked and sterilized

- Mixing during parallel particle formation by pipettes may not be as vigorous as done by vortexing. This can affect particle self-assembly in some instances.

## 3.5 REFERENCES


1. Partridge, K.A. & Oreffo, R.O.C. Gene delivery in bone tissue engineering: Progress and prospects using viral and nonviral strategies. *Tissue Eng* **10**, 295-307 (2004).
2. Thomas, C.E., Ehrhardt, A. & Kay, M.A. Progress and problems with the use of viral vectors for gene therapy. *Nat Rev Genet* **4**, 346-358 (2003).
3. Pack, D.W., Hoffman, A.S., Pun, S. & Stayton, P.S. Design and development of polymers for gene delivery. *Nature Reviews Drug Discovery* **4**, 581-593 (2005).
4. Merdan, T., Kopecek, J. & Kissel, T. Prospects for cationic polymers in gene and oligonucleotide therapy against cancer. *Adv Drug Delivery Rev* **54**, 715-758 (2002).
5. Putnam, D. Polymers for gene delivery across length scales. *Nat Mat* **5**, 439-451 (2006).
6. Lynn, D.M. & Langer, R. Degradable poly(beta-amino esters): Synthesis, characterization, and self-assembly with plasmid DNA. *J Am Chem Soc* **122**, 10761-10768 (2000).
7. Green, J.J. et al. Biodegradable polymeric vectors for gene delivery to human endothelial cells. *Bioconjug Chem* **17**, 1162-1169 (2006).
8. Anderson, D.G., Lynn, D.M. & Langer, R. Semi-automated synthesis and screening of a large library of degradable cationic polymers for gene delivery. *Ang. Chem. Int. Edn* **42**, 3153-3158 (2003).
9. Akinc, A. & Langer, R. Measuring the pH environment of DNA delivered using nonviral vectors: Implications for lysosomal trafficking. *Biotechnol Bioeng* **78**, 503-508 (2002).

10. Sonawane, N.D., Szoka, F.C. & Verkman, A.S. Chloride accumulation and swelling in endosomes enhances DNA transfer by polyamine-DNA polyplexes. *J Biol Chem* **278**, 44826-44831 (2003).

11. Akinc, A., Thomas, M., Klibanov, A.M. & Langer, R. Exploring polyethylenimine-mediated DNA transfection and the proton sponge hypothesis. *J Gene Med* **7**, 657-663 (2005).

12. Anderson, D.G. et al. A polymer library approach to suicide gene therapy for cancer. *Proc. Natl. Acad. Sci. U.S.A.* **101**, 16028-16033 (2004).

13. Green, J.J. et al. Electrostatic ligand coatings of nanoparticles enable ligand-specific gene delivery to human primary cells. *Nano Lett* **7**, 874-879 (2007).

14. Green, J.J. et al. Combinatorial modification of degradable polymers enables transfection of human cells comparable to adenovirus. *Adv Mat*, (in press) (2007).

15. Zugates, G.T., Anderson, D.G. & Langer, R. in *Gene Transfer: Delivery and Expression of DNA and RNA*. (eds. T. Friedmann & J. Rossi) 547 - 554 (Cold Spring Harbor Laboratory Press, New York, NY; 2007).

# Chapter 4: Design of Biodegradable Polymeric Vectors*

## 4.1 INTRODUCTION

Cardiovascular disease and cancer are the leading causes of death in the United States. Gene therapy has the potential to treat many cardiovascular conditions including peripheral arterial disease, restenosis, and myocardial ischemia as gene delivery enables long term expression of target genes useful for treatments such as therapeutic angiogenesis and inhibition of cell proliferation.[1-3] Endothelial cells are a significant cell target in cardiovascular disease as they control vascular function. Endothelial cells are also an important cell type for cancer treatments that target against vasculogenesis and angiogenesis.[4, 5] In these experiments, we use Human Umbilical Vein Endothelial Cells (HUVECs) as a model primary cell system to test the efficacy of gene delivery vectors. This is a challenge as primary endothelial cells have higher intrinsic resistance to gene delivery than other cell lines.[6]

There are two main approaches to gene delivery: viral and non-viral. The primary advantages of viral delivery are efficient infection of cells and long-term gene expression.[7, 8] However, problems with viral vectors as compared to non-viral vectors include limited cargo capacity, resistance to repeated infection, production and quality control issues, and safety.[7, 9]

* Reproduced with permission from *Bioconjugate Chemistry* 17(5), 1162-1169. ©2006 American Chemical Society

Specific safety concerns include acute toxicity, cellular immune response, and oncogenicity due to insertional mutagenesis.[7] Non-viral vectors are attractive for gene delivery as they do not have these viral vector limitations.

To improve stability and uptake of DNA, numerous biomaterials have been used to create synthetic gene delivery vectors. The main biomaterials that have been studied include cationic polymers, cationic lipids, liposomes, chitosans, inorganic nanoparticles, and dendrimers.[8-10] Though these biomaterials improve transfection in comparison to naked DNA, they still have relatively low transfection efficacy, and many of these materials are cytotoxic.

Recently, a large library of 2350 structurally unique poly(β-amino esters) was developed using high-throughput combinatorial chemistry.[11] Poly(β-amino esters) are promising for non-viral gene delivery due to their 1) ability to condense DNA into nanoparticles, 2) ability to buffer the endosome, 3) ability to promote endosomal escape, 4) low cytotoxicity compared to other cationic polymers, 5) biodegradability via hydrolytic cleavage of ester groups, and 6) large potential for structural diversity.[12-16]

Previously, we have shown that top performing poly(β-amino ester) vectors have particle sizes smaller than 150 nm, positive zeta potentials, polymer weight to DNA weight ratios greater than or equal to 40, molecular weights above 10,000, amine-terminated chains, and other structural similarities.[11, 13, 17, 18] However, all of these assays and measurements were conducted in serum-free conditions, and the role of serum interactions on biophysical properties and transfection efficacy of poly(β-amino ester) vectors has not previously been studied. Important particle properties such as size, zeta potential, and particle stability are dependent on the local aqueous environment and gene delivery particles demonstrated to have certain biophysical characteristics in a buffer may not have the same characteristics in the presence of serum or *in*

*vivo*.[19, 20] Here we demonstrate that poly(β-amino esters) as a class, and C32 in particular, transfect human primary endothelial cells better than several top commercially available reagents. Analysis of the biophysical properties of poly(β-amino ester)/DNA complexes as a function of media and over time provide insight into serum stability and efficacy of these complexes.

## 4.2 EXPERIMENTAL PROCEDURES

### *4.2.1 Cell Culture*

Human Umbilical Vein Endothelial Cells (HUVECs) (Cambrex, Walkersville, MD, USA) were cultured in EGM-2 media supplemented with SingleQuot Kits (Cambrex). HUVEC cells were used by passage five and in accordance to the manufacturer's instructions. Cells were grown at 37°C at a humid 5% CO2 atmosphere.

### *4.2.2 Polymer Synthesis*

Monomers were purchased from Aldrich (Milwaukee, WI, USA), TCI (Portland, OR, USA), Pfaltz & Bauer (Waterbury, CT, USA), Matrix Scientific (Columbia, SC, USA), Scientific Polymer (Ontario, NY, USA), and Dajac Monomer–Polymer (Feasterville, PA, USA). Optimal amine/diacrylate stoichiometric ratios for each polymer were determined from previous work.[13] To synthesize each polymer, 400 mg of amino monomer was weighed into a 1 mL sample vial with Teflon-lined screw cap. Next, the appropriate amount of diacrylate was added

to the vial and a small Teflon-coated stir bar was then put in each vial. Polymers were then synthesized on a multiposition magnetic stir-plate residing in an oven at either 95°C and solvent free or 60°C with 2 ml DMSO added. High temperature synthesis was performed for approximately 12 h, and low-temperature synthesis was performed for 2 days. After completion of reaction, all vials were removed from the oven and stored at 4°C. All polymers were analyzed by gel-permeation chromatography (GPC) as previously discussed.[13]

### *4.2.3 Polymeric Vectors*

The non-viral vectors are formed through electrostatic interactions between poly(β-amino esters) and plasmid DNA. Depending on transfection experiments, plasmid DNA encoding either pEGFP enhanced green fluorescent protein (ElimBiopharmaceuticals, South San Francisco, CA, USA) or pCMV-Luc firefly luciferase (ElimBiopharmaceuticals, South San Francisco, CA, USA) was used. By varying the amount of DNA used in preparation, the amount of DNA loading per cellular well was varied. At a fixed DNA basis, by varying the weight of polymer, the charge ratio (N/P) of polymer nitrogen (N) to DNA phosphate (P) was varied. To ease handling, polymer stock solutions (100 mg/ml) were prepared in DMSO solvent prior to use. Working dilutions of each polymer were prepared in 25 mM sodium acetate buffer (pH 5). For 96-well plate experiments, twenty-five microliters of the diluted polymer was added to 25 microliters of DNA and mixed well. The mixtures were then incubated at room temperature for 10 min to allow for complex formation. For 24-well experiments and for biophysical characterization experiments, the same steps were followed but all volumes were scaled up appropriately.

### *4.2.4 Biophysical Characterization*

Particle size and ζ potential measurements were measured by using a ZetaPALS dynamic light scattering detector (Brookhaven Instruments Corp., Holtsville, NY, USA, 15-mW laser, incident beam 676 nm). Samples were prepared for biophysical characterization in the same manner and at the same concentrations as they were for transfections, but the media/polymer/DNA solution was scaled up to a final volume of 1.6 mL. Generally, particles were first sized in 25 mM NaAc buffer while initial polymer/DNA complexation occurred and then added to 12% serum EGM-2 media and sized dynamically in time for up to 8 days. Particle stability was determined by changes to particle size over time. Polymer/DNA ratios shown are those determined to have the highest transfection efficacy unless otherwise stated. Correlation functions were collected at a scattering angle of 90°, and particle sizes were calculated using the MAS option of BICTs particle sizing software (version 2.30) using the viscosity and refractive index of water at 25°C. Particle sizes are expressed as effective diameters assuming a log-normal distribution. Average electrophoretic mobilities were measured at 25°C using BIC PALS ζ potential analysis software, and ζ potentials were calculated using the Smoluchowsky model for aqueous suspensions.

### *4.2.5 Luciferase Transfections*

Non-viral vector transfections were performed on HUVECs with and without the presence of serum. HUVECs were seeded (15,000 cells/well) into each well of an opaque white 96-well plate (Corning-Costar, Kennebunk, ME, USA) 24 hours prior to transfection to allow for

growth to confluence. Vectors were constructed as previously mentioned and then 30 μL of each polymer/DNA solution was added to either 200 μL of Opti-MEM with sodium bicarbonate (Invitrogen), EGM-2 media (2% Serum), or FBS supplemented EGM-2 media (12% Serum) in 96-well polystyrene plates. The growth medium was removed from the cells using a 12-channel aspirating wand (V&P Scientific, San Diego, CA, USA) after which 150 μL of the Media/polymer/DNA solution was immediately added. Complexes were incubated with the cells for 1-4 hours and then removed using the 12-channel wand and replaced with 100 μL of warm EGM-2 media. Final DNA loading was 0.3 or 0.6 μg per well depending on the experiment. Cells were then allowed to grow for 48 hours and then analyzed for luciferase expression. Control experiments were also performed with PEI (MW 25,000; Sigma–Aldrich), jetPEI (Qbiogene, Irvine, CA, USA), jetPEI-HUVEC (Bridge Bioscience Corporation, Portsmouth, NH, USA) and Lipofectamine 2000 (Invitrogen). PEI transfections were performed as described above using a polymer/DNA weight ratio of 1/1. Jet PEI, Jet-PEI-HUVEC, and Lipofectamine 2000 transfections were performed as described by their vendors. The same quantity of DNA per well and incubation time was used with the control vectors as with the poly(β-amino ester) vectors. Luciferase expression was analyzed using Bright-Glo assay kits (Promega, Madison, WI, USA). Briefly, 100 μL of Bright-Glo solution was added to each well of the 96-well plate containing cell medium and cells. Luminescence was measured using a Mithras luminometer (Berthold, Oak Ridge, TN, USA).

### *4.2.6 GFP Transfections*

GFP transfections paralleled the luciferase transfections except that all volumes were scaled up five-fold and the experiments were conducted in clear 24-well plates (Becton Dickinson, Franklin Lakes, NJ, USA) with 3 ug GFP DNA per well. Cells were seeded at 75,000 per well, 24 hours prior to transfection, and cells were transfected with 750 μL of media/polymer/DNA solution. Cells were aspirated prior to transfection using a 6-channel aspirating wand (V&P Scientific, San Diego, CA, USA). After a 1-4 hr incubation, the non-viral vector solution was aspirated off and replaced with 500 μL of warm EGM-2 media. After a 48 hrs, transfected and untransfected control cells were washed, removed from the 24-well plates by trypsinization, microcentrifuged, and resuspended in 1 mL of FACS running buffer (98% PBS / 2% FBS / 1:200 propidium iodide solution (Invitrogen)) for FACS analysis.

### *4.2.7 Flow Cytometry*

GFP expression was measured using Fluorescence Activated Cell Sorting (FACS) on a FACSCalibur (Becton Dickinson, San Jose, CA, USA). Propidium iodide staining was used to exclude dead cells from the analysis and 20,000 live cells per sample were acquired. Two-dimensional gating was used to separate increased autofluorescence signal from increased GFP signal to more accurately count positively expressing cells. Gating and analysis was performed using FlowJo 6.3 software (TreeStar, Ashland, OR, USA).

### *4.2.8 Cell Viability Measurements*

To measure cytotoxicity and cell viability, cellular metabolic activity was measured using the Cell Titer 96 Aqueous One Solution assay kit (Promega , Madison, WI, USA). Metabolic activity was measured using optical absorbance on a Victor3 Multilabel plate counter (Perkin Elmer Life Sciences, Boston, MA, USA). Measurements of treated cells were converted to percent viability by comparison to untreated controls.

### *4.2.9 Statistics*

Statistical calculations were carried out using GraphPad Prism 4.0 for Windows. Results are reported as mean±standard deviation. For comparison of gene delivery vectors, statistical significance was obtained by using unpaired, two-tailed, Student's *t*-tests with 99% confidence.

## 4.3 RESULTS AND DISCUSSION

### *4.3.1 Polymer Synthesis and Gene Delivery Vector Formulation*

Poly(β-amino esters) are synthesized by the conjugate addition of amine monomers to acrylate esters. The acrylate and amine monomers used in this experiment and their synthesis scheme can be seen in Figure 4A. High-throughput screening and synthesis of a large library of over 2,000 poly(β-amino esters) was conducted.[11] The top 486 polymers were then

resynthesized on a larger scale at a range of molecular weights[13]. Based on transfection efficacy to COS-7 cells in serum-free conditions, 11 of the best performing polymers were then selected for further analysis and optimization for transfection to human primary cells in the presence of serum.

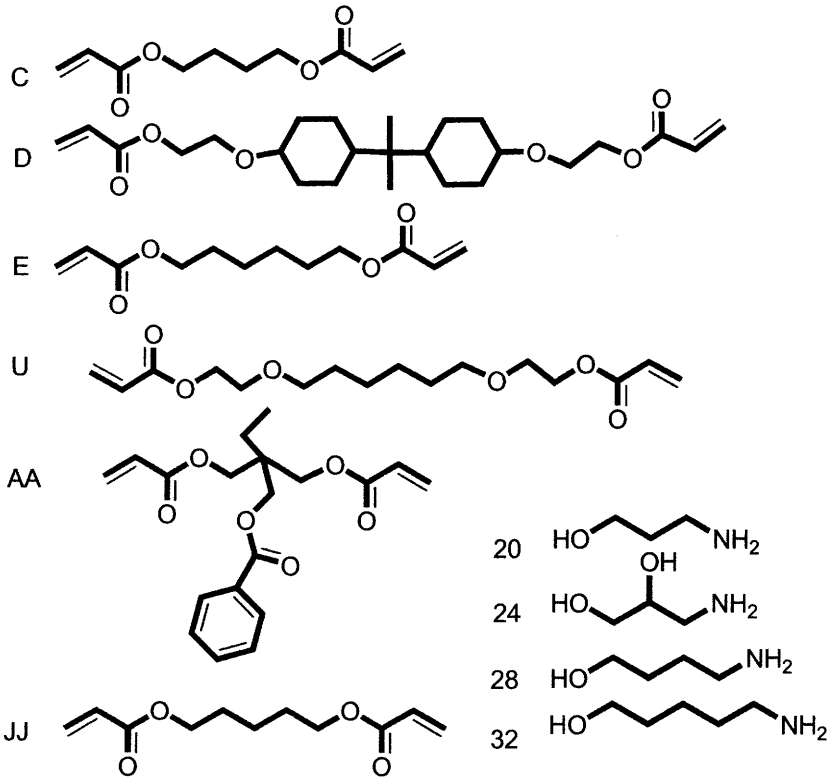


**Figure 4.1A.** Diacrylate esters and amine monomers.

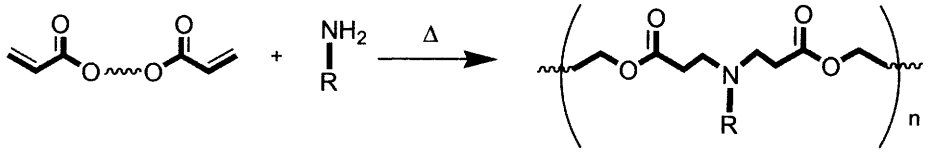


**Figure 4.1B.** Synthesis of poly(β-amino esters).

Cationic polymeric gene delivery vectors were formed in sodium acetate buffer solution. It was determined that particles quickly self-assemble and that a 10 min complexation time is optimal for transfection efficacy. Adding poly(β-amino esters) to DNA was found to create vectors that were significantly more effective than those vectors formed by adding DNA to the polymers. These results parallel earlier results found with PEI[21] and suggest that this mixing order may be a general rule for all cationic polymers used to condense DNA.

### *4.3.2 Biophysical Characterization*

Previously, nanoparticle size and zeta potential of poly(β-amino ester) vectors in PBS buffer was reported. For the top performing vectors, particle sizes were smaller than 150 nm and zeta potentials were positive.[13] We hypothesized that these biophysical properties change during actual transfections when the complexes are added either to serum-free OptiMem or cell culture media with differential levels of serum. As it has been reported that non-viral vector formulations have low efficacy in the presence of serum[19, 20], we wanted to determine how media and serum might change the biophysical properties of these vectors and if serum proteins inhibited poly(β-amino ester) vector transfection.

Figure 4.2. shows the effect of media type on poly(β-amino ester) vector particle size and stability over time. In this figure, gene delivery particles are prepared at the same concentrations as they are for typical *in vitro* bio-assays. This figure demonstrates that C32/DNA particles delivered in OptiMem are significantly larger than those delivered in cell culture media with serum. This figure also demonstrates that in OptiMem, these particles are unstable and the biophysical properties of the particles change over time. This is important as during transfection,

the population of functional gene delivery nanoparticles can be dynamically changing in time. In contrast, serum proteins are shown to differentially reduce particle size and instability, presumably, from negative electrostatic repulsions.

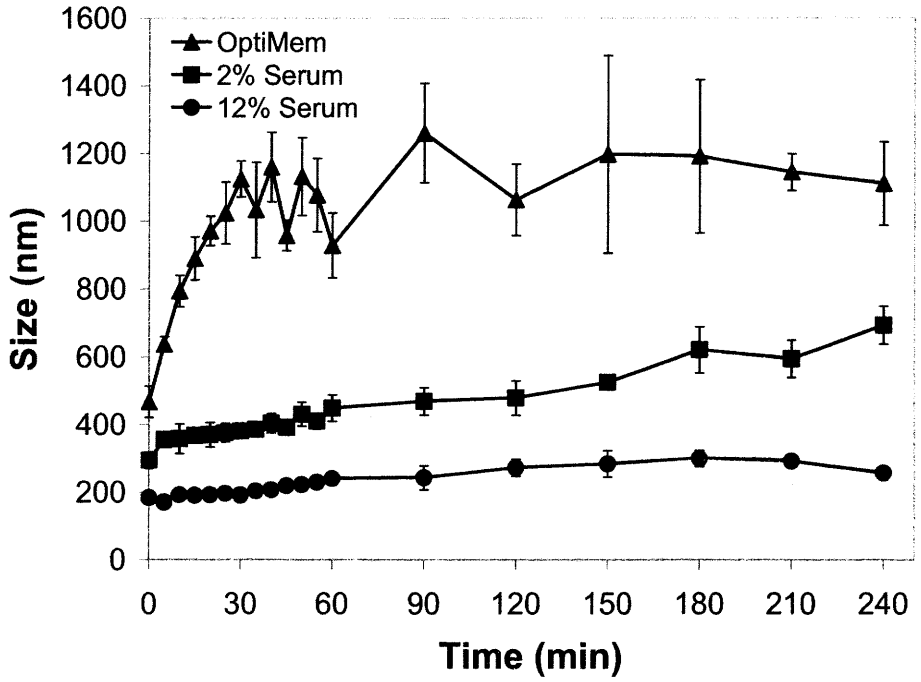


**Figure 4.2. C32/DNA (50 w/w) particle size and stability is dependent on media type and serum concentration and can change dynamically in time. Error bars are the standard deviations of triplicate samples.**

The size of a polymeric gene delivery complex is known to dramatically affect transfection efficacy.[13, 19, 22] However, there is some controversy in the literature about what size is optimal for delivery. Some researchers have found that for *in vitro* experiments, large aggregated particles transfect better than small particles.[19, 23, 24] This is believed to be from a sedimentation effect of large particles. Interestingly, the reverse has also been reported.[13, 22] In

either case, for an *in vivo* application, larger particles could cause problems due to physical size exclusions in capillaries and tissues. Small particles that are stable in serum are typically preferred.

Figure 4.3. demonstrates that the choice of aqueous solution used during bio-assays can result in dramatic differences in the biophysical characteristics of closely related biomaterials. In this figure, poly(β-amino ester) vectors are first sized in sodium acetate buffer and then sized in high-serum containing media. Whereas all vectors condensed DNA into small nanoparticles below 150 nm while in buffer, particle size dramatically changed when these particles were sized in serum. Some vectors such as C32, JJ32, and E28 formed small, stable particles in the 200 nm range whereas other vectors such as D24 aggregated in serum to large particles in the 1 um range. The biophysical characteristics of a gene delivery vector in a high-serum environment are likely one important indicator in predicting effectiveness for *in vivo* cardiovascular gene delivery.

Figure 4.4. shows how particle size depends on poly(β-amino ester) to DNA N/P ratio (and weight ratio) for top performing and poor performing vectors in the poly(β-amino ester) library. This figure shows that E28, a representative top performing vector, forms uniformly sized small nanoparticles over a range of weight ratios whereas a poor performing vector, such as D24, forms large, aggregating particles that are differentially sized according to N/P ratio.

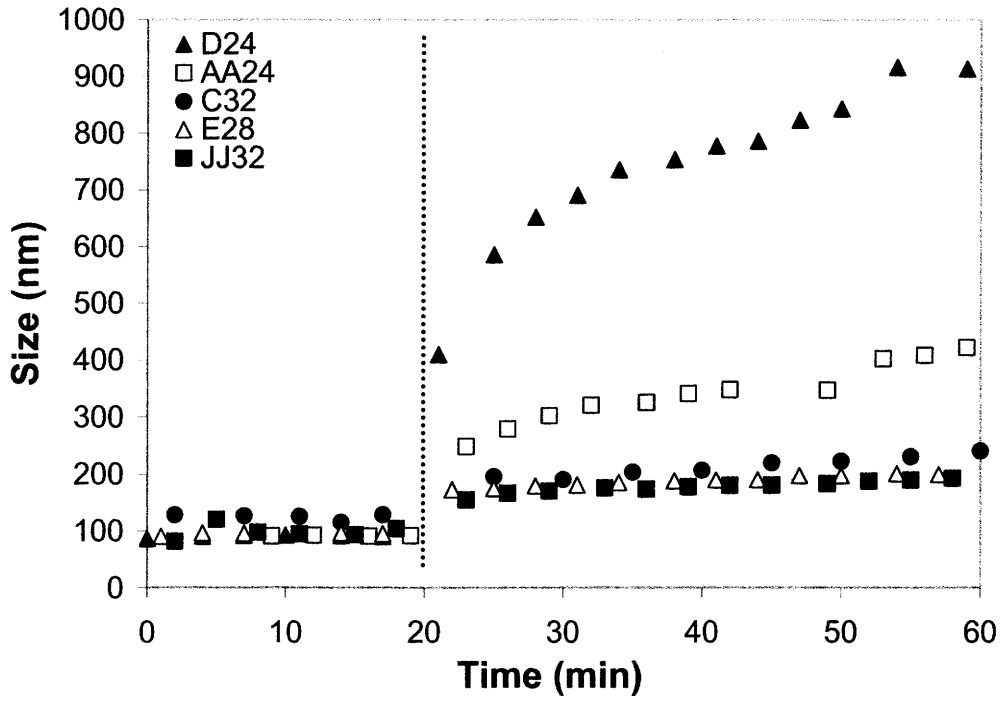


**Figure 4.3.** Particle size and stability is dependent on polymer type. All particles have a similar <150 nm size in NaAc buffer, but grow disparately in size when added to 12% serum-containing media (indicated by the vertical line). Size in serum-containing media correlated to transfection efficacy.

Figure 4.5. shows the long term stability of C32/DNA gene delivery vectors. C32/DNA vectors were found to stay stable for at least eight days in OptiMem, 2% low-serum enhanced media, and 12% high-serum enhanced media. For all the poly(β-amino ester) vectors tested, particles that aggregated tended to do so within the first hour of formation and then remained relatively stable for subsequent time points. Non-aggregating particles were stable for all time points tested. Particle stability is advantageous for effective delivery by circulating nanoparticles, consistent transfections, and for storage.

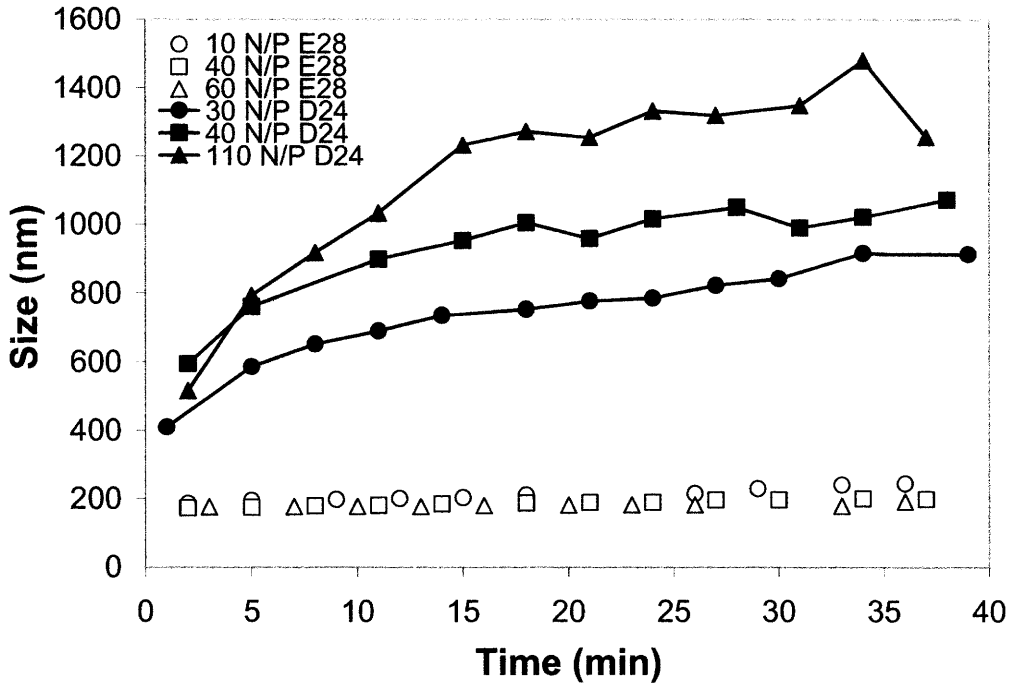


**Figure 4.4.** Particle size and stability in 12% serum is dependent on polymer type and the N/P (and w/w) ratios of polymer to DNA. E28/DNA particles show stability over a range of N/P ratios whereas D24/DNA complexes grow increasingly large based on their N/P ratio. E28/DNA particles were found to transfect well whereas D24/DNA particles were found to transfect poorly.

Table 4.1 shows the optimized polymer weight ratios (w/w), nitrogen to phosphate charge ratios (N/P), and biophysical parameters for the poly(β-amino ester) vectors in 12% serum-containing media. This table demonstrates that for efficient transfection of HUVECs in serum, a higher w/w ratio and N/P ratio was generally required as compared to our previous work in COS-7 cells without the presence of serum.[13] As previously mentioned, gene delivery particle sizes in PBS were all sub-150 nm, but in serum varied greatly from 200 nm to 1 um. Zeta potential was found to go from positive in PBS to negative in serum. This is likely due to negatively charged

serum proteins adsorbing to the positively charged nanoparticles and coating them to have an overall net negative surface charge.

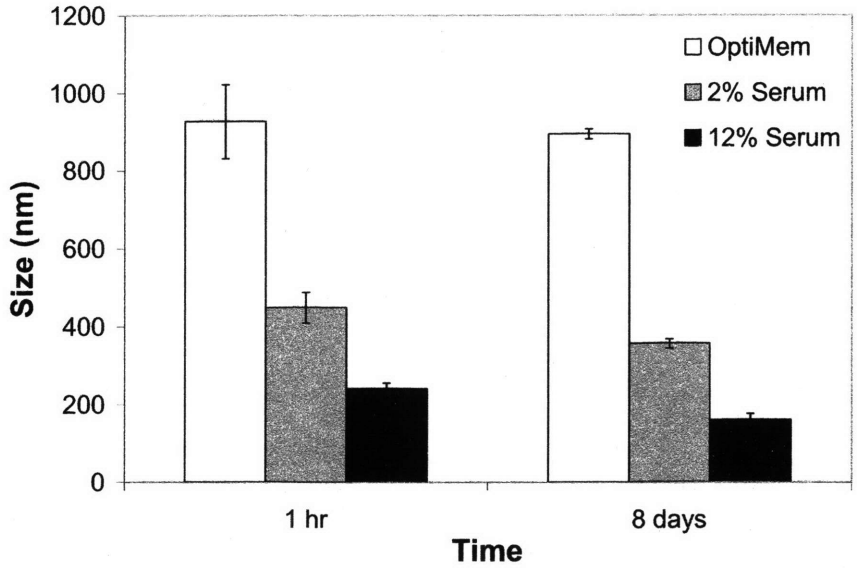


**Figure 4.5.** C32/DNA (50 w/w) particles are stable over a long time period while in various media conditions. Error bars are the standard deviations of triplicate samples.

Among the different types of polymers, zeta potential was found to vary depending on polymer type from near neutral to strongly negative. Interestingly, the difference in zeta potential and size between similar vectors in serum seems to correlate to single atom changes to their constitutive monomers. For example, at the same fixed N/P ratio of 60, JJ32 vectors have near neutral zeta potential and small size (-6 mV and 193 nm), JJ28, which has one less carbon on its amine monomer, forms larger, more negatively charged vectors (-14 mV and 226 nm), and JJ20, which is missing yet another carbon on its amine monomer forms vectors still more negative in charge and larger in size (-22 mV and 251 nm). JJ32, with the longest amine monomer chain

and forming the most neutral and smallest JJ-based particle overall, transfected best in serum followed next by JJ28 and lastly JJ20. This analysis highlights the use of a large polymeric library in elucidating structure/function relationships.

| Acrylate | Amine | MW | w/w | N/P | % Positive | Size (nm) | ζ Potential (mV) | HUVEC Rank | COS-7 Rank |
|---|---|---|---|---|---|---|---|---|---|
| C | 32 | 25101 | 100 | 110 | 46.9 | 236 | -13 | 1 | 1 |
| JJ | 32 | 19400 | 57 | 60 | 29.7 | 193 | -6.0 | 2 | 9 |
| E | 28 | 14300 | 38 | 40 | 25.8 | 199 | -14 | 3 | 11 |
| AA | 28 | 20900 | 40 | 30 | 13.8 | 206 | -4.9 | 4 | 7 |
| JJ | 28 | 16800 | 55 | 60 | 13.5 | 226 | -14 | 5 | 2 |
| AA | 24 | 5304 | 53 | 40 | 12.8 | 422 | -12 | 6 | 8 |
| AA | 20 | 16200 | 29 | 24 | 6.3 | 208 | -13 | 7 | 5 |
| U | 28 | 15600 | 147 | 120 | 2.9 | 327 | -10 | 8 | 4 |
| C | 28 | 27900 | 122 | 140 | 2.7 | 309 | -12 | 9 | 3 |
| D | 24 | 9542 | 47 | 30 | 0.3 | 913 | -12 | 10 | 10 |
| JJ | 20 | 20200 | 52 | 60 | 0.2 | 251 | -22 | 11 | 6 |

**Table 4.1** Optimized polymer weight ratios (w/w), nitrogen to phosphate charge ratios(N/P), biophysical parameters, and efficacy for poly(β-amino ester) vectors in 12%serum-containing media.

### *4.3.3 Luciferase Transfections*

Transfection experiments are commonly performed *in vitro* on immortal cancerous cell lines under serum-free conditions. Immortal cancerous cell lines are frequently chosen as they are easier to propagate and manipulate than primary cells, and are often easier to transfect. Primary endothelial cells in particular have been shown to have an intrinsic resistance to the uptake of exogenous genes compared to other cell lines.[6] Serum-free conditions are routinely employed to prevent unwanted electrostatic interactions between positively charged nanoparticles and

negatively charged serum proteins. Though these conditions are known to maximize *in vitro* transfection, they do not closely correspond to the conditions likely to be found *in vivo*.

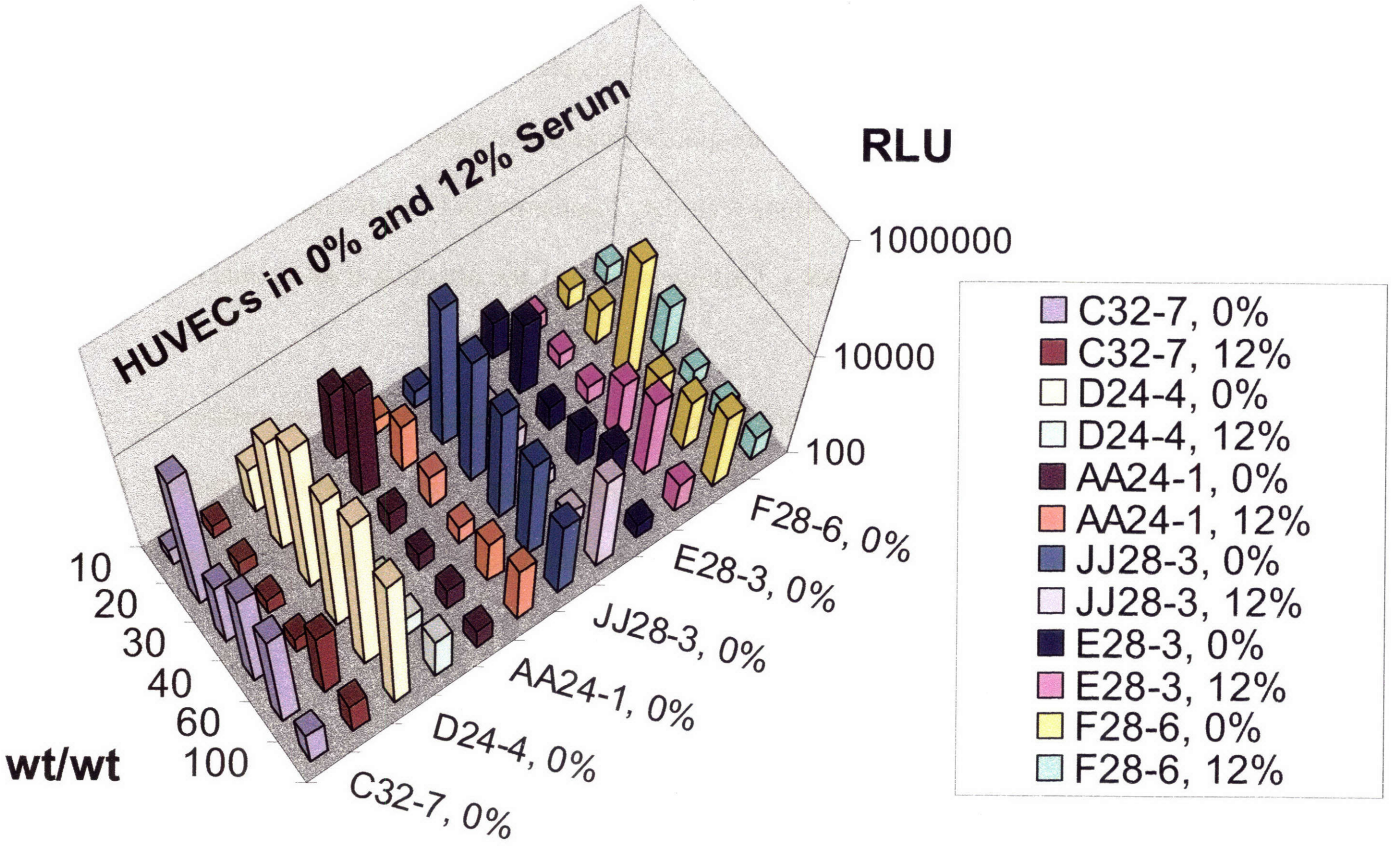


**Figure 4.6A.** High-throughput screening of vectors. At standard transfection conditions (300 ng DNA/well and 1 hr incubation) transfection is high in serum-free media, but poor in serum containing media.

Poly(β-amino ester)/DNA vector transfections to confluent HUVECs in 12% serum containing media were initially found to be relatively poor when using particle formulations optimized for serum-free media conditions. The differences in transfection performance among

several poly(β-amino ester)/DNA vectors in different media conditions as a function of polymer type, polymer to DNA w/w ratio, and DNA loading can be seen in Figure 4.6A-D. In these figures, optimal transfection of HUVECs in high-serum containing media occurs at much higher w/w ratios (and higher N/P ratios) than in non-serum containing media (polymers C32 and AA24). Other polymers like C28, are unable to transfect well in serum-containing media at any weight ratio tested even though they are quite efficacious in non-serum containing media. In non-serum conditions, peak transfection is relatively insensitive to DNA loading (300 ng vs. 600 ng per well) whereas the higher DNA loading is needed for effective transfection in serum-containing media.

These results highlight the differences in polymer vector design depending on the application conditions. Given the previous biophysical characterization results, it appears that particle size, stability, and surface charge changes are likely factors that are in part responsible for these differences in efficacy.

### *4.3.4 GFP Transfections*

While high-throughput screening gives a measurement of the total gene expression per microtiter plate well, this is an aggregate measurement without any information on individual cells. To learn the transfection efficacy to individual cells we used Fluorescent Activated Cell Sorting (FACS) and enhanced green fluorescent protein (GFP) DNA.

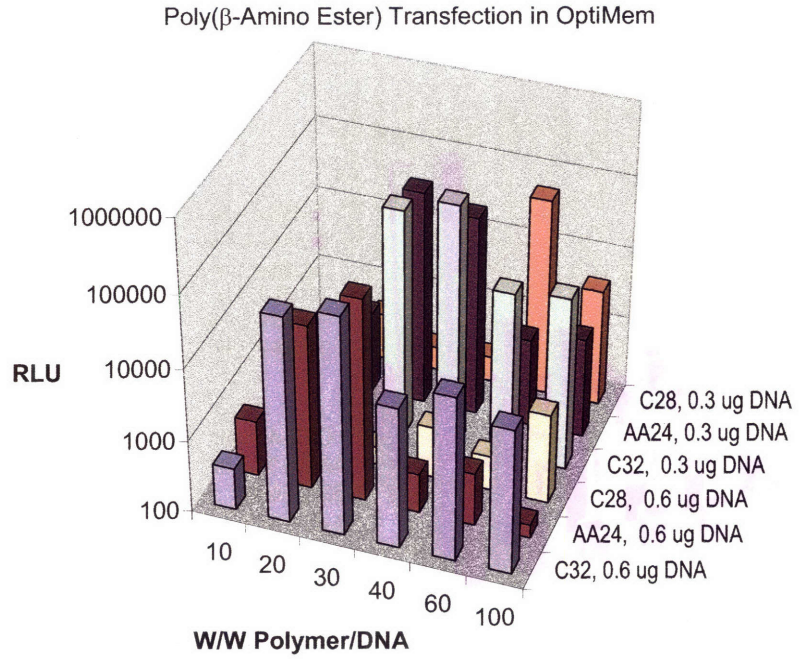


**Figure 4.6B and Figure 4.6C.** Optimal transfection (RLU) is dependent on DNA loading, polymer weight ratio (N/P ratio), type of polymer, and presence of serum.

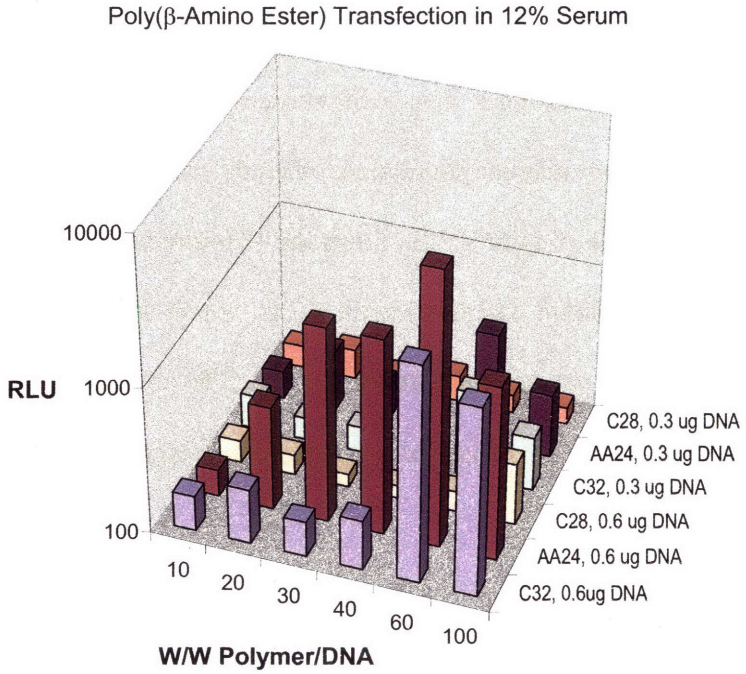

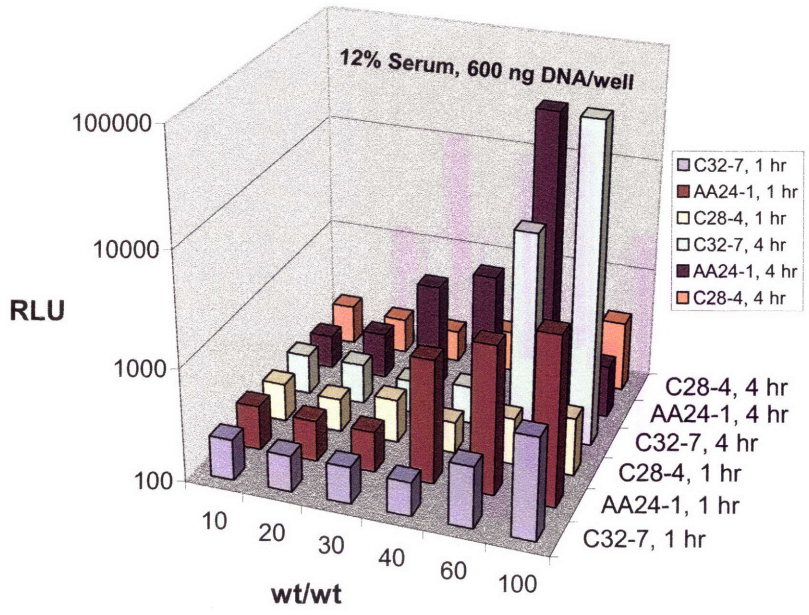


**Figure 4.6D.** High-throughput screening of vectors. A longer incubation time is necessary, but not sufficient, for high transfection in high-serum containing media.

FACS data was interpreted by using a two-dimensional density plot that compares the ratio of GFP channel fluorescence (x-axis) to yellow channel autofluorescence (y-axis). This method was chosen as it separates changes in autofluorescence from changes in actual GFP signal and divides the cells into two distinct populations, thereby reducing the over-counting of falsely positive cells. For example, Figure 4.7.B shows the two-dimensional density plot of a C32/DNA transfection as 45% positive whereas Figure 4.7.C, which shows a one-dimensional histogram of the same experiment, would count the cells to be 57% positive. All FACS results of poly(β-amino ester) vectors and control vectors were calculated using this more conservative two-dimensional analysis.

The best previously known transfecting polymers from the poly(β-amino ester) library[13] were re-optimized for transfecting HUVECs in high-serum and the results are shown in Figure

4.8.. This figure demonstrates that high transfection to COS-7 cells in the absence of serum is not a guarantee of efficacy to primary human endothelial cells in serum. However, Figure 4.8. also demonstrates that several poly(β-amino ester) vectors were indeed found to transfect HUVECs at high levels, particularly polymers C32, JJ32, and E28.

Interestingly, the best performing polymers all share a near identical structure, and single molecular differences in the polymers' structure were found to correlate to transfection efficacy. For example, polymers formed with C, JJ, and E differ by only the length of their acrylate monomer carbon chain (4, 5, and 6 carbons respectively). Similarly, polymers formed with 20, 28, and 32 differ by only the length of their amine monomer carbon chain (3, 4, and 5 carbons respectively). Yet, these small changes to molecular structure lead to dramatic differences in transfection efficacy. For example, increasing the length of the number of carbons in the constituent amine monomer was found to correlate to increased transfection efficacy. Polymers formed with the same acrylate monomer but different length amine monomers, transfected differentially according to length: 32 (5 carbons) > 28 (4 carbons) > 24 (3 carbons + hydroxyl group) > 20 (3 carbons). It has been reported that amine groups on a polymer are functionally responsible for the ability of a gene delivery vector to bind and unpack DNA[25] and to buffer the endosome to promote osmotic swelling and rupture.[26] We hypothesize that that the seemingly small changes to constituent amine monomer length may play a role in at least one of these gene delivery bottlenecks. This analysis highlights the utility of a combinatorial library approach to designing a non-viral gene delivery vector, as similarly structured, but functionally different vectors can be obtained and analyzed.

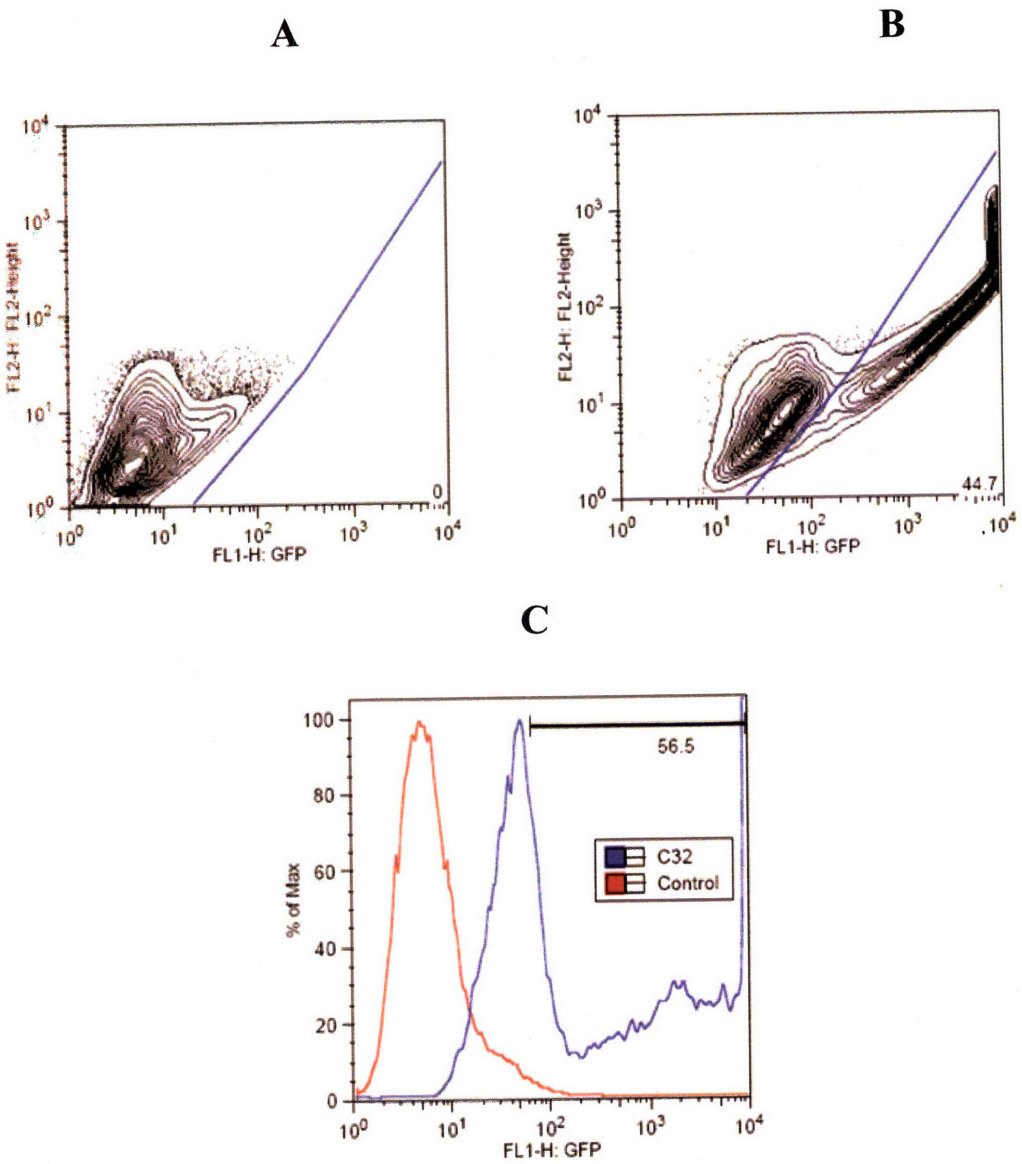


**Figure 4.7.** (A) FACS density plot and gating for negative control (0% positive) and comparison to (B) C32/DNA vector transfection (44.7% positive). Ratio of GFP fluorescence (x-axis) to background fluorescence (y-axis) was used to accurately gate positive cells. (C) The same FACS data shown in a one-dimensional histogram plot. C32/DNA transfected cells (56.5% positive) includes some falsely positive cells that are excluded during the two-dimensional analysis used in Figure 4.7.B.

The ranked order of the efficacy of these polymers shows similarities and differences between the two cell systems tested. Table 4.1 shows relative effectiveness of poly(β-amino ester) vector transfections to HUVECs in high-serum media versus transfections to COS-7 cells in OptiMem based on our previous work.[13] Generally, higher w/w ratios of polymer to DNA (and correspondingly higher N/P ratios) were needed for effective delivery in high-serum containing media. Polymer C32 was reinforced as the lead poly(β-amino ester) vector, but interestingly other vectors performed differentially between these two cells types. C28 and U28 were previously found to be in the top 5 transfecting vectors of the whole class, but were found to transfect HUVECs in serum rather poorly. In contrast, JJ32 and E28 which were previously seen as mediocre vectors, were found to transfect HUVECs in serum with high efficacy. These findings demonstrate that a vector able to transfect well in serum-free conditions may not necessarily transfect human primary cells well in high-serum conditions.

High transfection in serum-free OptiMem with poly(β-amino ester) vectors may be due in part to large particle size and positive surface charge, both promoting physical interaction of the gene delivery complexes with cells through sedimentation and attractive electrostatic forces respectively. However in serum containing media, zeta potential of these particles is neutral to negative and particle size changes according to weight ratio and polymer material properties as previously indicated in the biophysical characterization section. Thus, serum interactions are potentially responsible for poorer transfection by reducing particle uptake. This hypothesis was furthered by experiments that varied particle incubation time and found that in OptiMem or serum-free media, a one hour incubation is sufficient for high expression, whereas in serum-containing media, a four hour incubation is necessary (but not sufficient) to achieve high expression.

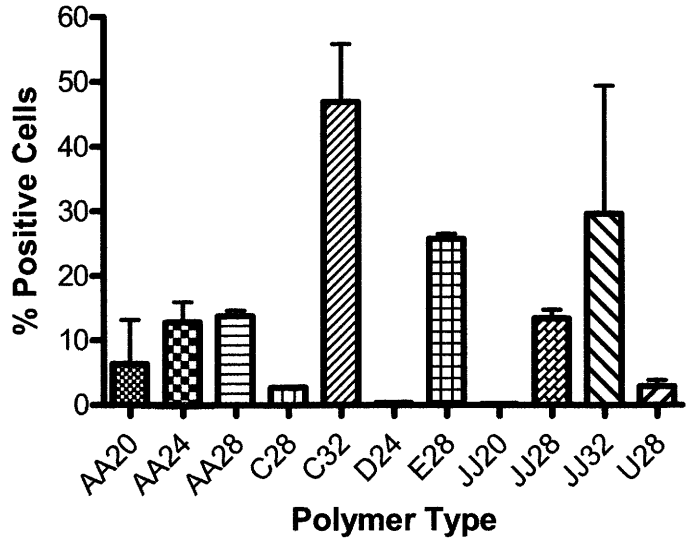


**Figure 4.8.** HUVEC FACS transfection results in 12% serum media. Each polymer type is shown at its optimal polymer weight to DNA weight (w/w) ratio. Error bars are standard deviations.

Biophysical properties of the particles in serum were found to correlate to HUVEC transfection in serum whereas biophysical properties in buffer were unable to give the same predictive information. For example, as mentioned above, all poly(β-amino ester) vectors tested were able to condense DNA into small nanoparticles below 150 nm while in buffer, but some vectors such as C32, JJ32, and E28 formed small, stable particles while in high-serum containing media, whereas other vectors such as D24, aggregated in serum to form large particles in the micron range. C32, JJ32, and E28 were found to be the highest transfecting vectors for HUVECs in serum whereas D24 and other aggregating polymers were found to transfect much more poorly. The top five performing polymeric vectors in serum formed particles in the 193-236 nm range whereas the bottom performing polymers tended to form particles larger than 250 nm in the presence of high-serum containing media. Thus, the formation of small, stable gene

delivery particles in serum was found to be predictive for high efficacy in serum containing media and the formation of large and/or aggregating particles in serum was found to correlate to poor efficacy. On the other hand, particle size of these polymers in buffer was not found not to be predictive of transfection performance in serum.

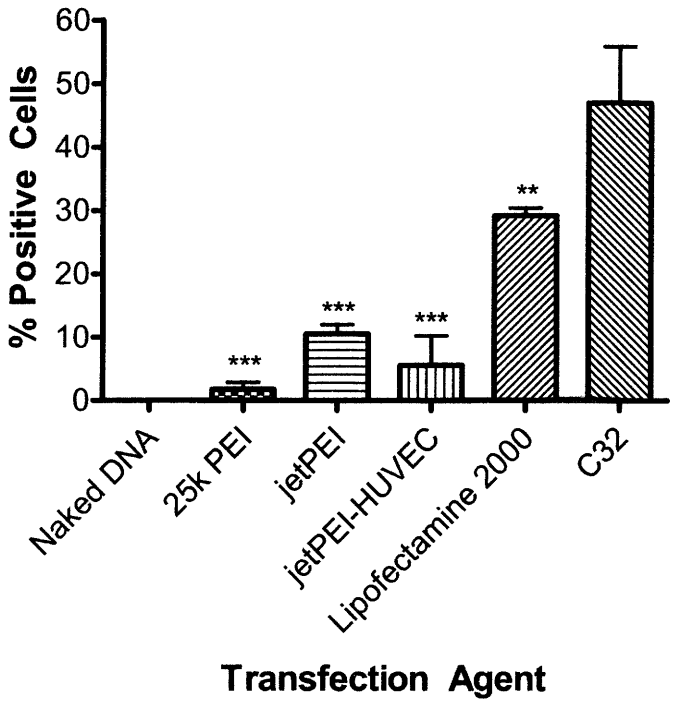


**Figure 4.9.** Comparison of vectors for HUVEC transfection in 12% serum-containing media. Each vector is shown at its optimal formulation. Error bars are standard deviations ($n \geq 4$). As compared to C32, (**) and (***) indicate statistical significance of $p<0.01$ and $p<0.001$ respectively.

As compared to other top commercially available non-viral transfection vectors, poly(β-amino ester) vectors as a class, and C32 in particular, were found to be very efficacious. Figure 4.9. compares the best-performing poly(β-amino ester), C32, to other commonly used non-viral vectors. Polymeric vector C32 averages 47±9% positively transfected HUVECs which is

statistically significant versus the control vectors 25k PEI (2±1%, $p<0.001$ ), jetPEI (11±2%, $p<0.001$), jetPEI-HUVEC (6±5%, $p<0.001$), and Lipofectamine 2000 (29±1%, $p<0.01$).

Other researchers have recently shown that tetraglucose-grafted L-PEI (jetPEI-HUVEC) is a top performing non-viral transfection agent for transfection of HUVECs as compared to other commercially available reagents.[27] To our knowledge, C32 and other poly(β-amino ester) vectors can transfect HUVECs significantly higher than any reported non-viral vector system. It is important to note that this high transfection took place under conditions generally seen as difficult for *in vitro* transfection, but important for an *in vivo* cardiovascular application: fully confluent primary cells in the presence of a high concentration of serum proteins. The percentage of HUVECs positively transfected by C32 approach those achieved with viral systems. Recently, 70% *in vitro* transfection of HUVECs was reported by using an engineered vesicular stomatis virus G-protein (VSV-G)-pseudotyped lentiviral vector and a nuclear localizing signal (NLS) tagged lacZ gene.[28] Improvements to C32 to allow for cellular targeting and nuclear targeting are hypothesized to further narrow this gap between viral and non-viral vectors.

### *4.3.5 Cell Viability*

We have previously shown that poly(β-amino ester) vectors are biodegradable and generally non-cytotoxic.[16, 18] In this study, C32 was non-cytotoxic to HUVECs. Figure 4.10. shows the cell viability of HUVECS transfected with C32 gene delivery particles as compared to non-transfected controls. Over a range of polymer to DNA w/w ratios and DNA loadings, C32/DNA vectors were determined to be non-cytotoxic. In comparison, jetPEI particles are

found to be cytotoxic, particularly at high concentrations of gene delivery particles and higher DNA loading. It is also interesting to note that the C32/DNA particles are non-cytotoxic at polymer concentrations as high as ~500 ug/mL (600 ng DNA, 120 w/w C32) over two orders of magnitude more concentrated than when jetPEI shows cytotoxicity, indicating the relative safety of poly(β-amino esters). Of note, C32 has been shown to have good in vivo biocompatibility,[12] in contrast to certain viral systems.[29]

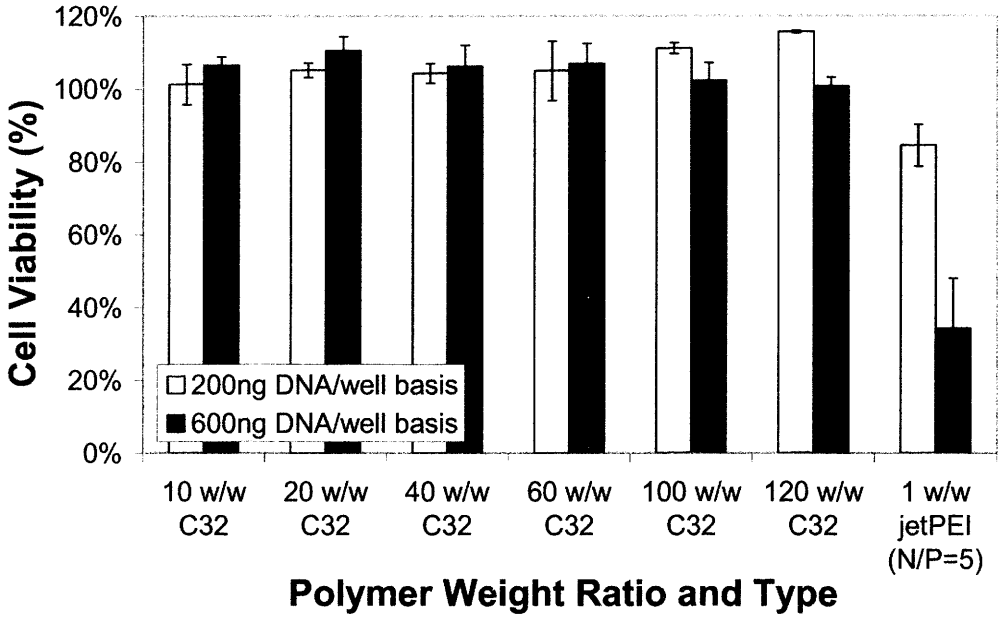


**Figure 4.10.** Poly(β-amino ester) C32 is non-cytotoxic to HUVECs in contrast to the premiere commercially available polymeric vector jetPEI. Error bars are the standard deviations of quadruplicate samples.

## 4.4 CONCLUSIONS

We have demonstrated that poly(β-amino esters) as a class, and C32 specifically, transfect human primary endothelial cells better than several leading commercially available reagents. We have determined that these particles have high efficacy, are stable in the presence of serum proteins, and are non-cytotoxic. It was also demonstrated that analyzing biophysical properties of poly(β-amino ester)/DNA complexes including size, stability, and zeta potential in the proper media conditions and dynamically over time provides good correlation to transfection efficacy and can pick up phenomenon missed when biophysical particle properties are only tested in buffer. We optimized vector parameters including DNA loading and polymer to DNA weight ratio and determined efficacy with and without serum-containing media. As biodegradable polymers have certain safety advantages over viruses, poly(β-amino ester) gene delivery vectors may prove useful in various clinical applications.

## 4.5 REFERENCES


1. Nabel, E.G. Gene therapy for cardiovascular diseases. *Journal of Nuclear Cardiology* **6**, 69-75 (1999).
2. Shah, P.B. & Losordo, D.W. Non-viral vectors for gene therapy: clinical trials in cardiovascular disease. *Adv Genet* **54**, 339-361 (2005).
3. Jones, J.M. & Koch, W.J. Gene therapy approaches to cardiovascular disease. *Methods Mol Med* **112**, 15-35 (2005).

4. Segura, I. et al. Inhibition of programmed cell death impairs in vitro vascular-like structure formation and reduces in vivo angiogenesis. *FASEB J* **16**, 833-841 (2002).

5. Muller, K., Nahde, T., Fahr, A., Muller, R. & Brusselbach, S. Highly efficient transduction of endothelial cells by targeted artificial virus-like particles. *Cancer Gene Ther* **8**, 107-117 (2001).

6. Suh, W., Han, S.O., Yu, L. & Kim, S.W. An angiogenic, endothelial-cell-targeted polymeric gene carrier. *Mol Ther* **6**, 664-672 (2002).

7. Kay, M.A., Glorioso, J.C. & Naldini, L. Viral vectors for gene therapy: the art of turning infectious agents into vehicles of therapeutics. *Nature Medicine* **7**, 33-40 (2001).

8. Partridge, K.A. & Oreffo, R.O.C. Gene delivery in bone tissue engineering: Progress and prospects using viral and nonviral strategies. *Tissue Eng* **10**, 295-307 (2004).

9. Merdan, T., Kopecek, J. & Kissel, T. Prospects for cationic polymers in gene and oligonucleotide therapy against cancer. *Adv Drug Delivery Rev* **54**, 715-758 (2002).

10. Wagner, E., Kircheis, R. & Walker, G.F. Targeted nucleic acid deliver into tumors: new avenues for cancer therapy. *Biomed Pharmacother* **58**, 152-161 (2004).

11. Anderson, D.G., Lynn, D.M. & Langer, R. Semi-automated synthesis and screening of a large library of degradable cationic polymers for gene delivery. *Ang. Chem. Int. Edn* **42**, 3153-3158 (2003).

12. Anderson, D.G. et al. A polymer library approach to suicide gene therapy for cancer. *Proc. Natl. Acad. Sci. U.S.A.* **101**, 16028-16033 (2004).

13. Anderson, D.G., Akinc, A., Hossain, N. & Langer, R. Structure/property studies of polymeric gene delivery using a library of poly(beta-amino esters). *Mol Ther* **11**, 426-434 (2005).

14. Akinc, A. & Langer, R. Measuring the pH environment of DNA delivered using nonviral vectors: Implications for lysosomal trafficking. *Biotechnol Bioeng* **78**, 503-508 (2002).

15. Lynn, D.M., Anderson, D.G., Putnam, D. & Langer, R. Accelerated discovery of synthetic transfection vectors: parallel synthesis and screening of a degradable polymer library. *J Am Chem Soc* **123**, 8155-8156 (2001).

16. Lynn, D.M. & Langer, R. Degradable poly(beta-amino esters): Synthesis, characterization, and self-assembly with plasmid DNA. *J Am Chem Soc* **122**, 10761-10768 (2000).

17. Akinc, A., Anderson, D.G., Lynn, D.M. & Langer, R. Synthesis of poly(beta-amino ester)s optimized for highly effective gene delivery. *Bioconjug Chem* **14**, 979-988 (2003).

18. Akinc, A., Lynn, D.M., Anderson, D.G. & Langer, R. Parallel synthesis and biophysical characterization of a degradable polymer library for gene delivery. *J Am Chem Soc* **125**, 5316-5323 (2003).

19. Ogris, M. et al. The size of DNA/transferrin-PEI complexes is an important factor for gene expression in cultured cells. *Gene Ther* **5**, 1425-1433 (1998).

20. Guo, W. & Lee, R.J. Efficient gene delivery via non-covalent complexes of folic acid and polyethylenimine. *J Control Release* **77**, 131-138 (2001).

21. Boussif, O. et al. A versatile vector for gene and oligonucleotide transfer into cells in culture and in vivo: polyethylenimine. *Proc Natl Acad Sci U S A* **92**, 7297-7301 (1995).

22. Thomas, M. & Klibanov, A.M. Non-viral gene therapy: polycation-mediated DNA delivery. *Appl Microbiol Biotechnol* **62**, 27-34 (2003).

23. Zuber, G., Dauty, E., Nothisen, M., Belguise, P. & Behr, J.P. Towards synthetic viruses. *Adv Drug Delivery Rev* **52**, 245-253 (2001).

24. Ogris, M., Steinlein, P., Carotta, S., Brunner, S. & Wagner, E. DNA/polyethylenimine transfection particles: Influence of ligands, polymer size, and PEGylation on internalization and gene expression. *Aaps Pharmsci* **3**, art. no. 21 (2001).

25. Schaffer, D.V., Fidelman, N.A., Dan, N. & Lauffenburger, D.A. Vector unpacking as a potential barrier for receptor-mediated polyplex gene delivery. *Biotechnol Bioeng* **67**, 598-606 (2000).

26. Akinc, A., Thomas, M., Klibanov, A.M. & Langer, R. Exploring polyethylenimine-mediated DNA transfection and the proton sponge hypothesis. *Journal of Gene Medicine* **7**, 657-663 (2005).

27. Zaric, V. et al. Effective polyethylenimine-mediated gene transfer into human endothelial cells. *J Gene Med* **6**, 176-184 (2004).

28. Totsugawa, T. et al. Successful lentivirus-based delivery of a LacZ gene into human endothelial cells. *Transplant Proc* **35**, 499-500 (2003).

29. Thomas, C.E., Ehrhardt, A. & Kay, M.A. Progress and problems with the use of viral vectors for gene therapy. *Nat Rev Genet* **4**, 346-358 (2003).

# Chapter 5: Nanoparticle Coatings for Ligand-Specific Delivery*

## 5.1 INTRODUCTION

Gene therapy has the potential to treat many diseases including cancer and cardiovascular disease, but it is currently limited by the inability to deliver genes in a safe and effective manner. Delivering genes specifically to targeted cells and/or tissues is also particularly challenging. Here, we demonstrate a general approach for coating nanoparticles to functionalize them for ligand-specific delivery to human primary cells. Though we have used DNA as the drug cargo in this application, this nanoparticle coating method may be general enough to be used with other payloads and other charged nanoparticles.

Viral gene delivery is currently plagued by multiple problems including acute toxicity, cellular immune response, oncogenicity due to insertional mutagenesis, limited cargo capacity, resistance to repeated infection, and production and quality control issues.[1,2] Non-viral vector nanoparticles have been formed with numerous biomaterials including calcium phosphate, cationic lipids, cationic polymers, dendrimers, and cyclodextrins, but although generally safer than viruses, these methods have much lower transfection efficacy.[3] Recently, a large library of 2350 structurally unique poly(β-amino esters) was developed using high-throughput

* Reproduced with permission from *Nano Letters* 7(4), 874-879. ©2007 American Chemical Society

combinatorial methods.[4] These polymers have shown considerable promise for drug delivery both in vitro and in vivo.[5-9]

A number of methods for functionalizing nanoparticles have been tested. For example, commonly used gene delivery polymers, such as polylysine and polyethylenimine (PEI), have been covalently modified to include poly(ethylenegylcol) (PEG) and/or targeting ligands such as EGF[10], transferrin[11] and RGD[12,13] peptide to promote specific uptake. The results of these experiments have been mixed, with some researchers demonstrating dramatically improved targeting and others showing little improvement.[11-15] Peptides containing the amino acid sequence Arg-Gly-Asp (RGD) can be used for specific targeting to integrin receptors, including the vitronectin receptor $\alpha v\beta 3$, which is known to be highly upregulated in certain tumors.[13]

One of the problems with covalently coupling targeting ligands to a polymer is that it can change the biophysical properties of that polymer and the corresponding polymer/DNA nanoparticle. For example, several researchers have found that as ligand substitution (either targeting or shielding) increases, overall gene delivery can decrease, presumably due to alteration of the original polymer's functionality for DNA condensation and endosomal buffering.[14,16] Furthermore, gene delivery nanoparticles are generally positively charged, and these positively charged nanoparticles are taken up non-specifically.[15] Cell-specific nanoparticulate delivery requires both specific uptake by the target cell and inhibition of delivery to non-specific cell types. Coatings that reduce the positive charge of gene delivery nanoparticles could potentially reduce this non-specific uptake while still enabling receptor-mediated uptake. Gene delivery nanoparticles at overall neutral or negative charge may also be desirable to prevent unwanted serum interactions.[17]

Here, we show that electrostatic interactions can drive peptide coating of nanoparticles and enable ligand-specific gene delivery to human primary cells. Our general approach to electrostatically coat gene delivery nanoparticles with ligands provides a simple method of ligand addition as well as a mechanism to neutralize nanoparticle charge. These coatings reduce non-specific delivery to HUVECs and may similarly affect other cell types. While we use RGD-containing peptide as a model system to investigate nanoparticle coating and ligand-specific delivery to primary endothelial cells, many other peptide ligand sequences, such as those made from antibody fragments, could potentially be readily incorporated into this system as well.

## 5.2 EXPERIMENTAL PROCEDURES

### *5.2.1 Cell Culture*

Human Umbilical Vein Endothelial Cells (HUVECs) (Cambrex, Walkersville, MD, USA) were cultured in EGM-2 media supplemented with SingleQuot Kits (Cambrex). HUVEC cells were used by passage five and in accordance to the manufacturer's instructions. Cells were grown at 37°C at a humid 5% $CO_2$ atmosphere.

### *5.2.2 Polymer Synthesis*

Monomers were purchased from Aldrich (Milwaukee, WI, USA) and Scientific Polymer (Ontario, NY, USA). An optimal amine/diacrylate stoichiometric ratio of 1.2:1 for C32 was determined from previous work.[6] To synthesize C32, 400 mg of 5-aminopentanol was weighed into a 1 mL sample vial with a Teflon-lined screw cap. Next, 640 mg of 1,4-butanediol diacrylate was added to the vial along with a small Teflon-coated stir bar. The monomers were then polymerized on a magnetic stir-plate residing in an oven at 95°C for 1 day. After completion of reaction, the vial was removed from the oven and stored at 4°C. C32 was analyzed by gel-permeation chromatography (GPC) as previously described.[1]

### *5.2.3 Peptide-Coated Polymeric Nanoparticles*

Non-viral gene delivery nanoparticles are formed through electrostatic interactions between poly(β-amino ester) C32 and plasmid DNA encoding pEGFP, enhanced green fluorescent protein (ElimBiopharmaceuticals, South San Francisco, CA, USA). To ease handling, polymer and peptide stock solutions (100 mg/ml) were prepared in DMSO solvent prior to use. Working dilutions of polymer and peptide were prepared in 25 mM sodium acetate buffer (pH 5). To form nanoparticles, 75 μL of diluted polymer (5.52-9.20 μg/μL in 25 mM NaAc depending on polymer to DNA weight ratio) was added to 75 μL of DNA (0.184 μg/μL in 25 mM NaAc), mixed well, and then the mixture was incubated at room temperature for 10 min. 75 μL of anionic peptide solution or buffer only control (0-10.7 μg/μL in 25 mM NaAc) EEEEEEEEEEEEGGGGGGGRGDS or EEEEEEEEEEEEGGGGGGGRDGS (MIT

Biopolymers Laboratory, Cambridge, MA) was then mixed with the cationic nanoparticles and the nanoparticles were incubated at room temperature for an additional 5 min. At a fixed basis of DNA and polymer, by varying the weight of peptide coating, the charge ratio was varied.

Polyethylenimine (PEI) (Branched, $M_w \sim 25{,}000$ Da, Sigma-Aldrich) and Lipofectamine 2000™ (Invitrogen) were used as gene delivery positive controls. PEI/DNA vectors were formed at a 1:1 polymer to DNA weight ratio (N/P=8) using the same DNA basis and protocol used with C32/DNA particles except that PEI/DNA particles were formed in 150 mM NaCl as previously described.[24] Lipofectamine™ 2000 was used following manufacturer instructions.

### *5.2.4 Transmission Electron Microscopy (TEM)*

Nanoparticles were formed as they were for transfection experiments and then single drops of nanoparticle solution were dropped on to TEM Cu grids coated with carbon film. TEM microstructure was determined using a JEOL 200CX operating at 200kV.

### *5.2.5 Agarose Gel Electrophoresis Retardation Assay*

Polymer/DNA nanoparticles with or without peptide coatings were prepared as described above and run on a 1% agarose gel (TAE buffer, 110 V, 1hr). The free DNA control and the nanoparticles in buffer were loaded at a concentration of 1 μg DNA per well. The nanoparticles in 12% serum media were diluted in serum media and were then loaded at a concentration of 250

ng DNA per well. DNA bands were visualized by ethidium bromide staining. Free DNA is able to migrate through the gel and encapsulated DNA is unable to migrate through the gel.

### *5.2.6 Biophysical Characterization*

Particle size and ζ potential measurements were measured by using a ZetaPALS dynamic light scattering detector (Brookhaven Instruments Corp., Holtsville, NY, USA, 15-mW laser, incident beam 676 nm). Correlation functions were collected at a scattering angle of 90°, and particle sizes were calculated using the MAS option of BICTs particle sizing software (version 2.30) using the viscosity and refractive index of water at 25°C. Particle sizes are expressed as effective diameters assuming a log-normal distribution. Average electrophoretic mobilities were measured at 25°C using BIC PALS ζ potential analysis software, and ζ potentials were calculated using the Smoluchowsky model for aqueous suspensions.

Samples were prepared for biophysical characterization in the same manner and at the same concentrations as they were for transfections, but the media/polymer/DNA/peptide solution was scaled up to a final volume of 1.6 mL. Particle stability was determined by changes to particle size over time.

### *5.2.7 GFP Transfections*

Non-viral nanoparticle transfections were performed on confluent HUVECs in the presence of 12% serum. HUVECs were seeded (75,000 cells/well) into clear 24-well plates

(Becton Dickinson, Franklin Lakes, NJ, USA) at 24 hours prior to transfection to allow for growth to confluence. Nanoparticles were constructed as previously mentioned above creating a polymer/DNA/peptide nanoparticle solution containing a DNA basis of 0.0613 μg/μL in 25 mM NaAc buffer. To transfer 6 μg DNA as a final DNA dose per well, 150 μL of this nanoparticle solution was first added to 1.00 mL of FBS supplemented EGM-2 media (12% Serum). The growth medium was next removed from the seeded cells using a 6-channel aspirating wand (V&P Scientific, San Diego, CA, USA) after which 750 μL of the nanoparticle/media solution was immediately added. Nanoparticles were incubated with the cells for 4 hours and then removed using the 6-channel wand and replaced with 500 μL of warm EGM-2 media. After 48 hrs, transfected and untransfected control cells were washed, removed from the 24-well plates by trypsinization, microcentrifuged, and resuspended in 500 μL of FACS running buffer (98% PBS / 2% FBS / 1:200 propidium iodide solution (Invitrogen)) for FACS analysis. To confirm integrin receptor-mediated gene delivery of the RGD coated nanoparticles, fibronectin active fragment peptide RGDS (Peptides International, Louisville, KY, USA), an integrin binding competitor, was added at 100 nM to the cell media prior to transfection. Following the standard 4 hr incubation with the gene delivery nanoparticles, the RGDS containing media was removed using a 6-channel wand and replaced with 500 μL of warm EGM-2 media.

### *5.2.8 Flow Cytometry*

GFP expression was measured using Fluorescence Activated Cell Sorting (FACS) on a FACSCalibur (Becton Dickinson, San Jose, CA, USA). Propidium iodide staining was used to exclude dead cells from the analysis and 20,000 live cells per sample were acquired. Two-

dimensional gating was used to separate increased autofluorescence signal (y-axis) from increased GFP signal (x-axis) to more accurately count positively expressing cells. Gating and analysis was performed using FlowJo 6.3 software (TreeStar, Ashland, OR, USA) using untransfected cells as the primary negative control. For an additional negative control, 50 w/w ratio C32/DNA nanoparticles were assembled using a luciferase-encoding plasmid, pCMV-Luc, rather than the typical EGFP-encoding plasmid (ElimBiopharmaceuticals, South San Francisco, CA, USA). The FACS gating for these nanoparticles is shown in Figure 4.7.B.

### *5.2.9 Cell Viability Measurements*

To measure cytotoxicity and cell viability, cellular metabolic activity was measured using the Cell Titer 96 Aqueous One Solution assay kit (Promega , Madison, WI, USA). Transfections were performed as described above for 24-well plates, but scaled down five-fold. Metabolic activity was measured using optical absorbance on a Victor3 Multilabel plate counter (Perkin Elmer Life Sciences, Boston, MA, USA). Measurements of treated cells were converted to percent viability by comparison to untreated controls. HUVECs were treated with a wide range of nanoparticle formulations including a DNA basis of 200 ng – 1200 ng per well, 50 wt/wt ratio C32, and 1.35-55.0 overall N/P ratio depending on level of E12-RGD or E12-RDG coating. Cell viability was determined to be 80%-100% depending on dose.

## 5.3 RESULTS AND DISCUSSION

### *5.3.1 Nanoparticle Formation and Peptide Coating*

Polymer C32 is synthesized by the conjugate addition of 5-aminopentanol to 1,4-butanediol diacrylate. The acrylate and amine monomers used in this experiment and their synthesis scheme can be seen in Figure 5A. Cationic polymeric gene delivery nanoparticles were formed in sodium acetate buffer solution through self-assembly of C32 with plasmid DNA.

**A**

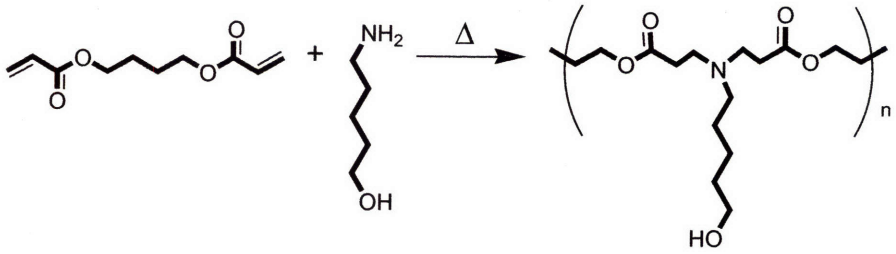


**B**

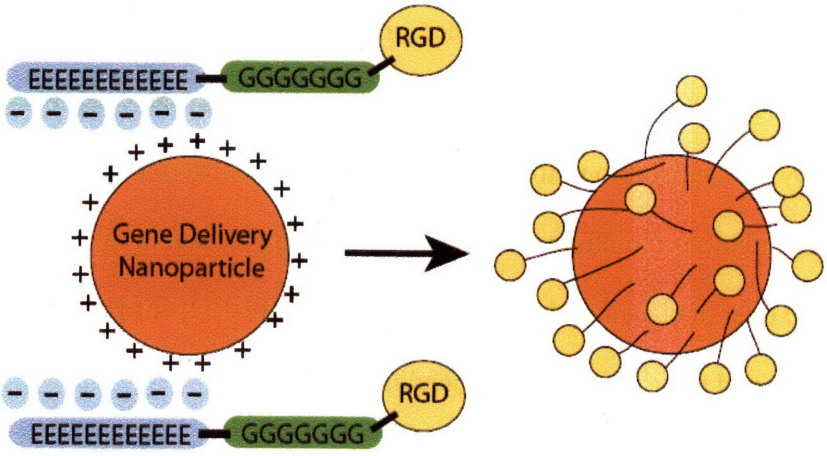


**Figure 5.1.** Synthesis Schemes. (A) Poly(β-amino ester) C32 structure and synthesis; (B) Electrostatic self-assembly of ligand coated nanoparticle.

After a 10 min incubation period, anionic peptide was added to electrostatically coat the cationic nanoparticles as demonstrated in Figure 5B. As this self-assembly is driven simply by opposing electrostatic charge, virtually any other cationic polymer (polyethylenimine, poly(β-amino ester), or other) could be potentially used to form similarly coated nanoparticles. The peptide sequence EEEEEEEEEEEEGGGGGGGRGDS (E12-RGD) was used as a sequence with specific binding to integrin receptors expressed by HUVECs and the near-identical peptide sequence EEEEEEEEEEEEGGGGGGGRDGS (E12-RDG) was used as a non-integrin binding control sequence.[18] As the actual fraction of protonated amines in cationic polymeric gene delivery systems is not typically known, charge ratio is frequently reported as a ratio of amine groups on the cationic polymer (N) to phosphate groups on the anionic plasmid DNA (P). Here, we slightly modify the N/P ratio to also include the carboxylic acid groups on the anionic peptide in a manner analogous to what has been done previously[19]:

$$N/P = \frac{[N]}{[P]+[COO^-]}$$

We use w/w to refer to the weight ratio balance between the polymer and DNA (μg/μg), whereas N/P refers to the overall charge ratio of the nanoparticles, which can vary with peptide coating composition at a fixed polymer/DNA w/w ratio. The molecular weight of the polymer C32 has been previously optimized[6] and is not varied in these experiments. The molecular weight of the peptide coating is varied by the number of the glutamic acid residues: 8, 12, 16, 20, with the glycine linker and RGD/RDG ligand remaining fixed.

To verify the formation and particle integrity of the nanoparticles, transmission electron microscopy (TEM) was performed (Figure 5.2.). The nanoparticles were coated with peptide and incubated in media prior to imaging. Dried particles were determined to be ~100 nm in size. To determine DNA encapsulation efficiency, uncoated and coated nanoparticle formulations

were tested by gel electrophoresis (Figure 5.3.). For all nanoparticle formulations tested (30 w/w, 40 w/w, and 50 w/w C32/DNA nanoparticles), no free DNA was detected, indicating 100% encapsulation of DNA. The presence of ligand coatings and/or serum media did not change this DNA encapsulation.

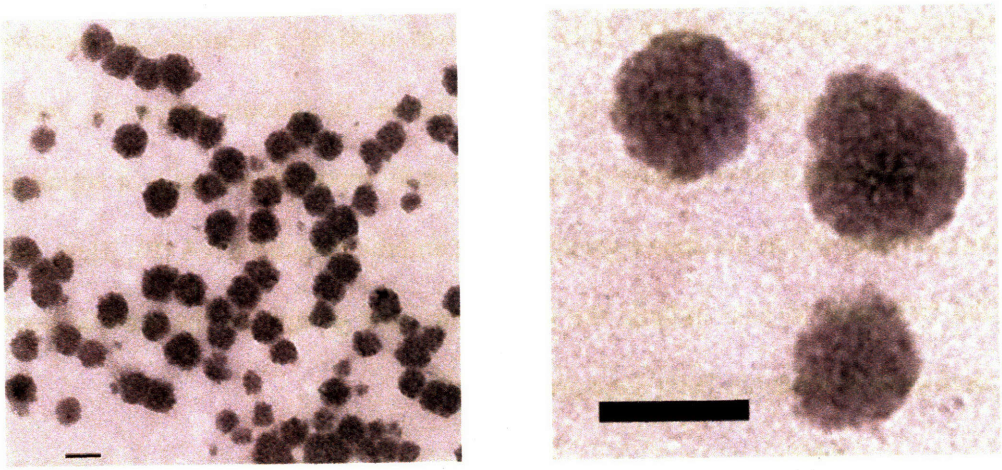

**Figure 5.2.** 40 w/w C32 particles coated with 19 w/w E12RGD in serum media. Scale Bar is 100 nm in both figures.

### *5.3.2 Biophysical Characterization*

Previously, we have demonstrated that the size and ζ potential of gene delivery nanoparticles can change depending on the type of aqueous environment in which they are analyzed. Furthermore, we have also shown that these changes to biophysical properties directly

affect transfection efficacy.[20] Thus in these experiments, the nanoparticles were measured in the actual conditions used during transfection, 12% serum-containing media.

Figure 5.4. shows the size and stability of the C32/DNA nanoparticles with and without peptide coating over time. Gene delivery particles are prepared at the same concentrations as they are for typical *in vitro* bio-assays. This figure demonstrates that particles formed at 40 w/w

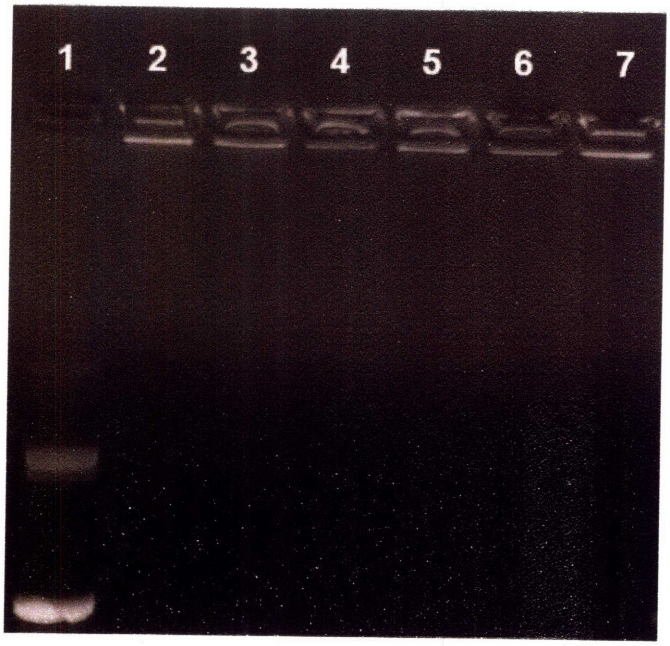


**Figure 5.3.** Gel showing full DNA encapsulation of particles. (1) DNA only control, (2) 30 w/w C32/DNA particles, (3) 40 w/w C32/DNA particles, (4) 50 w/w C32/DNA particles, (5) 40 w/w C32/DNA + 19 w/w RGD coated particles, (6) 40 w/w C32/DNA particles in serum media, (7) C32/DNA + 19 w/w RGD coated particles in serum media.

and 50 w/w C32/DNA have a small size of ~200 nm and are stable in serum over time. The diameter determined by dynamic light scattering in solution is larger than the ~100 nm size found by TEM of dried samples. This is likely due to the difference in size of the hydrated polymeric nanoparticle versus the dried particle. Coated 50 w/w C32/DNA particles were

determined to be 27.2 – 32.8 nm larger than uncoated particles and coated 40 w/w C32/DNA particles were 36.8 – 60.7 nm larger than uncoated particles (95% CI). Importantly, coated nanoparticles have a stable, small size in 12% serum-containing media over time. Thus, E12-RGD coating slightly increases particle size while maintaining serum stability. Small size and serum stability are conditions necessary for many therapeutic *in vivo* applications.[3] Particle stability is also advantageous for consistent transfections and for storage.

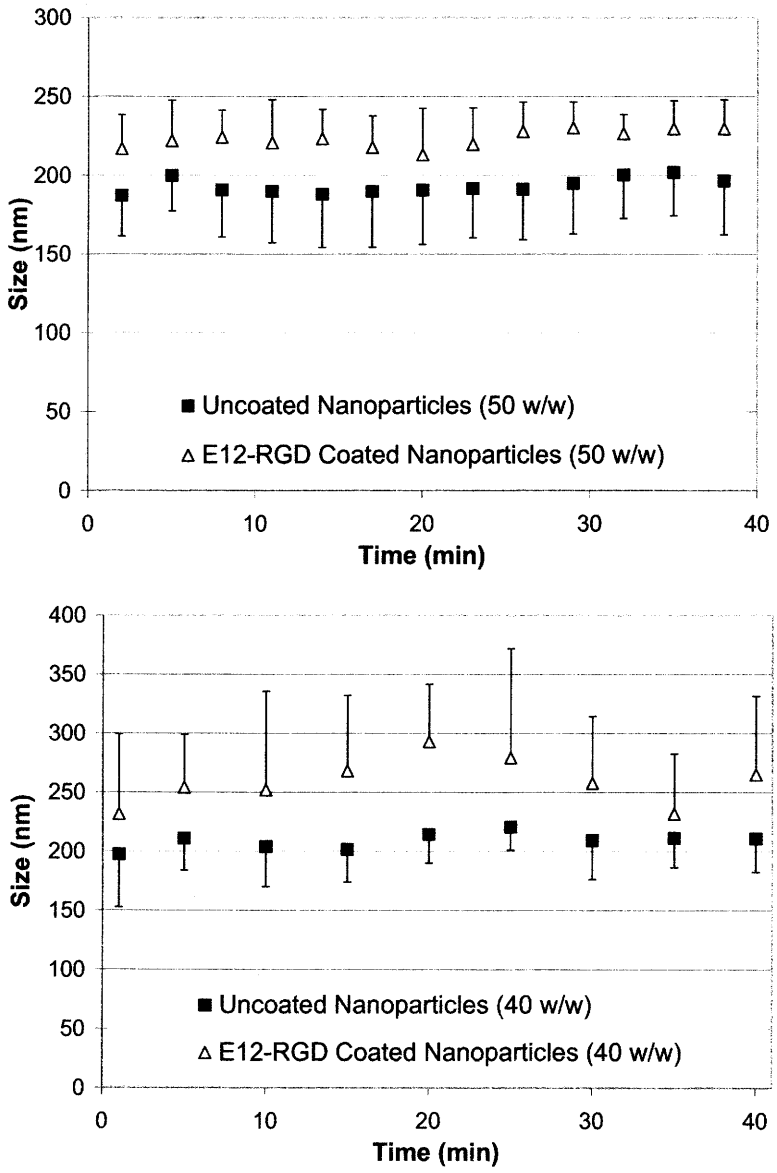


**Figure 5.4.** Ligand coated nanoparticles are slightly larger in size than uncoated nanoparticles. Nanoparticles are formed with 50 w/w or 40 w/w C32/DNA and peptide coats with an overall N/P of 1.55. Coated nanoparticles have a stable, small size in 12% serum-containing media over time. Error bars are standard deviations of independently prepared particle batches.

Figure 5.5. shows the ζ potential of E12-RGD coated and non-coated C32/DNA nanoparticles in 12% serum containing media. The C32/DNA nanoparticles have a negative ζ potential due to serum interactions with the particles. Ligand coated 40 w/w C32/DNA nanoparticles have equivalent negative charge to uncoated nanoparticles while

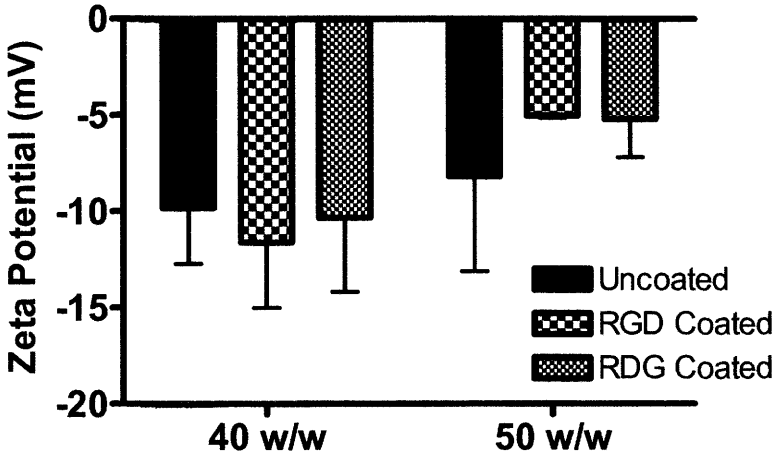


**Figure 5.5.** Ligand coated 40 w/w C32/DNA nanoparticles have equivalent negative charge to uncoated nanoparticles while in 12% serum-containing media whereas 50 w/w C32/DNA nanoparticles are slightly more neutrally charged. Nanoparticles are formed with peptide coats with an overall N/P of 1.55. RGD ligand coated nanoparticles have equal charge to RDG ligand coated nanoparticles. Error bars are standard deviations of independently prepared particle batches.

in 12% serum-containing media whereas 50 w/w C32/DNA nanoparticles have a more neutral ζ potential. The anionic peptide coating may be able to reduce serum interactions. Reduction of serum interactions may be beneficial for an *in vivo* application as serum proteins are known to promote clearance from the blood and to interfere with transfection.[3,17] Ligand coated nanoparticles had equal charge whether RGD ligand peptide coats or RDG control peptide coats were used.

### *5.3.3 GFP Transfections*

Fluorescent Activated Cell Sorting (FACS) and enhanced green fluorescent protein (EGFP) DNA were utilized to determine the efficacy of nanoparticle gene delivery. FACS data was interpreted by using a two-dimensional contour plot that compares the ratio of EGFP channel fluorescence (x-axis) to yellow channel autofluorescence (y-axis) for greater accuracy than a one-dimensional histogram as previously described.[20] Figure 5.6. shows the two-dimensional contour plot of representative C32/DNA/E12-RGD and C32/DNA/E12-RDG transfections. These experiments took place under conditions generally seen as difficult for *in vitro* transfection, but important for an *in vivo* cardiovascular application: fully confluent, and therefore non-dividing, primary cells in the presence of a high concentration of serum proteins.[2] To further ensure appropriate gating and counting of positively transfected cells, 50 w/w C32/DNA nanoparticles formed using DNA that encodes luciferase protein (Luc) rather than EGFP was also used as a negative control. Luciferase DNA nanoparticles resulted in 0.0% GFP positive signal (Figure 5.7.B).

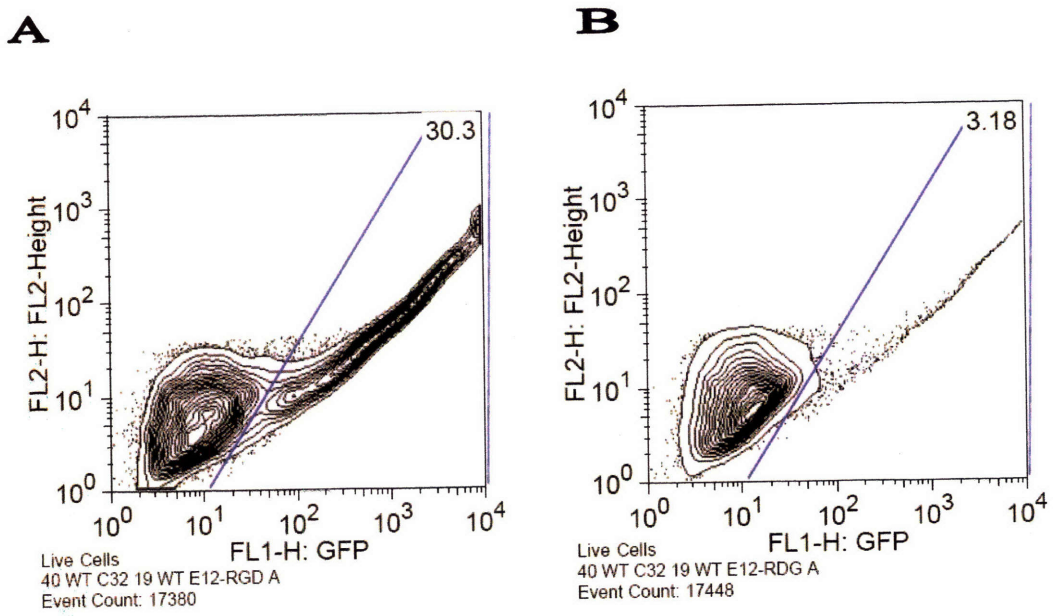


**Figure 5.6.** FACS results showing the gating of transfected HUVECs. (A) E12-RGD (ligand) coated nanoparticles significantly transfect HUVECs whereas (B) E12-RDG (control) coated nanoparticles do not. Nanoparticles are formed with 40 w/w C32 and overall N/P of 1.55. These results are representative samples from quadruplicate experiments.

### *5.3.4 Cell Viability*

We have previously shown that poly(β-amino ester) nanoparticles are biodegradable and generally non-cytotoxic to multiple cell types including HUVECs.[8,20,21] In this study C32/DNA/E12-RGD and C32/DNA/E12-RDG coated nanoparticles were also found to be non-cytotoxic to HUVECs (80%-100% cell viability depending on dose, see materials and methods for further information).

### 5.3.5 *Glutamic Acid-based Coats Enable Ligand-Specific Gene Delivery of Poly(β-amino ester)/DNA nanoparticles to Human Primary Cells*

Polyglutamic acid-based peptides were used to coat poly(β-amino ester)/DNA nanoparticles for ligand-based gene delivery. As Figure 5.7. shows, at low weight ratios (w/w) of peptide, the nanoparticles have equivalent transfection whether E12-RGD peptide, E12-RDG peptide, or no coating at all is used. However, at higher weight ratios of anionic peptide, the overall charge ratio of the complexes decreases and efficacy changes occur. When the overall N/P (charge) ratio nears neutrality, E12-RGD coated nanoparticles transfect human endothelial cells significantly better than the same nanoparticles coated with the near identical E12-RDG scrambled sequence, our negative control. Concurrently, as additional anionic peptide coating is added beyond a threshold, overall transfection decreases. Thus, there is a relatively narrow window where (1) The nanoparticles are ligand-specifically targeted and (2) The nanoparticles maintain high efficacy. The results found using this coating system are consistent with previous findings that showed that polylysine conjugated EGF gene delivery particles allow specific binding and internalization only at a relatively narrow window of charge.[10]

Figure 5.7. also demonstrates that C32 ligand coated nanoparticles are 50-fold more effective than the widely-used gene delivery polymer, polyethylenimine (PEI), and equivalent to the leading commercially available liposome-based transfection reagent, Lipofectamine 2000. Without polymer, free DNA itself (100% release from polymer) was unable to transfect the HUVECs (0.0% positive). This demonstrates that for effective gene delivery to at least some human primary cells, the DNA cargo must initially remain encapsulated and be internalized into the cell via an appropriate nanoparticle formulation before later intercellular release.

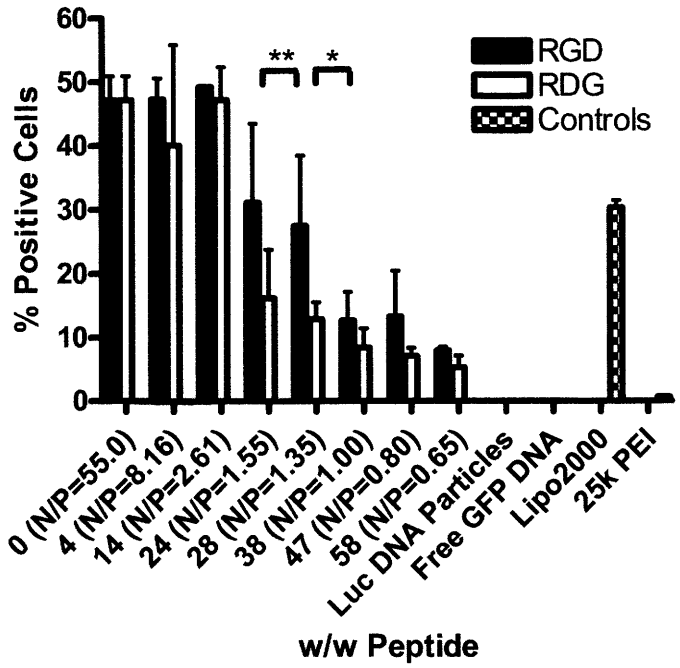


**Figure 5.7.** (A) Efficacy and specificity of E12-RGD/E12-RDG ligand coated gene delivery nanoparticles is dependent on w/w peptide and N/P ratio. Nanoparticles are formed at 50 w/w C32 and are delivered to HUVECs in 12% serum containing media. Error bars are standard deviations and (*) and (**) indicate statistical significance of $p<0.05$ and $p<0.01$ respectively.

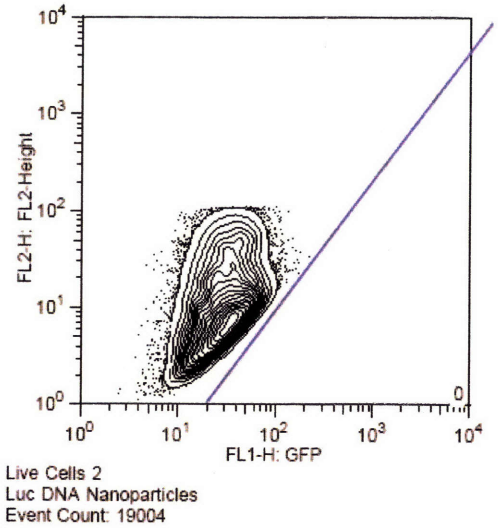


**Figure 5.7.(B).** FACS gating of 50 w/w ratio C32/DNA nanoparticles formed using luciferase DNA.

### *5.3.6 Polymer Weight Ratio, Overall Charge Ratio, and Peptide Length are Important Parameters for Ligand-Specific Gene Delivery*

Nanoparticle and coating parameters including polymer weight ratio, peptide weight ratio, overall charge ratio, and peptide length were analyzed to determine optimal conditions. C32/DNA nanoparticle formulations formed at 30 w/w, 40 w/w, and 50 w/w polymer to DNA weight ratios showed the same trends: at low amounts of anionic peptide coating there is no difference in gene delivery between RGD integrin-binding sequence, RDG non-binding sequence, or uncoated controls, but at near neutral N/P ratio, peptide coats formed with RGD integrin-binding sequences delivered DNA much more effectively than the identically formed

peptide coated nanoparticles with RDG scrambled sequences. These transfection results of the near-neutrally charged particles can be seen in Figure 5.8.. Interestingly, at 40 w/w C32/DNA and an N/P ratio of 1.55, integrin-binding E12-RGD coated nanoparticles transfected a six-fold higher percentage of HUVECs as compared to the scrambled sequence E12-RDG coated control particles, our negative control. On an individual cell basis, the most positive cells express GFP at levels 1,000-fold higher than the background. Representative FACS data from these experiments (n≥4) can be seen in Figure 5.6.. The electrostatic ligand coatings provide a

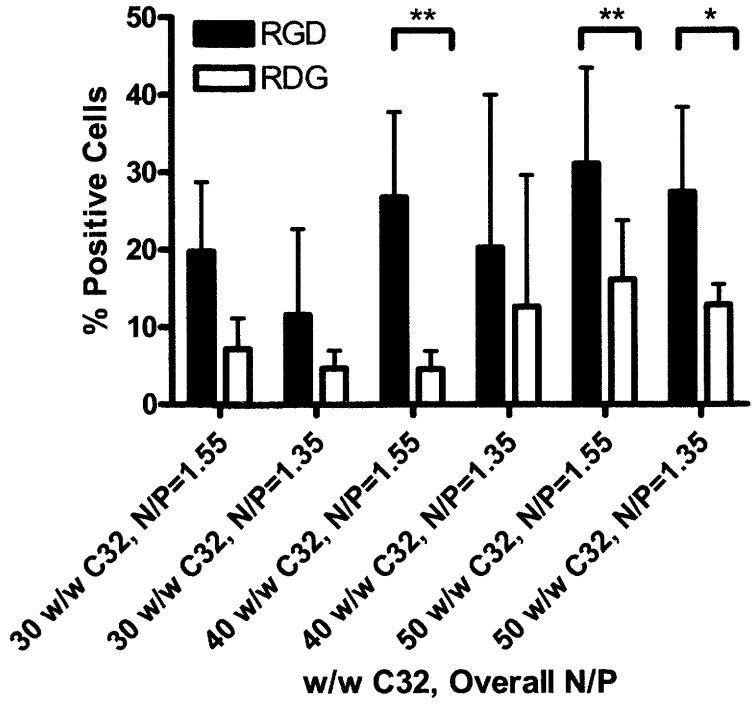


**Figure 5.8.** Efficacy and specificity of E12-RGD/E12-RDG ligand coated gene delivery nanoparticles is dependent on w/w C32 and N/P ratio. Nanoparticles are delivered to HUVECs in 12% serum containing media. Error bars are standard deviations and (*) and (**) indicate statistical significance of $p<0.05$ and $p<0.01$ respectively.

mechanism to neutralize nanoparticle charge and reduce non-specific cellular uptake, while simultaneously allowing receptor-specific uptake. To confirm integrin receptor-mediated gene delivery of the RGD coated nanoparticles, fibronectin active fragment peptide RGDS, an integrin binding competitor,[22] was added to the cells prior to transfection. 100 nM RGDS peptide was found to reduce significantly gene delivery of RGD coated nanoparticles ($p=0.0043$) while not affecting gene delivery of RDG coated nanoparticles ($p=0.48$) as shown in Figure 5.9.. To test whether free RGDS may have some other effect on the cells that non-specifically reduces transfection efficiency,

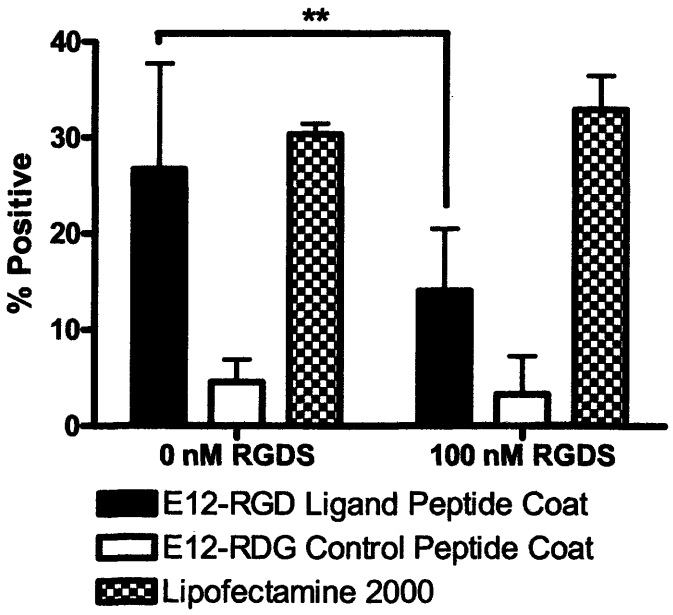


**Figure 5.9.** Competitive inhibition experiment with E12-RGD (ligand) and E12-RDG (control) coated gene delivery nanoparticles and free RGDS peptide fragment. Nanoparticles are formed at 40 w/w C32, N/P=1.55, and are delivered to HUVECs in 12% serum containing media. Error bars are standard deviations and (**) indicates statistical significance of $p<0.01$.

Lipofectamine 2000 was also tested at high RGDS concentration and maintained a constant level of transfection efficiency without regard to the amount of RGDS present.

Peptide length was also determined to be important for effective ligand coatings. Figure 5.10. demonstrates that while both intermediate length E12-RGD and E16-RGD coatings allowed for specific delivery, E8-RGD and E20-RGD coatings did not. While the biophysical basis of this trend is unclear, we hypothesize that linker length can affect both accessibility and avidity of ligands to their target receptors. Our data show that it is important to optimize peptide coat lengths in order to both reduce non-specific delivery and enable ligand-mediated nanoparticle delivery.

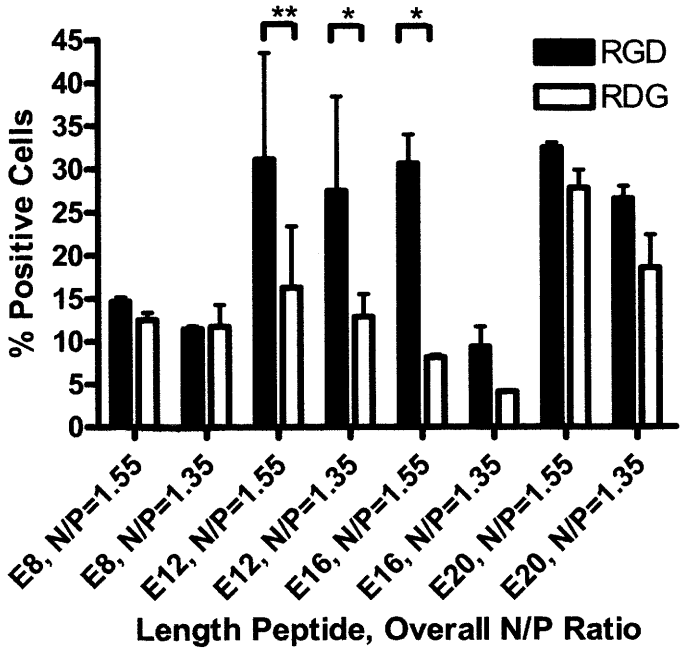


**Figure 5.10.** Efficacy and specificity of E12-RGD (ligand) and E12-RDG (control) coated gene delivery nanoparticles is dependent on peptide length and N/P ratio. Nanoparticles are formed at 50 w/w C32 and are delivered to HUVECs in 12% serum containing media. Error bars are standard deviations and (*) and (**) indicate statistical significance of $p<0.05$ and $p<0.01$ respectively.

### *5.3.7 Statistics*

Statistical calculations were carried out using GraphPad Prism 4.0 for Windows. Results are reported as mean±standard deviation. For comparison of gene delivery vectors, statistical significance was obtained by using unpaired, two-tailed, Student's *t*-tests with 95% confidence. For comparisons of coated vs. uncoated particle size over time, paired, two-tailed, Student's *t*-tests with 95% confidence were used.

## 5.4 CONCLUSIONS

In these experiments, we use Human Umbilical Vein Endothelial Cells (HUVECs) as a model primary cell system due to the following: (1) HUVECs are more difficult to transfect than other cell lines[16] and (2) Endothelial cells are prime therapeutic targets against cancer (anti-angiogenesis) and cardiovascular disease (therapeutic angiogenesis, prevention of restenosis, etc). We have also recently shown that poly(β-amino ester) nanoparticles transfect HUVECs significantly better than the leading commercially available non-viral vectors including PEI and Lipofectamine2000 and functionalizing these nanoparticles for targeted delivery would further increase their clinical utility.[20] Here we have shown that these nanoparticles can be coated for not only high efficacy, but now also for receptor-mediated delivery.

Previously, electrostatic components have been used with poly(β-amino esters) to construct erodible multilayered films.[23] Here we demonstrate that this concept can be extended to drug delivery nanoparticles to enable single or potentially multi-layered coats for

functionalized poly(β-amino ester)-based delivery. Polyacrylic acid and other polycarboxylic acids have also been recently shown to combine with polyethylenimine to form tertiary-component gene delivery nanoparticles that have reduced serum inhibition and enhanced nonspecific transfection efficacy.[17] As compared to this technique, our technology enables ligand-specific delivery in a biodegradable system. These nanoparticles are composed of biodegradable materials -- poly(β-amino esters), such as C32, are readily degradable via the hydrolysis of its ester groups as previously described[8]. Peptides are also known to degrade in vivo.

This nanoparticle peptide coating approach allows for easy incorporation of a potentially wide range of ligands. Though a peptide sequence containing RGD, such as that used here, can be used for targeting to integrin receptors and/or tumors, many other peptide ligand sequences could be incorporated into this system as well.

We have demonstrated a novel method of coating nanoparticles for ligand-based gene delivery. This method is both flexible and general enough for potentially varied nanoparticle applications. This work also highlights the importance of multiple factors including polymer weight ratio, peptide weight ratio, overall charge ratio, and ligand length when developing coated gene delivery nanoparticles. A biphasic efficacy relationship was found for peptide weight ratio, overall charge ratio, and ligand length, with intermediate values of coating being optimal. This finding demonstrates that a balance is required when seeking to design the nanoparticles to have reduced non-specific uptake, but increased ligand-specific uptake. As this nanoparticulate drug delivery system has high efficacy, ligand-based specificity, biodegradability, low cytotoxicity, and certain safety advantages over viruses, ligand coated poly(β-amino ester) gene delivery nanoparticles may be potentially useful in several clinical applications.

## 5.5 REFERENCES


1. Kay, M.A., Glorioso, J.C. & Naldini, L. Viral vectors for gene therapy: the art of turning infectious agents into vehicles of therapeutics. *Nature Medicine* **7**, 33-40 (2001).
2. Merdan, T., Kopecek, J. & Kissel, T. Prospects for cationic polymers in gene and oligonucleotide therapy against cancer. *Adv Drug Delivery Rev* **54**, 715-758 (2002).
3. Pack, D.W., Hoffman, A.S., Pun, S. & Stayton, P.S. Design and development of polymers for gene delivery. *Nature Reviews Drug Discovery* **4**, 581-593 (2005).
4. Anderson, D.G., Lynn, D.M. & Langer, R. Semi-automated synthesis and screening of a large library of degradable cationic polymers for gene delivery. *Ang. Chem. Int. Edn* **42**, 3153-3158 (2003).
5. Anderson, D.G. et al. A polymer library approach to suicide gene therapy for cancer. *Proc. Natl. Acad. Sci. U.S.A.* **101**, 16028-16033 (2004).
6. Anderson, D.G., Akinc, A., Hossain, N. & Langer, R. Structure/property studies of polymeric gene delivery using a library of poly(beta-amino esters). *Mol Ther* **11**, 426-434 (2005).
7. Akinc, A. & Langer, R. Measuring the pH environment of DNA delivered using nonviral vectors: Implications for lysosomal trafficking. *Biotechnol Bioeng* **78**, 503-508 (2002).
8. Lynn, D.M. & Langer, R. Degradable poly(beta-amino esters): Synthesis, characterization, and self-assembly with plasmid DNA. *J Am Chem Soc* **122**, 10761-10768 (2000).

9. Lynn, D.M., Anderson, D.G., Putnam, D. & Langer, R. Accelerated discovery of synthetic transfection vectors: parallel synthesis and screening of a degradable polymer library. *J Am Chem Soc* **123**, 8155-8156 (2001).

10. Schaffer, D.V. & Lauffenburger, D.A. Optimization of cell surface binding enhances efficiency and specificity of molecular conjugate gene delivery. *J Biol Chem* **273**, 28004-28009 (1998).

11. Ogris, M. et al. Tumor-targeted gene therapy: strategies for the preparation of ligand-polyethylene glycol-polyethylenimine/DNA complexes. *J. Controlled Release* **91**, 173-181 (2003).

12. Zuber, G., Dauty, E., Nothisen, M., Belguise, P. & Behr, J.P. Towards synthetic viruses. *Adv Drug Delivery Rev* **52**, 245-253 (2001).

13. Kunath, K., Merdan, T., Hegener, O., Haberlein, H. & Kissel, T. Integrin targeting using RGD-PEI conjugates for in vitro gene transfer. *Journal of Gene Medicine* **5**, 588-599 (2003).

14. Kursa, M. et al. Novel shielded transferrin-polyethylene glycol-polyethylenimine/DNA complexes for systemic tumor-targeted gene transfer. *Bioconjug Chem* **14**, 222-231 (2003).

15. Thomas, M. & Klibanov, A.M. Non-viral gene therapy: polycation-mediated DNA delivery. *Appl Microbiol Biotechnol* **62**, 27-34 (2003).

16. Suh, W., Han, S.O., Yu, L. & Kim, S.W. An angiogenic, endothelial-cell-targeted polymeric gene carrier. *Mol Ther* **6**, 664-672 (2002).

17. Trubetskoy, V.S. et al. Recharging cationic DNA complexes with highly charged polyanions for in vitro and in vivo gene delivery. *Gene Ther* **10**, 261-271 (2003).

18. Tosatti, S. et al. RGD-containing peptide GCRGYGRGDSPG reduces enhancement of osteoblast differentiation by poly(L-lysine)-graft-poly(ethylene glycol)-coated titanium surfaces. *J. Biomed. Mater. Res. A* **68**, 458-472 (2004).

19. Sullivan, M.M.O., Green, J.J. & Przybycien, T.M. Development of a novel gene delivery scaffold utilizing colloidal gold-polyethylenimine conjugates for DNA condensation. *Gene Ther* **10**, 1882-1890 (2003).

20. Green, J.J. et al. Biodegradable Polymeric Vectors for Gene Delivery to Human Endothelial Cells. *Bioconjug Chem* **17**, 1162-1169 (2006).

21. Akinc, A., Lynn, D.M., Anderson, D.G. & Langer, R. Parallel synthesis and biophysical characterization of a degradable polymer library for gene delivery. *J Am Chem Soc* **125**, 5316-5323 (2003).

22. Ruoslahti, E. The RGD story: a personal account. *Matrix Biol* **22**, 459-465 (2003).

23. Zhang, J., Fredin, N.J., Janz, J.F., Sun, B. & Lynn, D.M. Structure/property relationships in erodible multilayered films: influence of polycation structure on erosion profiles and the release of anionic polyelectrolytes. *Langmuir* **22**, 239-245 (2006).

24. Boussif, O. et al. A versatile vector for gene and oligonucleotide transfer into cells in culture and in vivo: polyethylenimine. *Proc Natl Acad Sci U S A* **92**, 7297-7301 (1995).

# Chapter 6: Investigation of Polymer/DNA Binding as a Gene Delivery Bottleneck

## 6.1 INTRODUCTION

Gene therapy, the therapeutic delivery of nucleic acids to cells, has great medical potential that has not yet been realized. Viral gene therapy is unsafe and non-viral gene therapy is ineffective. To design an improved non-viral gene delivery vector, one promising approach is to elucidate structure/function relationships between gene delivery biomaterials and the nucleic acid cargo they carry. These relationships are believed to be key in maximizing gene delivery efficacy by overcoming specific delivery bottlenecks.

When using polymers as carriers to deliver genes, one main hurdle is DNA/polymer binding. Polycations condense DNA in a reversible transition from linear polymer to globule.[1] For efficient transfection, it is crucial that DNA is condensed to protect the DNA, maintain particle stability, and allow for efficient uptake of the complexes.[1, 2] Polymer/DNA binding determines particle stability, which can be key to ensure that the DNA stays protected from nucleases and degradation. Furthermore, stable DNA-encapsulating particles are needed for efficient uptake. DNA uptake efficiency is significantly reduced if the DNA is released by the encapsulating particles prematurely. Lastly, polymer/DNA interactions are also important in

shaping the biophysical properties of the resulting nanoparticles as we have recently demonstrated for poly(β-amino esters) (Chapter 4).[3, 4]

It is important to also consider that the particle should not bind or encapsulate the DNA so tightly, as to prevent the timely release of the DNA into the cytoplasm once the gene delivery particle has entered the cell. For DNA transcription to occur, the DNA must unpack from the gene delivery vector and translocate into the nucleus. Furthermore, once inside the nucleus, the transported DNA must eventually be free from polymer and other potentially competitive binding biomolecules so that it can be efficiently transcribed into mRNA. It has been shown that polymeric vector/DNA complexation significantly inhibits RNA synthesis and that above an optimal length, overall transfection decreases as polylysine length increases.[5] Similarly, 25 kDa PEI vectors are known to have higher transfection efficacy that those formed with higher molecular weight PEIs.[1] Thus, it appears that there may be a biphasic relationship between vector/DNA binding and transfection efficacy among a broad range of polymers.

When developing new biomaterials for gene delivery, researchers typically look at DNA/polymer binding qualitatively, rather than quantitatively, by using techniques such as agarose gel electrophoresis to measure binding. [6, 7] However, polymer/DNA binding is important for other gene delivery steps beyond initial condensation of DNA and gel electrophoresis is insufficient to provide quantitative measurements such as polymer/DNA binding constants that would be useful to evaluate these subsequent steps. If DNA binding constants could be calculated quickly and easily and correlated to structural properties and transfection efficacy, these biomaterials could be rationally designed to better overcome this bottleneck. Recently, a few researchers have quantitatively investigated some non-viral vector/DNA binding constants, but have done so only after making several simplifying

assumptions. Zelikin *et al.*'s technique did not take into account McGhee and von Hippel binding isotherms and subsequently calculated "effective" relative binding constants.[8] Plank *et al.*'s work, though more rigorous in form, required making assumptions about the binding constant of the reference ligand and of the site size of the known and unknown ligands.[9] An improved high-throughput assay that can determine absolute DNA binding constants for unknown vector ligands with minimal assumptions is presented here. This assay is then applied for the first time to a library of biomaterials to quantitatively measure nucleic acid binding constants and investigate structure/function relationships.

## 6.2 EXPERIMENTAL PROCEDURES

### *6.2.1 Polymer Synthesis*

Monomers for the primary poly(β-amino ester) synthesis were purchased from Aldrich (Milwaukee, WI, USA), TCI (Portland, OR, USA), Pfaltz & Bauer (Waterbury, CT, USA), Matrix Scientific (Columbia, SC, USA), Scientific Polymer (Ontario, NY, USA), and Dajac Monomer–Polymer (Feasterville, PA, USA). Amine capping reagents were purchased from Sigma-Aldrich, Alfa Aesar, Acros Organics/Fisher Scientific (Pittsburgh, PA, USA), TCI America (Portland, OR, USA), Molecular Biosciences (Boulder, CO, USA), and Toronto Research Chemicals (Toronto, Ontario, Canada). Anhydrous DMSO was purchased from Sigma-Aldrich (St. Louis, MO, USA) and a 25 mM sodium acetate buffer solution pH 5.2 (NaAc

buffer) was prepared by diluting a 3 M stock (Sigma-Aldrich). All chemicals were used as received without any further purification.

To synthesize the poly(β-amino esters), optimal amine/diacrylate stoichiometric ratios for each polymer were determined from previous work.[4] For each synthesis, 400 mg of amino monomer was weighed into a 1 mL sample vial with Teflon-lined screw cap. Next, the appropriate amount of diacrylate was added to the vial and a small Teflon-coated stir bar was then put in each vial. Polymers were then synthesized on a multiposition magnetic stir-plate residing in an oven at either 95°C and solvent free or 60°C with 2 ml DMSO added. High temperature synthesis was performed for approximately 12 h, and low-temperature synthesis was performed for 2 days. After completion of reaction, all vials were removed from the oven and stored at 4°C. All polymers were analyzed by gel-permeation chromatography (GPC) as previously discussed.[4] The monomers used to create the polymers and the synthesis scheme can be seen in Figure 6.1A and Figure 6.1B respectively.

To form the end-modified polymers, a two-step process was utilized (Figure 6.2A). First, acrylate-terminated polymers were synthesized, followed by post-polymerization end-chain conjugation of amine molecules (Figure 6.2B). In the first step, acrylate-terminated poly(β-amino ester) C32-Ac was synthesized by mixing the corresponding diacrylate and amine monomers in a 1.2:1 ratio. C32-Ac was prepared by mixing 793 mg of 1,4-butanediol diacrylate (4 mmol) with 344 mg of 5-amino-1-pentanol (3.3 mmol). Polymerizations were performed in Teflon-lined screw cap vials under magnetic stirring at 90°C for 24 hours. Gel permeation chromotography (GPC) of the C32-Ac polymer resulted in a $M_w$ = 8800 Da (polydispersity = 1.9).

Acrylate-terminated polymers were dissolved in DMSO at 31.13% wt/wt. Amine capping reagents were dissolved in DMSO at 0.25 M. End chain capping reactions were performed by mixing 321 mg of polymer/DMSO solution with 800 μl of amine solution. Reactions were performed in eppendorf tubes with constant agitation for 24 hours. End-chain coupling conditions were optimized in DMSO to prevent inter-chain crosslinking and aminolysis reactions, as determined using GPC and NMR. Polymers were stored at -20°C until used for each experiment.

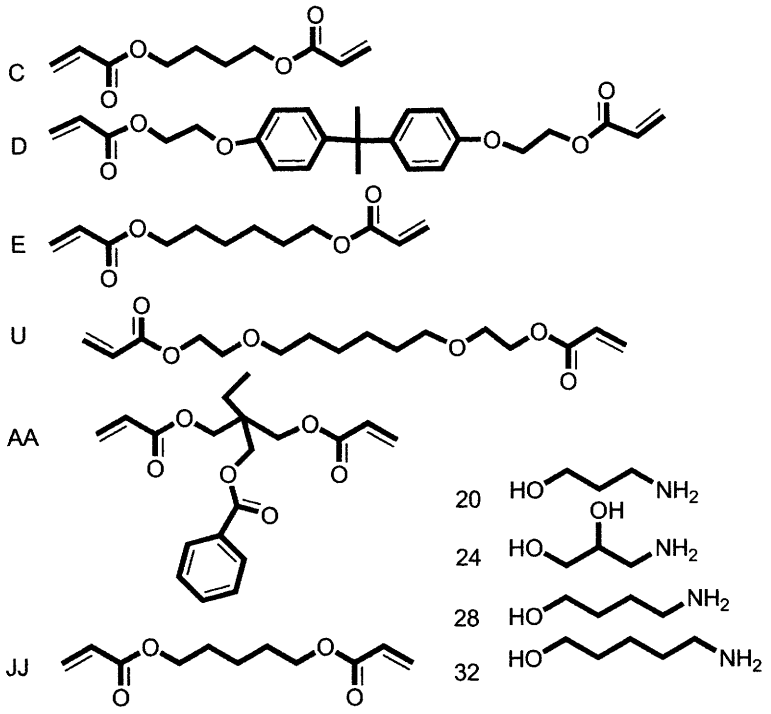


**Figure 6.1A.** Amine and acrylate monomers used for poly(β-amino ester) synthesis.

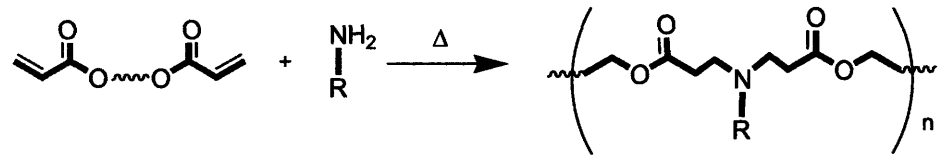

**Figure 6.1B.** Synthesis of poly(β-amino esters).

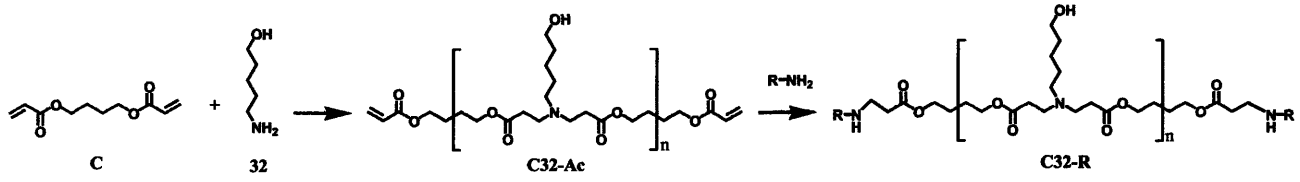


**Figure 6.2A.** Synthesis of end-modified poly(β-amino esters) by reaction of acrylate-terminated C32 polymer with primary diamine molecules in DMSO.

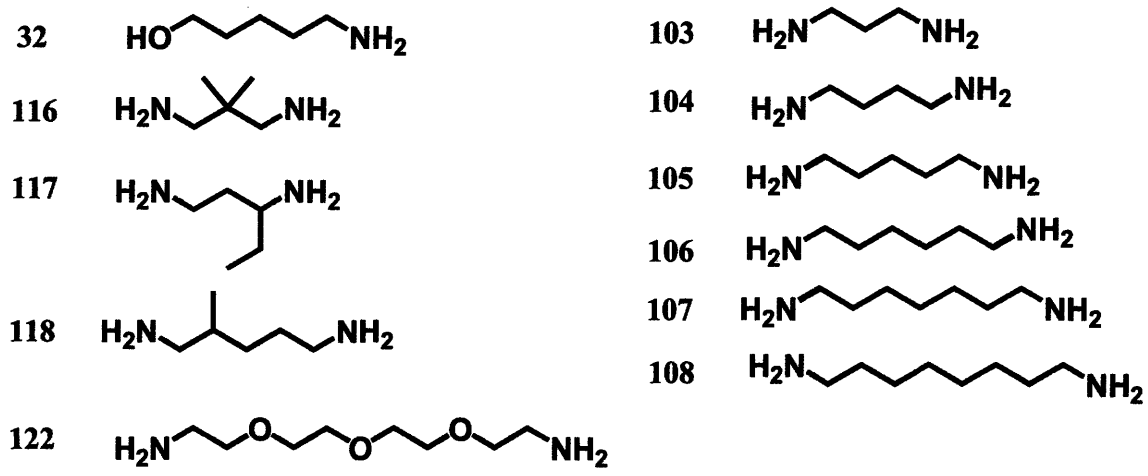


**Figure 6.2B.** Structures of amine-capping molecules.

### *6.2.2 DNA Binding Assay*

Biochemists have investigated how DNA binds to biomolecules such as proteins to better understand molecular biology mechanisms. The theoretical aspects of these DNA-protein

interactions were delineated in the work of McGhee and von Hippel in 1974.[10] This approach takes into account the observed deviations from linearity due to multivalent ligands binding to a lattice where binding site "overlap" can occur. It quantifies how, as a lattice becomes saturated, there is an entropic resistance to further binding. Cationic polymers, like other multivalent ligands, electrostatically bind and unbind from a large DNA lattice following McGhee and von Hippel binding isotherms. An extension of this approach for modeling two competing ligands binding to the same lattice was developed by Wolfe and Meehan.[11]

To quantify unlabelled polymer/DNA binding equilibrium, the oxazole yellow dye YO-PRO-1 (Invitrogen, Carlsbad, CA, USA), was utilized as a competing reference ligand. YO-PRO-1 is a very sensitive DNA binding dye with a high signal to background ratio. When YO-PRO-1 binds DNA at the concentrations used here, the fluorescent signal was found to be over 300-fold higher than the signal from unbound YO-PRO-1 ($F_{bound} >> F_{Free}$). First the binding thermodynamics of YO-PRO-1/DNA were determined using the McGhee and von Hippel binding isotherm and then these parameters were used to model the competition experiments performed using polymer, YO-PRO-1, and DNA all together. To conduct binding experiments, a 96-well plate format was utilized for high throughput assays. All binding experiments (with and without polymer) were conducted in the same conditions as *in vitro* polymer/DNA transfections: preparation in 25 mM sodium acetate buffer (pH = 5.2) with 5 kbp EGFP-N1 plasmid DNA.

For the YO-PRO-1 / DNA assays, a constant amount of YO-PRO-1 was used across rows and a reverse titration of lattice (dilution series of DNA) was used in the columns. Each data point was replicated in quadruplicate with a single plate measuring 24 lattice concentrations. A wide range of [YO-PRO-1]:[DNA bp] ratios (1:0.03125 to 1:4096) was used to assay binding at

multiple YO-PRO-1 ratios. To perform the titrations, first 1000 μL of DNA dissolved in 25 mM NaAc was added to top-right most well (A12) of a 2.0 mL deep 96-well plate and 500 μL of 25 mM NaAc is added to the other wells in the row (A1-A11). Then to perform the dilution series, 500 μL was transferred from A12 to A11 and mixed, then 500μL from A11 to A10 and so on through A2. A1 was left without any DNA as a control to measure fluorescence of free unbound ligand. A 12-channel pipette was then used to transfer 100 μL of DNA at each concentration across the row to four quadruplicate rows of ligand in the 96-well plate. YO-PRO-1 was diluted at the appropriate concentration in 25 mM NaAc, transferred to a reservoir, and a 12-channel pipette was used to transfer 100 μL per well to the quadruplicate DNA wells and mix. All plates were kept wrapped in foil to protect the samples from light. After a 15 min wait, which was determined to be sufficient for reaching equilibrium, the samples were measured for fluorescence using a Perkin Elmer Victor3 plate reader (Perkin Elmer Life Sciences, Boston, MA, USA) with a FITC filter set (excitation 485 nm, emission 535 nm). To calculate the concentration of YO-PRO-1 ligand bound, the relevant equations are:

$$F_{obs} = F_{Bound}L_{Bound} + F_{Free}L_{Free}$$
$$L_{Total} = L_{Bound} + L_{Free}$$

Where $F_{obs}$ is the observed fluorescence, $F_{Bound}$ is the fluorescence per bound ligand, $F_{Free}$ is the fluorescence per free unbound ligand, $L_{Bound}$ is the concentration of bound ligand, and $L_{Free}$ is the concentration of free ligand. At very high concentrations of lattice ([DNA] >> [L]) and with a ligand such that $F_{bound} >> F_{Free}$, it can be assumed that $F_{obs\_max} = F_{Bound}L_{Total}$, enabling solving for $F_{Bound}$. Similarly, when no lattice is present, $F_{obs\_min} = F_{Free}L_{Total}$, determining $F_{Free}$. Thus, $L_{Bound}$

can be determined for each point by solving the original system of two equations. Once $L_{Bound}$ is determined, it can be fit using MatLab to the McGee and von Hippel's lattice model to determine $K_a$, the binding constant, and n, the binding site size:

$$\frac{v}{L_{Free}} = K_a \cdot f \cdot \left( \frac{f}{f+v} \right)^{n-1}$$

$$L_{Free} = L_{Total} - vD$$

$$v = \frac{L_{Bound}}{D}$$

$$f = 1 - n \cdot v$$

**Figure 6.3.** McGhee and von Hippel binding isotherm for a ligand binding to an infinite lattice. $L_{Bound}$, $L_{Total}$, and D (lattice concentration) are known. v, fraction of lattice bound by ligand, f, fraction of lattice free, and $L_{free}$ are defined in these equations. The binding association constant, $K_a$, and the site size, n, can be solved for computationally.

When the ligand is monovalent, these equations reduce to the more familiar Scatchard equation:

$$\frac{v}{L_{Free}} = K_a \cdot (1 - v)$$

Overall these equations for binding can be perhaps best understood as :

$$\frac{Average\_number\_of\_ligands\_bound/_{lattice}}{L_{Free}} = K \cdot \left( \frac{Average\_number\_of\_free\_ligand\_binding\_sites}{lattice} \right)$$

Once the binding parameters of the fluorescent reference competitor (YO-PRO-1) are known, it can be used to determine the unknown binding parameters of a whole library of gene delivery polymers. The relevant equations for two non-cooperative binding n-mers is given by the theoretical method developed by McGee and von Hippel and shown below in a form below adapted from Plank *et al.*[9, 10]:

$$\frac{v_1}{L_{1Free}} = K_1 f \cdot \left( \frac{f}{f + v_1 + v_2} \right)^{n_1 - 1} \qquad \frac{v_2}{L_{2Free}} = K_2 f \cdot \left( \frac{f}{f + v_1 + v_2} \right)^{n_2 - 1}$$

$$L_{1Free} = L_{1Total} - v_1 D \qquad L_{2Free} = L_{2Total} - v_2 D$$

$$v_1 = \frac{L_{1Bound}}{D} \qquad v_2 = \frac{L_{2Bound}}{D}$$

$$f = 1 - n_1 v_1 - n_2 v_2$$

**Figure 6.4.** Modified McGhee and von Hippel binding isotherm for two ligands competing to bind to an infinite lattice.

The following variables are known: D, the lattice concentration, $L_{1Total}$, the total concentration of the reference ligand, $L_{2Total}$, the total concentration of the polymer, $K_1$, the reference ligand-DNA association constant, $n_1$, the number of reference ligand-DNA lattice binding sites per reference ligand, and $v_1$, the reference ligand binding density as measured by the spectroscopic signal. The unknown variables are $K_2$, the polymer-DNA association constant, $n_2$, the number of polymer-DNA lattice binding sites per polymer, and $v_2$, the polymer binding density. A non-linear fit was used to calculate these values based on the experimental data.

To perform the polymer / YO-PRO-1 / DNA binding titrations for a single polymer, a 12-channel pipette was first used to transfer 50 μL of 1 μM DNA basepairs in 25 mM NaAc to each of four replicate rows containing 12 wells each. Next, 50 μL of 1 μM YO-PRO-1 in 25 mM

NaAc was similarly transferred at transfer to each of these same wells and mixed with the DNA. As before, the plates were covered in aluminum foil to prevent exposure to light. The polymer was prepared in a 2.0 mL deep 96-well plate for a dilution series, just as the DNA was in the polymer-free binding experiments. A polymer concentration range of 1:0.25 – 1:256 YO-PRO-1 dye : polymer monomer units was used for all polymers. 50 μL of polymer in 25 mM NaAc was transferred to 11 of the 12 YO-PRO-1 / DNA wells, mixed well, and the fluorescence was measured after a 15 min wait for equilibrium. For the $12^{th}$ well, 50 μL of 25 mM NaAc without polymer was transferred instead. The concentration of monomer units was calculated based on the molecular weight of the polymer and corresponds to the concentration of lattice DNA basepairs that could be potentially occupied by the polymer. This range was sufficient to achieve full quenching of the YO-PRO-1 dye for all polymers tested.

### *6.2.3 Cell Culture and Transfection*

Human Umbilical Vein Endothelial Cells (HUVECs) (Cambrex, Walkersville, MD, USA) were cultured in EGM-2 media supplemented with SingleQuot Kits (Cambrex). HUVEC cells were used by passage five and in accordance to the manufacturer's instructions. pEGFP-N1 plasmid DNA stock solution (1 mg/ml in water) was obtained from Elim Biopharmaceuticals (Hayward, CA, USA). The non-viral gene delivery particles are formed through electrostatic interactions between poly(β-amino esters) and plasmid DNA. To ease handling, polymer stock solutions (100 mg/ml) were prepared in DMSO solvent prior to use. Working dilutions of each polymer were prepared in 25 mM sodium acetate buffer (pH 5). GFP transfections of unmodified poly(β-amino esters) were conducted using a final dose of 3 μg GFP DNA per cell

well at individually optimized polymer to DNA weight ratios (ranging from 30:1 to 150:1 see Chapter 4).[3] Acrylate-terminated C32 (C32-Ac) transfections and all end-modified polymer transfections were conducted using a 6 μg GFP DNA final dose per well and a constant, relatively low polymer to DNA weight ratio of 30:1. HUVECs were seeded (75,000 cells/well) into clear 24-well plates at 24 hours prior to transfection to allow for growth to confluence.

For each replicate, 75 μL of polymer solution in 25 mM NaAc buffer was added to 75 μL of DNA solution also in NaAc buffer, well mixed, and allowed to sit for 10 min for self-assembly to occur. Next, this 150 μL polymer/DNA particle solution was added to 1.0 mL of EGM-2 media supplemented with FBS (12% serum). The growth medium was removed from the seeded cells using a 6-channel aspirating wand (V&P Scientific, San Diego, CA, USA) after which 750 μL of the nanoparticle/media solution was immediately added to each well. Polymeric gene delivery nanoparticles were incubated with the cells for 4 hours and then removed using the 6-channel wand and replaced with 500 μL of warm EGM-2 media. After 48 hrs, transfected and untransfected control cells were washed, removed from the 24-well plates by trypsinization, microcentrifugation, and resuspension in 500 μL of FACS running buffer (98% PBS / 2% FBS / 1:200 propidium iodide solution (Invitrogen)) for FACS analysis.

GFP expression was measured using Fluorescence Activated Cell Sorting (FACS) on a FACSCalibur (Becton Dickinson, San Jose, CA, USA). Propidium iodide staining was used to exclude dead cells from the analysis and 20,000 live cells per sample were acquired. Two-dimensional gating was used to separate increased autofluorescence signal from increased GFP signal to more accurately count positively expressing cells. Gating and analysis was performed using FlowJo 6.3 software (TreeStar, Ashland, OR, USA).

## 6.3 RESULTS AND DISCUSSION

### *6.3.1 Determination of YO-PRO-1 Binding Constant and Site Size*

The binding of YO-PRO-1 to DNA was determined by the change in fluorescence signal upon binding. A representative figure showing this binding equilibrium is Figure 6.5 which shows YO-PRO-1 (2.5 x $10^{-7}$ M) following reverse titration with DNA. Maximum fluorescence is reached at ~$10^{-5}$ M base pairs of DNA.

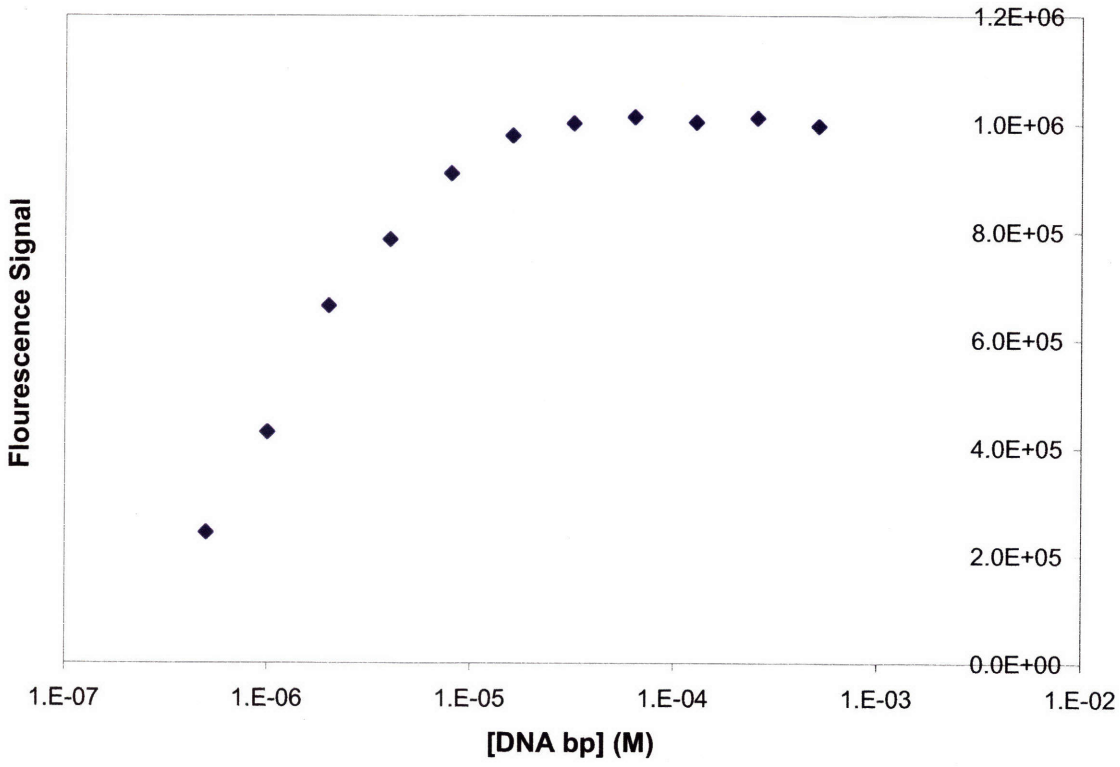


**Figure 6.5.** Plot showing the binding of YO-PRO-1 to DNA. Extent of binding is determined by fluorescence upon binding. YO-PRO-1 is 2.5 x $10^{-7}$ M.

Fitting conducted using MatLab and nonlinear least squares determined $K_a$ to be 1.4 x $10^6$ $M^{-1}$ and the binding site size, n, to be 3.1. This agrees with the literature that found that the observed binding site size of YO-PRO-1 is between 2.7-3.8 depending on salt conditions.[12] Compared to previous work of others, the DNA binding constant for Yo-Pro-1 fitted here is on the same order ($10^6$ $M^{-1}$), but slightly lower.[12] Variance in the constant is likely due to differences in the experimental conditions employed including different type and concentration of salt (25 mM sodium acetate) and use of supercoiled plasmid DNA rather than calf thymus DNA. This fit can be seen in Figure 6.6.

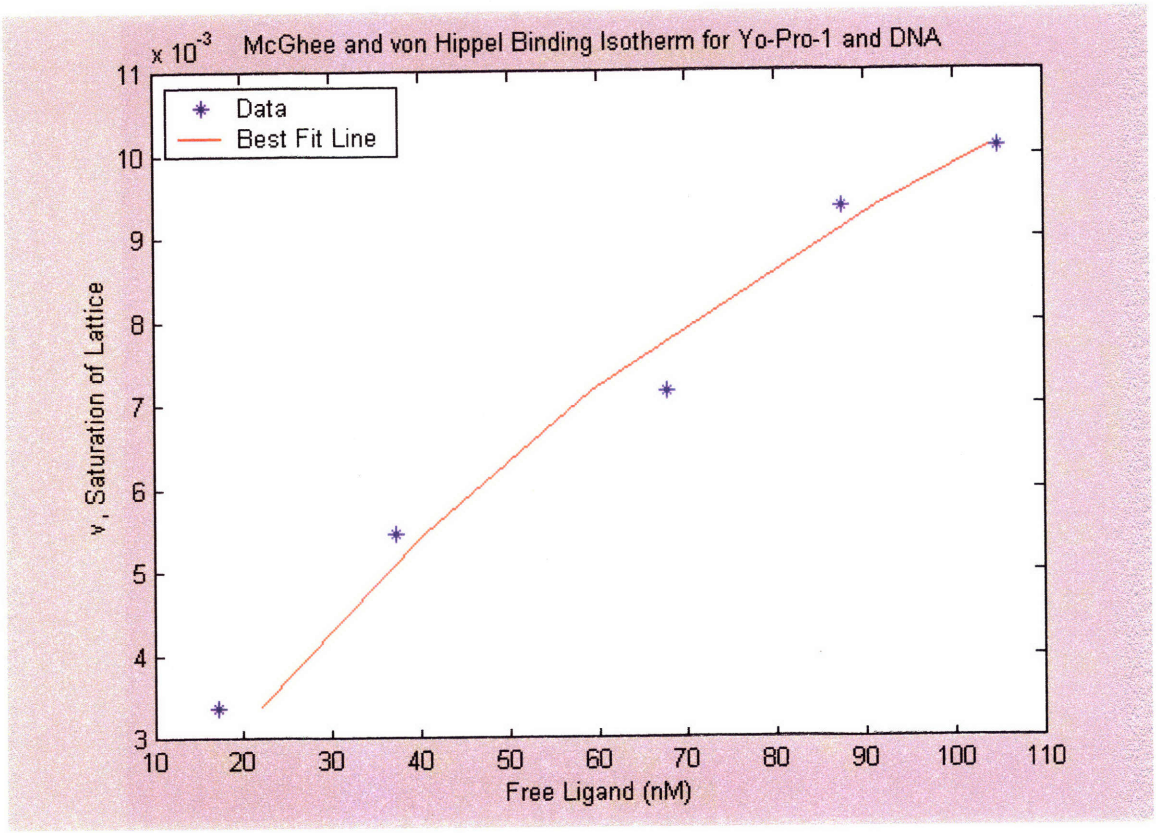


**Figure 6.6.** Plot showing fit to McGhee and von Hippel Binding isotherm for YO-PRO-1/DNA.

### 6.3.2 *Determination of Polymer/DNA Binding Constants*

The simultaneous equations found in Figure 6.4 for the binding isotherm for two ligands binding to an infinite lattice were solved using MatLab. For a given polymer site size, $n_2$, a well defined polymer DNA binding constant $K_2$ was determined. By cycling through all possible site sizes, $n_2$, the optimal combination of site size and binding constant could be found by minimizing the residual least square error of the fitting function. Figure 6.7 shows the data points and fit for polymer C32. Representative fits for C32 and the weakest binding polymer, U28, are shown in Figure 6.8 and Figure 6.9 respectively.

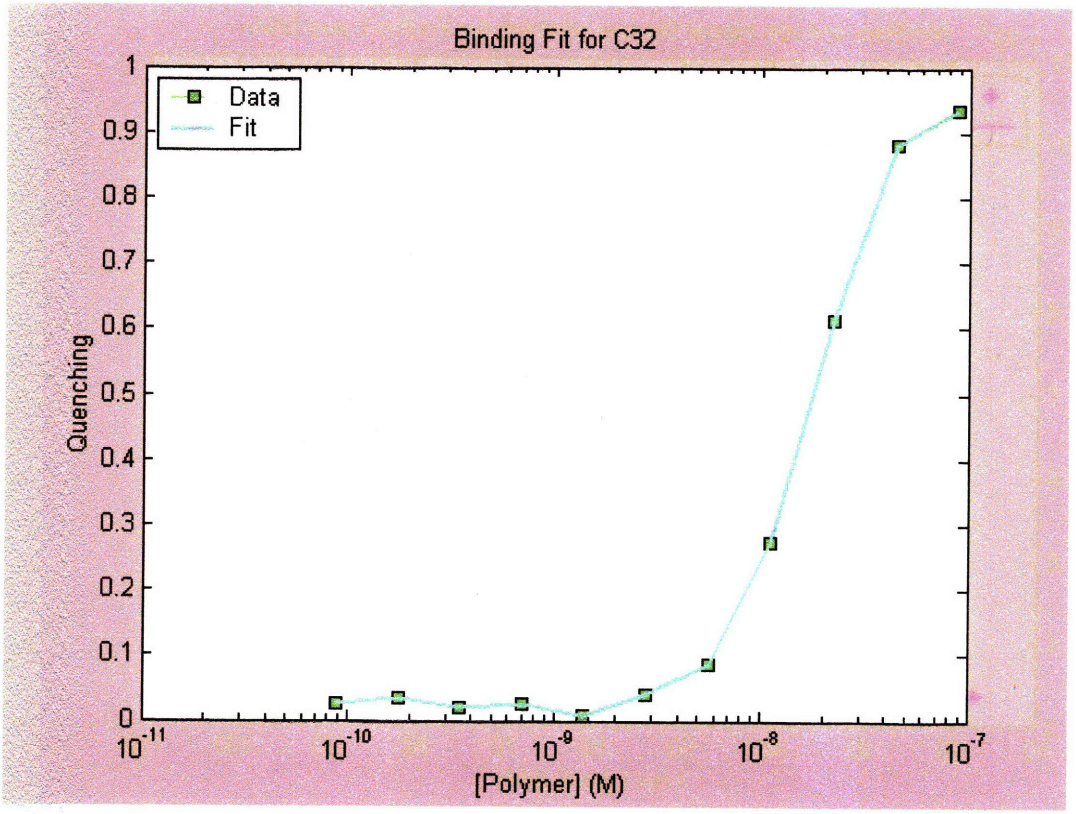


**Figure 6.7.** C32 and YO-PRO-1 competing to bind DNA. Quenching of fluorescence is determined by polymer C32 binding to DNA and displacing YO-PRO-1.

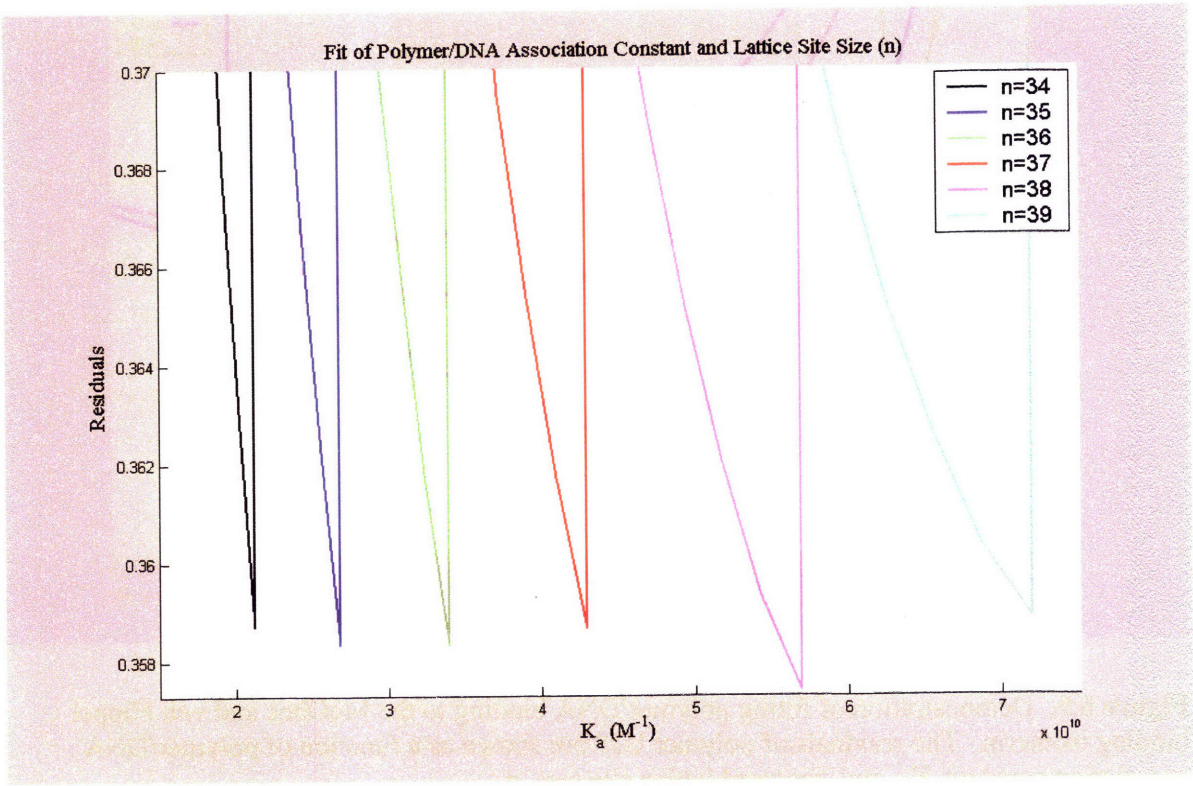


**Figure 6.8.** Demonstration of fitting polymer/DNA binding to the McGhee and von Hippel binding isotherm. The residuals of polymer C32 are shown as a function of polymer/DNA association constant, $K_a$, and observed lattice site size, n.

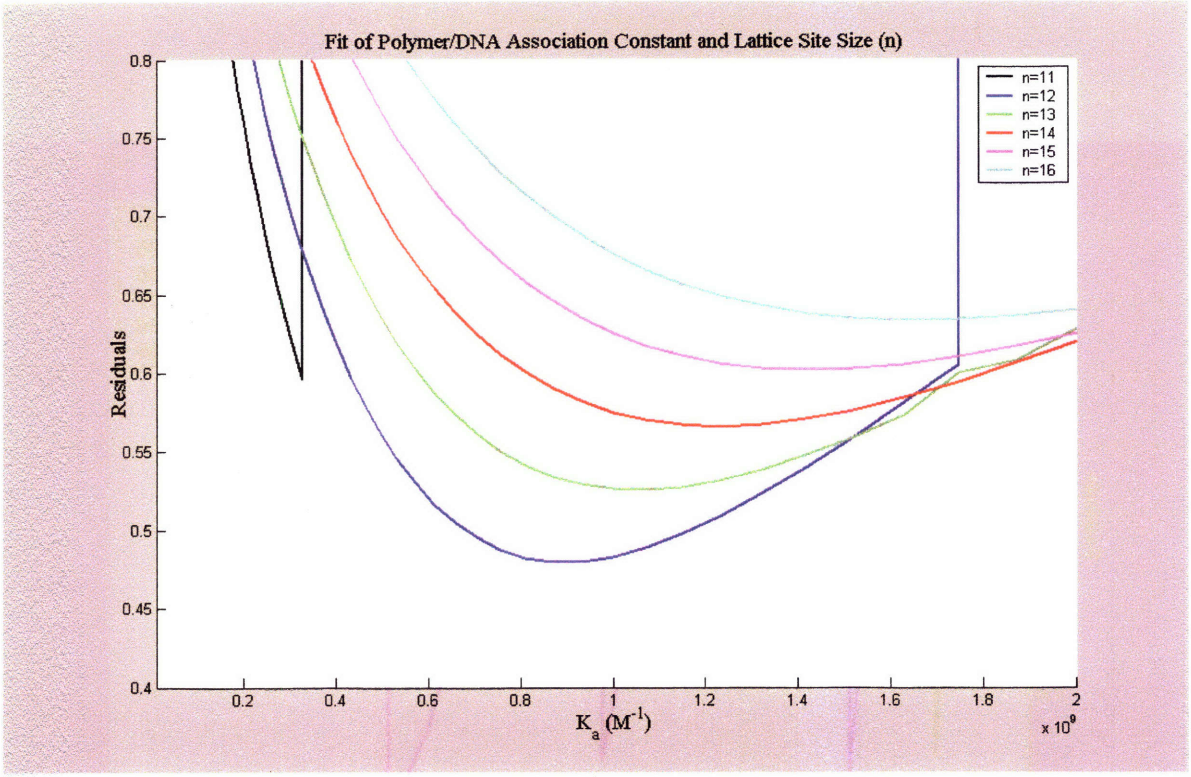


**Figure 6.9.** Demonstration of fitting polymer/DNA binding to the McGhee and von Hippel binding isotherm. The residuals of polymer U28 are shown as a function of polymer/DNA association constant, $K_a$, and observed lattice site size, n.

These fits indicate that global minima were achieved. A wide range of $n_2$ values were tried, only the six best fitted values are shown above, The quenching of YO-PRO-1 by the polymers in the library can be seen in Figure 6.10 (polymer basis) and Figure 6.11 (monomer unit of polymer basis). The difference in basis highlights a potential effect of the differences in molecular weight of the polymers. While Figure 6.10 shows actual polymer ligand concentration as fit for binding constants, Figure 6.11 reveals the intrinsic binding on a per monomer repeat unit that corresponds to the maximum binding site size. The color and shape of the markers used in these and subsequent figures, reveal information on structure of the polymers in the library.

The color corresponds to the acrylate monomer used to form the polymer (AA, C, D, E, JJ, and U) and the shape corresponds to the amine monomer used (20, 24, 28, and 32). The structures of these monomers are shown in Figure 6.1A. It is important to take note that acrylate monomers C, JJ, and E differ by only single carbons in the acrylate interior (the number of carbons being 4, 5, and 6 respectively). Similarly, amine monomers 20, 28, and 32 differ by only single carbons as well (3, 4, and 5 respectively). The eleven polymers analyzed here were selected based on top-performance in an *in vitro* gene delivery screen using over 2,000 unique polymer structures and molecular weights.[6]

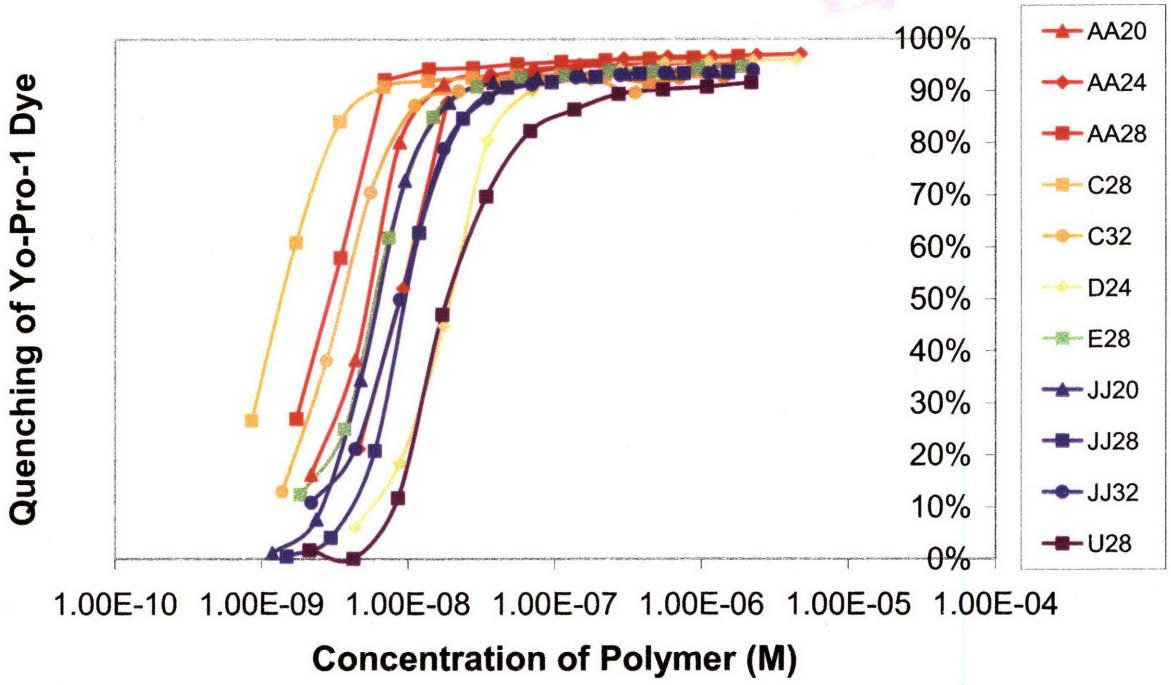


**Figure 6.10.** Comparison of poly(β-amino esters) binding to DNA (v.s. concentration of polymer).

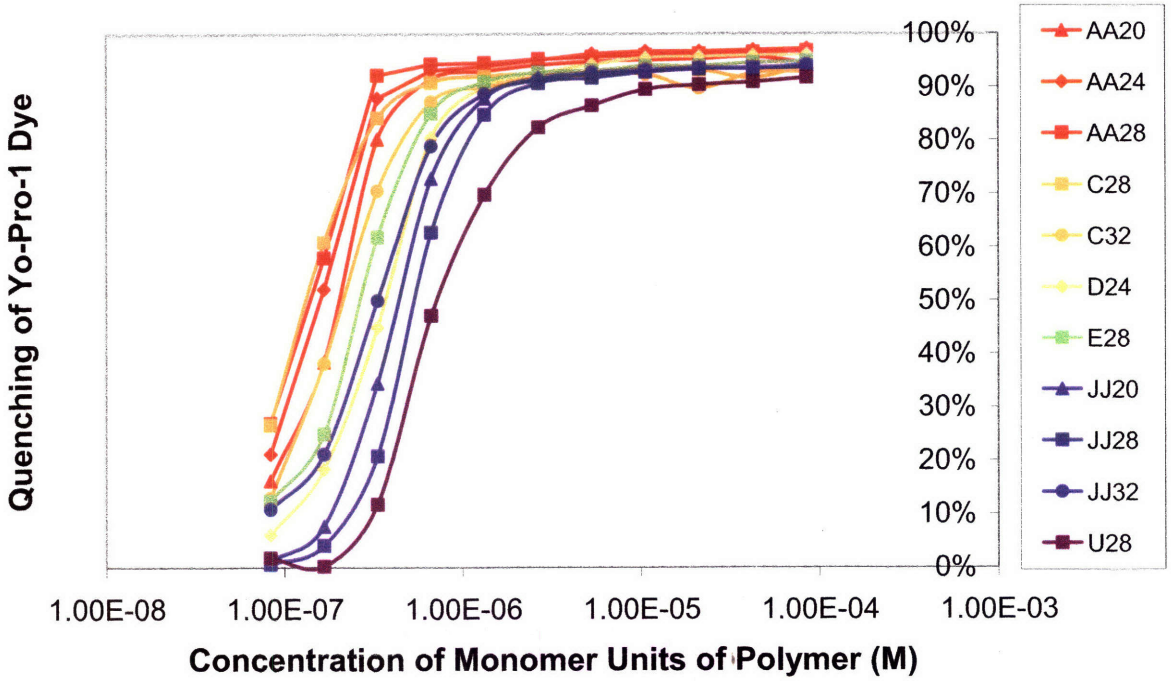


**Figure 6.11.** Comparison of poly(β-amino esters) binding to DNA (vs. concentration of monomer units comprising polymer).

A table comparing the molecular weights (MW), the maximum and observed lattice binding site size ($n_{max}$ and $n_{obs}$), and the association constant, $K_a$, are shown in Table 6.1. Maximum binding site size ($n_{max}$) comes from the number of amine units on each polymer which is directly calculated from the molecular weight whereas $n_{obs}$ is fitted. Generally, $n_{obs}<n_{max}$, indicating that the actual number of interacting units of the polymer with the lattice is fewer than the maximum number of monomer units comprising the polymer. This is expected as the electrostatically interacting groups of the monomer are the amines that may not be fully charged. Based on previous work on this class of polymers,[13, 14] it was determined that poly(β-amino

esters) function for gene delivery through the "proton sponge" mechanism[15, 16] to escape the endosomal compartment into the cytoplasm. In this mechanism, polymers with titratable amine groups at endosomal pH buffer endosomal acidification, cause endosomal $Cl^-$ ion accumulation due to the maintenance of charge neutrality, and lead to osmotic swelling and rupture of the endosome.[16] Thus, these amine groups likely have $pK_a$s in the range of the endosomal compartment (pH~6) to allow efficient proton buffering and may be less than fully charged in the 25 mM sodium acetate buffer (pH=5.2) used here for binding studies and also used for nanoparticle formation.[3, 4] Furthermore, the maximum lattice site size may not be physically possible due to steric effects and conformational limitations of the polymer.

| Polymer | MW (Da) | $n_{max}$ | $n_{obs}$ | $K_a$ (1/M) |
|---|---|---|---|---|
| AA20 | 16200 | 39 | 21 | 2.1E+10 |
| AA24 | 8058 | 19 | 21 | 1.6E+10 |
| AA28 | 20900 | 49 | 43 | 1.1E+13 |
| C28 | 27900 | 98 | 79 | 7.1E+16 |
| C32 | 18100 | 61 | 38 | 5.7E+10 |
| D24 | 9542 | 20 | 20 | 2.0E+09 |
| E28 | 14300 | 46 | 29 | 8.9E+10 |
| JJ20 | 20200 | 71 | 37 | 1.9E+12 |
| JJ28 | 16800 | 57 | 32 | 7.8E+10 |
| JJ32 | 12100 | 39 | 24 | 4.2E+10 |
| U28 | 15600 | 40 | 12 | 9.1E+08 |

**Table 6.1.** Table of polymer properties. This table shows molecular weights (MW), the maximum and observed lattice binding site size ($n_{max}$ and $n_{obs}$), and the association constant, $K_a$.

It is interesting to note that just as many of these top-performing polymers show a convergence in structure, they also show a convergence to binding constant to $K_a \sim 10^{10}$ $M^{-1}$. However, it is also interesting to note extreme differences caused by single carbon changes. For example, a single carbon change between a gene delivery-optimized formulation using C32 (5 carbons on amine alcohol monomer) and a similarly optimized formulation using C28 (4 carbons on amine alcohol monomer) resulted in an increase in binding constant by over six orders of magnitude. These results demonstrate the utility of using a large polymer library to elucidate structure/function relationships for biomaterials. Single molecule and even single atomic changes can be seen to cause dramatic effects.

### *6.3.3 Polymer/DNA Binding Constant Correlates to Transfection Efficacy*

As previously mentioned, the eleven poly(β-amino esters) used here were chosen based on their top gene delivery performance from a library of over 2,000 materials.[6] However, this screening took place in an easy-to-transfect immortalized cell line in serum free conditions. It is widely known that *in vitro* gene delivery efficacy often do not translate to *in vivo* efficacy. One of the reasons for this is the primary cells are much more difficult to transfect and serum proteins found in the blood can quickly deactivate gene delivery nanoparticles. To account for this, transfections presented here take place in conditions seen as difficult for an *in vitro* gene delivery assay, fully confluent human primary cells (HUVECs) in the presence of a high concentration of serum. The importance of binding constant to transfection efficacy is likely much pronounced in this case as the binding interaction is responsible for keeping the gene delivery nanoparticles small and stable in the presence of serum proteins. Additionally, as these cells are harder to

transfect, the balance between keeping the DNA protected inside the cell vs. ultimately releasing the DNA for expression is perhaps more sensitively assayed. Polymer/DNA binding constants were indeed found to correlate to transfection efficacy as seen in Figure 6.12 and Figure 6.13 which highlight a side by side comparison of poly(β-amino ester) binding constants and their gene delivery efficacy to human primary cells.

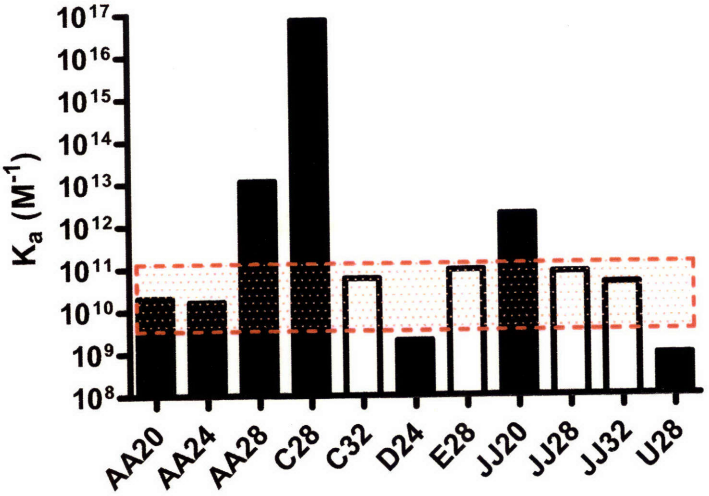


**Figure 6.12.** Binding association constants for top-performing polymers in the poly(β-amino ester) library. The top four performing polymers for gene delivery are shown in white.

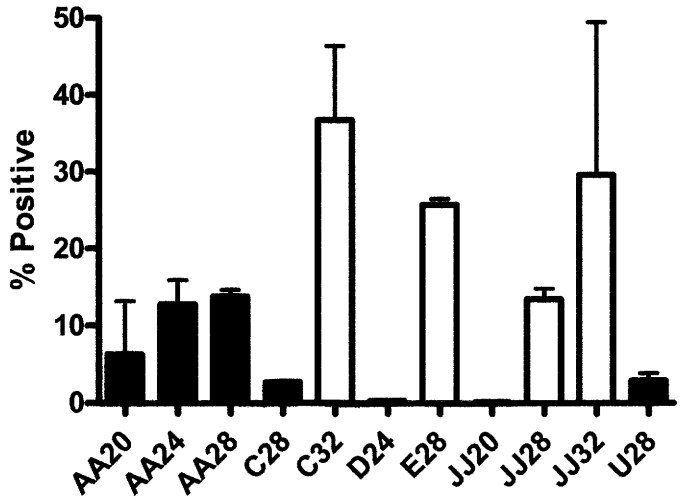


**Figure 6.13.** Transfection efficacy of poly(β-amino esters) in HUVECs. Top-performing polymers for gene delivery are shown in white.

Interestingly, there is a biphasic relationship between polymer/DNA binding constant and transfection efficacy. All four of the top-performing gene delivery polymers here have a polymer/DNA binding constant in the narrow range of 4-9 x $10^{10}$ $M^{-1}$. Both below (D24 and U28) and above (C28 and JJ20) this intermediate value for $K_a$, there is dramatically reduced transfection to baseline levels. An important exception to this relationship, is the AA-based polymers. For this case, it is very important to note that all of the acrylate structures are very similar, except for acrylate monomer AA (Figure 6.1A). This acrylate has a much more hydrophobic structure and is believed to function differently than the other polymers. For example, polymers formed with this monomer, unlike the others (C, D, E, JJ, U), are able to self-assemble without DNA into nanoparticles (data not shown). It is believed that this self-assembly is into micelle-like or liposome-like structures. These AA-based polymers are also much more

cytotoxic than the other acrylate-polymers and this is believed to be due to a different hydrophobic interaction of these polymers with biological membranes.

These binding results add further evidence that the AA-based polymers (left side of figures) deliver DNA by an alternative mechanism than the other acrylate based polymers (C, D, E, JJ, and U). For example, while all of the other PBAE polymers tested here show a rather steep biphasic dependence of binding constant, $K_a$, on gene delivery, AA-based polymers show no dependence on binding constant with gene delivery efficacy. The hydrophilic polymers must bind DNA electrostatically to form particles (favors high $K_a$) and then release DNA electrostatically (favors low $K_a$) for delivery to occur. This conflicting relationship of how $K_a$ affects gene delivery results in the biphasic relationship elucidated here. However, in contrast, the hydrophobic AA-based polymers can self-assemble with or without DNA in a manner that is independent of $K_a$. If DNA is present in solution, it could then become encapsulated in a process that is much less sensitive to binding. Similarly, if this hydrophobic polymer is membrane disruptive (as potentially indicated by its hydrophobic structure and much larger toxicity), release of DNA could also be accomplished in a binding insensitive manner. This binding assay could potentially be useful in not only quantifying DNA binding constants and effective binding lattice site size, but also as an assay to determine the mechanism of DNA encapsulation by examining the sensitivity of $K_a$ to gene delivery efficacy. AA-based polymers may not have the same DNA binding bottleneck for gene delivery as some of other gene delivery polymers, but instead have a different bottleneck. Unfortunately, their corresponding toxicity limits their utility (data not shown), but a similar structural derivative may make a very promising gene delivery polymer.

Of the eight non-AA-based polymers, four of them are found to have almost the same intermediate binding constant and all four of these polymers work well for gene delivery. The two polymers with lower binding constant (D24 and U28) fail presumably because they are unable to bind DNA tightly enough to efficiently condense DNA into a small and stable particle and/or sufficiently protect DNA from degradation. This has been verified by our biophysical analysis of the nanoparticles formed using these polymers.[3] On the other hand, the two polymers with higher binding constants (C28 and JJ20) fail presumably because they bind too tightly and are unable to efficiently release their DNA cargo once inside the cell. For the hydrophilic polymers tested here (C, D, E, JJ, and U), this assay combined with our polymer library approach provides insight into how to design a polymer with an optimal DNA binding constant.

### *6.3.4 Small Modifications of C32 Base Polymer Enables Polymer/DNA Binding Constant Tuning and Increased Transfection Efficacy*

The polymer library approach used here to investigate how polymer structure affects binding affinity and how binding affinity affects gene delivery efficacy is quite interesting. However, one confounding variable is that these polymers were all chosen based on their maximal efficacy in early gene delivery screening, and consequently for each polymer there was a different optimal molecular weight (~10-20 kDa). We next wanted to control the effect of molecular weight and look exclusively at polymer structure. We also wanted to develop a method to take an effective (or non-effective) gene delivery polymer and be able to "tune" its

structure to change its binding constant and hopefully, gene delivery efficacy. We hypothesized that the addition of small diamines to the ends of an acrylate-terminated base polymer could increase polymer/DNA binding and increase transfection efficacy. We chose C32 as the base polymer since it performed the best in earlier transfection screens on multiple cell types and a variety of conditions.[3, 6]

End-modified C32-based polymers were assayed and fitted following the same protocol as the other poly(β-amino esters). As all of the end-modified polymers were based on the same base polymer, they all have approximately the same molecular weight (~9 kDa). From this molecular weight, $n_{max}$ was calculated for reference (all fitting for $K_a$ and $n_{obs}$ are independent of $n_{max}$). The base polymer (C32-Ac) has two fewer maximum binding sites per polymer since it lacks the amine end-capping of the other polymers. The binding isotherms of these polymers and a table of their fitting parameters can be found in Figure 6.14 and Table 6.2 respectively.

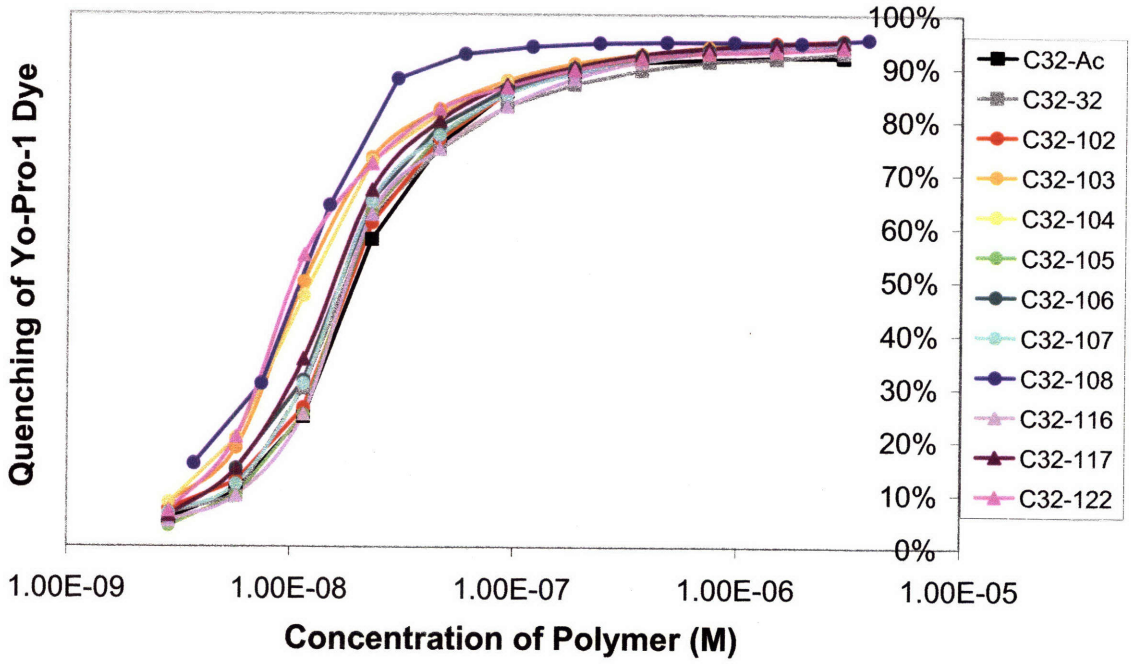


**Figure 6.14.** End-modified C32 polymer isotherms. Unlike the broader class of poly(β-amino esters) used earlier, each of these polymers has the same molecular weight.

Small end-modifications to the same base polymers were found to have disparate affects on the overall change $K_a$. This ranged from a small decrease (C32-102) to an order of magnitude increase in $K_a$ (C32-108). We had hypothesized that this modification technique could be used to tune $K_a$, but an order of magnitude change is surprising as the end-modifications only change ~2-3% of the total molecular weight of the polymer. The only end-modified polymer that had an $n_{obs}$ significantly different from the other end-modified polymers is C32-108, which had $n_{obs} = 18$, whereas the average of $n_{obs}$ for the other end-modified polymers is 15±1. It may be that this

relatively long end-chain modification caused the overall polymer ligand to fully occupy two additional lattice sites when bound.

| Polymer | $n_{max}$ | $n_{obs}$ | $K_a$ ($10^9$/M) |
|---|---|---|---|
| C32-Ac | 28 | 16 | 1.2 |
| C32-32 | 30 | 17 | 1.7 |
| C32-102 | 30 | 15 | 1.0 |
| C32-103 | 30 | 14 | 3.7 |
| C32-104 | 30 | 13 | 2.7 |
| C32-105 | 30 | 17 | 1.8 |
| C32-106 | 30 | 15 | 1.9 |
| C32-107 | 30 | 16 | 1.8 |
| C32-108 | 30 | 18 | 11 |
| C32-116 | 30 | 16 | 1.0 |
| C32-117 | 30 | 15 | 2.4 |
| C32-118 | 30 | 16 | 2.0 |
| C32-122 | 30 | 13 | 2.7 |

**Table 6.2** Table of end-modified C32 polymer properties. This table shows the maximum and observed lattice binding site size ($n_{max}$ and $n_{obs}$), and the association constant, $K_a$.

Figure 6.15 and Figure 6.16 highlight how structural changes to the end-capping diamine affect binding constant, $K_a$, and gene delivery efficacy. Effects of single carbon changes to linear diamine monomers C32-102 (2 carbons) through C32-108 (8 carbons) may be indicative of physical overlap of amine groups along the polymer with anionic charges on the lattice. It

may be that end groups on C32-102 (2 carbons spacer) partially block the binding of their adjacent amine group reducing binding affinity. C32-103, (3 carbon spacer) in contrast, may be just the right size to augment the binding of the amine groups adjacent to the polymer end groups. C32-108 (8 carbon spacer), as previously mentioned, may increase binding by increasing the ligand site size by a full count on each side of the polymer. Intermediate lengths C32-104 (4 carbon spacer) through C32-107 (7 carbon spacer) show decreasing affinity with increasing length, possibly because as spacer length increases, the potential augmentation to polymer end binding is reduced (end-group modified group in combination of adjacent amine group). Structurally, C32-117 is the same as C32-103, but with an additional ethyl- group and C32-118 is the same as C32-105 except for an additional methyl- group. In these cases, the addition of the ethyl group reduces the increase in $K_a$ by about half, but addition of the methyl group does not significantly change $K_a$. In the case of C32-116, the steric effects of double methylation of the middle carbon in C32-103 abolish its $K_a$ enhancement altogether.

In terms of transfection efficacy, these studies elucidate the lower bound of optimal $K_a$. The three best end-modified C32 polymers were able to transfect greater than 50% of the primary human cells in serum, significantly greater than any of he unmodified polymers used previously. Importantly, this high efficacy also occurred using an efficiently low 30:1 polymer to DNA weight ratio and a relatively low polymer molecular weight of ~9 kDa. In contrast, the base polymer, acrylate-terminated C32 (C32-Ac) is ineffective for gene delivery. C32-32 (MW~9 kDa) is also ineffective for gene delivery due to a low $K_a$ compared with the higher molecular weight C32 polymer used in the earlier studies (MW~18 kDa). Also affecting the C32-32 comparison is the fact that in the earlier gene delivery efficacy studies (Figure 6.13),

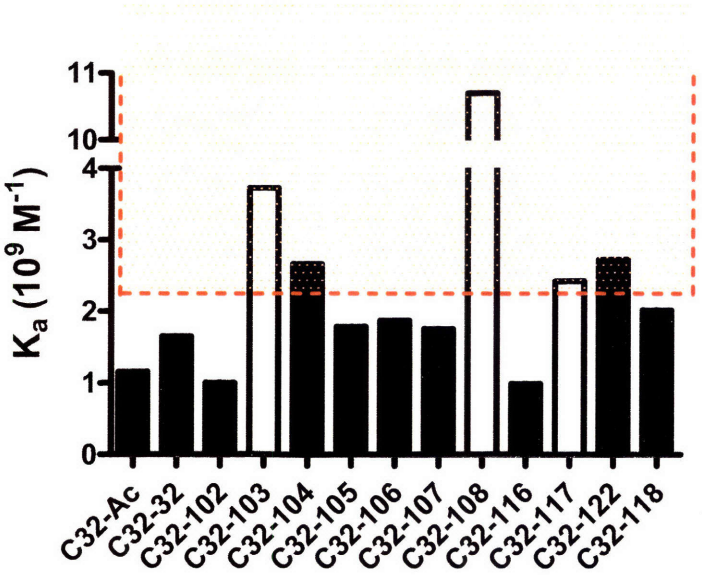


**Figure 6.15.** Small structural changes to diamine monomers used to end-cap C32-Ac base polymer tune the overall polymer/DNA binding constant for the whole polymer. Top-performing polymers for gene delivery are shown in white.

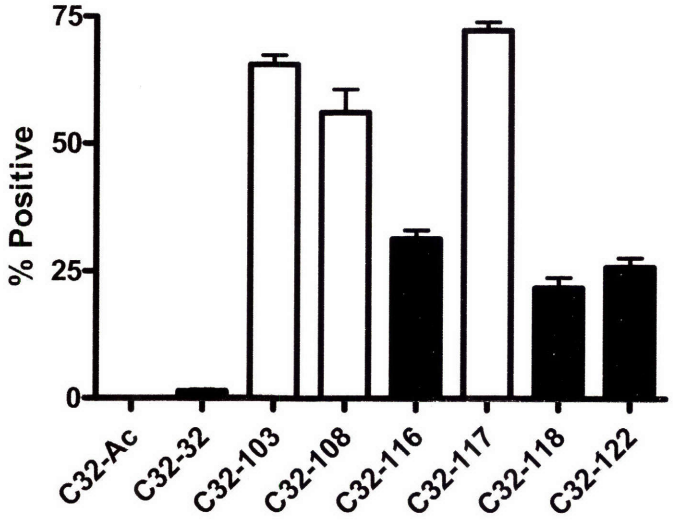


**Figure 6.16.** HUVEC transfection in serum containing media. All polymers are used at a 30:1 polymer to DNA weight ratio. Top-performing polymers for gene delivery are shown in white.

each polymer is used at its optimal polymer to DNA weight ratio and here (Figure 6.16), all polymers are used at a low constant 30:1 weight ratio for direct comparison of structure only (molecular weight and formulation conditions held constant). Based on these studies, a minimal $K_a$ of 2.4 x $10^9$ $M^{-1}$ is necessary, but may not be sufficient, for high gene delivery efficacy.

Combining the results from both the unmodified poly(β-amino esters) and the end-modified poly(β-amino esters) more clearly show the biphasic relationship between binding constant $K_a$ and gene delivery efficacy. Figure 6.17 highlights these findings. In this figure, the molecular structure of the polymers is indicated by their marker. The color of the marker is the component acrylate monomer and the shape of the marker is the component amine monomer. All amine structures are very similar, most differing only by a single carbon. All acrylate structures are very similar as well, except for acrylate monomer AA as previously discussed. Because of the different physicochemical properties of AA-based polymers and AA-based polymer/DNA nanoparticles, the AA-based polymers are highlighted in red in this figure, so that their unique $K_a$ – insensitive behavior can be better distinguished from the broader class of poly(β-amino esters). This figure demonstrates that our previous findings hold: that there is a relatively narrow range for optimal DNA binding constants and that modification to just the ends of a polymer can tune this binding constant.

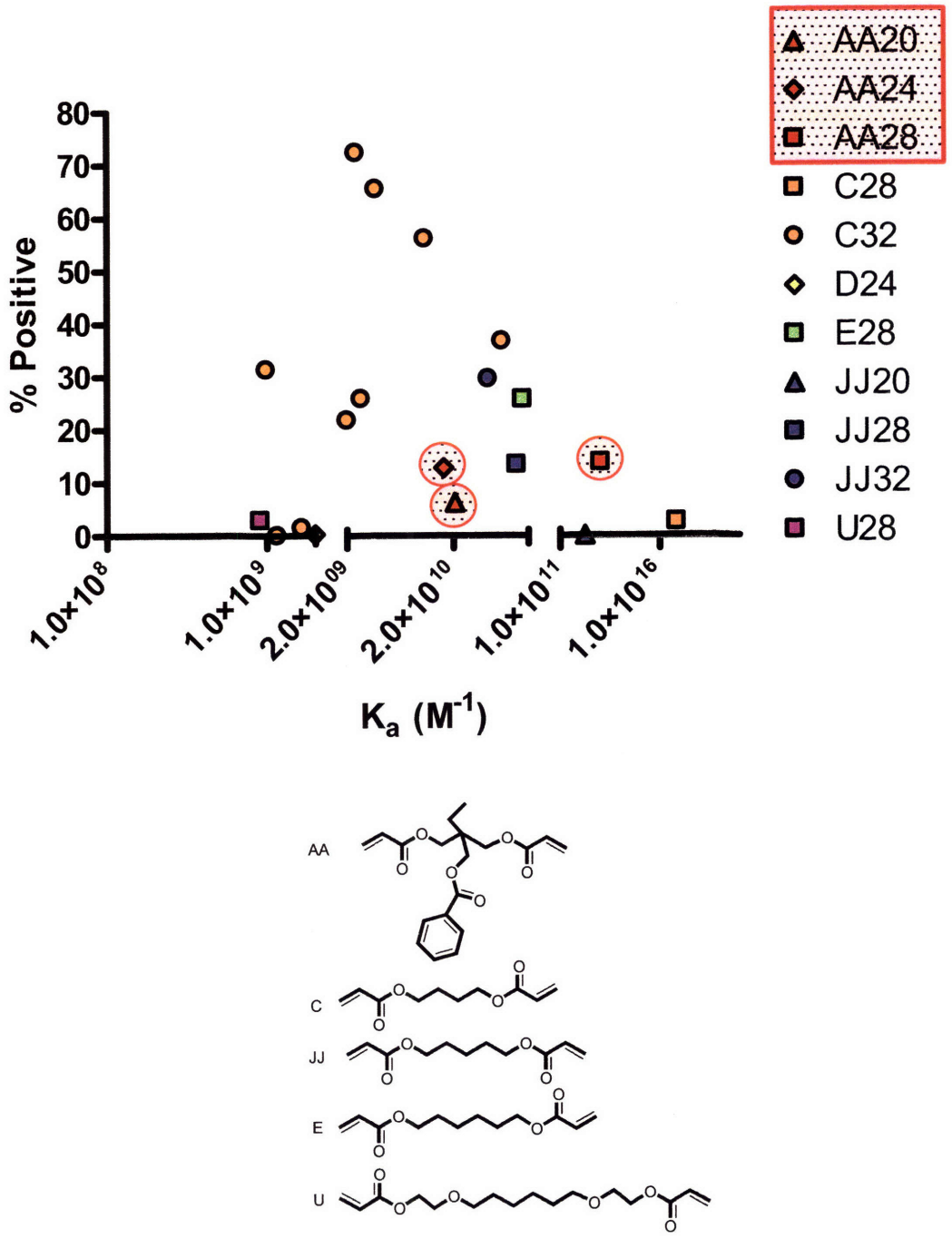


**Figure 6.17.** Comparison of $K_a$ vs. transfection efficacy. Polymer AA has different, more compact and hydrophobic structure than polymers C, JJ, E, and U. Polymer AA can self-assemble without DNA unlike the other polymers.

For the hydrophilic polymers tested, this high-throughput binding assay combined with our polymer library approach provides insight into how to design a polymer with an optimal DNA binding constant. For example, the literature shows that PEI and poly(β-amino esters) with molecular weights below 10 kDa exhibit poor transfection as compared to higher molecular weight versions.[4] However, some of the end-modified polymers used here (C32-103, C32-108, C32-117) are able to deliver DNA with high efficacy despite a low molecular weight of ~9 kDa. This binding study elucidates a mechanism for these findings, a more direct quantifiable parameter ($K_a$ rather than MW), and an *in situ* assay for designing and testing new polymers.

Whereas tight binding of the polymer to DNA is important, not all polymers that form small and stable gene delivery particles are subsequently proved to be effective for gene delivery. For example, we previously have investigated how polymer structure of poly(β-amino esters) correlates to biophysical properties including particle size and serum-stability (Chapter 4).[3] However, some particles that were small and stable still did not transfect well. One polymer in particular that failed to be effective was polymer C28. With the insights gained from the work presented here, it is now clear that this polymer failed because its binding constant was too high. In the future, drug delivery biomaterials that bind to and encapsulate nucleic acids can be quickly and easily screened *in situ* in under an hour using the assay presented here to find the most promising candidates before application to cells.

## 6.4 CONCLUSIONS

We have demonstrated a high-throughput method to screen polymers for DNA binding, computationally modeled DNA/binding constants and lattice site size, and correlated how DNA

binding constant affects transfection efficacy. Quantifying how polymers bind DNA is important to move forward in rational design for drug delivery. A striking, biphasic relationship was found between DNA binding and efficacy with an optimal $K_a$ in the range of $2.4 \times 10^9 - 8.9 \times 10^{10}$ $M^{-1}$ ($K_d \sim 11$ - 420 pM). This biphasic relationship held true for a range of different polymer structures from a poly(β-amino ester) library. To improve gene delivery biomaterials further, tuning $K_a$ is likely key, and small structural modifications were found to be effective at increasing $K_a$ and corresponding delivery efficacy. The assay used here was also helpful in discerning the mode of DNA association and encapsulation between a hydrophilic polymer and a hydrophobic polymer. The binding analysis used here is of importance to the design of polymeric drug delivery vehicles for a range of multivalent cargos (DNA, siRNA, etc) and diverse therapeutic applications.

## 6.5 REFERENCES


1. Thomas, M. & Klibanov, A.M. Non-viral gene therapy: polycation-mediated DNA delivery. *Appl Microbiol Biotechnol* **62**, 27-34 (2003).
2. Ogris, M., Steinlein, P., Carotta, S., Brunner, S. & Wagner, E. DNA/polyethylenimine transfection particles: Influence of ligands, polymer size, and PEGylation on internalization and gene expression. *Aaps Pharmsci* **3**, art. no. 21 (2001).
3. Green, J.J. et al. Biodegradable polymeric vectors for gene delivery to human endothelial cells. *Bioconjug Chem* **17**, 1162-1169 (2006).

4. Anderson, D.G., Akinc, A., Hossain, N. & Langer, R. Structure/property studies of polymeric gene delivery using a library of poly(beta-amino esters). *Mol Ther* **11**, 426-434 (2005).

5. Schaffer, D.V., Fidelman, N.A., Dan, N. & Lauffenburger, D.A. Vector unpacking as a potential barrier for receptor-mediated polyplex gene delivery. *Biotechnol Bioeng* **67**, 598-606 (2000).

6. Anderson, D.G., Lynn, D.M. & Langer, R. Semi-automated synthesis and screening of a large library of degradable cationic polymers for gene delivery. *Ang. Chem. Int. Edn* **42**, 3153-3158 (2003).

7. Lynn, D.M. & Langer, R. Degradable poly(beta-amino esters): Synthesis, characterization, and self-assembly with plasmid DNA. *J Am Chem Soc* **122**, 10761-10768 (2000).

8. Zelikin, A.N., Trukhanova, E.S., Putnam, D., Izumrudov, V.A. & Litmanovich, A.A. Competitive reactions in solutions of poly-L-histidine, calf thymus DNA, and synthetic polyanions: Determining the binding constants of polyelectrolytes. *J Am Chem Soc* **125**, 13693-13699 (2003).

9. Plank, C., Tang, M.X., Wolfe, A.R. & Szoka, F.C. Branched cationic peptides for gene delivery: Role of type and number of cationic residues in formation and in vitro activity of DNA polyplexes. *Hum Gene Ther* **10**, 319-332 (1999).

10. Mcghee, J.D. & Hippel, P.H.V. Theoretical Aspects of DNA-Protein Interactions - Cooperative and Non-Cooperative Binding of Large Ligands to a One-Dimensional Homogeneous Lattice. *J Mol Biol* **86**, 469-489 (1974).

11. Wolfe, A.R. & Meehan, T. Use of binding site neighbor-effect parameters to evaluate the interactions between adjacent ligands on a linear lattice. Effects on ligand-lattice association. *J Mol Biol* **223**, 1063-1087 (1992).

12. Petty, J.T., Bordelon, J.A. & Robertson, M.E. Thermodynamic Chacterization of the Association of Cyanine Dyes with DNA. *J. Phys. Chem. B.* **104**, 7221-7227 (2000).

13. Akinc, A. & Langer, R. Measuring the pH environment of DNA delivered using nonviral vectors: Implications for lysosomal trafficking. *Biotechnol Bioeng* **78**, 503-508 (2002).

14. Akinc, A., Lynn, D.M., Anderson, D.G. & Langer, R. Parallel synthesis and biophysical characterization of a degradable polymer library for gene delivery. *J Am Chem Soc* **125**, 5316-5323 (2003).

15. Akinc, A., Thomas, M., Klibanov, A.M. & Langer, R. Exploring polyethylenimine-mediated DNA transfection and the proton sponge hypothesis. *J Gene Med* **7**, 657-663 (2005).

16. Sonawane, N.D., Szoka, F.C. & Verkman, A.S. Chloride accumulation and swelling in endosomes enhances DNA transfer by polyamine-DNA polyplexes. *J Biol Chem* **278**, 44826-44831 (2003).

# Chapter 7: Poly(β-amino ester) Nanoparticles With Efficacy Comparable to Adenovirus

## 7.1 INTRODUCTION

Viral gene therapy has high efficacy, but is plagued by serious safety risks, production and manufacturing challenges, and other limitations including nucleic acid cargo capacity.[1] In contrast, non-viral gene delivery systems, while addressing these challenges, remain less effective.[2] Here we develop end-modified poly(β-amino ester)s, easy-to-synthesize degradable polymers, that are able to deliver DNA to primary human umbilical vein endothelial cells (HUVECs) at levels comparable to adenovirus at a Multiplicity of Infection (MOI) between 100 and 500, and two orders of magnitude better than the commonly used non-viral polymeric vector, polyethylenimine (PEI). Interestingly, small structural changes were found to have dramatic effects on multiple steps of gene delivery including the DNA binding affinity, nanoparticle size, intracellular DNA uptake, and final protein expression. *In vivo*, these polymer modifications dramatically enhance DNA delivery to ovarian tumors. We believe the development of polymeric vectors with gene delivery efficacy comparable to adenovirus could set a new benchmark in non-viral transfection capability.

Numerous polymeric materials have been used for gene delivery including poly(L-lysine), polyethylenimine, poly(amidoamine) dendrimers, poly(α-[4-aminobutyl]-L-glycolic acid),

chitosan, cyclodextrin, and others.[2,3] While significant strides have been made in improving delivery, efficacy remains generally low, particularly for primary cells in the presence of serum.[4] Poly(β-amino ester)s are promising materials that bind and self-assemble with DNA to form stable nanoparticles that effectively enter cells, escape the endosomal compartments, and degrade via hydrolytic cleavage of backbone ester groups.[5-8] While good *in vitro* and *in vivo* activity has been described,[5,9] structural diversity of existing poly(β-amino ester) was limited by chemical requirements of conjugate addition.[5-8,10] We hypothesized that the exploration of an expanded chemical space through combinatorial modification of poly(β-amino ester)s could optimize performance. To this end, and to better understand structure-function relationships, we synthesized a library of end-modified poly(β-amino ester)s using C32 diacrylate-terminated polymer as a base polymer and twelve amine end-capping reagents (Figure 7.1.). Chemical methods were developed to allow a simple, one step modification of the base polymer with several different amine capping agents. In this way, the combined effects of internal structure and amine termination on poly(β-amino ester) transfections could be systematically assessed. Once synthesized, polymers were characterized by $^{1}$H NMR and GPC (see experimental procedures).

## 7.2 EXPERIMENTAL PROCEDURES

### *7.2.1 Materials*

Polyethylenimine (water free, $M_w$ ~ 25 kDa, $M_n$ ~ 10 kDa), 3-amino-1-propanol (99%), N,N'-dimethylethylenediamine (99%), and anhydrous DMSO were purchased from Sigma-Aldrich (St. Louis, MO, USA). A 25 mM sodium acetate buffer solution pH 5.2 (NaAc buffer) was prepared by diluting a 3 M stock (Sigma-Aldrich). 1,4-Butanediol diacrylate (99+%) and 5-amino-1-pentanol (97%) were from Alfa Aesar (Ward Hill, MA, USA); Amine capping reagents were purchased from Sigma-Aldrich, Alfa Aesar, Acros Organics/Fisher Scientific (Pittsburgh, PA, USA), TCI America (Portland, OR, USA), Molecular Biosciences (Boulder, CO, USA), and Toronto Research Chemicals (Toronto, Ontario, Canada). All chemicals were used as received without any further purification.

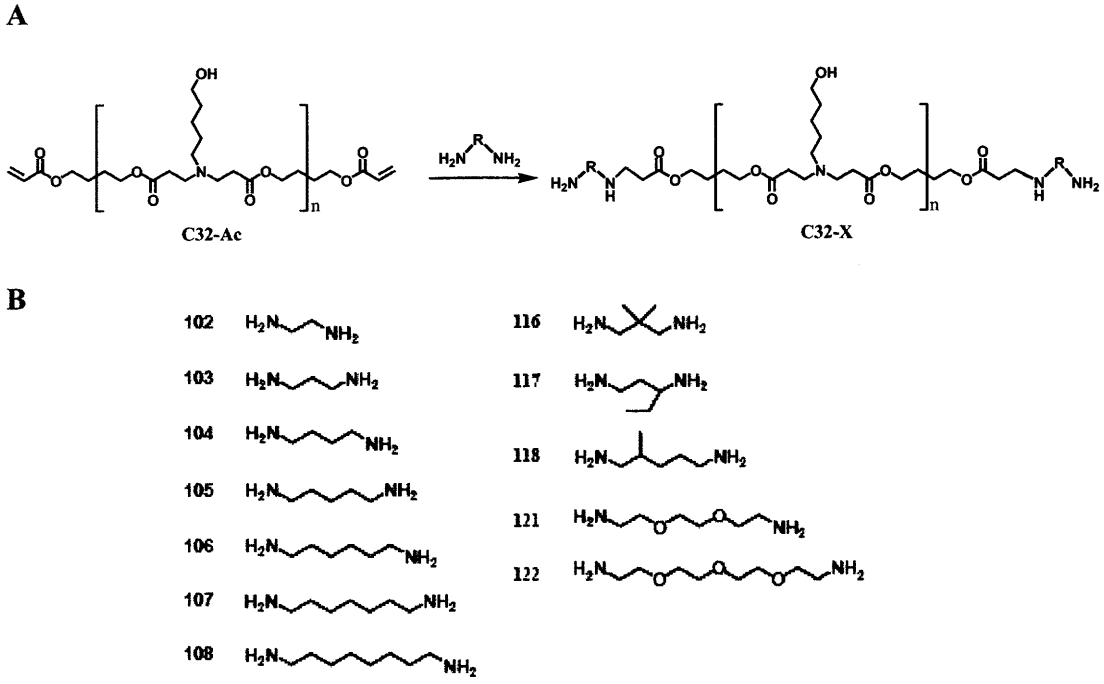


**Figure 7.1.** (A) Synthesis of end-modified poly(β-amino ester)s by reaction of acrylate-terminated C32 polymer with primary diamine molecules in DMSO; (B) Structures of amine-capping molecules.

### *7.2.2 Polymer Synthesis*

End-modified polymers were synthesized using a two-step process. First, acrylate-terminated polymers were synthesized, followed by post-polymerization end-chain conjugation of amine molecules (Figure 7.1.A). In the first step, acrylate-terminated poly(β-amino ester) C32-Ac was synthesized by mixing the corresponding diacrylate and amine monomers in a 1.2:1 ratio. C32-Ac was prepared by mixing 793 mg of 1,4-butanediol diacrylate (4 mmol) with 344 mg of 5-amino-1-pentanol (3.3 mmol). Polymerizations were performed in Teflon-lined screw

cap vials under magnetic stirring at 90°C for 24 hours. $^1$H NMR of C32-Ac ($d_6$-DMSO): δ (ppm) 1.2-1.4 (m, -$NCH_2(C\boldsymbol{H_2})_3CH_2OH$), 1.6 (bs -$N(CH_2)_2COOCH_2C\boldsymbol{H_2}$- and $CH_2CHCOOCH_2C\boldsymbol{H_2}$-), 2.3-2.4 (m, -$COOC\boldsymbol{H_2}CH_2N$- and –$NC\boldsymbol{H_2}(CH_2)_4OH$), 2.6-2.7 (m, -$COOCH_2C\boldsymbol{H_2}N$-), 3.4 (bs, -$N(CH_2)_4C\boldsymbol{H_2}OH$), 4.0 (bs, -$N(CH_2)_2COOC\boldsymbol{H_2}CH_2$-), 4.1 (m, $CH_2CHCOOC\boldsymbol{H_2}CH_2$-), 4.4 (bs, -$N(CH_2)_5O\boldsymbol{H}$), 5.9 (m, $C\boldsymbol{H_2}CHCOOCH_2CH_2$-), 6.1-6.2 (m, $CH_2C\boldsymbol{H}COOCH_2CH_2$-), 6.3-6.4 (m, $C\boldsymbol{H_2}CHCOOCH_2CH_2$-). Gel permeation chromotography (GPC) of the C32-Ac polymer resulted in a $M_w$ = 8800 Da (polydispersity = 1.9).

Acrylate-terminated polymers were dissolved in DMSO at 31.13% wt/wt. Amine capping reagents were dissolved in DMSO at 0.25 M. End chain capping reactions were performed by mixing 321 mg of polymer/DMSO solution with 800 μl of amine solution. Reactions were performed in eppendorf tubes with constant agitation for 24 hours. End-chain coupling conditions were optimized in DMSO to prevent inter-chain crosslinking and aminolysis reactions, as determined using GPC and NMR. The use of concentrated polymer in DMSO, containing residual unreacted amine that did not affect cell viability, permitting the final end-modified polymers to be used directly in all transfection assays, without prior purification of each polymer. This enabled end-modified derivatives of each polymer to be rapidly synthesized and screened in parallel. Polymers were stored at -20 degC until used for each experiment.

$^1$H NMR of C32-Ac capped with 1,3-Diaminopropane (C32-103) ($d_6$-DMSO): δ (ppm) 1.2-1.5 (m, -$NCH_2(C\boldsymbol{H_2})_3CH_2OH$ and –$NHCH_2C\boldsymbol{H_2}CH_2NH_2$), 1.6 (bs -$N(CH_2)_2COOCH_2C\boldsymbol{H_2}$-), 2.2-2.4 (m, -$COOC\boldsymbol{H_2}CH_2N$- and –$NC\boldsymbol{H_2}(CH_2)_4OH$), 2.4-2.7 (m, -$COOCH_2C\boldsymbol{H_2}N$- and -$NHC\boldsymbol{H_2}CH_2C\boldsymbol{H_2}NH_2$), 3.3 (t, $J$ = 6.6 Hz, -$N(CH_2)_4C\boldsymbol{H_2}OH$), 4.0 (bs, -$N(CH_2)_2COOC\boldsymbol{H_2}CH_2$-).

### *7.2.3 Luciferase Transfection*

COS-7 cells were obtained from ATCC (Manassas, VA, USA) and maintained in phenol red-free DMEM supplemented with 10% fetal bovine serum and 100 units/ml of penicillin/streptomycin. HepG2 cells were obtained from ATCC and grown in MEM supplemented with 10% fetal bovine serum, 2 mM L-glutamine, 0.1 mM non-essential amino acids, 100 units/ml of penicillin/streptomycin, and 1 mM sodium pyruvate. All cell culture reagents were purchased from Invitrogen Corporation (Carlsbad, CA, USA) unless otherwise noted. All cell lines were grown at 37°C, 5% $CO_2$ atmosphere. pCMV-Luc plasmid DNA stock solution (1 mg/ml in water) was obtained from Elim Biopharmaceuticals (Hayward, CA, USA).

COS-7 cells (15,000 cells/well) or HepG2 cells (5,000 cells/well) were plated in opaque 96-well plates and allowed to adhere overnight. Polymers at 100 mg/ml in DMSO were diluted accordingly into NaAc buffer to concentrations that yield the different polymer:DNA weight ratios. One hundred microliters of diluted polymer solution was mixed vigorously with 100 µl of DNA (60 µg/ml in NaAc buffer) in a 96-well polystyrene plate. The solutions were left undisturbed for 5 minutes after which time 120 µl of each was added to 800 µl of cell culture media in a deep-well polypropylene plate. The media over the cells was then removed with a 12-channel aspirator wand and followed by the addition of 150 µl/well of polymer-DNA complex solution. Complexes were incubated over the cells for one hour after which time they were aspirated off and replaced with 105 µl/well of fresh cell culture media. Cells were allowed to grow for three days at 37°C, 5% $CO_2$ and then analyzed for luciferase protein expression.

Luciferase expression was analyzed using Bright-Glo™ assays kits purchased from Promega Corporation (Madison, WI). Briefly, 100 µl/well of Bright-Glo solution was added to

the cell plates. The plates were gently agitated to promote mixing for 2 minutes. Luminescence was then measured on a Perkin Elmer Victor 3 plate luminometer using a 1% neutral density filter and a one second per well counting time.

### *7.2.4 DNA Binding Assay*

Polymer solutions at 100 mg/ml in DMSO were diluted into NaAc buffer to a final concentration of 6 mg/ml. In a half area 96-well plate, 50 μl/well of diluted polymer was added to 50 μl/well of DNA (60 μg/ml in NaAc buffer). The solutions were mixed vigorously and allowed to sit undisturbed for 5 minutes to allow for polymer-DNA complexation. After this time, 100 μl/well of PicoGreen solution was added. PicoGreen working solution was prepared by diluting 80 μl of the purchased stock into 15.2 ml NaAc buffer. After 5 minutes, 30 μl/well of polymer-DNA-PicoGreen solution was added to 200 μl/well of DMEM media in black 96-well polystyrene plates. The plate fluorescence was then measured on a Perkin Elmer Victor 3 plate reader using a FITC filter set (excitation 485 nm, emission 535 nm). The relative fluorescence (RF) was calculated using the following relationship:

$RF = (F_{sample} - F_{blank})/(F_{DNA} - F_{blank})$

where $F_{sample}$ is the fluorescence of the polymer-DNA-PicoGreen sample, $F_{blank}$ is the fluorescence of a sample with no polymer or DNA (only PicoGreen), and $F_{DNA}$ is the fluorescence of DNA-PicoGreen (no polymer).

### *7.2.5 Particle Sizing*

Polymer solutions at 100 mg/ml in DMSO were diluted into NaAc buffer the appropriate concentration. Concentrations were adjusted for each polymer so that the final polymer:DNA ratio was the same that produced the highest transfection. To prepare polymer:DNA complexes, 100 μl of diluted polymer was added to 100 μl of DNA (60 μg/ml in NaAc) and pipetted vigorously. Complexation was allowed to proceed undisturbed for 5 minutes after which time 150 μl of the sample was diluted into 1.8 ml of DMEM media. Polymer:DNA complex size was measured on a ZetaPALS dynamic light scattering detector (Brookhaven Instruments Corporation, Holtsville, NY, USA; 15 mW laser; 676 nm incident beam, 90° scattering angle). Effective particle diameters were calculated from the autocorrelation function using the MAS option of the BIC particle sizing software assuming a log normal distribution. The solution viscosity and refractive index were assumed equal to pure water at 25°C.

### *7.2.6 DNA Uptake Assay*

Uptake measurements of polymer-DNA complexes were performed essentially as described for the transfection experiments but using a β-galactosidase (β-gal) plasmid. Instead of quantifying protein expression levels after three days, total cellular DNA was isolated four hours post-transfection using a DNeasy 96 Tissue Kit (Qiagen; Valencia, CA, USA) following the manufacturer instructions. Total DNA was quantified using a Redi-Plate 96 PicoGreen dsDNA Quantification kit following the supplied instructions. The amount of β-gal DNA delivered was quantified using RT-PCR with a custom Taqman primer and probe set specific for

the β-gal plasmid (Applied Biosystems; Foster City, CA, USA). The primers and probe spanned an 80 bp sequence in the β-gal coding region of the plasmid and had the following sequences: forward primer 5'-TTA CAG GGC GGC TTC GTC T-3', reverse primer 5'-TAA GCC GAC CAC GGG TTG-3' and the Taqman probe 5'-6FAM-CTG GGT GGA TCA GTC GCT GAT TAA ATA TGA TG-TAMRA-3'. The primers and probes were used at concentrations of 400nM and 25nM respectively. After activating the Taq enzyme at 95°C for 10 minutes, 40 cycles of amplification were performed, with each cycle consisting of 95°C for 15 seconds, 60°C for one minute, followed by a fluorescent plate read using a Chromo4 Continuous Fluorescence Detector (MJ Research; Waltham, MA, USA). Plasmid copy numbers were determined by comparing the RT-PCR cycle threshold values to a plasmid standard curve and analyzed using the Opticon Monitor 3 software package (MJ Research).

### *7.2.7 GFP Transfection*

Human Umbilical Vein Endothelial Cells (HUVECs) (Cambrex, Walkersville, MD, USA) were cultured in EGM-2 media supplemented with SingleQuot Kits (Cambrex). HUVEC cells were used by passage five and in accordance to the manufacturer's instructions. pEGFP-N1 plasmid DNA stock solution (1 mg/ml in water) was obtained from Elim Biopharmaceuticals (Hayward, CA, USA). GFP transfections paralleled the luciferase transfections except that all volumes were scaled up five-fold, the experiments were conducted in clear 24-well plates with 6 μg GFP DNA per well, and C32 was used at an optimized 50:1 polymer:DNA weight ratio and the other poly(β-amino ester)s at a 30:1 ratio. HUVECs were seeded (75,000 cells/well) into clear 24-well plates at 24 hours prior to transfection to allow for growth to confluence. 150 μL

of each polymer/DNA complex solution was added to 1.0 mL of EGM-2 media supplemented with FBS (12% serum). The growth medium was removed from the seeded cells using a 6-channel aspirating wand (V&P Scientific, San Diego, CA, USA) after which 750 μL of the nanoparticle/media solution was immediately added to each well. Polymeric gene delivery nanoparticles were incubated with the cells for 4 hours and then removed using the 6-channel wand and replaced with 500 μL of warm EGM-2 media. After 48 hrs, transfected and untransfected control cells were washed, removed from the 24-well plates by trypsinization, microcentrifuged, and resuspended in 500 μL of FACS running buffer (98% PBS / 2% FBS / 1:200 propidium iodide solution (Invitrogen)) for FACS analysis.

PEI/DNA vectors were formed at a 1:1 polymer to DNA weight ratio (N/P=8) using the same DNA basis and protocol as the other polymers except that PEI/DNA complexes were formed in 150 mM NaCl as previously described.[11] Lipofectamine™ 2000 (Invitrogen) was used following manufacturer instructions. AdenoExpress™ adenovirus, Ad5.CMV-GFP, was obtained from Qbiogene (Montreal, QC, Canada). Both pEGFP-N1 plasmid DNA and Ad5.CMV-GFP utilize the CMV promoter. Ad5.CMV-GFP expresses sgGFP™ which based on vendor information has equivalent brightness to EGFP and is ~3-fold brighter than wtGFP. Ad5.CMV-GFP adenovirus was added directly to the cells in 750 μL of fresh 12% serum media, but unlike with the non-viral vectors, adenoviral particles were not aspirated out after 4 hours, but instead allowed to remain in the medium for the entire 48 hour duration of the experiment as instructed by the vendor.

GFP expression was measured using Fluorescence Activated Cell Sorting (FACS) on a FACSCalibur (Becton Dickinson, San Jose, CA, USA). Propidium iodide staining was used to exclude dead cells from the analysis and 20,000 live cells per sample were acquired. Two-

dimensional gating was used to separate increased autofluorescence signal from increased GFP signal to more accurately count positively expressing cells. Gating and analysis was performed using FlowJo 6.3 software (TreeStar, Ashland, OR, USA). GFP fluorescent micrographs were taken at 24 hrs post-transfection using a Zeiss fluorescent microscope equipped with AxioVision 3.1 using a 10x objective lens and 0.5 sec exposure time.

### *7.2.8 Mice*

Hemizygous MISIIR/TAg male transgenic mice[12] were bred to C57BL/6J females (Jackson Laboratory) to generate hemizygous MISIIR/TAg female mice. Ovarian tumors were detected by palpation. All procedures on mice were done in accordance with a protocol approved by the Lankenau IACUC.

### *7.2.9 Intraperitoneal Administration*

To prepare polymer/DNA complexes, 100 μg pCAG/luc DNA in 50 μl $H_2O$ was mixed with 50 μl diluted polymer [20 – 30 μl polymer (1 mg/10μl stock) diluted in 50mM NaAc buffer, pH5.2], a polymer:DNA ratio of 20:1 to 30:1. Following a 5 min. incubation at room temperature, 20 μl of a 30% (w/v) solution of glucose in PBS was added to the polymer/DNA mixture (5% glucose final conc.). The resulting 120 μl volume was injected immediately into the peritoneal cavity of a mouse using a 28G $^1/_2$ in insulin syringe.

### *7.2.10 Optical Imaging*

Optical bioluminescence imaging was performed on whole bodies of mice and then on harvested tumors 6 hr following injection of polymer/DNA complexes using an IVIS imaging system as previously described.[9] LIVE IMAGE acquisition and analysis software was used to quantify luciferase expression from the optical images.

### *7.2.11 Statistics*

Statistical calculations were carried out using GraphPad Prism 4.0 for Windows. Results are reported as mean±standard deviation. Statistical differences between modified polymers and C32H were determined for each cell line using a one-way ANOVA with a Dunnett multiple comparison test. For head-to-head comparison of gene delivery vectors to viral vectors or unmodified C32H, statistical significance was determined by using unpaired, two-tailed, Student's *t*-tests with 95% confidence. For bioluminescence imaging, statistical differences between C32-117 and unmodified C32 were determined using a Student's *t*-test with 95% confidence on log-transformed data (* $p < 0.05$; ** $p < 0.01$; *** $p < 0.001$).

## 7.3 RESULTS AND DISCUSSION

Polymer C32 was chosen as the base polymer as high-throughput screening studies have identified polymer C32 as the most effective poly(β-amino ester) to date for gene delivery.[5,6] This base polymer was end modified with twelve amine capping reagents (Figure 7.1.B). Primary diamine molecules were selected for chain termination to increase the cationic charge density of the polymers, which we hypothesized to increase the DNA binding, cellular uptake and ultimately the gene delivery efficiency.

Initial transfection testing of end-modified poly(β-amino ester)s was performed on COS-7 fibroblasts and HepG2 hepatocytes. To identify polymers that were effective at a low polymer concentration and in the presence of serum proteins, end-modified polymers were tested at a 20:1 polymer:DNA weight ratio in cell culture media containing 10% serum. A positive control, unmodified C32 polymer, was also prepared as described previously[5] and tested at both a low (20:1) and high (100:1) polymer:DNA weight ratio. The top performing polymers were then selected for testing in human primary cell culture.

To investigate a possible mechanism of delivery enhancement, two known gene delivery bottlenecks, DNA/vector binding and cellular uptake of DNA, were examined (Figure 7.2.). Lead modified polymers C32-103 and C32-117 were found to bind DNA with significantly higher affinity than C32, which also translated to the formation of smaller polymer-DNA complexes. We reason that the diamine end group modification increases the polymers' cationic charge, improving the polymer/DNA binding dynamics and the condensation of DNA into nanoparticles. This may also enhance overall gene delivery by better protecting DNA from degradation. Concurrently, it is also known that nanoparticles of smaller size tend to be more

efficiently internalized by cells[5,13] By using quantitative PCR to measure DNA internalization, C32-103 and C32-117, which formed nanoparticles that were ~30% smaller than those formed with unmodified C32, were found to increase cellular DNA uptake up to five-fold compared to C32. Interestingly, these higher levels of DNA binding and cellular uptake of end-modified polymer vectors were achieved at relatively low polymer weight ratios compared to optimized C32, further demonstrating the efficiency gains due to end-capping.

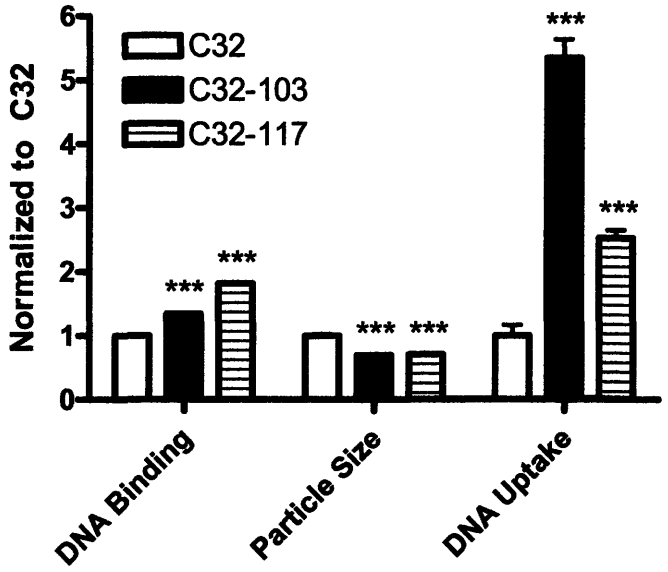


**Figure 7.2.** Comparison of optimized formulations of unmodified C32 to modified C32-103 and C32-117 for ability to bind DNA, form nanoparticles, and facilitate DNA uptake into COS-7 cells (particle size of normalized C32/DNA particles is 152 nm, *** indicates $p<0.001$).

End-modified C32 poly(β-amino ester)s were tested on Human Umbilical Vein Endothelial Cells (HUVECs) since primary endothelial cells are particularly difficult to transfect[14] and an important cell target for treatments against cardiovascular disease[15,16] and

cancer[17]. A commercially available GFP-expressing replication-deficient adenoviral vector that uses the same cytomegalovirus (CMV) promoter/enhancer as the plasmid DNA was chosen as a viral vector positive control (Ad5.CMV-GFP). Using fluorescent activated cell sorting (FACS) to measure the number of GFP-expressing cells, the adenovirus was found to transfect 75.6 ±0.1% of HUVECs at a multiplicity of infection (MOI) of 100. These results are comparable to, but slightly lower than, those reported by other researchers who found 90% positively expressing HUVECs at 100 MOI.[18] This difference is likely due, in part, to the differences in transfection conditions employed. Instead of using serum-free conditions for the transfections, we performed both non-viral and viral transfections in 12% serum containing media to more closely simulate *in vivo* conditions. It is known that serum proteins can inhibit both viral[19] and non-viral[4] gene delivery.

Figure 7.3.A shows a FACS histogram comparing the HUVEC GFP expression levels measured using an end-modified poly(β-amino ester), C32-103, and an adenovirus at a reasonably high level of infectivity (MOI=100). C32-103 is comparable to adenovirus both in terms of the average expression per cell and percentage of cells transfected. Interestingly, the mode of C32-103 treated cells is $10^4$ times the background level of controls, whereas for adenovirus, this peak is $\sim 10^2$.

The gene delivery efficacy of end-modified C32 polymers is shown in Figure 7.3.B. This figure demonstrates that some polymers, such as C32-118 and -122, have lower efficacy compared to optimized C32, whereas other polymers, including C32-103, -108, and -117, have higher efficacy than C32 and are comparable to adenovirus. It is important to note that all of the end-modified C32 polymers are more effective than the control C32 polymer at the same

polymer:DNA ratio, indicating that chain termination with primary diamine molecules is a useful way to improve the delivery efficiency. For effective gene delivery, unmodified C32 polymer

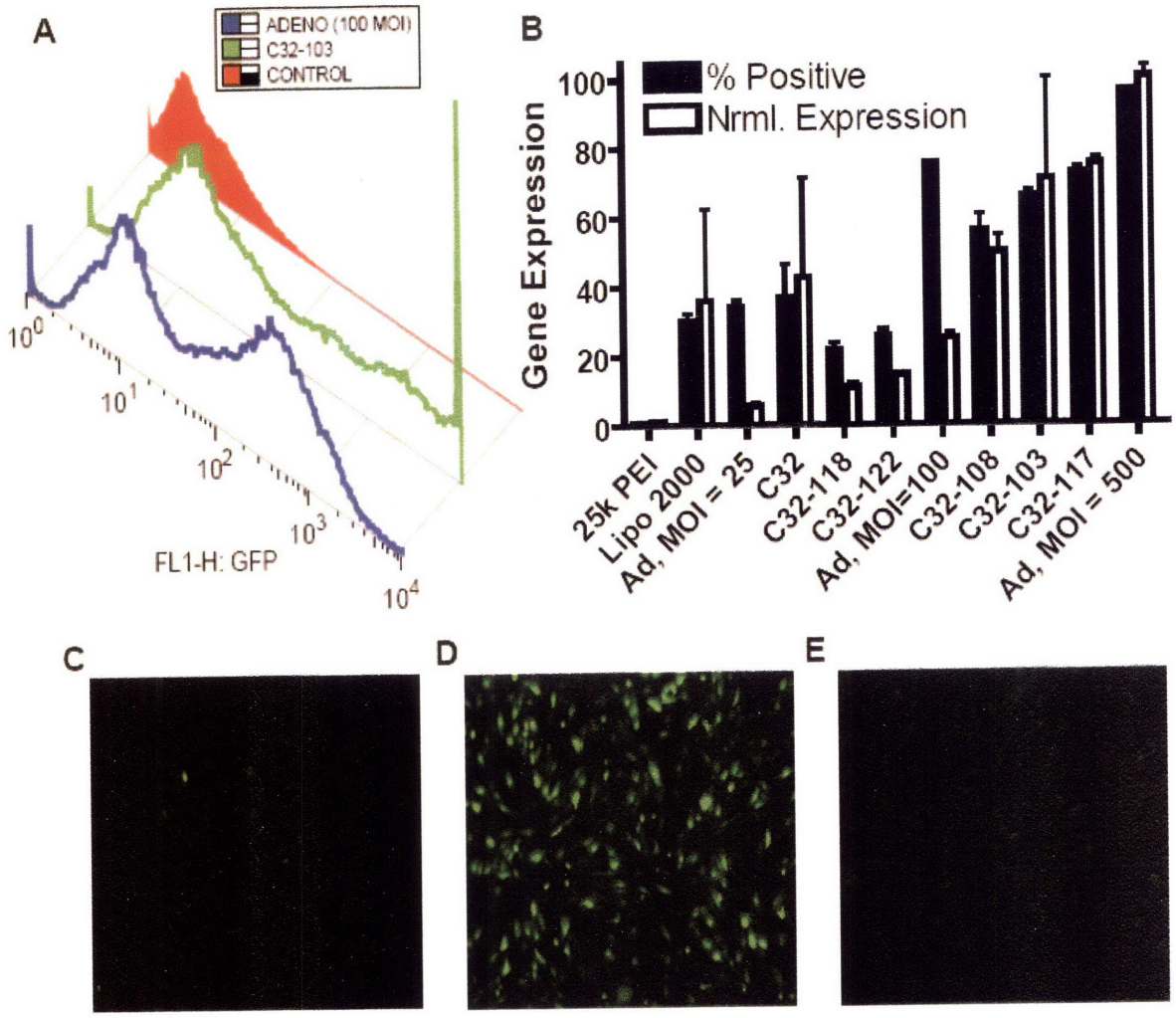


**Figure 7.3.** Gene expression of leading non-viral polymeric vectors as compared to adenovirus vectors. (A) Histogram showing gene expression in HUVECs at 48 hrs post-transfection with polymeric vector C32-103 as compared to adenovirus and a negative control. The mode of C32-103 cells are those expressing at $10^4$ times the background level of negative controls. (B) Gene expression is compared on both the basis of the percentage of cells positively transfected and normalized total gene expression per cell at 48 hrs post-transfection. Representative micrographs of GFP-expressing cells 24 hrs after transfection with (C) PEI, (D) C32-103, and (E) adenovirus at MOI=500.

required at least 70% more polymer (≥50:1 polymer to DNA weight ratio) than the end-modified versions of C32 did (30:1 polymer to DNA weight ratio). Since the base molecular weight of all these materials is the same, and the only modification is at the terminus, this demonstrates that single atom differences at the chain ends can alter the transfection levels significantly. We hypothesize that a polymer whose transfection activity is reduced by interior conjugation of targeting ligands, PEG chains or other molecules, may be potentially restored or improved by end-chain functionalization.

The most effective polymers are C32-103 and C32-117, which are twice as effective as an optimal C32 formulation. Having a three carbon spacer between terminal amines may be the ideal length for effective gene delivery with C32 polymers. These polymers also transfect more than twice as many cells as the leading commercially available non-viral transfection reagent, Lipofectamine 2000. Furthermore, by both measures of gene delivery, percentage of cells transfected and average expression per cell, these polymers are two orders-of-magnitude more effective than 25 kDa polyethylenimine (PEI). This improvement over PEI can also be seen by comparing the fluorescent micrographs of GFP expressing cells produced using PEI (Figure 7.3.C) and C32-103 (Figure 7.3.D).

End-modified poly(β-amino ester)s were found to have comparable gene expression to adenovirus even at high titer. Only at a very high MOI of 500, is the percentage of cells transfected (96.0 ±0.1%), beyond what is attained by polymers C32-103 (65.5 ±1.9%) and C32-117 (72.3 ±1.6%). However, on a gene expression per cell basis, the adenovirus, even at this high titer, is not statically better than C32-103 ($p=0.25$). In fact, at 24 hrs post-transfection, the GFP expression per cell via C32-103 vectors (Figure 7.3.D) is dramatically higher than GFP expression via adenovirus at high titer (500 MOI, Figure 7.3.E).

For viral gene therapy, one alternative approach to adenovirus is the retrovirus.[1] Researchers using an engineered vesicular stomatis virus G-protein (VSV-G)-pseudotyped lentiviral vector to transfect HUVECs have reported an efficacy of 70% positive cells[20]. C32-103 and C32-117 degradable polycations have achieved gene delivery efficacy comparable to these reported results.

To examine the activity of these optimized polymers *in vivo* as possible vectors for the systemic treatment of ovarian cancer, we injected C32 and C32-117 polymer/pCAGluc DNA complexes into the peritoneum of MISIIR/TAg female transgenic mice bearing bilateral ovarian tumors. These mice develop ovarian tumors as a result of expression of SV40 T antigen in ovarian epithelial cells[19]. Optical images of mice taken 6 hours post-administration of the complexes showed strong luciferase expression in mice injected with end-modified C32 complexes, but not with C32 complexes (Fig. 4A). Quantification of the bioluminesce emitted from tumors showed that C32-117 delivered DNA over two-orders-of-magnitude more efficiently to the tumor than C32 (Fig. 4B). This result shows that small modifications to the termini of a polymer can significantly increase its *in vivo* activity, and the specific end-modified polymers described here may have utility in the treatment of ovarian cancer.

(A)

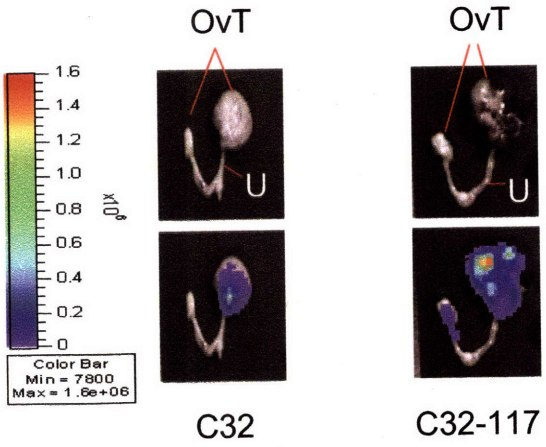


(B)

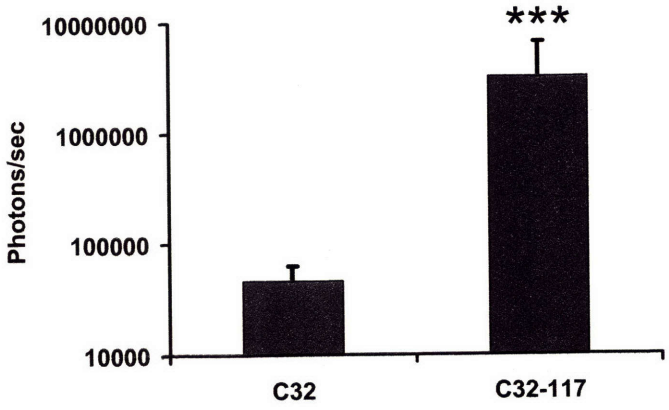


**Figure 7.4.** (A) Optical images of ovarian tumors and uteri from MISIIR/TAg mice 6 hr following *i.p.* injection with polymer/DNA (pCAG/luc) complexes. Grayscale images are shown in the top row. OvT = ovarian tumors; U = uterus. In the bottom row, corresponding pseudocolor images representing emitted bioluminescence are superimposed over grayscale images. RLUs/pixel are indicated in the color scale bar on the left. (B) Quantification of luciferase expression in ovarian tumors 6 hr following *i.p.* injection with C32 (n = 6) or C32-117 (n = 9) delivered pCAG/luc DNA (100 μg). Results are expressed as mean transfection levels (± SD).

## 7.4 CONCLUSIONS

To our knowledge, this is the first time that a polymeric vector has been shown to have comparable efficacy to a viral vector in a head-to-head test in human primary cells. It is also the first time that specific combinatorial modifications of just the termini of polymers has been shown to lead to large changes to gene delivery efficacy via known
gene delivery bottlenecks including DNA binding and cellular uptake. As degradable polymers C32-103 and C32-117 have many attractive properties over a virus including high safety, low immunogenicity, high nucleic acid cargo capacity, ease in manufacture, and flexibility for future design improvements including targeting, we believe that these polymers may provide promising alternatives for therapeutic gene delivery applications.

## 7.5 REFERENCES


1. Thomas, C.E., Ehrhardt, A. & Kay, M.A. Progress and problems with the use of viral vectors for gene therapy. *Nat Rev Genet* **4**, 346-358 (2003).
2. Pack, D.W., Hoffman, A.S., Pun, S. & Stayton, P.S. Design and development of polymers for gene delivery. *Nature Reviews Drug Discovery* **4**, 581-593 (2005).
3. Park, T.G., Jeong, J.H. & Kim, S.W. Current status of polymeric gene delivery systems. *Adv Drug Delivery Rev* **58**, 467-486 (2006).
4. Merdan, T., Kopecek, J. & Kissel, T. Prospects for cationic polymers in gene and oligonucleotide therapy against cancer. *Adv Drug Delivery Rev* **54**, 715-758 (2002).

5. Anderson, D.G., Akinc, A., Hossain, N. & Langer, R. Structure/property studies of polymeric gene delivery using a library of poly(beta-amino esters). *Mol Ther* **11**, 426-434 (2005).

6. Green, J.J. et al. Biodegradable Polymeric Vectors for Gene Delivery to Human Endothelial Cells. *Bioconjug Chem* **17**, 1162-1169 (2006).

7. Akinc, A. & Langer, R. Measuring the pH environment of DNA delivered using nonviral vectors: Implications for lysosomal trafficking. *Biotechnol Bioeng* **78**, 503-508 (2002).

8. Lynn, D.M. & Langer, R. Degradable poly(beta-amino esters): Synthesis, characterization, and self-assembly with plasmid DNA. *J Am Chem Soc* **122**, 10761-10768 (2000).

9. Anderson, D.G. et al. A polymer library approach to suicide gene therapy for cancer. *Proc. Natl. Acad. Sci. U.S.A.* **101**, 16028-16033 (2004).

10. Anderson, D.G., Lynn, D.M. & Langer, R. Semi-automated synthesis and screening of a large library of degradable cationic polymers for gene delivery. *Ang. Chem. Int. Edn* **42**, 3153-3158 (2003).

11. Boussif, O. et al. A versatile vector for gene and oligonucleotide transfer into cells in culture and in vivo: polyethylenimine. *Proc Natl Acad Sci U S A* **92**, 7297-7301 (1995).

12. Connolly, D.C. et al. Female mice chimeric for expression of the simian virus 40 TAg under control of the MISIIR promoter develop epithelial ovarian cancer. *Cancer Res* **63**, 1389-1397 (2003).

13. Thomas, M. & Klibanov, A.M. Non-viral gene therapy: polycation-mediated DNA delivery. *Appl Microbiol Biotechnol* **62**, 27-34 (2003).

14. Tanner, F.C., Carr, D.P., Nabel, G.J. & Nabel, E.G. Transfection of human endothelial cells. *Cardiovasc Res* **35**, 522-528 (1997).

15. Brewster, L.P., Brey, E.M. & Greisler, H.P. Cardiovascular gene delivery: The good road is awaiting. *Adv Drug Delivery Rev* **58**, 604-629 (2006).

16. Shah, P.B. & Losordo, D.W. Non-viral vectors for gene therapy: clinical trials in cardiovascular disease. *Adv Genet* **54**, 339-361 (2005).

17. Li, C.G., Guo, B.Q., Bernabeu, C. & Kumar, S. Angiogenesis in breast cancer: The role of transforming growth factor beta and CD105. *Microsc Res Techniq* **52**, 437-449 (2001).

18. Riccioni, T., Cirielli, C., Wang, X., Passaniti, A. & Capogrossi, M.C. Adenovirus-mediated wild-type p53 overexpression inhibits endothelial cell differentiation in vitro and angiogenesis in vivo. *Gene Ther* **5**, 747-754 (1998).

19. Vincent T, H.B. et al. Rapid assessment of adenovirus serum neutralizing antibody titer based on quantitative, morphometric evaluation of capsid binding and intracellular trafficking: population analysis of adenovirus capsid association with cells is predictive of adenovirus infectivity. *J. Virol* **75**, 1516-1521 (2001).

20. Totsugawa, T. et al. Successful lentivirus-based delivery of a LacZ gene into human endothelial cells. *Transplant Proc* **35**, 499-500 (2003).

# Chapter 8: Applications to Genetic Vaccines

## 8.1 INTRODUCTION

One field that gene delivery can impact dramatically is immunotherapy. The delivery of genes could be used for multiple immunological applications including both vaccines against infectious diseases and vaccines against non-infectious diseases such as cancer.[1] DNA-based genetic vaccines have numerous potential advantages over conventional viral or protein based vaccines. These include high induction of cellular immunity, potentially high safety, ease in manufacture, cost-savings, and the potential for co-expression of multiple antigens.[2] The comparative ease in DNA manufacture makes DNA vaccines especially advantageous against new or rapidly mutating pathogens that conventional vaccines find technologically challenging such as HIV or a future influenza pandemic.[3] An overview of the mechanism of DNA vaccines is shown in Figure 8.1.

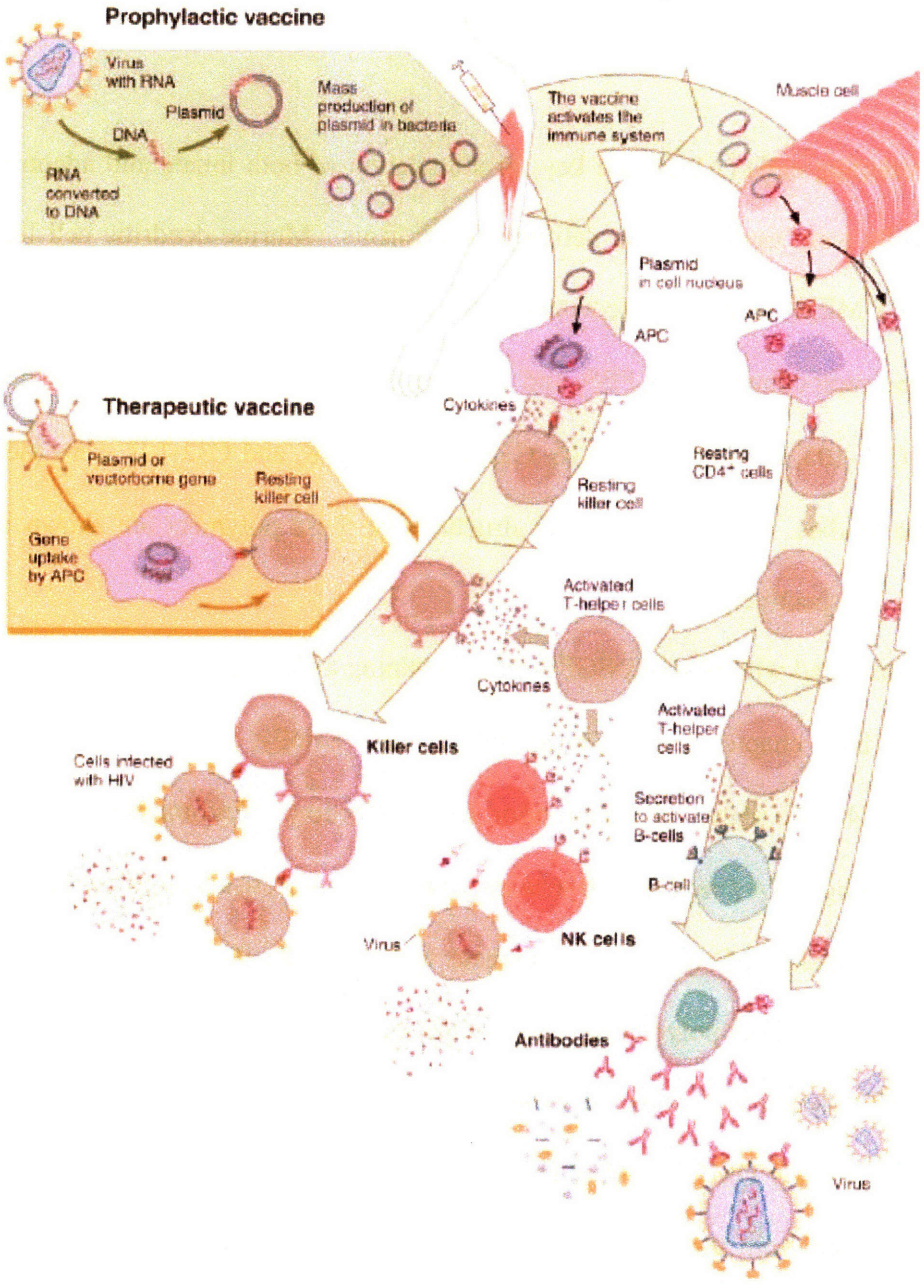


**Figure 8.1.** Overview of DNA vaccine mechanism.[1]

## 8.2 METHODS

As antigen presenting cells (APCs) are key for stimulation of both innate and adaptive immunity, dendritic cells were used for gene delivery experiments. Murine dendritic cell line DC2.4 was grown in DMEM media supplemented with 20 mM HEPES buffer, 2 mM L-glutamine, 50 μM β-mercaptoethanol, 10% FBS, and 1% penicillin/streptomycin. End-modified poly(β-amino esters) C32-103, C32-108, C32-116, C32-117, C32-118, and C32-122 were used in these DNA vaccine studies. The synthesis and structures of these polymers are shown in Figure 8.2and Figure 8.3 respectively.

Cells were transfected with plasmid EGFP-N1 (containing a CMV promoter) following the "standard protocol" from chapter 3, using 6 μg DNA / well. Briefly, cells were seeded at 75,000 per well to a 24-well plate, 24 hours prior to transfection. End-modified PBAE nanoparticles formed at 6 μg DNA / well and 30 w/w polymer to DNA were added to the cells in 10% serum containing DMEM and were left to incubate with the cells for 4 hours. Control polymers were used at their optimal polymer to DNA weight ratios (unmodified C32 polymer at 50 w/w and 25 kDa PEI polymer at 1 w/w). Afterwards, the media was aspirated and replaced with 500 μL of warm, complete DMEM. After a 48 hrs, transfected and untransfected control cells were washed, removed from the 24-well plates by trypsinization, microcentrifuged, and resuspended in 1 mL of FACS running buffer (98% PBS / 2% FBS / 1:200 propidium iodide solution) for FACS analysis as previously described.

To ascertain cell viability, cellular metabolic activity was measured using the Cell Titer 96 Aqueous One Solution assay kit. Metabolic activity was measured using optical absorbance on a Victor3 Multilabel plate counter. Measurements of treated cells were converted to percent

viability by comparison to untreated controls. High-throughput cell viability assays were conducted using 96-well plates with correspondingly scaled down cell seeding (15,000 cells/well) and poly(β-amino ester) nanoparticle doses (1.2 ug DNA/well basis). Polymers were tested for cell viability / cytotoxicity at the same formulation conditions used for gene delivery efficacy studies.

To test these PBAE nanoparticles *in vivo*, serum antibody generation was measured in response to pCI-BP2, a β-galactosidase encoding plasmid. This plasmid is driven by a CMV promoter and encodes a fusion protein of β-galactosidase and peptide SIYRYYGL, an agonist for the 2C T-cell receptor when bound to the H-2K$^b$ allele of MHCI in B6 mice.[4] Young B6 mice were vaccinated with 200 μL intraperitoneal injections containing 50 μg DNA and 30 w/w poly(β-amino ester) three times with each injection 72 hrs apart. The nanoparticles were first prepared in 25 mM sodium acetate and then diluted in phosphate buffered saline supplemented with 5% glucose. Intraperitoneal injection of β-galactosidase protein and naked pCI-BP2 intramuscular injections were used as positive controls. At four weeks, all mice were then challenged with an intraperitoneal injection of 50 μg of β-galactosidase protein. Whole blood was sampled from mice tail veins at two weeks, five weeks, and six weeks following initial injection. Serum was stored at -80 °C and was then tested by an ELISA specific for mouse anti-β-galactosidase IgG.

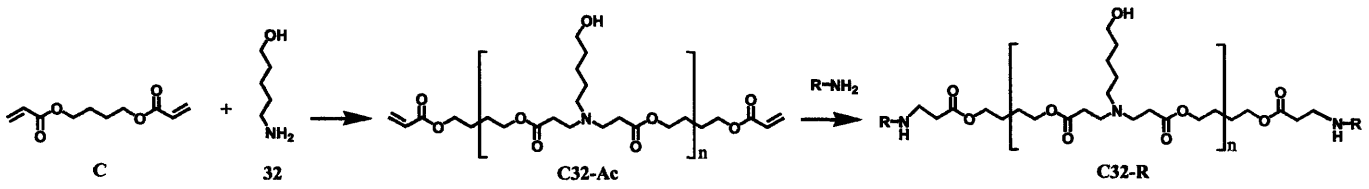


**Figure 8.2.** Synthesis of end-modified C32 poly(β-amino esters).

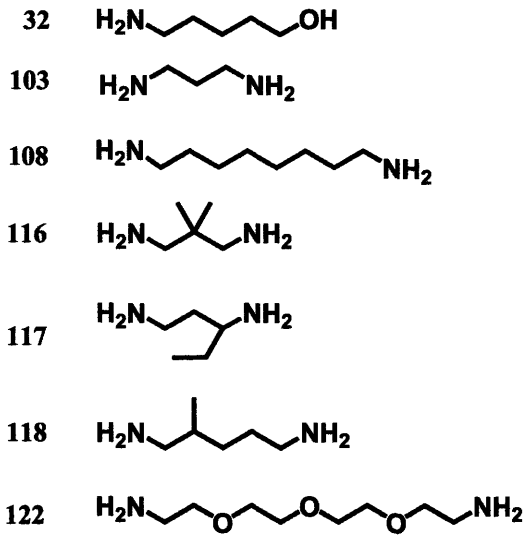


**Figure 8.3.** End-capping monomers used to create C32-based poly(β-amino esters) for use as genetic vaccines.

## 8.3 RESULTS AND DISCUSSION

Almost all poly(β-amino esters) tested including, C32-103, C32-116, C32-117, and C32-118 transfected DC 2.4s significantly better than 25 kDa PEI. These results can be seen in Figure 8.4. Interestingly, C32-108, with a structure vary similar to the other polymers, did not transfect DC 2.4 cells. This is interesting as it shows that certain polymers can be quite effective

in one cell line, while ineffective in another. Similarly, the two best-performing polymers, C32-116 and C32-118, were able to transfect dendritic cells more effectively than C32-103 and C32-117, polymers found to be the most effective at transfecting primary human umbilical vein endothelial cells. The observation that seemingly small molecular changes to polymer structure can cause transfection cell-specificity among various cell types may be potentially useful for cell targeting. Fluorescent micrographs showing EGFP dendritic cell transfection use polymers C32-116 and C32-118 are also shown in Figure 8.5.

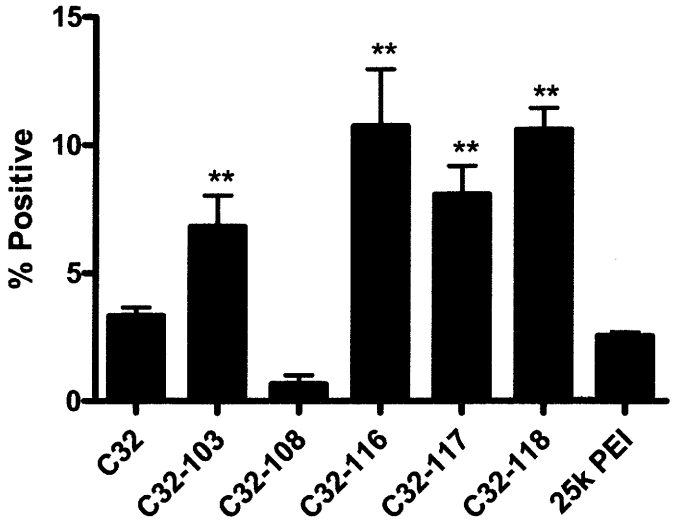


**Figure 8.4.** Transfection of dendritic cell line DC 2.4 in serum containing media. Graph shows means ± SD. One-way ANOVA shows $p<0.0001$. (**) indicates $p<0.01$ for Dunnett's Multiple Comparisons post-test.

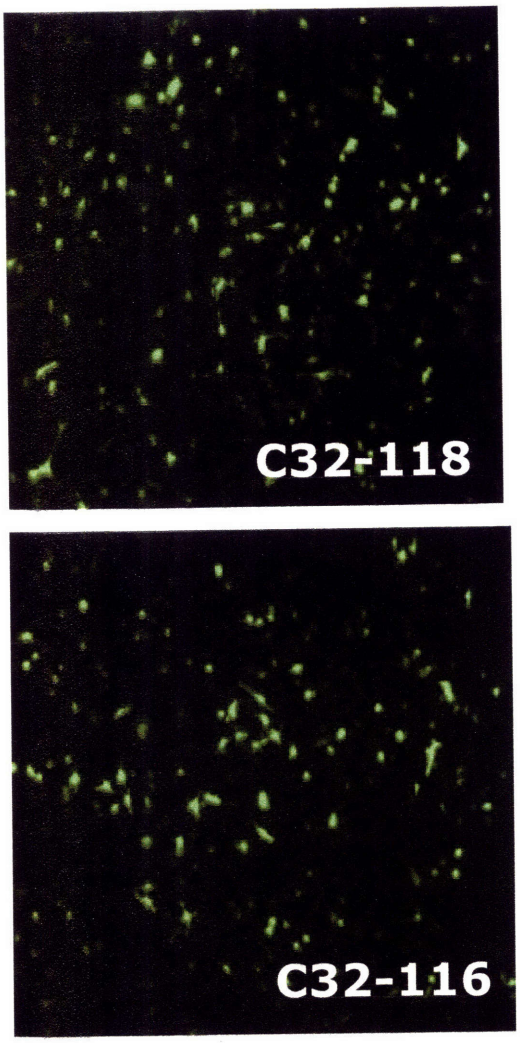


**Figure 8.5.** Fluorescent micrographs of DC 2.4 EGFP transfection using PBAE nanoparticles.

Poly(β-amino ester) nanoparticles have minimal toxicity to dendritic cells. Figure 8.6 demonstrates that the end-terminated C32 polymers, are non-toxic at the concentrations used for transfection, 0.24 μg/μL. In contrast, Lipofectamine 2000 shows cytotoxicity at 0.024 μg/μL. This demonstrates that poly(β-amino esters) are non-toxic to DC 2.4 dendritic cells and at least an order of magnitude less toxic than Lipofectamine 2000. Dose response for two polymers are shown in Figure 8.7. C32-116 is found to be non-toxic for all doses tested and C32-118 only first shows slight cytotoxicity at 0.8 μg/μL, a concentration over three-fold higher than the dose at which it is used.

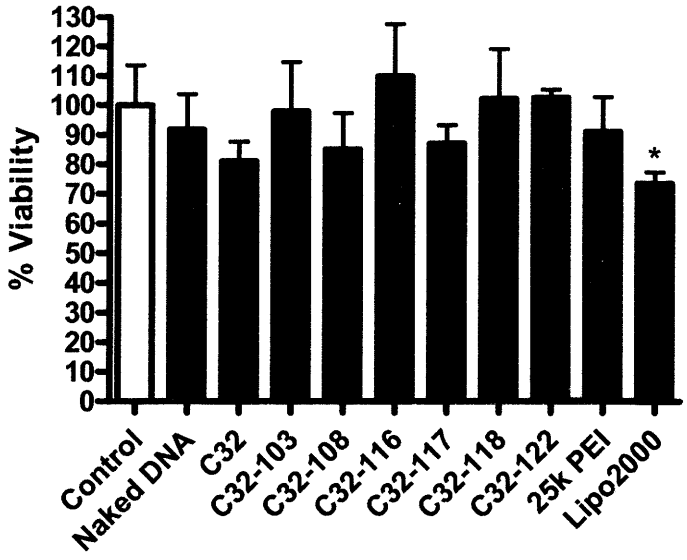


**Figure 8.6.** Transfection of dendritic cell line DC 2.4 in serum containing media. Graph shows means ± SD. (*) indicates $p<0.05$ for Dunnett's Multiple Comparisons post-test. The modified PBAE polymers are non-toxic at two orders of magnitude higher concentration. Unmodified C32 at 50 w/w, 0.40 μg/μL, modified C32 derivatives at 30 w/w, 0.24 μg/μL, PEI at 1 w/w, 0.008 μg/μL, Lipofectamine 2000 at 0.024 μg/μL.

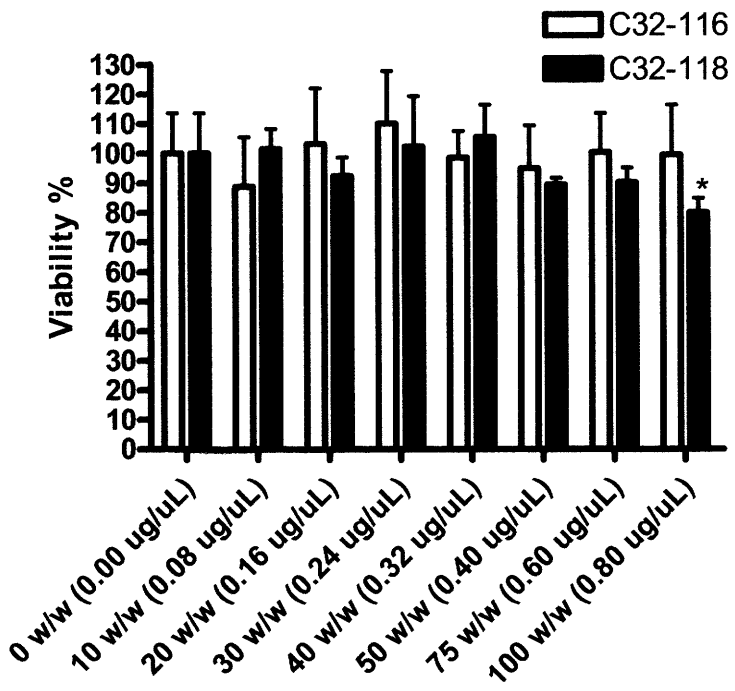


**Figure 8.7.** Viability of dendritic cell line DC 2.4 in serum containing media. Graph shows means ± SD. (*) indicates $p<0.05$ for Dunnett's Multiple Comparisons post-test. Only at the highest polymer concentration (100 w/w, 0.80 μg/μL) does C32-118 show cytotoxicity. C32-116 does not show cytotoxicity for the concentrations tested.

These results demonstrate that poly(β-amino ester)-mediated DNA vaccine delivery to dendritic cells can be safe and effective *in vitro*. This may be important for an *ex vivo* application where dendritic cells can be transfected and/or T-cells activated *in vitro* and then these cells can be re-injected *in vivo* for a therapeutic response. However, for most applications, direct *in vivo* DNA delivery would be preferred. Mice vaccinated by PBAE/BP2 DNA nanoparticles were found to have high levels of antibody production, especially following the β-galactosidase challenge. Average serum antibody levels for the polymeric DNA vaccines at two

weeks, five weeks, and six weeks can be seen in Figure 8.8. Figure 8.9 shows the antibody response in more detail for individual mice at the six week time point.

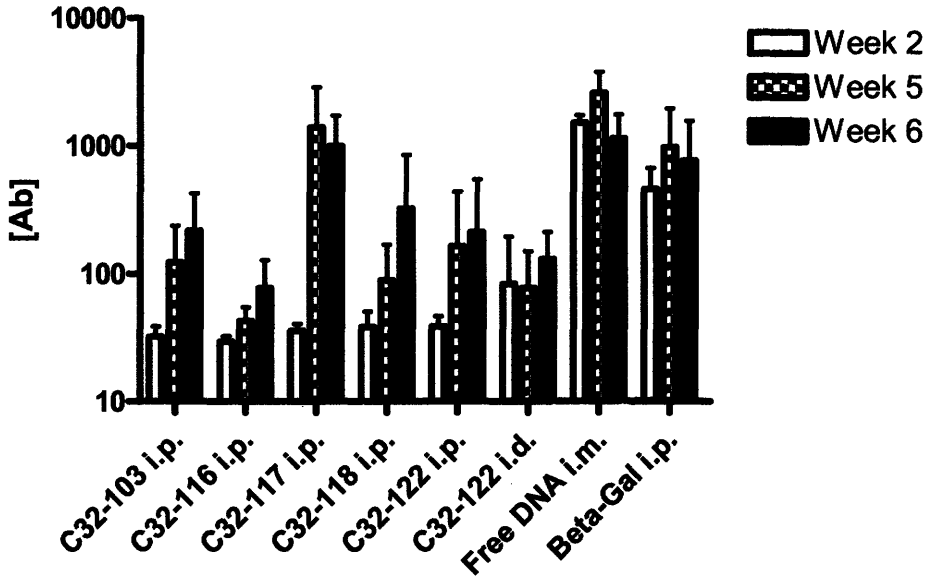


**Figure 8.8.** Antibody production in mice following injection of PBAE nanoparticles means ± SD (n=5).

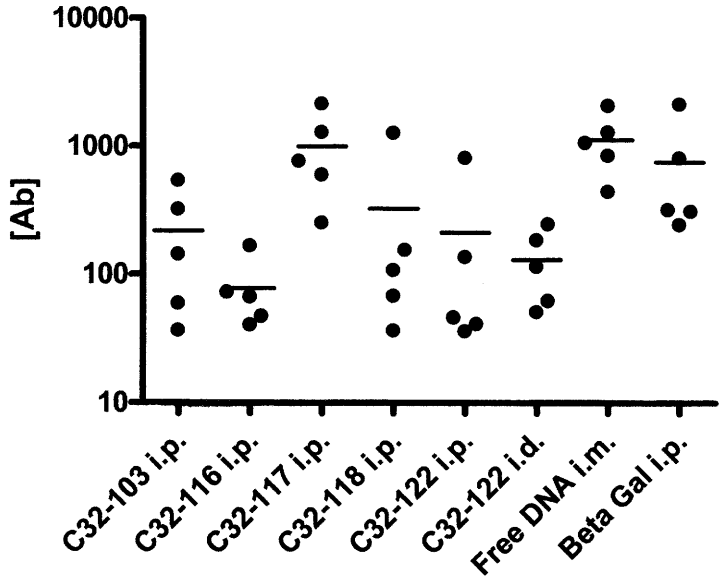


**Figure 8.9.** In vivo antibody production at 6 weeks (n=5).

These results demonstrate that C32-117 and C32-118, top polymers during *in vitro* testing, also mediated high antibody responses *in vivo* and may therefore be promising as genetic vaccines. Tissue pathology studies of transfected mice also revealed minimal inflammation and toxicity. The particularly sharp, almost two orders of magnitude, increase in serum antibody concentrations for C32-117 between 2 weeks and 5 weeks is indicative of a very strong memory response following antigen challenge. C32-117 also matched the antibody concentrations of intramuscular free DNA injections and intraperitoneal injection β-galactosidase protein itself. This is important as these are the gold standards for determining *in vivo* efficacy of genetic vaccines in a mouse model. However, intramuscular DNA injections have failed in numerous human trials and have proven ineffective for therapy. Similarly, conventional protein vaccination has associated manufacturing concerns and does not induce a cytolytic T lymphocyte

response. Thus, the demonstration of C32-117 nanoparticles to rival these two positive controls shows its promise for potential use as a DNA vaccine.

Interestingly, small structural changes were found to make a big difference to *in vivo* efficacy. Additional preliminary data recently obtained both *in vitro* and *in vivo* (data not shown) suggest that these polymeric nanoparticles can also activate cytolytic T lymphocytes for efficient cell-mediated immunity. In particular, C32-118 appears to be especially efficient at this whereas C32-117 does not. This ongoing work may further reveal how the choice of an ideal polymer for gene delivery may be increasingly application-dependent and how small structural changes to a polymer can lead to dramatic changes in biological function. The work highlights how future applications using poly(β-amino ester) nanoparticles as DNA vaccines are highly promising.

## 8.4 REFERENCES


1. Donnelly, J.J., Wahren, B. & Liu, M.A. DNA vaccines: progress and challenges. *J Immunol* **175**, 633-639 (2005).
2. Bivas-Benita, M., Ottenhoff, T.H., Junginger, H.E. & Borchard, G. Pulmonary DNA vaccination: concepts, possibilities and perspectives. *J Control Release* **107**, 1-29 (2005).
3. Forde, G.M. Rapid-response vaccines--does DNA offer a solution? *Nat Biotechnol* **23**, 1059-1062 (2005).
4. Udaka, K., Wiesmuller, K.H., Kienle, S., Jung, G. & Walden, P. Self-MHC-restricted peptides recognized by an alloreactive T lymphocyte clone. *J Immunol* **157**, 670-678 (1996).

# Chapter 9: Future Directions

## 9.1 SUMMARY

Poly(β-amino esters) are promising for non-viral gene delivery due to their 1) ability to condense DNA into nanoparticles, 2) ability to buffer the endosome, 3) ability to promote endosomal escape, 4) low cytotoxicity compared to other cationic polymers, 5) biodegradability via hydrolytic cleavage of ester groups, and 6) large potential for structural diversity.[1-5] In the chapters of this thesis, we have demonstrated that these particles can be formulated to be stable in the presence of serum proteins and have high efficacy without toxicity to human primary cells (Chapter 4). It was also demonstrated that analyzing biophysical properties of poly(β-amino ester)/DNA nanoparticles including size, stability, and zeta potential in the proper media conditions and dynamically over time provides good correlation to transfection efficacy and can pick up phenomenon missed when biophysical particle properties are only tested in buffer. We optimized vector parameters including DNA loading and polymer to DNA weight ratio and determined efficacy with and without serum-containing media.

Cell-specific nanoparticle delivery requires both specific uptake by the target cell and inhibition of delivery to non-specific cell types. Researchers have found that as ligand substitution of a polymer increases (either targeting or shielding), overall gene delivery can decrease, presumably due to alteration of the original polymer's functionality for DNA condensation and endosomal buffering.[6, 7] Coatings that reduce the positive charge of gene delivery nanoparticles could potentially reduce non-specific uptake while still enabling receptor-

mediated uptake and may also be desirable to prevent unwanted serum interactions.[8] Here, we have shown that electrostatic interactions can drive peptide coating of nanoparticles and enable ligand-specific gene delivery to human primary cells (Chapter 5). Our general approach to electrostatically coat gene delivery nanoparticles with ligands provides a simple method of ligand addition as well as a mechanism to neutralize nanoparticle charge and reduce electrostatic interactions with undesirable cell types. While we use RGD-containing peptide as a model system to investigate nanoparticle coating and ligand-specific delivery to primary endothelial cells, many other peptide ligand sequences, such as those made from antibody fragments, could be readily incorporated into this system as well.

This work also highlights the importance of multiple factors including polymer weight ratio, peptide weight ratio, overall charge ratio, and ligand length when developing coated gene delivery nanoparticles. A biphasic efficacy relationship was found for peptide weight ratio, overall charge ratio, and ligand length, with intermediate values of coating being optimal. This finding demonstrates that a balance is required when seeking to design the nanoparticles to have reduced non-specific uptake, but increased ligand-specific uptake.

We also have demonstrated a high-throughput method to screen polymers for DNA binding and determine DNA/binding constants and lattice site size parameters (Chapter 6). A striking, biphasic relationship was found between DNA binding and efficacy with an optimal $K_a$ in the range of $2.4 \times 10^9 - 8.9 \times 10^{10}$ $M^{-1}$ ($K_d \sim 11$ - 420 pM). This biphasic relationship held true for a range of different polymer structures from a poly(β-amino ester) library and revealed interesting structure/function relationships. Small structural modifications were found to be effective at increasing $K_a$ and corresponding delivery efficacy. The assay used here was also helpful in discerning the mode of DNA association and encapsulation between a hydrophilic

polymer and a hydrophobic polymer. This binding analysis may be used to design polymeric drug delivery vehicles for a range of multivalent cargos (DNA, siRNA, etc) and diverse therapeutic applications.

Finally, we develop end-modified poly(β-amino ester)s, easy-to-synthesize degradable polymers, which are able to deliver DNA to primary human umbilical vein endothelial cells (HUVECs) at levels comparable to adenovirus at a Multiplicity of Infection (MOI) between 100 and 500 (Chapter 7). By both measures of gene delivery, percentage of cells transfected and average expression per cell, these polymers are two orders-of-magnitude more effective than 25 kDa polyethylenimine (PEI) without toxicity. Interestingly, small structural changes were found to have dramatic effects on multiple steps of gene delivery including the DNA binding affinity, nanoparticle size, intracellular DNA uptake, and final protein expression. We show that small modifications to the termini of a polymer can significantly increase its *in vivo* activity and demonstrate potential utility of these polymers in the fields of cancer therapy (Chapter 7), genetic vaccines (Chapter 8), and stem-cell engineering (Chapter 9). To our knowledge, this is the first time that a polymeric vector has been shown to have comparable efficacy to a viral vector in a head-to-head test in human primary cells. It is also the first time that specific combinatorial modifications of just the termini of polymers has been shown to lead to large changes to gene delivery efficacy via known gene delivery bottlenecks including DNA binding and cellular uptake.

We believe the development of polymeric vectors with gene delivery efficacy comparable to adenovirus could set a new benchmark in non-viral transfection capability. As the enhanced polymeric gene delivery nanoparticles described here have many attractive properties over a virus including high safety, low immunogenicity, high nucleic acid cargo capacity, ease in

manufacture, a coating method for targeted delivery, and flexibility for future design improvements, we believe that these polymeric nanoparticles may provide promising alternatives for therapeutic gene delivery applications.

## 9.2 FUTURE DIRECTIONS

The poly(β-amino ester) nanoparticles described here can be utilized in numerous additional *in vitro* and *in vivo* applications. Specific use of poly(β-amino ester) nanoparticles as potential cancer therapeutics and genetic vaccines were presented in previous chapters and use as agents to transform human embryonic stem cells are briefly described here. These examples show the future directions that polymeric gene delivery can play in the fields of cancer research, immunotherapy, and regenerative medicine. Future directions for the rational design of further improved non-viral gene delivery systems are also discussed.

### *9.2.1 Applications to Stem Cells and Tissue Engineering*

#### 9.2.1.1 Introduction

The delivery of genes to stem cells also has large potential for the advancement of cell-based therapies and the field of tissue engineering. A depiction for a combined strategy of gene therapy and stem cell therapy is shown in Figure 9.1. Given the right conditions, pluripotent stem cells can potentially differentiate into any cell of the body, allowing wide therapeutic utility

including treatments for autoimmune diseases, spinal chord injury, Parkinson's disease, and cardiac tissue engineering, among many others.[9] Gene delivery could possibly allow for directed differentiation from a pluripotent stem cell into specific cell types of interest and/or could reprogram a differentiated cell back into a pluripotent state. Recently, it was reported that through the use of viral gene delivery, mouse fibroblasts could be reprogrammed into an ES-like pluripotent state through ectopic expression of four transcription factors: Oct4, Sox2, c-Myc, and Klf4.[10] While the retrovirus approach used here is not practical for human use due to safety concerns, a non-viral approach may be feasible. Such a safe and effective method for gene delivery to stem cells would be invaluable for the creation of new cell-based therapies.

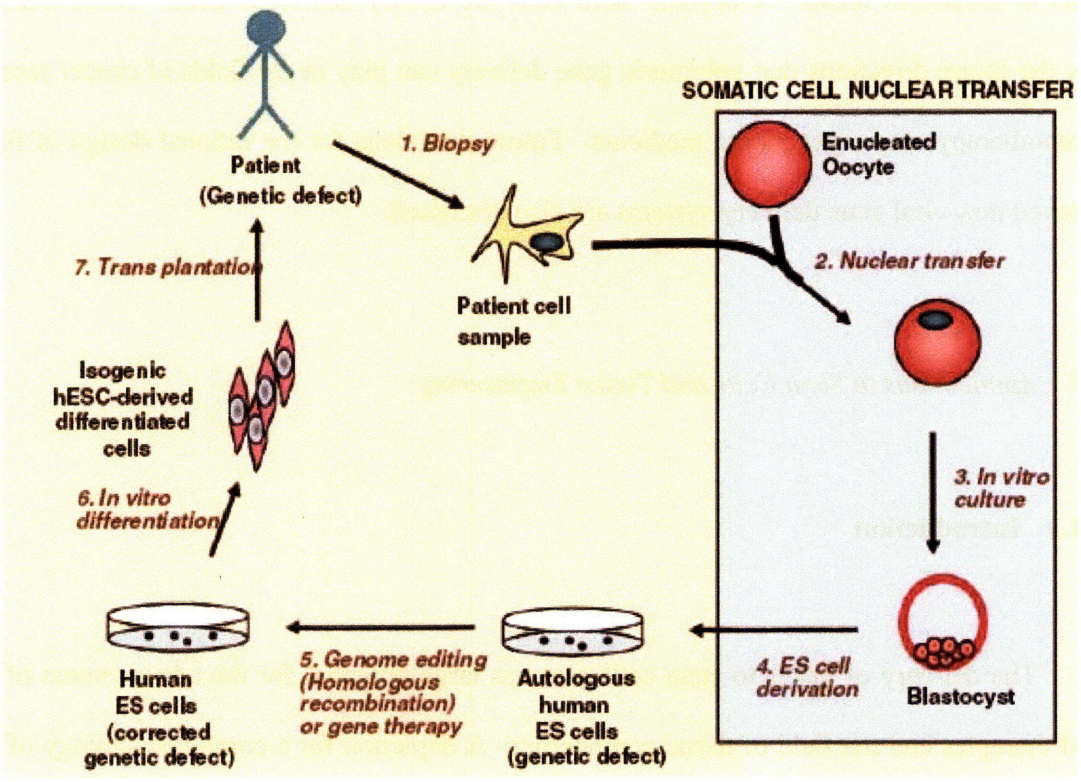


**Figure 9.1.** Combined gene and stem cell therapy[9]

#### 9.2.1.2 Methods

Human embryonic stem (hES) cells were grown according to standard protocols. hES cells may be transfected while on feeder cells, but transfection is enhanced if they are first transferred to Matrigel.™ For GFP experiments, cells were transfected with plasmid EGFP-N1 following the "standard protocol" from chapter 3, using 20 μg DNA / well in a 6-well plate format or 10 μg DNA / well in a 12-well plate format. Colonies were plated 24 hours prior to transfection. End-modified PBAE nanoparticles were formed at 50 w/w polymer to DNA were added to the cells in reduced serum media and left to incubate with the cells for 4 hours. Lipofectamine 2000 was used according to manufacturer instructions. After the incubation, the media was aspirated and replaced with regular warm media. At 48 hrs, transfected and untransfected control cells were analyzed by FACS as previously described.

#### 9.2.1.3 Results and Discussion

End-modified poly(β-amino ester) nanoparticles encapsulating GFP DNA were found to be efficacious for gene delivery to human embryonic stem cell colonies (hES). Dramatically, C32-118 is able to significantly transfect hES colonies whereas Lipofectamine 2000, the leading commercially available non-viral vector is only able to transfect cells on the periphery. Representative fluorescent micrographs of this transfection can be seen in Figure 9.2 and Figure 9.3 respectively. For this particular transfection, it is important to note that some of these cells may be differentiated and others may be feeder cells. To avoid this, for subsequent experiments modified GFP positive hES cells were utilized instead and they were transfected on Matrigel™

rather than feeders. These modified hES cells have been previously stably transfected to have GFP expression driven by Oct4. If these hES cells remain undifferentiated, they are GFP positive. However, if they become differentiated, the GFP expression stops and they become GFP negative. In this manner, undifferentiated hES cells can be distinguished from differentiated stem cells and/or feeder cells.

With this new cell system, red fluorescent protein (RFP) was transfected instead of GFP, and positive transfection of undifferentiated hES cells was determined by counting cells positive for both RFP and GFP. The results for polymeric gene delivery to undifferentiated hES cells that remain undifferentiated following transfection are shown in Figure 9.4. PBAEs clearly show superior gene delivery efficacy compared to Lipofectamine 2000 and suggest that they can be effective agents to deliver genes to hES colonies. Such genetically reprogrammed cells may prove very useful for future cell-based therapies.

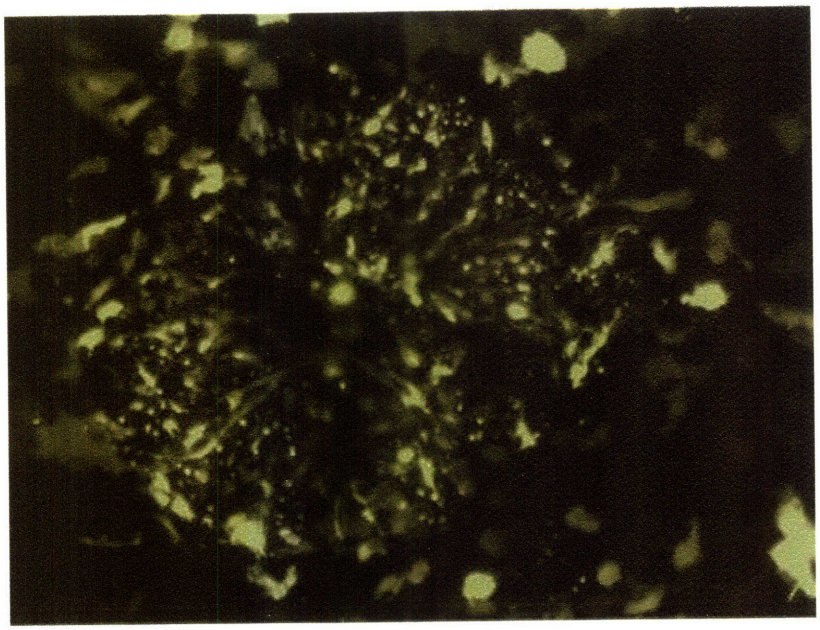

Figure 9.2. Transfection of hES colony by C32-118

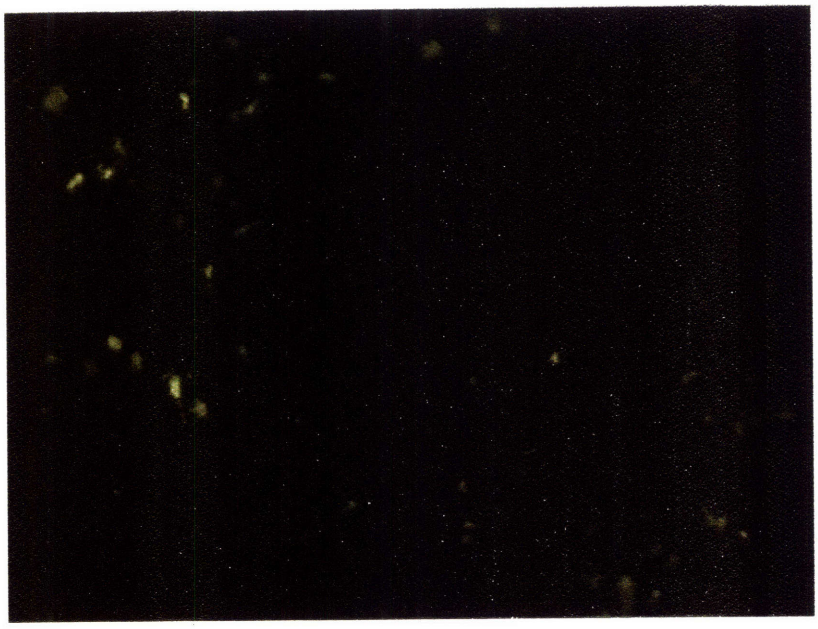

**Figure 9.3.** Transfection of hES colony by Lipofectamine 2000

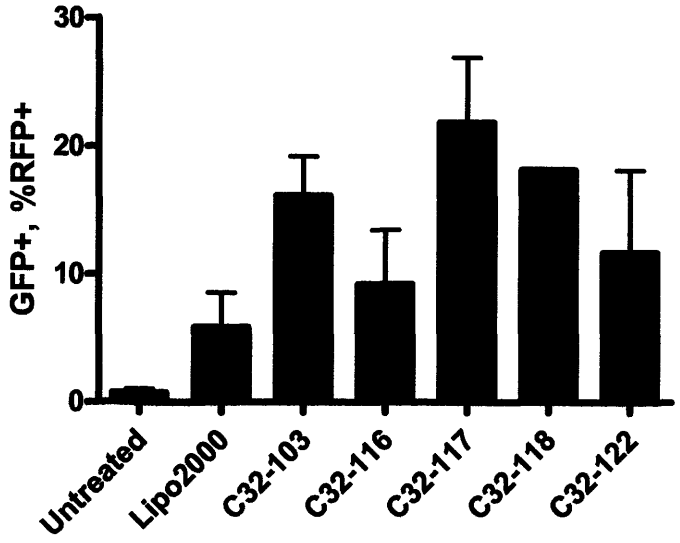


**Figure 9.4.** PBAE gene delivery to undifferentiated hES colonies.

### *9.2.2 Towards Further Rational Design*

While we have demonstrated in part how polymer structure and nanoparticle properties affect gene delivery function, much still remains unknown. Novel assays and quantitative computational models are one approach to further elucidate design properties and delivery mechanisms. The development of differential equation models for mass action kinetics of gene delivery transport[11, 12] are a very important step in this direction. What is needed next is additional quantitative biomaterial-specific empirical data to take the place of computationally fitted parameters and to have related models that can predict how changes to biomaterial structure will change these key model parameters. Validation of such a combined model would

enable high-throughput *in silico* experiments to take the place of high-throughput *in vitro* experiments[13] currently used to generate data sets.

Additionally, beyond efficient delivery to the cytoplasm, for gene therapy to be efficacious, the delivered DNA must make its way inside the nucleus, be transcribed into mRNA, and subsequently translated into protein. Whereas many viruses have evolved mechanisms for efficiently transmitting their genetic material into the nucleus for high expression[14], plasmid DNA generally does not have this advantage. Plasmid DNA also generally has only transient expression, with the gene of interest being either degraded[15], methylated and transcriptionaly silenced[16], or dramatically reduced in dividing cells presumably through dilution.[17] For these reasons, to truly optimize non-viral gene delivery, both the gene delivery nanoparticle and the DNA cargo itself need to be designed.

To engineer plasmids for efficient nuclear import, nuclear localization sequence (NLS) can be utilized either through peptide nucleic acid (PNA) to hybridize to DNA,[18] covalent modification of DNA to include an NLS,[19] or engineering of plasmid DNA to contain endogenous DNA-binding proteins containing NLS sequences themselves.[20] Further DNA design strategies are inclusion of a tissue specific promoter, removal of immunostimulatory unmethylated CpG motifs,[16] and depending on the level of gene expression desired, the creation of a mechanism for site-specific integration and/or inducible expression. The combination of a more rationally designed DNA construct with a highly efficient and safe gene delivery system would be very desirable for therapeutic gene therapy.

## 9.3 REFERENCES


1. Anderson, D.G. et al. A polymer library approach to suicide gene therapy for cancer. *Proc. Natl. Acad. Sci. USA.* **101**, 16028-16033 (2004).
2. Anderson, D.G., Akinc, A., Hossain, N. & Langer, R. Structure/property studies of polymeric gene delivery using a library of poly(beta-amino esters). *Mol Ther* **11**, 426-434 (2005).
3. Akinc, A. & Langer, R. Measuring the pH environment of DNA delivered using nonviral vectors: Implications for lysosomal trafficking. *Biotechnol Bioeng* **78**, 503-508 (2002).
4. Lynn, D.M., Anderson, D.G., Putnam, D. & Langer, R. Accelerated discovery of synthetic transfection vectors: parallel synthesis and screening of a degradable polymer library. *J Am Chem Soc* **123**, 8155-8156 (2001).
5. Lynn, D.M. & Langer, R. Degradable poly(beta-amino esters): Synthesis, characterization, and self-assembly with plasmid DNA. *J Am Chem Soc* **122**, 10761-10768 (2000).
6. Kursa, M. et al. Novel shielded transferrin-polyethylene glycol-polyethylenimine/DNA complexes for systemic tumor-targeted gene transfer. *Bioconjug Chem* **14**, 222-231 (2003).
7. Suh, W., Han, S.O., Yu, L. & Kim, S.W. An angiogenic, endothelial-cell-targeted polymeric gene carrier. *Mol Ther* **6**, 664-672 (2002).
8. Trubetskoy, V.S. et al. Recharging cationic DNA complexes with highly charged polyanions for in vitro and in vivo gene delivery. *Gene Ther* **10**, 261-271 (2003).
9. Yates, F. & Daley, G.Q. Progress and prospects: gene transfer into embryonic stem cells. *Gene Ther* **13**, 1431-1439 (2006).

10. Wernig, M. et al. In vitro reprogramming of fibroblasts into a pluripotent ES-cell-like state. *Nature* (2007).

11. Varga, C.M., Hong, K. & Lauffenburger, D.A. Quantitative analysis of synthetic gene delivery vector design properties. *Mol Ther* **4**, 438-446 (2001).

12. Varga, C.M. et al. Quantitative comparison of polyethylenimine formulations and adenoviral vectors in terms of intracellular gene delivery processes. *Gene Ther* **12**, 1023-1032 (2005).

13. Anderson, D.G., Lynn, D.M. & Langer, R. Semi-automated synthesis and screening of a large library of degradable cationic polymers for gene delivery. *Ang. Chem. Int. Edn* **42**, 3153-3158 (2003).

14. Thomas, C.E., Ehrhardt, A. & Kay, M.A. Progress and problems with the use of viral vectors for gene therapy. *Nat Rev Genet* **4**, 346-358 (2003).

15. Abdelhady, H.G. et al. Direct real-time molecular scale visualisation of the degradation of condensed DNA complexes exposed to DNase I. *Nucleic Acids Res* **31**, 4001-4005 (2003).

16. Hodges, B.L., Taylor, K.M., Joseph, M.F., Bourgeois, S.A. & Scheule, R.K. Long-term transgene expression from plasmid DNA gene therapy vectors is negatively affected by CpG dinucleotides. *Mol Ther* **10**, 269-278 (2004).

17. Biamonti, G. et al. Fate of exogenous recombinant plasmids introduced into mouse and human cells. *Nucleic Acids Res* **13**, 5545-5561 (1985).

18. Branden, L.J., Mohamed, A.J. & Smith, C.I.E. A peptide nucleic acid-nuclear localization signal fusion that mediates nuclear transport of DNA. *Nat Biotechnol* **17**, 784-787 (1999).

19. Zanta, M.A., Belguise-Valladier, P. & Behr, J.P. Gene delivery: A single nuclear localization signal peptide is sufficient to carry DNA to the cell nucleus. *Proc Natl Acad Sci U S A* **96**, 91-96 (1999).

20. Dean, D.A., Dean, B.S., Muller, S. & Smith, L.C. Sequence requirements for plasmid nuclear import. *Exp Cell Res* **253**, 713-722 (1999).

# Chapter 10: Conclusions

The potential of gene therapy to treat disease and improve human health is tremendous. Safe and effective gene delivery to humans would usher in a whole new era of genetic therapies, in many ways revolutionizing medicine. Although viral vectors initially captured the interest of scientists and doctors as the way to move forward in gene therapy, many concerns remain that need to be overcome including limited cargo capacity, manufacturing challenges, and especially safety. The failure of viral gene therapy clinical trials due to toxicity, immunogenicity, and carcinogenicity has been tragic and strongly motivates a non-viral approach.

This alternative, the use of engineered biomaterials rather than viruses to deliver genes, has progressed from materials that were scarcely able to deliver genes at all, to the biomaterials that are presented here which can rival the top viral approaches, adenovirus and lentivirus, for gene delivery efficacy to primary human cells in serum. Compared to the previous "gold standard" for polymeric transfection, 25 kDa PEI, the poly(β-amino ester) nanoparticles presented here have two orders of magnitude higher efficacy while simultaneously having two orders of magnitude lower toxicity. Furthermore, the development of coatings for these nanoparticles for ligand-specific delivery may lead to efficacious and specific cell targeting of these gene delivery nanoparticles *in vivo*. Lastly, by more fully understanding structure/function relationships of these particles including how polymer properties correlate to nanoparticle biophysical properties, how small structural changes to the ends of polymers lead to dramatic changes in DNA binding affinity, particle uptake, and transfection efficacy, and how there is a narrow window of charge

ratio between efficient non-specific particles and ligand-specific particles, future next-generation gene delivery polymers can be better designed. With the continued work of research groups world-wide, the 21st century may very well see a bright future in genetic medicine.